The Characteristics and Perception of Small Wind System Noise

Jennifer Taylor MEng (Hons)

Thesis submitted to the University of Nottingham
for the degree of Doctor of Philosophy

September 2011

Abstract

The UK has committed to sourcing 15% of its energy from renewable sources by 2020 and wind turbines have the potential to contribute towards this target. Due to the Feed-In-Tariffs introduced by the UK Government in 2010, the potential uptake of micro-generation methods such as small wind is likely to increase. However, many barriers exist which prevent widespread implementation, such as noise concerns. There is little work available in the open literature quantifying the problem because much of the existing research focuses on large scale turbines. The need for an increase in interdisciplinary research in this area has also been called for.

This research fills the gap in the literature by seeking to better understand the noise levels generated by small wind systems, the characteristics of the noise and people's reactions to this noise. The research is interdisciplinary, incorporating engineering, to measure, characterise and model the noise from small wind systems and psychology, to identify the type of people who are most likely to perceive the noise.

Environmental noise measurements have been taken at small wind system installations to quantify and characterise the noise levels. This work included an assessment of the attenuation of the noise.

Studies have been carried out on individuals living close to small wind system installations, as well as individuals being played recordings of wind turbine noise to investigate the level and type of noise they perceive and to link this to an individual's attitude towards wind turbines, personality traits and symptom reporting.

CFD has been used to model the flow fields around 2D blade sections to identify the likely noise mechanisms associated with small wind systems by observing the turbulent regions near the aerofoil wall.

Finally, a comparison of the three methods has been carried out to identify that the overall level of small wind system noise is low but it is the nature of the sounds that increase the likely perception of the noise.

Acknowledgements

I would like to thank my supervisors, Carol Eastwick, Claire Lawrence and Robin Wilson, for their guidance and encouragement throughout the duration of my PhD.

The financial support awarded to me by the UK Energy Research Centre is kindly acknowledged, as is the friendly assistance and approachability of the staff at UKERC headquarters.

I am also grateful to the external contributors to my research, particularly the wind turbine installations who were willing to participate in the study and especially Encraft for accompanying me on many turbine visits. Thank you also to Ampair for providing me with data to facilitate my studies.

I would also like to thank my friends and colleagues at the University of Nottingham, who made the duration of my studies enjoyable.

Last, but not least, I give my special thanks to my family for their support and understanding during the years of my study.

Conferences and Publications List

Conferences

EOn Energy Program and Poster Competition June 2008, University Nottingham	Poster and Short Presentation - 1st Prize
UKERC Summer School June 2008, Roehamptom	Poster Presented
U21 Energy Conference September 2008, University Birmingham	Poster Presented
BWEA Small Wind Committee meeting January 2009, London	Invited to present research
Bridging the Gaps Poster Event March 2009, University Nottingham	Won 1st Prize in category
NERC Directors Visit July 2009, University Nottingham	Poster Presented
IOA Wind Turbine Noise Conference January 2010, Cardiff	Presented
Renewable UK Small Wind Conference April 2010, Glasgow	Presented a technical paper plus written paper
AWEA WINDPOWER 2010 May 2010, Dallas	Presented
Internal Division Seminar June 2010, University Nottingham	Presented
Cross Disciplinary Research Showcase July 2010, University Nottingham	Presented
Renewable UK 2010 November 2010, Glasgow	Presented
International Energy Audit October 2010, University Oxford	Poster Presented

Papers Submitted

The Influence of Negative Oriented Personality Traits on the Effects of Small Wind Turbine Noise
Submitted, Environment and Behaviour

Noise Levels and Noise Perception from Small and Micro Wind Turbines
Accepted pending corrections, Renewable Energy

Contents

Chapter 1

Introducing the Thesis Scope

1.1 Introduction

Globally the use of energy has increased dramatically over the last few decades [1] and the problems associated with excessive use of fossil fuels for energy purposes are coming to light. The evidence for global warming and the possible impacts of climate change is vast, extreme weather events worldwide and also in the UK are becoming more frequent. It has been suggested that with a business as usual scenario, the temperature of the earth will increase by up to 3°C by the end of the 21st century [2]. The following goals for the UK Government are outlined along with many others in the Energy White Paper published in 2007 [3]:

- To put ourselves on a path to cut the UK's carbon dioxide emissions by some 60% by about 2050, with real progress by 2020;
- To maintain the reliability of energy supplies;
- To promote competitive markets in the UK and beyond, helping to raise the rate of sustainable economic growth and to improve our productivity;
- To ensure that every home is adequately and affordably heated.

A number of coal and oil fired power stations are due to close over the next decade [4]; this means that the security of supply at peak times is a real concern. In addition to this the price of fossil fuels is increasing at a time when the UK relies increasingly on fossil fuel imports. For these reasons the need for new energy generation, storage, and supply technologies, and better understanding of renewable sources is being recognised. The task of finding more environmentally sustainable forms of energy production is a world-wide occupation, in addition to the goals above and as part of an EU wide directive, the UK has committed to sourcing 15% of its energy from renewable sources by 2020 [5]. The UK has the best wind resource in Europe [6]; therefore wind turbines have the potential to contribute a large amount towards this 15% target. In addition to this wind turbines are environmentally friendly compared to other energy generation methods such as oil and gas, so also have the potential to contribute to the UK Low Carbon Transition Plan to deliver emission cuts of 18% on 2008 levels by 2020 [7]. Over the last decade the installed capacity of wind turbines in the UK as well as Worldwide has increased dramatically. Figure 1.1.1 shows that since 2002 the installed capacity in the UK has increased year on year. Renewable UK quotes a total installed capacity of 5737.70 MW over 307 on and offshore wind farms in the UK to date (September 2011) [8]. However its further development is restricted largely by concerns relating to visual impact and noise, such that wind power is a subject that provokes substantial media coverage. In addition to this, although research has shown that there is general public support for renewable energy, when faced with having it implemented within their community, individuals adopt a 'not in my backyard' attitude and are against the construction of a wind farm in the vicinity of their community [9]. These NIMBY attitudes have been shown by Wolsink [10] to be owing to a feeling of equity and fairness. Wolsink suggests that in countries with a poor performance regarding the implementation of wind power, the planning process takes a hierarchical top down approach, i.e. sites are found and a plan drawn up before the public is involved. This is in contrast to more successful countries such as Denmark and Germany where a collaborative approach is taken and the public are involved at each stage of the selection and decision process. While noise and the potential detrimental effects of noise are clearly a reason for the negative reaction to wind turbines, it is not clear the extent to which this is due to other factors relating to the individuals themselves and specifically their sensitivity to such noise intrusion. It has been found that liaising with communities is important for wind power implementation and involving the public in the discussion of how wind power installation can be integrated into the landscape is required to promote positive attitudes towards wind turbines; this was noted by Devine-Wright [9] who found that studies suggest that local involvement, in either economic or political terms, tends to have a positive effect on public perceptions of wind power.

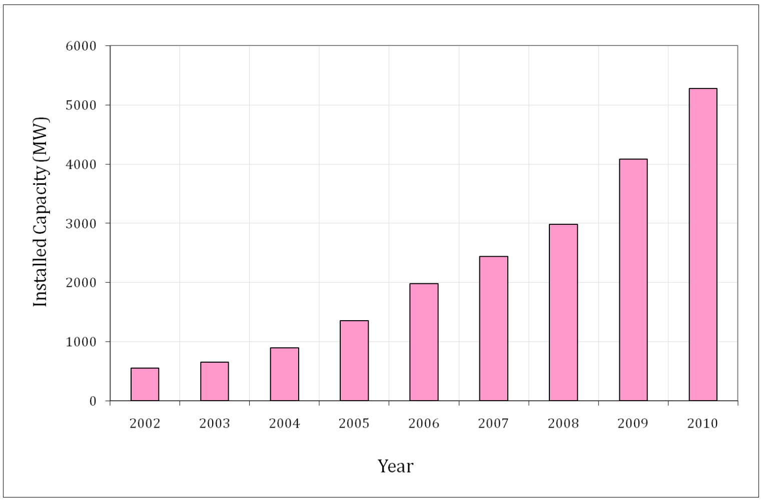

Figure 1.1.1: Graph showing the cumulative installed capacity of wind power in the UK up to 2010 - graph generated from Renewable UK statistics[8]

A study carried out by the Energy Saving Trust suggested that 30-40% of the UK's electricity demands could be met by micro-generation by the year 2050 [11]. As the increasing price of fossil fuels is transferred to the general public through energy bills, the attraction of generating electricity and heating supply on site is increasing. Community led initiatives to raise awareness of energy issues and solutions could encourage a tendency towards micro-generation projects and distributed energy, and could play an important role in the Government's energy strategy. Particularly as, in April 2010 Feed-In-Tariffs (or FITs) were introduced by the UK Government in order to help meet the UK's energy targets, where individuals are encouraged to generate their own green energy by being awarded financial incentives for every kWh of energy produced and bonus incentives to any additional kWh fed back to the grid.

Small and micro wind turbines are examples of micro-generation and for the purposes of this Thesis a micro turbine describes a turbine with a rated power below 2kW and a small turbine describes a turbine with up to 10kW rated power. Micro and small turbines will be described collectively as small wind systems. Renewable UK defines a small wind system as any turbine below 100kW where the target end user could be an individual household, school, or small community. The small wind system can generate all of the end user's energy needs or contribute towards this energy demand. Renewable UK stated in the 2011 Small Wind Market Report that 332 and 2036 small and micro wind turbines respectively were deployed in 2010, with projections for 1075 small and 2647 micro turbines in 2011 [12]. The Feed-In-Tariffs are expected to further increase the potential uptake of household, school and community (small) wind systems for the duration the scheme is offered. This increasing number of small wind systems could seriously reduce the strain on the national grid and provide a huge amount of carbon abatement if sited correctly. However, similar to large scale wind, many barriers exist which prevent the widespread implementation of small wind, such as noise concerns [13]. Small wind is generally sited closer to where individuals live and work than large scale wind projects so although noise levels for small wind are expected to be much lower than for large wind, the closer proximity to domestic dwellings and business properties may increase the likelihood of noise annoyance.

Planning applications for small and micro wind are often contested by the general public who oppose small wind due to noise issues even though there is limited understanding of the actual noise levels that are likely to be produced [14]. With little knowledge of the nature of noise from small wind systems and no standard policy for planning applications, different areas of the UK exhibit inconsistencies regarding granting installation permission [11]. PPS22, the Government's national planning policy statement of renewable energy [15] includes the following statements:

> "Small-scale projects can provide a limited but valuable contribution to overall outputs of renewable energy and to meeting energy needs both locally and nationally. Planning authorities should not therefore reject planning applications simply because the level of output is small."

And:

> "At the local level, planning authorities should set out the criteria that will be applied in assessing applications for planning permission for renewable energy projects."

In order for Renewable UK's small wind system projections to be met, it is essential that clear and consistent guidance for planning applications, siting and installations of small wind is available nationwide, this is currently not the case. A clear understanding of the noise characteristics from small wind systems and who is likely to perceive this noise will help achieve this.

In the case of small and micro turbines there is little work available in the open literature that quantifies the problem. Devine-Wright [9] concluded that much of the existing research examining wind turbine noise has focused on large scale wind turbines in rural environments as well as wind-farms and there is a gap in the body of research for smaller-scale and building integrated wind turbines in built up areas. Also stated in Devine-Wright's conclusions is that no attempt has been made to establish the underlying causes of psychological processes related to the perception of wind turbine noise – and the effect of this noise on individuals' health. The need for an increase in interdisciplinary research was also called for in Devine-Wright's review paper.

	Make and Model	Rated Power (kW)	Wind Speed Range (m/s)	Nominal Rotational Speed (rpm)	Rotor Diameter (m)	Hub Height (m)
Large	Vesta V-90	3000	4-25	16.1	90	105
Small	Evance Iskra	5	3-60	200	5.4	12/15
Micro	Ampair A600	0.6	3-Survival	300-1000	1.7	Varies

Table 1.1.1: Table showing property comparisons of different turbine sizes

It is not sufficient to apply research for large turbines to small wind systems. This is because characteristics are very different between different sized turbines, Table 1.1.1 describes examples of the various characteristics for a particular model of a turbine of each size and also shows the major differences between large scale turbines compared to micro and small. In Table 1.1.1, it is shown that micro turbines can rotate 75 times faster than large turbines and for small turbines rotation speed can be 12 times faster. This means that the noise mechanisms associated with large turbines may not be associated with small wind systems or they may manifest themselves as another sound at a different frequency. A discussion of the different noise mechanisms associated with wind turbines is provided in Section 1.2 of the Thesis. Small wind systems are also generally sited closer to where people live and work, often in highly populated areas and so potentially create more noise issues for individuals living nearby.

This research seeks to investigate the noise from small and micro wind turbines, who is likely to be affected by the noise, why this is the case and the potential impacts the noise will have on these individuals.

1.1.1 Objectives of the Research

The general aim of this research is to better understand the noise levels generated by small and micro wind turbines, the characteristics of the noise and people's reactions to this noise. The research fills a gap in the literature, which is currently principally based on large scale turbines in rural environments rather than small wind systems in built up areas. The research is interdisciplinary and will aim to create two models, incorporating the subject areas of Engineering, to measure and characterise the noise from small wind systems and to investigate the flow around aerofoil blade sections which is directly related to noise; and Psychology, to identify the type of people who are most likely to perceive small wind system noise and the effect this has on them.

There are three main objectives of the research:

1. **Noise Measurement -** to measure and characterise the noise levels and noise mechanisms at real small and micro wind turbine installations to estimate the turbine noise levels over and above the background noise at each installation, including a spectral analysis and assessment of the noise attenuation.

2. **Public Perceptions of Noise -** to survey individuals living close to small and micro wind turbine installations to investigate the level and type of noise perceived and to link this to individuals' attitudes towards wind turbines and personality and temperamental characteristics. To confirm the results with an experimental recordings study and compare the results of the two studies to the results of the noise measurements and noise modelling.

3. **Noise Modelling -** to identify the noise mechanisms associated with small wind systems by modelling the turbulent flow and hence noise around a turbine blade to compare to the noise measurement results.

The research will then provide the following benefits:

- A better understanding of the real levels of small wind system noise experienced by individuals living and working near where they are sited;
- Hence information to planners and policy makers for better guidance regarding siting of turbines;
- An accessible method to estimate the noise issues associated with small wind aerofoils for small wind system manufacturers;
- Information about the type of individuals likely to perceive small wind system noise and the effect this will have on their general health;
- Hence guidance on how information about small wind systems can be better relayed to the general public based on those who are likely to oppose installations.

1.1.2 Structure of the Thesis

The Thesis is divided into five Chapters. The first and current Chapter gives an introduction to the research and the overall objectives of the research. This is followed by an explanation of the noise mechanisms associated with wind turbines in Section 1.2 of Chapter 1; this is relevant to each of the three key methods involved in the research. In Section 1.3 of Chapter 1, the small and micro turbine types and the turbine installations used for the research are given.

Chapters 2, 3 and 4 contain the work carried out for the three key methods adopted to achieve the objectives of the research. These include the work associated with the noise measurement, the psychological and health impacts of small wind systems and noise modelling areas respectively.

The structure for each of the three main Chapters of the Thesis is the same:

1. The work for each of the three methods is put into context with the published literature via a specific literature survey;
2. An outline of the methodology employed for each of the three methods;
3. Analyses and discussion of results of each of the three key methods;
4. A brief conclusion of the results of each of the three key methods including recommendations for future work.

In the final Chapter, Chapter 5 of the Thesis, the conclusions of the research are given. Comparisons are made between the three methods of the research and recommendations for future work are given based on the key findings and conclusions of the work as a whole.

1.2 Wind Turbine Noise Mechanisms

A knowledge of the noise mechanisms associated with wind turbines is essential for each of the three key methods of the research and they have been well documented in the literature [16, 17, 18, 19]. In this Section of the Thesis an outline of aerodynamic noise mechanisms aerofoils generate, as well as other noise mechanisms wind turbines make will be given, with an overview of the most important noise mechanisms for wind turbines.

Noise from wind turbines can be categorised into two different types:

- Mechanical Noise
- Aerodynamic Noise

Mechanical noise originates from the working mechanisms within the turbine itself, such as gearboxes and generators. It is transmitted from the moving parts through the structure of the turbine and is then radiated from the surfaces of the turbine, such as the tower, the nacelle and the turbine blades. Mechanical noise is generally not a problem for small wind systems as they rarely have any mechanical equipment in their design and any mechanical noise that is present has been eliminated or reduced below the level of aerodynamic noise with improvements in mechanical design. Occasionally mechanical noise can be heard from small or micro wind turbines when there are faults, such as a bearing failure, or from the electro-mechanical parts if they are sited near the turbine as they often are for small wind turbines.

Aerodynamic noise is generated by a wind turbine either due to the interaction of its blades (aerofoils) with the natural atmospheric turbulence, due to turbulence within the boundary layer of the aerofoil itself ("self-noise") or due to unsteady loading and interaction with the wind turbine tower. There are several mechanisms of aerodynamic noise due to both atmospheric turbulence and "self-noise"; these mechanisms are discussed below. Aerodynamic noise can never be completely eliminated from a wind turbine as it is inherent to the way in which a wind turbine harnesses its power from the wind. However with careful design it can be substantially reduced to acceptable levels.

1.2.1 Inflow Turbulence Noise

A diagrammatic representation of inflow turbulence noise can be seen in Figure 1.2.3. The aerofoil encounters turbulent eddies present in unsteady atmospheric conditions. This effectively alters the angle of attack of the aerofoil and causes an unsteady loading on the blade. The frequency and amplitude of the noise generated is dependant on the size of the eddies. If the eddies are much greater than the aerofoil chord length then there is a fluctuation in blade loading and the blade is considered to be acoustically compact, the noise is of a dipole (see Appendix A for a description of a dipole sound source) nature and at a low frequency. If the turbulent eddies are smaller than the chord length, only local pressure fluctuations are experienced by the aerofoil and as a result, the noise will be of a higher frequency. Inflow turbulence noise contributes to broadband noise. It is very difficult to quantify mathematically because the atmospheric boundary layer is made up of random flow patterns which change constantly. Therefore, it is very difficult to predict how the natural atmospheric turbulence will behave and consequently quantify inflow turbulence noise.

1.2.2 Aerofoil "Self-Noise"

1.2.2.1 Tip Vortex Formation Noise

A diagrammatic representation of tip vortex formation noise is shown in Figure 1.2.1.

The difference in pressure on the suction side compared to the pressure side of the aerofoil causes an interaction of the two flows at the tip. Vortices are created which then propagate away from the aerofoil and interact with the trailing edge resulting in noise. In addition to this, local flow speeds at the tip are very high compared with speeds close to the hub and sound power is highly dependent of local flow velocities. This means that noise sources radiated at the tip will have a higher power than those radiated from close to the hub and will contribute more to the overall noise levels from a turbine. Indeed Brooks, Pope and Marcolini Brooks et al. [19] derived an expression to predict tip vortex noise using Mach number to the 5th power. Tip vortex formation noise is of broadband nature occurring at the high end of the frequency spectrum.

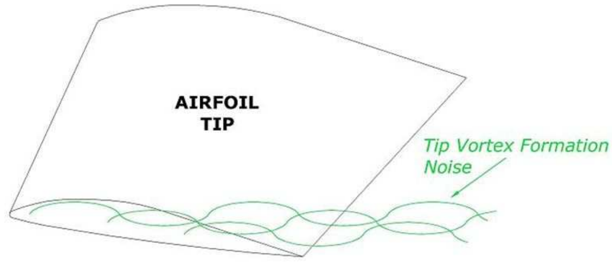

Figure 1.2.1: Aerofoil Tip Vortex Formation Noise Mechanism

1.2.2.2 Separation Stall Noise

A diagrammatic representation of separation stall noise is shown in Figure 1.2.2.

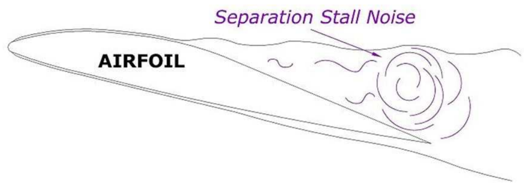

Figure 1.2.2: Separation Stall Noise Mechanism

Separation stall occurs when the aerofoil is at or past the limiting angle of attack. The boundary layer separates from the surface causing detached and unsteady flow. The point of separation along the chord depends on the angle of attack. Mildly separated stall causes sound radiation from the trailing edge but deep stall causes noise to radiate from the whole chord. Separation stall noise is of a broadband nature.

1.2.2.3 Laminar Boundary Layer Vortex Shedding Noise

A diagrammatic representation of laminar boundary layer vortex shedding noise is shown in Figure 1.2.3. At low Reynolds numbers of flow there is a laminar boundary layer which extends to the trailing edge. Instabilities in the laminar boundary layer can cause separation bubbles which may then form a vortex that propagates along the length of the chord eventually interacting with the trailing edge causing a noise source. Laminar boundary layer vortex shedding noise is tonal in nature at the high end of the frequency spectrum. The exact frequency of the tone is a function of the chord length and air velocity over the aerofoil and hence the Reynolds number of the flow.

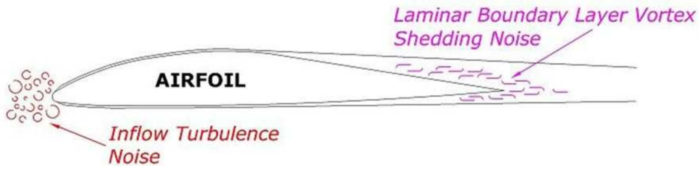

Figure 1.2.3: Inflow Turbulence and Laminar Boundary Layer Vortex Shedding Noise Mechanism

1.2.2.4 Trailing Edge Noise

There are two types of trailing edge noise; these are noise due to the bluntness of the trailing edge of an aerofoil, and noise due to turbulence within the boundary layer interacting with the trailing edge. Both are represented in Figure 1.2.4.

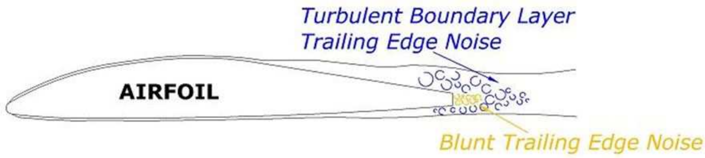

Figure 1.2.4: Turbulent Boundary Layer Trailing edge Noise and Blunt Trailing Edge Noise Mechanism

Blunt trailing edge noise is due to vortex shedding at the blunt edge. As long as the trailing edge bluntness is large compared to the boundary layer displacement thickness of the flow there will be a distinct secondary hump in the frequency spectrum showing a tonal noise of dipole nature. Sharpening the edge increases the peak frequency of the tone. Trailing edge bluntness noise can be avoided with careful design and by avoiding having a thick trailing edge.

Turbulent boundary layer trailing edge noise is due to the turbulent eddies present in the turbulent boundary layer of the aerofoil, these eddies are normally an inefficient sound source but when they encounter a sharp edge such as the trailing edge of an aerofoil they become much more efficient, thus producing a noise source emitted from the trailing edge and into the wake. Turbulent boundary layer trailing edge noise is of broadband nature.

1.2.3 Blade-Tower Interaction Noise

Atmospheric air flow is disturbed around the tower of a wind turbine both upstream and downstream (the flow is decelerated upstream of the tower and there is a wake downstream due to flow separation around the tower). When the blades of the wind turbine rotor encounter this disturbed flow, there is a rapid change in blade loading causing a dipole type noise source of low frequency heard as a thumping sound when each blade of the rotor passes the tower, the frequency of the noise is also dependant on the blade passing frequency. Blade-tower interaction noise is likely to be less important for small wind systems than large scale wind turbines because the towers have a relatively small diameter which disturbs the atmospheric flow less. As the blades on small or micro turbines are rotating at much faster rates, the low frequency thumping sound may be present as a much higher frequency noise source.

1.2.4 Vibration

Another source of noise, which has the potential to cause annoyance from micro and small turbines is vibrations present when the rotor is spinning. Smaller turbines can rotate at very high speeds, (as much as 1250rpm) so have the potential to cause significant vibrations. Many micro turbines are mounted directly onto the structure for which they are supplying energy; this could be a domestic dwelling or business and often the standard of mounting is insufficient to dampen out all vibrations from the rotating turbine. This means they are carried easily through the solid structure of the building and can be heard or felt as a continuous humming sound. This can also be a problem for micro or small turbines mounted on a mast close to a building. Vibration noise can be transmitted through the mast and into the building via the foundations.

1.2.5 Important Noise Mechanisms for Wind Turbines

Although all wind turbine noise mechanisms described in Section 1.2 can contribute to the overall noise levels from a wind turbine when it is operating, not all of them carry the same significance and therefore some can be considered of minor importance. Aerofoil "self-noise" mechanisms, if fully understood can either be reduced or eliminated. Laminar boundary layer vortex shedding noise and blunt trailing edge noise are of a tonal nature and can be removed with careful design [17].

Inflow turbulence is particularly hard to predict as it depends on many different factors which cause instabilities and turbulence in the atmosphere. These include buoyancy effects and interaction of the flow with surfaces due to shear. These factors are hard to measure and reproduce. Inflow turbulence is not yet fully understood but it is thought to be a major contributor to aerodynamic noise up to about 1000Hz [17] heard as a 'swishing' or 'swooshing' sound for large scale turbines. This frequency may be higher for small and micro turbines. The aerofoil leading edge and overall shape plays an important role in the generation of inflow turbulence noise [20] [21]. Turbulent boundary layer trailing edge noise is also perceived as a 'swishing' or 'swooshing' sound due to its broadband nature and the peak frequency associated with it lies in the 500-1500Hz for large scale turbines, again, this frequency may be higher for small and micro turbines. Trailing edge noise will provide a high contribution to the overall sound levels in the high frequency ranges provided the flow is attached [17].

There is some controversy surrounding the importance of tip noise and early research did not consider the contribution of tip noise to the overall noise levels, the only early publication addressing tip noise is that of Brooks, Pope and Marcolini [19] who suggested that tip noise could add an extra 1-2dB to the overall noise levels.

Separation stall noise is only an important contributing noise mechanism if the angle of attack of the aerofoil is high. Some wind turbines are stall regulated. This means that when wind speeds increase and the rotor speed is held constant, the flow angles over the blade sections increase and the flow becomes increasing separated to control the power generation of the wind turbine. For this type of turbine, separation stall noise can provide a substantial contribution to the overall noise levels. In some circumstances for deep stall noise levels from the turbine can be increased by up to 10dB [19].

Laminar boundary layer noise only occurs at low local Reynolds numbers. This is because if the flow around an aerofoil becomes sufficiently high the boundary layer will become turbulent. For modern, large turbines, laminar boundary layer noise is of minor importance as Reynolds numbers are high; however, it may be a contributing source to the overall noise levels of small wind systems as local flow speeds could be slower. Further investigation is needed for turbines of this size. One solution to laminar boundary layer noise is to trip the boundary layer at some distance along the chord from the leading edge of an aerofoil to change the boundary layer to turbulent flow.

Blunt trailing edge noise can be avoided by sharpening the trailing edge and for this reason it is not considered an important noise mechanism for wind turbine design. As discussed previously low frequency noise due to blade-tower wake interaction is of a lower importance for upwind turbines rather than downwind turbines and blade-tower interaction noise is not expected to provide any significant contribution to the overall noise levels of small wind systems as they are often mounted on masts which have a small diameter which causes little disturbance to the flow. In addition to this, small wind systems can rotate at high speeds, and as blade tower wake interaction noise is related to the blade passing frequency, it is expected that any noise due to this mechanism will manifest itself as a sound at a higher frequency which is likely to sound similar to the other noise sources from a turbine causing less distress to individuals.

The noise mechanisms considered to be most significant in previous research (which is predominantly applied to large wind turbines) are inflow turbulence noise, turbulent boundary layer trailing edge noise [18, 22] and tip noise [23]. It is expected that the same noise mechanisms will be significant for small wind systems, but that they may manifest themselves in different ways. A more detailed discussion of currently available noise prediction models and methods for modelling wind turbine noise can be found in Chapter 4.

A knowledge of noise mechanisms associated with wind turbines is relevant for all aspects of this PhD Thesis. As the way each noise mechanism manifests itself is known as well as the likely sound each mechanism will produce it is possible to use the well documented knowledge in the following ways:

- Each noise mechanism is present at a particular frequency band, either broadband or tonal. By taking measurements of actual turbine noise, it will be possible to identify the likely noise mechanisms associated with the small wind systems investigated by frequency analysis of the data. This part of the research is fully documented in Chapter 2 of the Thesis.
- By asking individuals living close to a small wind system installation which sounds they perceive from the turbine it is possible to identify the noise mechanisms associated with the turbine and

compare these results to noise measurement results. This part of the research is fully documented in Chapter 3 of the Thesis.

- By modelling noise, either directly or by observing turbulence around wind turbine aerofoils it will be possible to identify noise mechanisms from the turbines. These results can then be compared to the noise measurement data and results from the questionnaire data. This part of the research is fully documented in Chapter 4 of the Thesis.

In the following and final Section of this Chapter an outline of the small and micro wind turbine types used for the study as well as the installations where these types of turbines are sited will be given.

1.3 Installation Identification

To facilitate the aims of the research it was important to use real micro and small wind turbine installations for the study. This involved contacting known micro and small turbine installation owners to see if they were interested in participating in the research. A number of individuals and organisations were contacted to participate, selected as close to the Nottingham region as possible or in accessible locations with any manufacturer and type of micro or small turbine installed. Some installations contacted were not interested in participating in the study and others did not respond. Out of the remaining individuals or organisations contacted, it was decided that all installations would be used for the domestic study into the psychological and health impacts of small wind systems. This is because the surveys were sent out by post so it was easy to include all installations, even those inaccessible for measurements. Only seven of the installations were used for the noise measurement part of the study, this was for practical reasons.

Turbine Type	Rated Power (kW)	Rated Rotational Speed (rpm)	Number of Blades	Rotor Diameter (m)	Cut In Speed (m/s)	Cut Out Speed (m/s)	Rated SPL $L_{Wd,8m/s}$ (dBA)	Turbine Code
Small	5 (12m/s)	200	3	5.4	3	60 (Survival)	89.0	S1
Small	12.1 (11m/s)	>150	3	8.5	3.5	70 (Survival)	NA	S2
Micro	0.6 (12.6m/s)	1000	3	1.7	3	NA	89.5	M1
Micro	1.25 (NA)	NA	3	1.75	NA	NA	NA	M2
Micro	0.4 (16.5m/s)	1200	3	1.1	2.6	NA	NA	M3

Table 1.3.1: Turbine types included in the research

Table 1.3.1, shows the characteristics of the small and micro turbine types included in the study, the turbine types are coded for easy reference throughout the Thesis. Micro turbines of type M1 are installed at four of the installations willing to participate in the study, these installations were used for taking noise measurements. Small turbines of type S1 are installed at three of the installations participating in the study, these installation were also used for noise measurements. An outline of all thirteen installations willing to participate in the research is given in Table 1.3.2.

Letter Code	Location Code	Turbine Type	Location Type	Level of Background Noise
a	BGS	S1	Headquarters	Low
b	RUSH	S1	Country Park	Very Low
c	WBS	S1	School	Medium
d	TOW	M1	Social Housing	Medium
e	LILL	M1	Residential	Very High
f	HILL	M1	Public Gardens	Low
g	TAN	M1	Sheltered Housing for Elderly	High
h	WETH	S1	Residential	Low
i	CPR	S2	Park and Ride	High
j	SUM	M2	Residential	Medium
k	NORT	M2	Business Offices	Medium
l	DWB	M3	Residential	High
m	DELT	M3	Residential	High

Table 1.3.2: List of turbine installation codes used for the research

For more details of the three key methods used to achieve the aims of the research, see the relevant Chapters of the Thesis, Chapter 2 for Noise Measurement, Chapter 3 for the Psychological and Health Impact studies and Chapter 4 for the Noise Modelling. In each of the Chapters more details will be given regarding which turbine types and installations were used for each part of the study.

In the next and first of the three main Chapters, details of the noise measurement part of the study will be given, including a full literature review, methodology, results with discussion and a conclusion of the work, including recommendations.

Chapter 2

Noise Measurement

There is little understanding of the characteristics of noise from small wind systems. An introduction to the research and drivers for the current research has been given in Chapter 1. It is important to measure the noise attributed to small wind systems in order to have an idea of the level of noise experienced at real turbine installations and the noise mechanisms associated with measured frequency spectra (see Section 1.2 for a review of aerofoil noise mechanisms). An investigation of the attenuation of the sound at the key frequencies associated with small wind systems should also be carried out to get an overall picture of whether small wind system noise is a problem in built up areas. Small and micro wind turbine manufacturers must quantify the sound power level their turbines emit in order to get micro-certification but this sound power level does not account for the type of noises the turbines make and the actual noise experienced at different installations.

This Chapter of the research serves to achieve the noise measurement objectives of the research:

> To measure and characterise the noise levels and noise mechanisms at real small and micro wind turbine installations to estimate the turbine noise levels over and above the background noise at each installation, including a spectral analysis and assessment of the noise attenuation.

In this Chapter, methods for measuring noise available in the literature will be reviewed including standards relevant for the measurement and quantification of noise from small and micro wind turbines. The methodology for the chosen process will also be given. Finally a full analysis of the results and conclusions based on the findings will be given. Recommendation for future work will be included with the conclusions.

Noise Measurement Nomenclature

A	attenuation (dB)
D_C	directivity correction (dB)
f	frequency (Hz)
F	fast weighted
L_{eq}	equivalent continuous sound pressure level (dB)
L_p	sound pressure level (dB)
L_W	sound power level (dB)
LA_{eq}	A-weighted equivalent sound pressure level (dBA)
$LA(Inst)$	instantaneous A-weighted sound pressure level (dBA)
LA_{90}	A-weighted background noise (dBA)
LL_{eq}	L-weighted equivalent continuous sound pressure level (dB)
n	number of samples
p_A	instantaneous A-weighted sound pressure level (Pa)
p_f	instantaneous octave band sound pressure level (Pa)
p_i	initial sound pressure amplitude (Pa)
p_t	sound pressure amplitude (Pa)
p_0	reference sound pressure level (Pa)
s	attenuation distance (m)
S	wind speed dependence (dB)
SPL	sound pressure level (dB)
T	specified time interval (s)
α	pure tone attenuation coefficient (dB/m)

2.1 Noise Measurement Literature Review

An understanding of the work available in the literature is essential to develop a clear methodology for measuring and quantifying noise from small wind systems, including the propagation of this noise. It is unlikely that one method will be fully appropriate for the current research but a combination of several methods are likely to be adapted to suit achieving the objectives of this research. A knowledge of the research literature available is also necessary to help give an understanding of the noise mechanisms associated with wind turbines, both qualitatively and quantitatively.

In this Section of the Thesis, an outline of the available literature relating to noise measurement will be given. The standards for measuring wind turbine noise will be outlined, this will also include standards not specifically related to wind turbine noise but which are applicable to noise from small wind systems in the environment, as well as the propagation of this noise. The research available in the literature will also be examined to get an indication of the noise mechanisms associated with wind turbines and to identify methods for measuring the noise as developed and used by others. These methods will be assessed for their applicability to small wind systems.

2.1.1 Noise Testing Standards and Regulations

Standards and legislation exist for the measurement, rating, assessment and limiting of wind turbine noise but at present the large majority of these are designed for large scale wind turbines and wind farms, not small wind systems. Much of the guidance also incorporates standards dealing with industrial noise and the propagation of sound outdoors. In 2009, the microgeneration certification scheme [24] was introduced for micro and small wind turbines. This scheme requires turbine noise to be rated according to several measurement standards, including the BWEA Small Wind Turbine Performance and Safety Standard [25], which is to date the only standard directly related to small wind systems.

It is important to have an understanding of the standards associated with wind turbine noise in terms of this research because the methods developed in the standards could be adapted and adopted for the current research and should not be ignored. Publications relating to planning, safety and assessment that are applicable to wind turbine noise are outlined in this Section. For full details of each the reader is referred to the original texts.

2.1.1.1 BS EN 61400-11:2003 - Wind Turbine Generator Systems Acoustic Noise Measurement Techniques

The document BS EN 61400-11:2003 BSE [26] is a set of standards to include all aspects of acoustic noise measurement techniques for large scale individual turbines. The original text was developed in the mid 1980s and the current document is a revised version of this. It is the nationally accepted standard for assessing, testing and reporting wind turbine noise with the aim of allowing comparisons between turbines. The standard includes a number of data reduction methods to assess the noise emitted from the turbine, taking into account corrections such as those for background noise and is designed to give noise levels over a full range of wind speeds.

Noise measurements are made using a microphone board where the microphone is pointing towards the turbine at a reference distance from the hub which is related to rotor diameter and hub height. The microphone board should be flush with the ground (setup diagrams are shown in Figures 2.1.1, 2.1.3 and 2.1.2, reproduced from [26]). Additional measurements can be made at three other locations around the turbine to determine the directionality of the noise. At least 30 $LAeq$[1] measurements should be made for each centre frequency from 50Hz to 10kHz (measurements in one third octave bands[2]) and 30 measurements of background noise should also be made immediately before and after this. This must be carried out at a range of wind speeds from 6-10m/s. Wind speed measurements should be

[1] The **LAeq** is the equivalent continuous A-weighted sound level and is defined as the equivalent continuous sound which would contain the same sound energy as a varying sound over time, i.e. the average sound level over the measurement period. See equation 2.1.2 in Section 2.1.1.7 and equation 2.3.1 in Section 2.3.1 for mathematical descriptions of the $LAeq$. A-weighted sound levels are sounds corrected to the human hearing response by cutting off the low and high frequencies that the average human ear cannot hear. See Appendix B for A-weighting values.

[2] **Octave bands** have been developed to split the frequency spectrum into a range of discreet frequency bands. An octave band splits the spectrum into 10 bands and each centre frequency is twice the centre frequency of the previous band. When each octave band is split into three, it is called a third octave band. Third octave bands give a more detailed description of the sound. See Appendix B for the centre frequency of each third octave band.

made with an anemometer located on a mast between 10m and hub height and the equipment should have the capability of taking time averaged data in synchronisation with the sound level measurements.

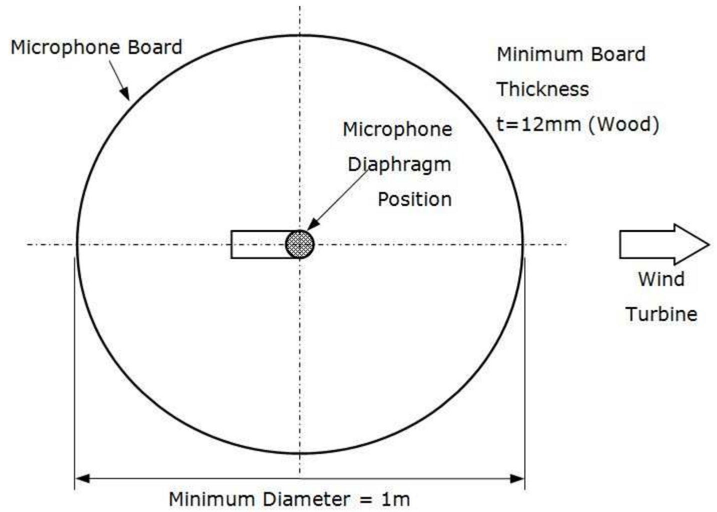

Figure 2.1.1: Plan View of Microphone Board Mounting

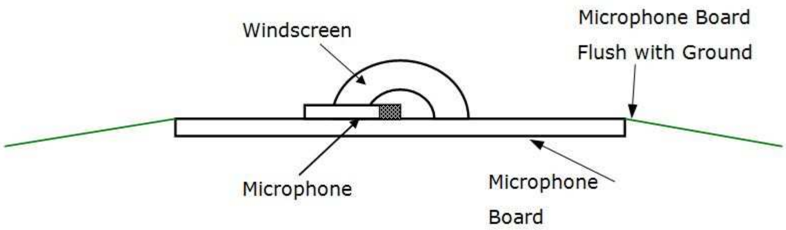

Figure 2.1.2: Cross Section of Microphone Board Mounting

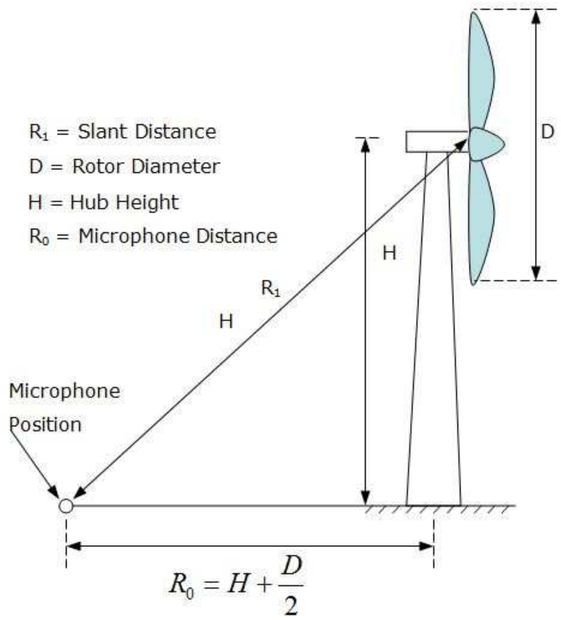

Figure 2.1.3: Microphone Board Distance from Turbine

The standard requires measurements that are complex and time consuming, equating to a high cost of specialist expertise and instrumentation. Acoustic and wind speed data capture and analysis are required simultaneously and there are tight tolerances on procedure, for example regarding the number of data points required, mast positions and number of measurements. Small wind systems tend to be dynamic in yaw so the standard would be very difficult to implement. Vick and Clark [27] identified that the BS EN 61400-11 standards do not apply well for small wind turbines because the standard requires a minimum averaging period of 1 minute for data collection. The rotor speed for the majority of small wind systems is extremely variable over a 1 minute period so collection of data as required by BS EN 61400-11 is difficult. In addition to this, 1 minute averaged data is required over the full range of wind speeds. These issues for small wind cause a large amount of scatter when plotting data collected. Vick suggests the use of the rotor tip speed as the independent variable instead of the wind speed when evaluating sound power levels from small wind systems. De Brujin et al. [28] also identified that rotor rotation speed is a more important parameter than the wind velocity when considering radiated noise. Because of the issues of applying the BS EN 61400-11 for small wind systems, adapted methodologies are needed for the measurement and assessment of noise from small wind systems. The set of standards are fit for the purpose which they were designed for (i.e. large scale turbines) but the exact procedure is not appropriate due to the nature of the turbine installations included in the study. The scope is also limited to the resources of the project.

2.1.1.2 ETSU-R-97 – The Assessment and Rating of Noise from Wind Farms

In August 1993, the Department of Trade and Industry (DTI) facilitated the establishment of a working group on noise from large scale wind turbines comprising experts in the environmental assessment of noise from wind turbines. The objectives of the working group were as follows:

- To review recent experience in the field of wind turbine noise.
- To define a framework that can be used to measure and rate the noise from wind turbines.
- To provide indicative noise levels thought to offer a reasonable degree of protection to wind farm neighbours and encourage best practice in turbine design and wind farm siting and layout.
- To encourage widespread adoption of the Working Group's recommendations.

The ETSU-R-97 report [29] describes the findings and recommendations of the working group, which are intended to serve as an informative guide to assessing the environmental impact of the noise from wind turbines.

The report includes:

- A review of current practice and guidance regarding wind farm noise
- A survey of public reactions related to noise from wind farms

- Current regulations on allowed noise limits from wind farms
- Recommended methods for the monitoring of noise from wind farms
- Details on the planning obligation

Planning Policy Statement 22 – "Renewable Energy" was published by the Office of the Deputy Prime Minister (ODPM), at present the Department of Communities and Local Government, in 2004 ODP [15]. The policies in the statement were designed to be taken into account by regional planning bodies in the preparation of regional spatial strategies and by local planning authorities in the preparation of local development documents. It is stated that they could also be used as material for decisions on individual planning applications.

The statement says:

> "Renewable technologies may generate small increases in noise levels (such as aerodynamic noise from wind turbines) and that local authorities should ensure that renewable energy developments have been located and designed in such a way to minimise increases in ambient noise levels."

The statement also recommends the use of ETSU-R-97 to assess and rate noise from wind energy development.

Like BS EN 61400-11, ETSU-R-97 does not apply well to small wind systems and is intended for assessing the noise from wind farms. Since the report in 1997 it has been recognised that there have been significant advancements in wind turbine design and technology and within the report it is suggested that a review should be carried out two years after the publication date, however, this has not yet occurred.

2.1.1.3 MCS 006 Product Certification Scheme Requirements: Micro and Small Wind Turbines

The MCS 006 [24] document was prepared by the MCS Working Group 3 "Micro and Small Wind Systems" and was approved by the Steering Group of the Microgeneration Certification Scheme (MCS). The document is designed to identify the evaluation and assessment requirements and practices for the purposes of certification and listing of small wind systems up to 50kW rated power (at 11.0 m/s wind speeds). The small wind system undergoing assessment for certification must meet and continue to meet the requirements of the BWEA Small Wind Performance and Safety Standard as outlined in Section 2.1.1.4 as verified by an independent body or third party. A certificate is then awarded to the small wind system once compliance with the MCS 006 document requirements have been met. In addition to the BWEA Small Wind Performance and Safety Standard, requirements include MCS 010 "Generic Factory Production Control Requirements", and MCS 011 'Testing acceptance criteria'. Any individual wishing to take advantage of the Feed-in-Tariffs (FITs) currently being offered by the government must install an MCS approved small wind system to benefit.

2.1.1.4 BWEA Small Wind Performance and Safety Standard

The BWEA "Small Wind Performance and Safety Standard" [25] published in 2008 contains elements from BS EN 61400-11:2003 but is much more fit for purpose for small wind systems. The standard was created by the small wind turbine industry, scientists, state officials and consumers to provide consumers with realistic and comparable performance rating and an assurance the small wind turbine products certified to this standard have been engineered to carefully meet considered standards for safety and operation. The performance and safety standard provides a method for the evaluation of wind turbine systems in terms of safety, reliability, power performance and acoustic characteristics.

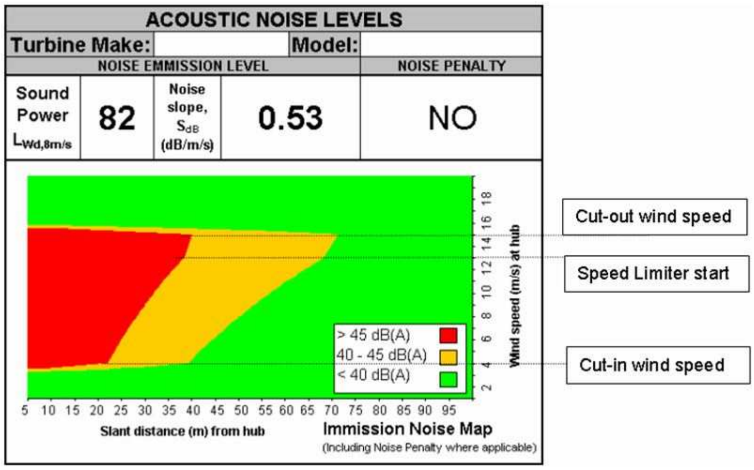

Figure 2.1.4: Example of a Small Wind Turbine Noise Label [25]

The acoustic noise from a small wind turbine shall be expressed as the following (summarised in a Noise Label, see Figure 2.1.4 for an example):

- Declared Apparent Emission Sound Power Level at wind speed 8m/s (L_W,8m/s)
- Wind Speed Dependence (S, dB)
- Immission[3] Sound Pressure Level at 60m (L_p,60m)
- Immission Sound Pressure Level at 25m (L_p,25m)
- Immission Noise Map
- Character of the turbine noise

The principles from BS EN 61400-11:2003 are applied to micro wind turbines and it takes into account the unique characteristics of micro wind turbines which are as follows:

- Higher and variable rotational speeds
- Dynamic in yaw and hence have a fast response to changes in the wind direction

[3] The amount of sound introduced at a receiver due to one or more sound sources

- Wider variety of geometries and modes of operation

The primary differences between BS EN 61400-11:2003 and the BWEA standards are the following:

- Relaxed anemometer mast position
- A downwind measurement position is adopted with no crosswind points
- A 1/3 octave band type character assessment is used and 1/3rd octave spectra are described in analysis
- The measurement averaging periods are a function of the turbine geometry and typically 4 times the rotor diameter ($t = 4D$ where D is the rotor diameter expressed in metres and the unit of t is seconds)

The methodology for certifying noise from small wind systems as used in the BWEA Small Wind Performance and Safety Standards is most appropriate for this research as the strict method from BS EN 61400-11:2003 has been adapted to be much more appropriate for small wind systems. Elements from the Performance and Safety standards method will be used for the current research. The methodology adopted for this research is given in Section 2.2.

2.1.1.5 BS 4142:1997 Method for rating industrial noise affecting mixed residential and industrial areas

BS 4142:1997 [30] describes methods for determining, at the outside of a building:

1. Noise levels from factories, or industrial premises, or fixed installations, or sources of an industrial nature in commercial premises and whether this noise is likely to cause complaints from individuals living in the building due to the industrial noise.
2. Background noise levels. The standard is not applicable when the background noise is below 30dB or the noise source sound power level is below 35dB.

Although the standard is not directly related to wind turbines, small wind systems could be described as a new noise source likely to cause a nuisance. This standard is not designed for assessing the sound power level from the noise source in question but to give a rating of the noise source in terms of its potential for nuisance by taking environmental noise levels close to locations where the noise may cause a nuisance. The methods adopted are applicable to the current research because an assessment of how small wind system noise is perceived is required to achieve the objectives of the research.

A brief outline from the standard of how measurements should be made is as follows:

- Microphones used to take measurements should be calibrated before and after measurements.

- Measurement positions should be chosen as close as possible to buildings where nuisance is likely to occur but 3.5m from any reflecting surface. Measurement height is at 1.2m-1.5m above the ground.
- The equivalent continuous A-weighted sound pressure level $LAeq_{,T}$ shall be taken for time interval T with a sound level meter at measurement positions chosen.
- Background sound measurements $LA_{90,T}$ should ideally be taken in the same location as sound levels from the noise source. If this is not possible, then an alternative location should be sought with equivalent background sound levels. Measurement time interval should be long enough to obtain a representative value of the background noise level.
- Take precautions against sound interference such as wind noise by using an appropriate wind screen, or rain noise.
- Report weather conditions.

To determine the specific noise level from the ambient noise by applying one of the following procedures:

- Ambient noise is comprised of the residual noise and the specific noise from the sound source. To minimise the residual noise take measurements when it has subsided to a low level.
- Compensate for the effect of the residual noise by subtracting the corrections from the ambient noise.
- Determine specific noise levels when residual noise is reduced from normal operating periods. If necessary the noise source may be switched on solely for the purpose of measurements.
- Determine the specific noise level by a combination of calculation and measurement.
- Determine the specific noise level by calculations alone.

To determine the background noise levels follow one of the procedures below:

- Take background noise measurements when the noise specific noise source would normally be operating but is not actually operating.
- Take background noise measurements when weather conditions are the same or similar to those when the specific noise source is at normal operation.

Certain acoustical features such as those that contain a discrete continuous tone or those that are impulsive in nature should carry an additional penalty by adding 5dB to the specific noise level to obtain the rating level of the noise source.

To then assess the likelihood of complaints the measured background noise levels should be subtracted from the noise source rating level. If this difference is +10dB or more then complaints are likely, and

+5dB is of marginal significance. Full information on all noise sources and how measurements were taken with final readings must be reported.

Although this standard is not directly related to small wind systems, they could be considered as a new industrial noise source likely to cause a nuisance. The method for assessing whether complaints are likely as outlined in BS4142 could be applied to small wind systems, since they are often sited close to where people live and work.

2.1.1.6 ISO 9613-1:1993 Acoustics attenuation of sound during propagation outdoors. Part 1: Calculation of the absorption of sound by the atmosphere

The ISO 9613 ISO [31, 32] standards are designed for the attenuation of any environmental noise and propagation outdoors and are therefore applicable to small wind system noise when the sound emitted by the turbine is modelled as a point source. Several noise mapping software packages use the ISO 9613 standards to predict the propagation of sound in outdoor environments, taking into account all attenuation effects as described by the standards. One such example of this is CadnaA, which will be used within the current research to indicate how the turbine noise is likely to propagate at each installation included in the study. A knowledge of the ISO 9613 standards is therefore required. The methodology for the noise mapping work will be given in Section 2.2.2 with the results in Section 2.3.3.

The ISO 9613-1 [31] standard provides an analytical method for calculating the attenuation of a sound due to atmospheric absorption in a variety of meteorological conditions. For pure tone sounds tabulated attenuation coefficients are given for the following conditions:

- frequency from 50Hz to 10kHz
- temperature from -20ºC to +50ºC
- relative humidity from 10% to 100%
- pressure of 101,325kPa

Formulae are also provided within the ISO 9613-1 standard for calculating the attenuation coefficient for a wider range of conditions other than those where tabulated values are given. For broadband sounds, where either discrete frequencies are present, no significant frequency components are present or where there is a combination of the two, a method for specifying the attenuation of this sound due to the atmosphere is given. Suggestions are also given within this standard to account for an inhomogeneous atmosphere and how sound attenuation should be handled in this case.

The basic expression for attenuation can then be used to calculate how a pure tone sound pressure has decreased over distance s:

$$p_t = p_i exp(0.1151 \alpha s) \tag{2.1.1}$$

Where, p_t is the sound pressure amplitude (Pa), p_i is the initial sound pressure amplitude (Pa) and α is the pure tone attenuation coefficient (dB/m).

In order to calculate attenuation for a broadband sound source which also has discrete tones present it is suggested in the standard that the frequency spectrum of source sound should be split into separate frequency bands. The attenuation coefficients and hence attenuation (Equation 2.1.1) can then be determined for each frequency band. This method will give the sound frequency spectrum at the receiver.

2.1.1.7 ISO 9613-2:1996 Acoustics attenuation of sound during propagation outdoors. Part 2: General method of calculation

Sound attenuation other than that due to atmospheric conditions is given in ISO 9613-2 [32]. The engineering methods in this standard are used to predict equivalent continuous A-weighted sound pressure levels of environmental noise, calculated as:

$$LA_{eq} = 10log\left\{\frac{\left[\left(\frac{1}{T}\right)\int_0^T p_A^2(t)dt\right]}{p_0^2}\right\} \tag{2.1.2}$$

Where $p_A(t)$ is the instantaneous A-weighted sound pressure level (Pa), p_0 is the reference sound pressure ($20 \times 10^{-6} Pa$) and T is the specified time interval (s).

Equivalent continuous downwind octave band sound pressure levels can be determined as follows:

$$L_{eq(f)}(DW) = 10log\left\{\frac{\left[\left(\frac{1}{T}\right)\int_0^T p_f^2(t)dt\right]}{p_0^2}\right\} \tag{2.1.3}$$

Where Where $p_f(t)$ is the instantaneous octave-band sound pressure downwind (Pa), the subscript (f) represents the nominal mid-band frequency of an octave-band filter.

Specific terms are given for the following physical effects:

- geometrical divergence
- atmospheric absorption
- ground effect
- reflection from surfaces
- screening by obstacles

Additional information is also given in the standard for propagation of sound through housing, foliage and industrial sites. The methods described are applicable for a wide variety of ground point noise sources and environments.

According to the standard, equivalent continuous downwind octave-band sound pressure levels for each point source should be calculated using:

$$L_{eq(f)T}(DW) = L_W + D_C - A \tag{2.1.4}$$

Where L_W is the octave band sound power level (dB), D_C is the directivity correction (dB) and A is the octave-band attenuation (dB) due to the physical effects described above.

$$A = A_{div} + A_{atm} + A_{gr} + A_{bar} + A_{misc} \tag{2.1.5}$$

- A_{div} is the attenuation due to geometrical divergence
- A_{atm} is the attenuation due to atmospheric absorption
- A_{gr} is the attenuation due to ground effects
- A_{bar} is the attenuation due to a barrier
- A_{misc} is the attenuation due to miscellaneous other effects.

Detailed methods for the calculation of the attenuation effect terms are described in the standard.

The propagation of noise is especially important in the case of wind turbines. Guidelines for noise limits as outlined by the World Health Organisation (WHO) [33] which should not be exceeded for planning applications to be accepted. The World Health Organisation has responded to an increase in daily noise exposure in two ways:

- By developing and promoting the concept of noise management
- By drawing up community noise guidelines

The current external maximum noise levels are 55dBA LAeq in the day time and 45dBA LAeq at night (this equates to 30dBA LAeq inside with an open window and taking into account the sound attenuation of the wall at night) to avoid sleep disturbance. There is ongoing discussion on reducing these levels further. These guideline levels are especially an issue when considering small and micro wind turbines as they are often located closer to where people live and work either building or mast mounted. A full understanding of how wind turbine noise will attenuate and propagate using methods such as those from the ISO 9613 standards is key.

The standards and legislation summarised in these Sections provide a very important background knowledge for this study. Elements from the standards will be used for assessing noise from small wind systems and to achieve objectives of the research. The detailed measurements required by BS EN 61400-11:2003 and ETSU-R-97 for rating the sound power levels from large scale wind turbines are not appropriate for the current research. However the more relaxed approach of these methods defined in The BWEA "Small Wind Performance and Safety Standard" would be more appropriate as the methods are adapted from small wind systems. The standards reviewed are not the only methods which should be considered for the current research, a consideration of the research literature available should also be considered to define the best approach of taking noise measurements to achieve the objectives of the research. A detailed literature review of noise measurement and estimation techniques in the available research literature is given in the following Section.

2.1.2 Research in the Literature

The method for measuring environmental noise levels is well established as outlined in the standards and policy documents in Section 2.1.1. Wind turbines are usually rated in terms of their sound power (L_W): BS EN 61400-11:2003 and ETSU-R-97 outline how this should be carried out for large wind turbines where the BWEA Small Wind Turbine Performance and Safety Standard outlines how the sound power should be mapped for small wind systems. Sound power levels are different from environmental noise levels. Environmental noise is the total noise at a receiver location irrespective of its source, whereas the sound power is the total sound emission from a particular sound source. In the case of a small wind system, it is the level of sound only attributable to the turbine separated from the background noise. The portion of noise at a receiver location due to a particular noise source is the sound pressure level (L_P), which will contribute to the overall environmental noise level. For an environment with a wind turbine it will be the total noise at the receiver, including the turbine and other background noise.

As well as the measurement standards for rating sound power from wind turbines, there has been much work in the literature assessing sound power from wind turbines and aerofoils or aerofoil sections. It is important to consider these studies in order to define the methodology for achieving the objectives of this research. The following Sections will summarise existing research in the literature, specifically acoustic measurements from wind turbines, single aerofoils and aerofoil sections and the methods available for doing so.

2.1.2.1 Microphone Board

The standard procedure for the measurement of the total sound power levels from working wind turbines is using a microphone board. This procedure is the same as that outlined in BS EN 61400-11:2003 (Section 2.1.1.1). Several research papers [34, 35, 36] have used a microphone board to measure and assess sound power levels from wind turbines (all sizes and not specifically small wind systems) as well as identifying significant noise mechanisms.

Migliore [35] used the BS EN 61400-11 standard to rigorously measure noise levels from a number of different sized small turbines from 0.4kW to 100kW at wind speeds from 6-10m/s. All requirements set out by the standard including microphone boards size and configuration, and measurement distances were adhered to. When there was sufficient separation between wind turbine noise and background noise the sound power level of each of the turbines was calculated. Three additional microphone boards were used to test directionality. It was found that for the quieter turbines at low wind speeds (where background noise fluctuates readily) and at high wind speeds (where wind noise masks some background and turbine noise) it was difficult to separate out turbine noise from background noise, the need for a quieter testing site was recognised. The tests carried out within this research were rigorous according to test standards. This is because the work was carried out at the National Renewable Energy Laboratory (NREL) where equipment and sufficient secure land use were available. Such facilities are not available for the current research so such rigorous tests will not be possible. Nii [37] also used the BS EN 61400-11 requirements to simulate measuring noise from wind turbines. However Nii wanted to investigate dependency on the ground board size and surrounding ground condition to see how this would affect the measurements taken. It was identified that measurements were more reliable the larger the board as long as bare soil was surrounding the board. Later Nii considered the performance of a vertical microphone board instead of the horizontal version [36]. The idea of the vertical microphone board was to minimise problems due to wind-induced noise, reflected sound waves from building facades and background noise as recommended by BS EN 61400-11. A microphone array was mounted on the board with results compared to free standing microphones. A microphone array is a number of microphones used in a fixed pattern, each measuring the noise at their location. This allows very detailed noise measurements, particularly when considering factors such as directionality. Other researchers have used the vertical board setup to develop a measurement station which could be controlled remotely to assess noise measurements at any site [38] with the intention for the measurement station to be portable so measurements can be easily taken at different distances from the turbine to investigate the effects of ground attenuation and wind direction.

Oerlemans' [34] method was slightly different from Nii's; the purpose of the research was to identify the significant noise mechanisms from a large scale wind turbine with a 58m rotor diameter within a wind farm. The wind turbine had one clean blade, one tripped blade and one untreated blade. Tripping was done using zigzag tape of 0.4mm thickness at 5% chord on both the suction and pressure sides of the blade. The purpose of tripping the blade was to assess the effect of blade roughness on trailing edge noise and to invoke turbulent, separated flow at the point of blade tripping. A microphone ground board was used, but instead of using a single microphone, a microphone array (148 microphones in an elliptical pattern) was mounted on a board with dimensions 15m by 18m. The research found that the majority of blade noise was produced on the downward movement of the blades at the outer part of the blade but not the very tip. The tripped blade emitted the most noise due to separation of the flow. The key mechanisms were therefore broadband trailing edge and separation noise. This research was carried out only for the turbine type tested and further work would be required to verify that the same would be the case for other turbine types.

Jung [39] used elements from BS EN 61400-11 to experimentally identify the characteristics of acoustic emission from each of a 1.5MW and a 660kW upwind wind turbine. In their study, emphasis was put on infra-sound and low frequency sound and it was found that blade-passing-frequency noise was dominant up to 6-7 harmonics in the 1-10Hz frequency range which is in the infrasound range. The findings from this study will not adapt well to small and micro wind turbine cases as they are unlikely to suffer from low frequency and infrasound noise problems as the blade-passing-frequencies are much higher due to the increased rotational speeds and sizes of the turbine rotors.

Each of the three methods adopted have different merits, largely, the ability to achieve detailed sound power level measurements from the wind turbines in question as long as the equipment and facilities are available. Results from the findings have shown that blade passing (unsteady loading) and broadband trailing edge noise are predominant noise sources. However, these findings are for research carried out on large scale turbines and consideration should be taken as to whether these findings would be the same for small wind systems. Although the microphone board method is a well established method for measuring sound power levels from wind turbines, the method does not adapt as well to small wind systems because they are extremely dynamic in yaw hence a ground board location would be difficult to determine. The majority of small wind system installations are in public areas where security of equipment and access is also a key issue. The cost of equipment and monitoring is also a factor in deciding whether the ground board method would be appropriate.

2.1.2.2 Wind Tunnel

Microphone boards and arrays are not only used according to the standards in field studies for whole wind turbines. They are also often used for wind tunnel tests where noise and sound power levels attributed to wind turbine aerofoils are measured. Wind tunnel use is an expensive option and therefore will not be used for the current research. However, a knowledge of the research carried out in using wind tunnel measurements will help to offer more of an insight into the qualitative description of small wind turbine noise. Since the mid-nineties, wind tunnels have been accepted as facilities for investigating wind turbine noise and some of the early noise prediction models used results from aerofoil wind tunnel experiments in order to develop the semi-empirical relationships such as Lowson [16], Brooks et al. [19]. One of the main driving forces for measuring aerofoil noise using wind tunnels was that it was recognised that there was a great need to improve wind turbine noise prediction models. This meant the separate noise mechanisms needed to be studied in more detail with the ability to change local flow conditions to prescribed experimental conditions. It is also possible within a controlled wind tunnel test to manipulate a large number of parameters such as aerofoil angles of attack and turbulence levels.

In the early nineties, two European facilities were set up to study aerodynamic noise from wind turbine aerofoil sections; these were at the University of Oldenburg in Germany and at NLR (National Aerospace Laboratory) in the Netherlands [17]. Both set-ups used a microphone array to assess the noise from different tip sections and 2-D blade sections respectively. It is recognised that separating out background noise from aerodynamic noise from the aerofoil sections can be a problem due to the noise from the wind tunnel itself. This is the case when the sound levels from the aerofoil are of the same or lower magnitude as the sound levels due to the fan or propeller of the wind tunnel. Separation of the two noise sources is also a problem when they both fall within the same frequency range. It is possible to separate out the background noise and there are methods to do this such as changing the positioning of the microphone array. Use of an anechoic wind tunnel is also possible when noise from a wind tunnel's fan is likely to be an issue. An anechoic wind tunnel is one where noise reflections are minimised and background noise due to the wind tunnel is reduced within a given frequency range. However, anechoic wind tunnels are expensive and are outside the capabilities of the current research.

Migliore and Oerlemans [40] used the anechoic wind tunnel and microphone array approach to measure the aero-acoustics of seven aerofoils intended for small wind turbines at low Reynolds numbers. The purpose of the research was to identify noise mechanisms associated with small aerofoils. The NACA 0012 aerofoil profile was also tested to act as a benchmark for data comparisons. A large number of high quality data were obtained from the tests and it was found that broadband trailing edge noise was dominant and that laminar boundary layer vortex shedding noise creates pure tones. It was also found that tripping the blades with zigzag tape of width equal to 5% chord over the entire model span at 2% and 5% chord on the suction and pressure sides respectively eliminated the tonal noise, as well as reducing the broadband noise levels. This is because tripping the blade invoked a turbulent boundary layer and eliminated the tonal noise associated with laminar boundary layer flow. In highly turbulent conditions, inflow turbulence noise became a dominant noise source. Cho [41] also took advantage of the wind tunnel and microphone array capabilities to take noise measurements, however an anechoic wind tunnel was not used and a 12% scale wind turbine rotating at 600rpm was tested instead of a single aerofoil section. The 12% scale model represents well the size of an actual micro wind turbine as being investigated in the current research. Results from the tests confirmed that aerodynamic noise associated with the wind turbine blades was significant within the 1kHz to 7kHz frequency range. After analysis of the noise contours, it was seen that the higher the frequency of the sound the further towards the tip of the blade the sound emanates from.

2.1.2.3 Flow Visualisation

Aero-acoustic analysis can be performed within a wind tunnel without the use of a microphone array but with flow visualisation. It is not possible to give absolute sound power values for wind turbine noise using this method but it is feasible to identify areas of the aerofoil that are likely to suffer from high noise by looking at the turbulence and vortices generated and associated with the noise mechanisms due to turbulence documented within the literature [19, 17]. It is also possible to make comparisons between aerofoils to identify which might suffer from the most noise. Measurements can also be taken for whole wind turbines where they have been scaled to fit the wind tunnel.

There are several methods for flow visualisation and the most common are:

- Surface flow visualisation - the surface in question can be coated with a thin film of material. When the flow interacts with the material a pattern can be observed on the surface of the body [42]. The most common types of surface visualisation are:

  - Surface tufts - a flexible material such as a thin fluorescent nylon monofilament is attached to the surface of the body. The tufts then align themselves with the local surface flow.
  - Oil film - the surface of the body is coated with a thin film consisting of an oil such as kerosene or light diesel mixed with a finely powdered pigment such as fluorescent pigment which can then be illuminated with a UV light source.
  - Shear-sensitive liquid crystal coating - used to identify surface flow separation and reattachment, transition and for measuring the continuous shear-stress vector distribution over an aerodynamic surface. Under aerodynamic shear, the liquid crystal coating selectively scatters incident white light as unique colours of visible light at unique orientations. The process is reversible and continuous. The colour change can be recorded using standard imaging equipment facing specific orientations compared to the flow where qualitative data are required. If more specific quantitative data are required, more advanced equipment is needed [43]. This surface visualisation method is preferred to the conventional oil-film method because the liquid crystal film can be kept sufficiently thin to avoid disruption of the flow and has been used by Nakano [44] to study the flow and noise characteristics of a NACA 0018 aerofoil.

- Flow direction and contour visualisation - a foreign body is released into the flow field and swept along with the mean flow in order to visualise the characteristics. The stream-lines, streak-lines and particle paths of the foreign body are captured using photographs or video. These methods are some of the oldest used but can only give an insight into the phenomena occurring in fluid flows and observations must be complemented with quantitative investigations.

  - Dye - a liquid dye is introduced into the flow field either upstream of the body or from small holes on the body surface itself. A well known example of the dye injection method is that of Osborne Reynolds who used the method to demonstrate transition from laminar to turbulent flow in a pipe.
  - Smoke - The principles of smoke visualisation are similar to those for dye visualisation. Smoke plumes are introduced into the flow field parallel to the flow direction, turbulence of the smoke is kept to a minimum to avoid early mixing with the mainstream flow. The smoke injected flow field is then illuminated and recorded with imaging methods such as photography to capture the characteristics of the flow. Research within the literature has used the smoke visualisation method to visualise the flow field around a rotating fan blade [45] and to analyse the turbulent characteristics of the flow around wind turbine rotors [46].

- Particle tracer methods - single foreign particles are introduced into the flow field. The concentration of the particles in the flow is small enough so the individual particles are distinguishable from one another. They are then tracked to show the flow field. Values such as flow velocities can also be determined using this method. Particles could be chosen due to their high visibilities or because there is low slip between particle and fluid flow. The particle should also be as small as possible to flow better and remain neutrally buoyant.

- Helium soap bubbles - helium soap bubbles are introduced into the flow field and are then illuminated and recorded to capture the characteristics of the flow. Research within the available literature has used the helium soap bubbles flow visualisation method to analyse the turbulent characteristics of the flow around wind turbine rotors [46].
- Particle Image Velocimetry (PIV) is commonly used for research within the literature to visualise the whole instantaneous velocity field around an aerofoil [47, 44, 45]. In contrast to the common dye and smoke injection methods and with the advancements in computer imaging technology PIV can provide quantitative results instead of simply qualitative results of flow visualisation. Generally olive oil or alcohol droplets are added to air flow in a wind tunnel as tracer particles. The particles are then illuminated in a plane of the flow using a pulsed laser, the light scattered by the tracer particles is recorded digitally ready for post processing. When post processing, the digital images are split into areas and each area is statistically analysed to determine flow patterns. It is assumed that all tracer particles move with the local flow velocity and the amount of movement is determined by this velocity. PIV is a well established method for investigating boundary layers, separated shear flows and unsteady flows. The capabilities of the PIV method provide a common ground with CFD theoretical modelling of fluid flow phenomena. For a full description of PIV the reader is referred to Raffel, Willert and Kompenhans [48] and Smits and Lim [43].

Some researchers have compared acoustic measurements taken in a wind tunnel with flow visualisation and PIV to verify results and obtain an understanding of the noise mechanisms present [47, 44]. Tomimatsu's comparisons found agreement between vortex shedding observed at the pressure side trailing edge of a symmetrical NACA 0018 aerofoil from the PIV analysis with the frequency of the generated noise. Nakano's [44] PIV analysis and liquid crystal visualisation agreed with Tomimatsu's comparisons. Separation bubbles were identified close to the trailing edge on the pressure surface from the liquid crystal visualisation, the separation bubbles cause a tonal noise due to the boundary layer instabilities with amplification near the trailing edge. The formation of periodic vortex structures near the trailing edge at small angles of attack was identified from the PIV analysis. The frequency of the vortex shedding again agreed with the frequency of the tonal noise present due to the NACA 0018 aerofoil.

The microphone array method with flow visualisation and PIV can be used to identify the velocity field around an aerofoil or full wind turbine as well as the noise sources or actual sound power levels. Nashimoto [45] analysed the flow around a rotating fan blade using PIV and smoke visualisation as well as taking acoustic measurements with a microphone array. In agreement with the analysis of the NACA 0018 aerofoil performed by Nakano, it was found that separation and reattachment of the flow occurred near the leading edge with tip vortices and vortex shedding occurring near the trailing edge. Noise was generated from the vortex structures around the trailing edge.

Flow visualisation is a valid method for identifying the noise mechanisms which are likely to be associated with wind turbine aerofoils and rotors by analysing the turbulence of the flow field. However, the methods do not generally allow quantification of the noise from small wind systems (except when using advanced PIV techniques) or give an insight into how this noise will be experienced at real wind turbine installation environments. This is needed to achieve the objectives of the research. For this reason, and due to the high cost of the methods, flow visualisations will not be used for the current research. However, the literature relating to flow visualisation will serve to offer an insight into the qualitative description of small wind turbine noise.

2.1.3 Summary of Noise Measurement Methods

Most of the standards and regulations outlined in Section 2.1.1 are not directly related to small and micro wind turbines, therefore the methods do not adapt well to quantifying small wind system noise. Only the Micro-Certification Scheme and the Small Wind Performance and Safety Standard are specifically designed for small wind. These standards adapt those for large scale turbines to the small scale to make them more appropriate to the characteristics of small wind systems. The standards alone are not sufficient to achieve the aims and objectives of the research. This is because an understanding of the way small wind system noise propagates and is experienced in the environment is needed. For this reason standards which identify how to rate noise sources in the environments in terms of their nuisance levels have been reviewed. A review of the research literature associated with wind turbine noise measurement and quantification given in Section 2.1.2 has summarised the methods adopted by other researchers and allowed an assessment of the noise levels and mechanisms associated with wind turbine aerofoils and rotors.

Having considered all the methods used in the standards and literature it has been decided that a combination of the methods observed, adapted for the current research, will be adopted. The standards for measuring noise will be followed as closely as possible and the propagation of the noise at each installation will also be assessed using the ISO 9613 standards within a commercial software package. The methodology chosen is designed to achieve the objectives of the research and is detailed fully in Section 2.2.

The specific aims of the noise measurement part of the research are as follows:

- To get an understanding of the actual noise levels at real small wind system installations
- To identify the noise levels which are likely to be experienced by residents living close to small wind systems
- To identify how noise propagates at a number of turbine installations and the Effect this will have on the sound levels from the turbine
- To carry out a frequency analysis of the measurement data to identify the noise mechanisms produced by small wind systems

- To compare measured noise mechanisms from the turbine with modelled noise
- To compare measured noise mechanisms with those reported by residents living near to each turbine installation

In the following Section details of the methodology for the noise measurement work will be given, followed by results of the noise measurement analysis and a conclusion of the results.

2.2 Noise Measurement Methodology

Noise measurements are required within this research as a tool to characterise the noise from small and micro wind turbines and how this noise attenuates. Measurements at each turbine installation will give an understanding of the type of sounds small and micro wind turbines make, how loud the noises are and how they will be experienced by individuals living nearby. Sound maps will show how wind turbine noise will propagate at each turbine installation (see Section 1.3 for the installations included in the research). These two methods combine to give an overall picture of the type of noise experienced from small wind systems at real installations as well as whether the noise is likely to be a problem in built up areas. In this Section of the Thesis, first the methodology for taking environmental noise measurements will be given by identifying the measurement locations at each installation, detailing the monitoring equipment used and the measurement process, followed by the process for transferring the data collected. Finally, the method for creating sound maps at each installation using the software package CadnaA will be given.

2.2.1 Environmental Noise Measurements

To achieve the aims and objectives of the research it is necessary to characterise the noise from small and micro wind turbines. Having reviewed the literature (see Section 2.1) it was decided that environmental noise measurements would be taken at a number of real turbine installations. From the measurement data, wind turbine noise over and above background noise will be identified. It is considered that taking environmental noise measurements will make best use of the time and security constraints and the equipment available. The procedure for taking the environmental noise measurements is outlined in this Section of the Thesis.

2.2.1.1 Measurement Locations

In order to understand the characteristics of noise from micro and small wind turbines, environmental noise measurements were taken at seven turbine installations summarised in Table 1.3.2. Ideally measurements should be taken inside and outside of every single domestic survey respondent's dwelling at a range of wind speeds and conditions, however this was not possible due to time constraints, issues of access and equipment limitations. In addition to this, respondents' experiences of the wind turbine noise are complex and difficult to link to quantitative measures of the exposure alone. The focus of this part of the research is therefore on the characteristics of the sounds from each turbine, making comparisons between turbine types and wind speeds. The seven installations chosen for the environmental noise measurement were selected on the basis of practicality (e.g. accessibility and proximity to Nottingham) and usability (i.e. to extract useful information by comparing data taken at different installations). The decision was made to take measurements at all installations of micro turbine type M1, installations (d), (e), (f) and (g) (see Tables 1.3.1 and 1.3.2 in Section 1.3) and all practical installations of small micro turbine type S1, installations (a), (b) and (c) (see Table 1.3.1 and 1.3.2 in Section 1.3). Environmental measurements were taken at each of the seven installations; measurement locations were determined at each site to adhere as closely as possible to the standards reviewed in Section 2.1. Therefore measurement locations were identified at each site at increasing distances from each turbine and at locations around the turbines. Measurements taken at these locations at each installation will give a good representation of how the noise from each turbine varies between installations, as well as how the noise characteristics vary relative to the turbine location. Maps identifying the turbines and measurement locations for each micro installation are shown in Figure 2.2.2 and for each small installation in Figure 2.2.1. Each turbine and measurement location is coded with two letters and a number to allow ease of discussion of the results in Section 2.3, for example Ma1. The first letter is either an M (measurement location) or a T (turbine), the second letter denotes the installation code from Table 1.3.2 and the number denotes either the measurement location number or the turbine number. Table 2.2.1 shows the slant distance (see Figure 2.1.3 in Section 2.1.1.1 for the definition of slant distance) of each measurement location to the turbine hub at each installation. The installation/turbine code is read vertically and the measurement number read horizontally in the table.

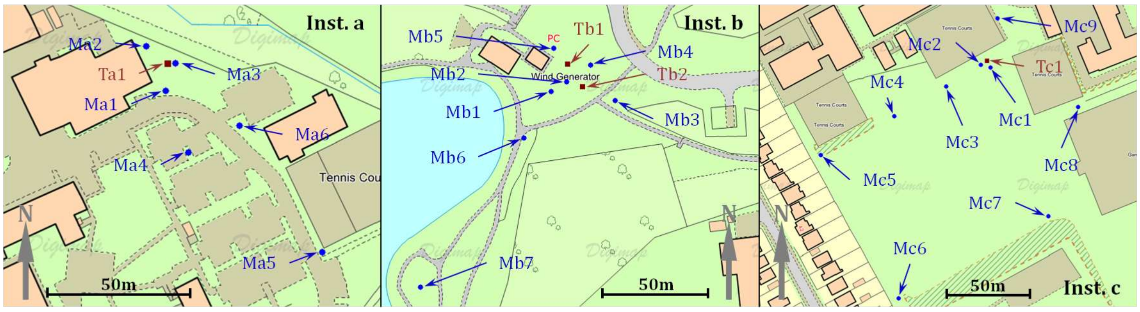

Figure 2.2.1: Maps showing the turbine locations (T) and measurement locations (M) at each small turbine installation

Figure 2.2.2: Maps showing the turbine locations (T) and measurement locations (M) at each micro turbine installation

M T	1 (m)	2 (m)	3 (m)	4 (m)	5 (m)	6 (m)	7 (m)	8 (m)	9 (m)
a1	17	17	13	36	85	37	-	-	-
b1	27	17	27	16	13	43	127	-	-
b2	23	14	18	19	21	40	122	-	-
c1	13	13	26	52	112	139	101	62	36
d1	12	28	63	-	-	-	-	-	-
d2	14	29	65	-	-	-	-	-	-
e1	12	19	49	35	INSIDE	-	-	-	-
f1	11	10	11	9	37	22	56	-	-
g1	14	33	26	-	-	-	-	-	-

Table 2.2.1: Table showing distances from measurement locations (M) to turbine hub (T) at each installation

2.2.1.2 Monitoring Apparatus

The equipment used for taking environmental noise measurements at each installation are as follows:

- Bruel and Kjaer 2260 Investigator with a pre-polarised free-field 1/2" condenser type microphone type 4189 installed (with windscreen) – a sound level meter or analyser which is most suitable for the measurement of environmental noise levels (or sound pressure levels) at each measurement location. Sound power levels are NOT measured using this equipment. The analyser works by measuring the voltage change signals across the microphone, the voltage change is taken through anti-aliasing filters to an A/D converter and then weighted through frequency weighting networks. The digital signals are processed and the required data is stored on the internal storage to be displayed at a later time or transferred to a computer for further analysis. The sound incidence correction for the microphone is set as frontal. The analyser has a number of frequency weightings and filter options which are set-up in advance of the measurements. The parameters chosen for the current research are outlined in the Measurement Process Section 2.2.1.3. The B&K investigator is mounted on a tripod at a height of 1.4m when taking measurements.

- Bushnell X500 range finder – a range finder to measure the slant distance from each measurement location to the nearby turbine hub to an accuracy of ± 0.91m (1 yard). Measurements are taken through a view finder where a cross is lined up over the turbine hub and a button depressed in order for the device to emit an infrared energy pulse which is then reflected off the target back to the range finder. The data times are processed to display the distance to the turbine hub.

- Garmin eTrex H GPS – a high-sensitivity GPS receiver used to store the measurement locations as way-points to allow the repeatability of measurements. The way-points are only used as a guide as the device is accurate to a 3m radius. The GPS is used in conjunction with the range finder to allow repeatability of the measurement locations.

- Tascam DA-P1 DAT (digital audio tape) recorder and DPA miniature omnidirectional microphone type 4060 series (with windscreen) – the microphone is a highly sensitive omnidirectional microphone which is used to simultaneously record the actual sound signal whilst taking noise measurements. The microphone is plugged into a power supply signal conditioning box (Type MPS6020 - MPS stands for miniature power supply), which is in turn plugged into the DAT recorder. The DAT recorder records the sound signal onto a digital audio tape which is used later for data transfer to a computer. The recording of the actual sound simultaneously with collecting noise measurement data using the B&K sound analyser is important for later analysis of the data. By listening to the sound recording, any unusual background noise identified during collection of the data can be removed from the analysis.

- Kestrel 4500 Pocket Weather Tracker – a piece of equipment which measures and data logs temperature, wind speed and relative humidity simultaneously while taking the sound measurements over a chosen averaging time length. The weather tracker was mounted on a wind vane on a tripod at a height of 1.66m as close to the wind turbine as possible.

- Noise Explorer Type 9815 – is the computer software used to post process the noise measurement data from the B&K 2260 once it has been transferred to a PC.

The process for taking measurements will be outlined in the following Section.

2.2.1.3 Measurements Process

Figure 2.2.3 shows a flow chart outlining the methodology for taking environmental noise measurements at each micro or small wind turbine installation. More details about the measurement process will be given in this Section.

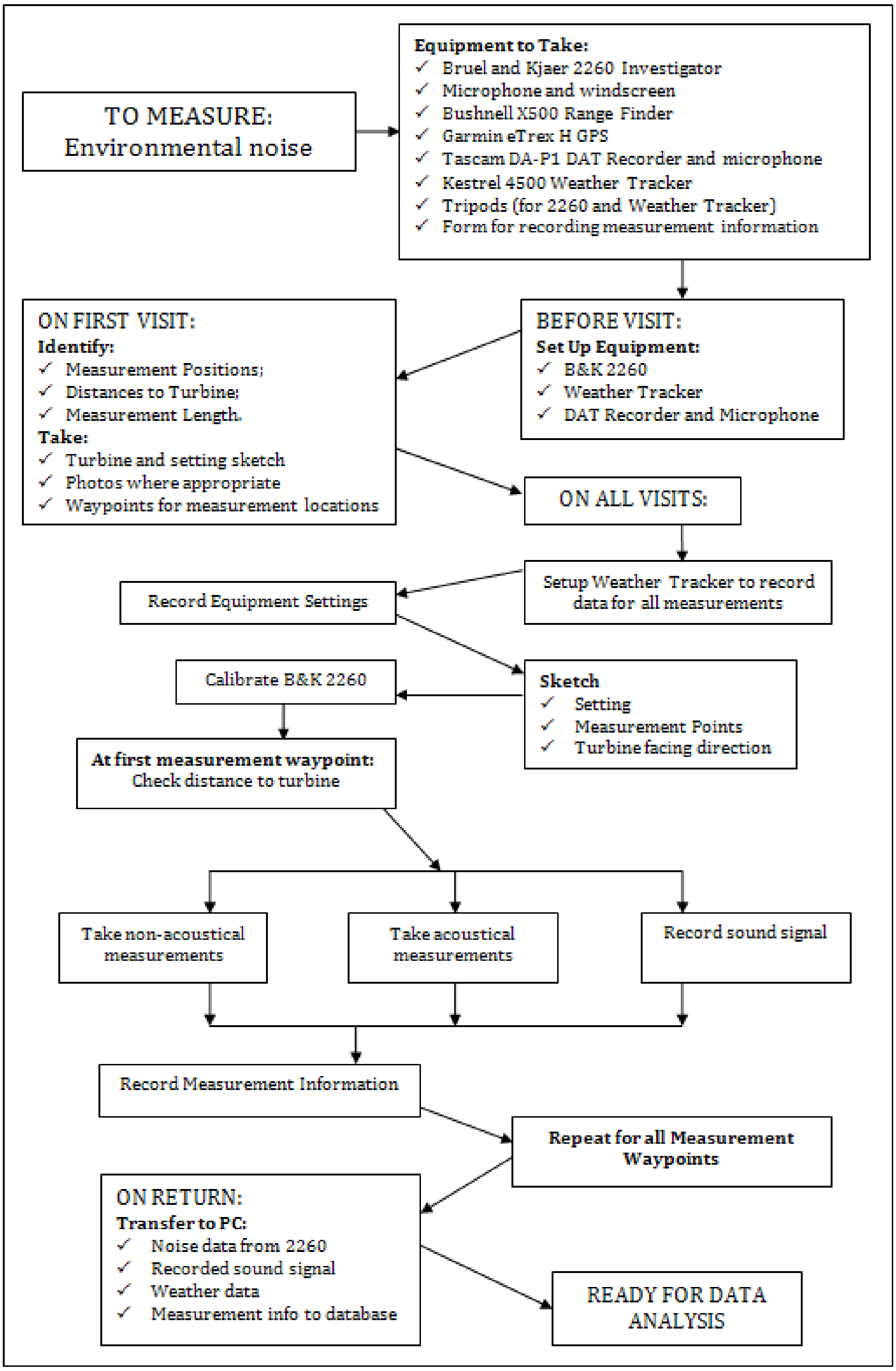

Figure 2.2.3: Flow chart to show methodology for measuring environmental noise levels

Bruel and Kjaer 2260 Investigator Before attending each of the turbine installations it was necessary to set up the B&K sound analyser as required. A storage directory for each installation was created within the B&K's internal memory so it was easy to keep track of all data before it was transferred to a PC.

Parameters The analyser was set to record fast (F) time weighted and A (corrected to the human hearing response - see Section 2.1.1.1 for a definition) and linear[4] frequency weighted data (A-weighted and L-weighted). The analyser has a large number of discrete broadband parameters which can be measured, processed and stored during each measurement for each sampling period. The parameters relevant for this research are as follows:

- The instantaneous A-weighted SPL ($LA(Inst)$) values set to display during the measurement time
- The equivalent continuous SPL level (LA_{eq} and LL_{eq})
- The above data is also recorded for each third octave band in the spectrum from 16Hz to 12500Hz
- For the spectrum, L-weighted equivalent continuous SPLs are recorded for each third octave band
- Single L-weighted and A-weighted equivalent continuous SPLs are recorded, calculated as a sum over all third octave bands
- Overload data, elapsed time, start and stop date and time and measurement number were also recorded.

An overload occurs when the noise data exceeds the range as set before measurements were taken. Depending on the wind speed on the day of measurement or the background levels at the installation the range was set to one of four values, 0dB-80dB, 10dB-90dB, 20dB-100dB or 30dB-110dB.

The parameters described above are relevant to this research as they allow an analysis of the overall sound level recorded at each measurement location, at each installation for every visit. Data for each third octave band over the frequency spectrum is essential to analyse the characteristics of the turbine noise at each installation. The time information stored simultaneously with the data is used to refer the measurement data to the information collected with the weather tracker and the sound signal recorded with the DAT recorder.

Measurement Control The B&K 2260 was set up so measurements were performed over a period of 2 to 5 minutes depending on the type of site (e.g. if there was a high level of background noise, measurement lengths were longer, however if a site had low levels of background noise a shorter measurement period was required.) Spectra were collected and logged over 10, 15 or 20 second averaging periods, the measurement technique evolved over the period when measurements were taken and it was recognised that a 10 second averaging time yielded better results for analysis. If anomalous background noise was identified during a measurement period, it is better to only remove a 10 second averaged sample than a 20 second sample, particularly if the anomalous noise is only present for a

[4]Linear weighted noise is unweighted across the frequency spectrum. The noise measured is not corrected to the response of the human ear and hence high and low frequency sounds which the human ear cannot easily detect are not cut out.

short time, this means less noise representative of the overall measurement is removed. The process for removing anomalous noise and more information about the type of noise that is considered as anomalous is given later in the Thesis in Section 2.3.1. All measurement data recorded was logged and stored to the measurement directory ready for transfer.

Calibration Before each measurement visit the B&K 2260 was calibrated using the B&K Sound Level Calibrator type 4231 (a reference sound source of 1kHz at 94dB) and the internal calibrate mode of the analyser. Additional calibration also occurred before and after each measurements using the charge injection calibration (CIC) function available allowing verification of the complete measurement chain taking into account the microphone. CIC allows the user to check that the external calibration of the analyser is still valid by checking a reference CIC value produced on any previous calibration with the new CIC value. A stable CIC ratio assures stable operation of all components of the measurement system within the sound analyser.

Kestrel 4500 Pocket Weather Tracker The weather tracker has the capability of logging and storing a number of weather parameters. The two most relevant for this research are the wind speed and direction. The weather tracker was set to automatically store average data every 10 seconds for the duration of the measurement visit and the time was synchronised with that on the B&K sound analyser. This means sampling times for both pieces of equipment were directly comparable for each 10 second sampling period.

At the beginning of each measurement visit the weather tracker was set up as close to the wind turbine as possible and set to auto-log the data. Once all measurements for the installation had been taken, auto-logging was disabled ready for the weather data to be transferred to a PC.

The wind speed measurements collected with the weather tracker at a height of 1.66m from the ground will be used as a reference wind speed as it is not possible to take absolute wind speed measurements at hub height of the turbines during the noise measurements. It is acknowledged that wind speeds at the turbine hub will be much higher than wind speeds at the height of the anemometer. This also means that small changes in wind speed measured at anemometer height will relate to a much higher change in wind speed at hub height. For this reason, the wind speeds measured will be referred to as the reference wind speeds for the remainder of the Thesis and serve to give a comparison between measurements taken on different days at different measurement locations.

Throughout the Thesis, low, mid and high reference wind speeds will be referred to. The magnitude of the reference wind speeds which are considered as low, mid or high depends on the installation. This is because the relationship between the reference wind speed measured by the anemometer and the wind speed at hub height will also vary between installations. In a highly built up area, the difference between the two wind speeds will be large. The difference will also depend on the turbine hub height. A higher turbine hub will mean a larger difference in the two wind speeds and vice versa. For example, at installation (a), 3.98m/s is considered as a high reference wind speed because although 3.98m/s is not a high wind speed per se, the anemometer location is sheltered and the turbine hub height is high at 15metres. This reference wind speed was taken on a day which was windy in comparison to other measurement days at installation (a). In contrast, at installation (b) the anemometer location is in an open area where wind speeds are undisturbed at the anemometer height, high wind speeds at this location are considered to be up to approximately 12m/s. The scatter plots for each installation found in the measurement results in Section 2.3.2 will show the reader the range of wind speeds for each installation.

Measurement Process On the first visit to each installation, measurement locations and the distance from each location to the turbine hub were identified (as outlined in Section 2.2.1.1). Each measurement location was then logged as a way-point using the Garmin eTrex H GPS to allow repeated measurements on future visits. Sketches of the turbine and surrounding area and photographs (where appropriate) were also taken on the first visit to further facilitate measurement repeatability.

On each measurement visit the B&K 2260 sound analyser and weather station were set up beforehand and on arrival as detailed previously in this Section. On arrival at each measurement visit, the turbine rotor orientation was sketched to identify the prevalent wind direction on the day of the measurement visit. At the first measurement location the method for collecting data was as follows:

1. All equipment is set up
2. The distance to the turbine was verified and noted using the Bushnell X500 range finder
3. The play button is pressed on the B&K sound analyser so its measurement process is started
4. CIC internal calibration commences and a note on the sound analyser alerting that this is taking place is displayed on the display
5. Meanwhile the DAT recorder is set to record the digital sound signal
6. Internal CIC finishes and the measurement process starts on the sound analyser
7. A note of the counter time on the DAT recorder is taken when the sound analyser measurement process starts
8. Once the measurement process has finished on the sound analyser a note is displayed on the sound analyser alerting that CIC internal calibration is taking place
9. The counter time on the DAT recorder when the measurement process on the sound analyser finished is noted. (This means that the digital recording can be split later to coincide with when measurements were actually taken)
10. A note of the file-name and directory where the measurement data is stored on the sound analyser is taken

This process is then repeated for all measurement locations at each installation. Once all data have been collected on a measurement visit the equipment is removed from the site, all data and measurement information is ready to be transferred to PC on return.

Measurements were taken over a period of 19 months with a measurement visit typically lasting between 1 and 2 hours. This 19 month duration allowed measurements to be taken in a variety of wind speeds and weather conditions over a range of seasons. However, this also meant that measurements at all wind speeds within the wind speed range were not available. In order to get data at all wind speeds continuous measurements would be needed and this was not possible for the current research. Table 2.2.2 shows the dates of measurement visits to each installation. See Table 1.3.2 in Section 1.3 for a full list of installations.

Inst.	21/05/09	01/06/09	25/06/09	20/07/09	22/07/09	31/07/09	06/08/09	07/08/09	08/09/09	10/09/09	22/10/09	19/11/09	15/12/09	09/02/10
(a)		X		X		X	X					X		
(b)	X		X	X			X			X		X		
(c)						X	X			X				
(d)					X			X	X		X		X	X
(e)					X			X	X		X			X
(f)					X			X	X					X
(g)									X		X			X

Inst.	16/02/10	19/02/10	23/02/10	06/05/10	30/07/10	24/08/10	06/09/10	24/09/10	04/10/10	19/10/10	29/10/10	23/11/10	24/11/10	09/12/10
(a)							X		X				X	X
(b)														
(c)	X	X						X	X					
(d)			X	X	X	X				X	X	X		
(e)			X	X	X	X				X	X	X		
(f)			X	X	X	X				X	X	X		
(g)			X											

Table 2.2.2: : Table showing the dates of measurement visits to each installation

2.2.1.4 Data Transfer Process

The following Sections detail how all data collected during the measurement process was transferred to PC after the measurements had taken place.

Recorded Measurement Information All measurement information is recorded into an MS Access database. Data includes measurement dates and times, and installation names where measurements took place. The order in which measurements at each installation were carried out is recorded with associated file-names for each measurement number as stored in the sound analyser internal storage recorded. The measurement length and sampling rate is recorded, with the associated DAT recorder counter time for the start and finish time of each measurement recorded. The names of the digital recording file and Excel file containing the weather data are referenced. The distances to the turbines on each visit are also stored along with any comments of any unusual circumstances associated with the measurements.

Weather Data All 10s sampled and averaged weather data from the weather tracker using the Kestrel USB Interface and Kestrel Communicator software is uploaded. The software reads the data directly from the weather tracker, then selected data can be exported to an Excel spreadsheet ready for analysis. Once in Excel, the data are split to correspond with the measurements they are associated with. This is done by noting the time and date for each measurement from the B&K sound analyser noise data and selecting the weather data which corresponds with this date and time. The weather data is then further split to the 10 second sampling periods and marked with the measurement and sampling number so comparisons can be made with the noise data when analysing. The names of all files are recorded in the measurement database.

B&K 2260 Sound Analyser Data Noise data from the B&K sound analyser is transferred in two ways.

Data is transferred directly to the Bruel & Kjaer noise explorer type 7815 software. This software package allows a general exploration of the data, i.e. all spectra can be shown for each sampling period and all relevant values stored by the sound analyser as outlined is Section 2.2.1.3 can be viewed. The data are transferred directly from the sound analyser in the program, where a directory or project is created within the software and all measurement data for a particular visit are uploaded into this project file. Data can also be exported to a spreadsheet from the noise explorer software. However this method for exporting the data to Excel is time consuming.

All noise data can also be printed to a text file directly from the sound analyser. This is done using the 2260 investigator link, the first noise data file for a measurement visit is called from the sound analyser internal directory and the investigator link is set to capture data (prompting for a file-name and directory for this noise data to be stored on the PC). The print button on the sound analyser is then pressed and all measurement data is printed to the text file specified with the investigator link. Data for all measurement on a measurement visit are automatically printed to the text file. The capture data function on the investigator link software is then disabled to stop data collection. A macro is created within Excel to open the text file and sort the data within Excel as required. For example, spectra data for each measurement can be copied to a separate spreadsheet ready for later manipulation and analysis.

Digital Sound Recording The digital sound recording from the DAT recorder must be transferred to PC so the signal can be split to correspond to the measurement data collected simultaneously with the recording of the sound. The DAT recorder is plugged into the sound card of the PC using its auxiliary outputs. The Audacity software is used to record the digital signal from the DAT recorder onto the PC, i.e. 'play' on the DAT recorder and 'record' within the Audacity software are pressed simultaneously. The digital recording is then copied onto PC ready to be split according to the counter start and finish times for each measurement. This is also done within the Audacity software, the required part of the digital recording corresponding to each measurement is selected and exported to a separate file. This sound recording is then used to identify any anomalous background noise data recorded by the B&K sound analyser.

All data is then ready for analysis. Full details of the analysis procedure and the results of the analysis of the data is given in Section 2.3. The following and final part of this Section outlines the methodology for creating sound maps of turbine noise attenuation at each installation using the software CadnaA.

2.2.2 Noise Mapping

The methodology for taking environmental noise measurements as detailed in the previous Section will allow an analysis of the frequency spectra associated with small wind systems as well as an idea of the key frequencies of small wind system noise. To get an overall picture of the likely levels of small wind system noise at real installations and how the noise propagates to buildings and areas near to the turbines sited at each installation it is important to create sound maps which show how sound at the key frequencies as measured with the environmental noise methodology attenuates over the topographical area. This was carried out using the DataKustik CadnaA 4.1 software package. The CadnaA software uses the ISO 9613 standards [31][32] "Acoustics attenuation of sound during propagation outdoors" to calculate the attenuation of sound over a topographical map.

The sound maps will be used first to help achieve the aims and objectives of the noise measurement part of the research, and second, in conjunction with manufacturer's data for the sound power level rating of each turbine type included in the study to provide a sound rating for each questionnaire respondent of the domestic study of the psychological and health impacts included in the research (more detail of this part of the research is given in Chapter 3 of the Thesis).

Using CadnaA it was possible to create a map of the topography at each installation by importing Ordnance Survey (OS) data of elevations, buildings and roads using the University's subscription to Edina online maps and data. The required data was imported into CadnaA in layers over a bitmap image of the OS map itself. By doing this, significant acoustic obstructions such as high fences or visual obstructions such as large bodies of trees and foliage could be traced over the OS image where data of these features were not available to import. Figure 2.2.4 shows a birds-eye image of the topographical map created for installation (d) (for a description of all measurement locations see Section 2.2.1.1 and Figure 2.2.2 for a map of installation (d)). In this image the roads and buildings are clearly visible, fences and similar significant obstructions are marked with a black line and contour lines are marked in blue.

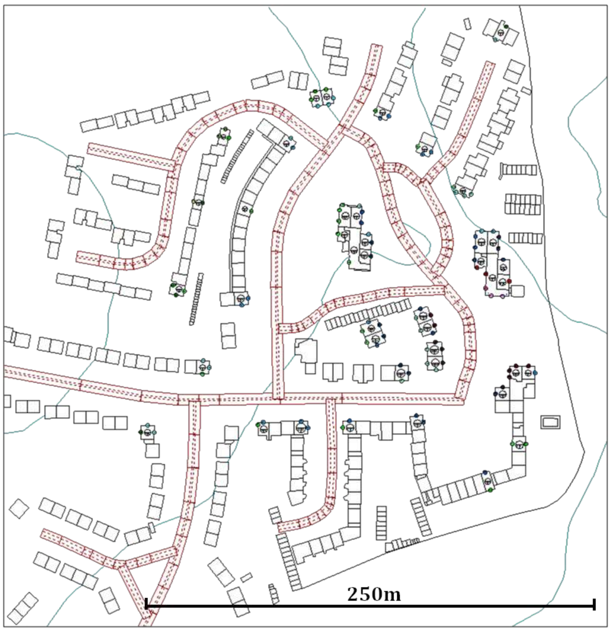

Figure 2.2.4: Birds eye view of the topography map for installation (d) showing buildings, roads, contour lines, and obstructions such as fences.

A three dimensional image looking in a south-easterly direction at micro turbine installation (d) is shown in Figure 2.2.5. On this 3D image the turbines are clearly visible marked as blue crosses at the top of the tower building on which they are mounted. Undulations in the land topography are also clearly visible in the 3D image. The building heights have been specified manually over the land topography. The maps created are an estimation of the area surrounding the turbines at each installation as accurate CAD layered images were not available.

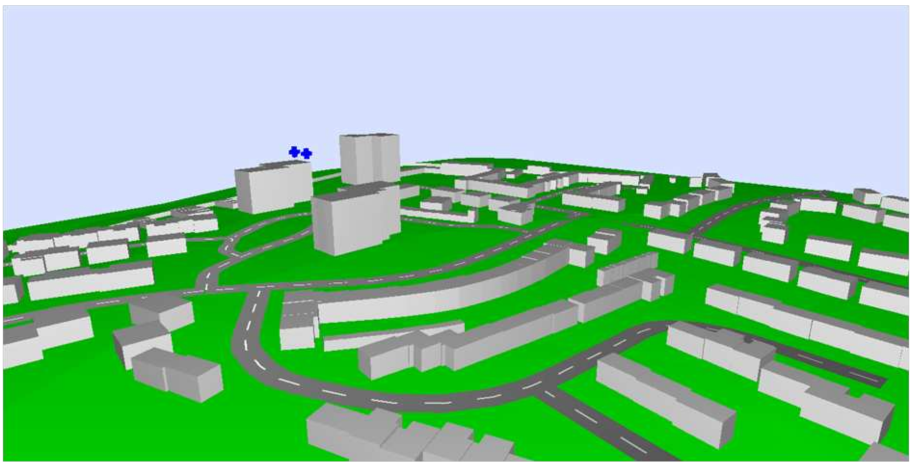

Figure 2.2.5: 3D View of installation (d) showing wind turbines as point sound sources marked as blue crosses

A similar 3D image looking in the north westerly direction at small wind turbine installation (c) is shown in Figure 2.2.6. Again the turbine is marked by a blue cross at the turbine hub. Similar 2D and 3D images were created for each of the seven installations where environmental noise measurements took place.

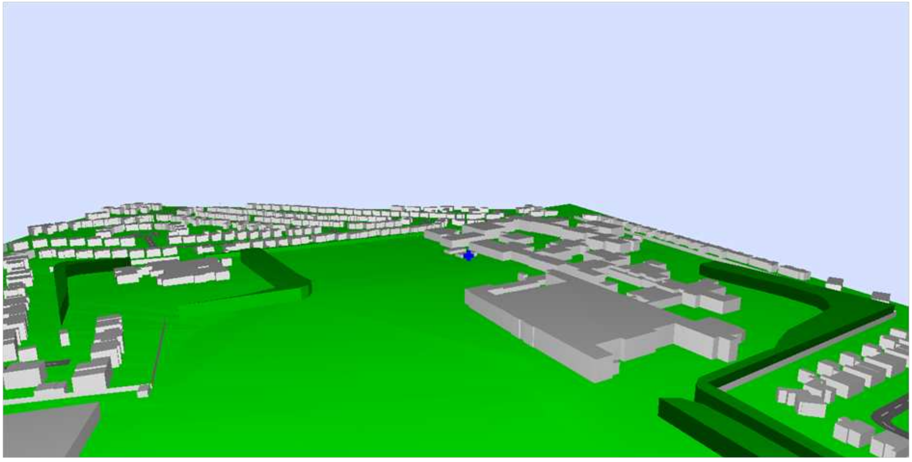

Figure 2.2.6: 3D View of installation (c) showing wind turbine as a point sound source marked as a blue cross

To create a sound map CadnaA automatically lays a grid of receivers spaced at 1m with a height of 1.2m over each topographical map. Random buildings over the map area were selected to display facade values at a height of 1.2m in addition to the sound map. The software calculates the sound pressure level at each receiver over the grid and assigns that receiver the associated colour corresponding to the sound pressure level. The colour sound map is then imposed over the topographical map. Building reflections were not selected as they did not show an effect on the overall results during preliminary investigations. Ground, building and obstruction absorptions were left as default as details of building materials and absorption factors for each specific installation were not available.

The interest of this part of the research is the attenuation of the sound and not the absolute levels at each receiver grid. For this reason, the turbines at each installation were set as a 50dB point source of sound with spherical sound radiation at each frequency of interest. Therefore, the sound pressure level at each receiver of the grid gives the amount the sound from the turbine has attenuated, rather than the absolute level. A separate sound map was created for each frequency at each installation. An analysis of whether the sound attenuates linearly at each frequency over a range of sound pressure levels was carried out during preliminary analyses. For example, the turbine at installation (a) was set as a point source of sound at a frequency of 1000Hz with a sound power level of 30dB, 50dB, 70dB and 100dB. Facade sound pressure levels at various buildings over the map topography were checked to determine whether the sound had attenuated by the same value over the whole sound power range at the given frequency. The same check was carried out at various frequencies over the frequency spectrum and the attenuation was found to be linear for all frequencies. This means, for a turbine with a higher or lower sound power compared to 50dB, the values of the sound pressure at each receiver can be scaled linearly accordingly. Figure 2.2.7 shows a sound map calculated for installation (c), the turbine is modelled as a 50dB point source at 50Hz. The figure shows, for example that the sound pressure levels experienced in the dark blue regions of the map due to the wind turbine sound power level are 5.0dB, meaning that there has been an attenuation of 45dB of the turbine sound to these regions. Colour regions on a map which show a negative sound pressure value simply mean that the sound has attenuated by a larger amount to these areas. For example, yellow regions on the maps correspond to a sound pressure level of -30dB where the turbines have been set as a point source of sound with a sound power level of 50dB. Therefore, the sound has attenuated by 80dB to the yellow regions on the sound map. If the sound power level at the turbine hub were 100dB instead of 50dB, the sound pressure level at the yellow regions on the map would be 20dB. In reality, it is possible to have sound pressure levels below zero, but these are below the threshold of human hearing. In addition to this, the absolute levels at each region on a map are not of interest for the current research, it is the attenuation values which will be used. It is important to note that background sounds are not modelled using these maps. They are used purely to show how sound due to the turbine will attenuate over the area of interest. This is with one exception. At installation (e), where traffic noise is high, an investigation was carried out for how the level of traffic noise affects the amount of micro turbine noise perceived. More details of this will be given with the results in Section 2.3.3. The colour palettes showing the sound pressure levels associated with the colours of the sound maps are given in Appendix D, Section D.1.

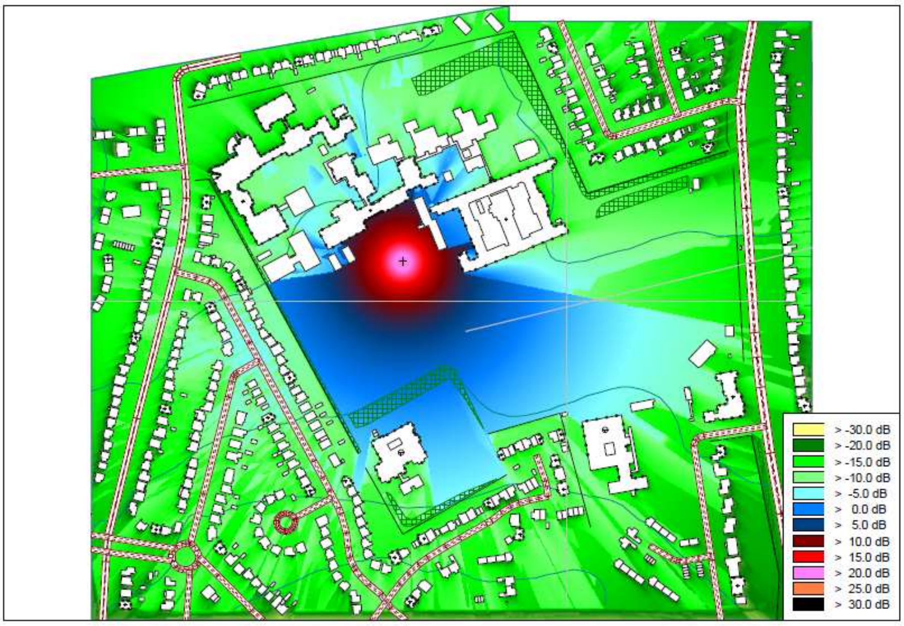

Figure 2.2.7: Sound map for installation (c) showing attenuation of sound from a 50dB turbine

In the next Section, full results of both the environmental noise measurements and the created sound maps using the methodologies specified will be given.

2.3 Noise Measurement Results

In this Section of the Thesis analysis of the noise measurement results will be given for each installation where measurements were taken (see Section 2.2.1.1 for details of the measurement locations). First, details of how the data were split and used will be given, followed by analysis of the overall environmental sound pressure levels at each installation. A spectral analysis of selected measurements will be given at each installation. Comparisons and observations will be drawn from these spectra. Finally sample sound maps will be shown that have been generated using the CadnaA software package for each installation. The results of the noise measurements should be considered in conjunction with the descriptions of turbine noise mechanisms as given in Section 1.2. Conclusions from the noise measurement Section including recommendations for future work will be given following the Results Section.

2.3.1 Data Processing

Data from equipment used for the noise measurements were uploaded as per Section 2.2.1.4 and all measurement information was stored in a database for reference when analysing. In order to interrogate the results the data had to be transferred to a format useful for analysis. To do this macro programs within Excel were used.

Data from the sound analyser had been uploaded to a text file for each visit to an installation. The data in this text file had to be sorted to create an Excel file with a separate sheet for each measurement on a given visit; a macro was used to do this. As each measurement may have had a different length or averaging period, the macro had to identify and account for this. For example, a 2-minute measurement length with 15 second averaging period would have produced 8 or 9 sets of data (due to the way the sound analyser stores data during the measurement process) containing summary information for that averaging period and, of key interest the unweighted sound pressure levels at each 1/3rd octave frequency band (for a list of 1/3rd octave frequency bands see Appendix B). It was necessary to A-weight each value in the 1/3rd octave spectra for each of the sets of data and then to calculate the LA_{eq} for each third octave frequency band for the two minute measurement length. This is not as straight-forward as calculating a simple average of the data sets for each frequency and a log average law must be used. The log average of the sound pressure levels measured during each averaging period over the measurement length at each frequency is calculated using Equation 2.3.1.

$$L_{eq} = 10log_{10}\left(\frac{10^{\frac{Lp1}{10}} + 10^{\frac{Lp2}{10}} + ... + 10^{\frac{Lpn}{10}}}{n}\right) \tag{2.3.1}$$

The overall un-weighted and A-weighted L_{eq} values representing the contribution from all frequencies were also given for each of the sets of data. The raw data had to be A-weighted because it is the human response to the wind turbine noise which is of interest. The A-weight values convert the sound to an equal-loudness contour for human hearing for all frequencies taking into account how the ear responds to sounds of different frequencies. A chart has been produced for each measurement showing a frequency spectra of the A-weighted values for each of the sets of data as well as the A-weighted L_{eq} for each frequency for the whole measurement length (see Figure 2.3.1). A-weighting correction values are given in Appendix B.

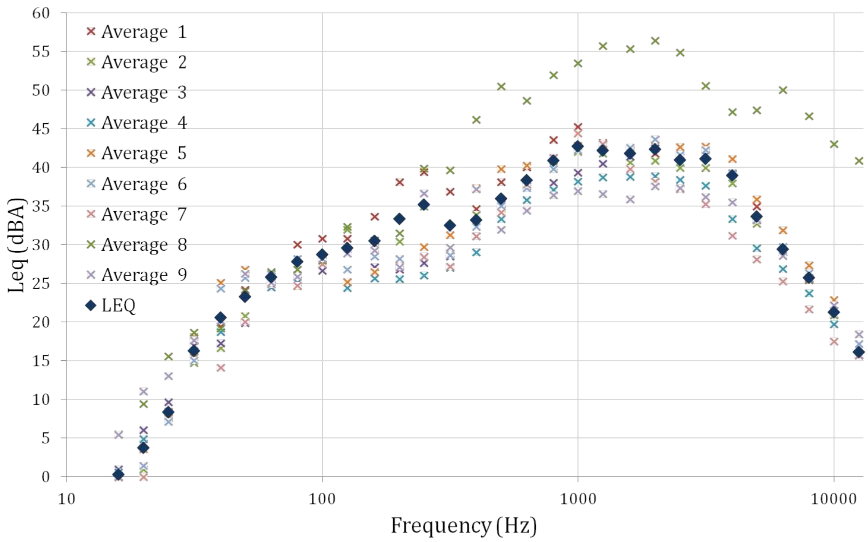

Figure 2.3.1: Chart showing the A-weighted frequency spectra for each averaging period of a two minute measurement with the equivalent sound pressure level at each frequency for the whole measurement.

It was necessary to remove any anomalous background noise from each measurement. Anomalous background noise is described as a sound which is not representative of the usual level of background noise at an installation. For example, at an installation with low background noise a heavy truck driving past would be classed as anomalous. However, at an installation with a high level of traffic noise, a heavy truck would not necessarily be depicted as anomalous. Most of the installations included in the study have a very low level of background noise so even conversation noise would be classed as anomalous. The frequency spectra plots as in Figure 2.3.1 help to distinguish anomalous background noise by identifying any sample that does not follow the trend of the other samples for a given measurement (for example Average 8 in Figure 2.3.1 does not follow the trend of the other samples in the high frequency[5] range). This was carried out with caution because in some instances, a sample that did not follow the trend was due to increased or unusual turbine noise for that averaging period, in which case it was of key interest rather than an averaging period which should be removed from the analysis. To avoid removing measurements of interest, the sound signal recorded in conjunction with taking the measurement data was listened to. Any extraneous noise was identified and the associated averaging period for a given noise measurement could be removed from the calculation of the A-weighted L_{eq} for each frequency for the measurement period using Equation 2.3.1. Any turbine noise of interest could also be identified with this method and the A-weighted frequency spectrum associated with the noise of interest could be identified. The method for removing any extraneous background noise also served to reduce the range of error on the spectra shown in Section 2.3.2. By removing any extraneous background noise, the error in all figures shown in Section 2.3.2 was reduced to ±2.5dB in the frequency ranges of interest; in many cases the error was as low as ±1dB. For frequencies below

[5] For the purpose of this research, a low frequency sound is considered to be below 200Hz, a high frequency sound is considered to occur above 2000Hz and all sounds in between are considered to be in the mid frequency range.

100Hz, the error could be higher at up to ±4dBA. This was of no concern as the human ear is less sensitive to sounds at these low frequencies. The error can be attributed to the changes in wind speed during the measurement length and hence changes in the noise levels due to these wind changes. The error range is the best that can be expected for the type of measurements taken.

The overall sound pressure level representing the sum of all the frequencies for each measurement is also of key interest. The method for removing extraneous noise as described above was used and the A-weighted overall L_{eq} for each measurement was plotted against the reference wind speed for that measurement to identify how the environmental noise changes as the wind speed increases. To capture the associated wind speed, the time stamp from each measurement was read from the acoustic data file. The average reference wind speed from the anemometer measurements corresponding to the time of the acoustic data file time stamp was calculated.

In the following Section, results from analysis of the noise measurement data will be given at each installation where measurements were taken.

2.3.2 Measurement Data Analysis

In this Section, noise measurement results at all installations where measurements were taken will be given. See Section 2.2.1.1 for details of the turbine installations included and the codes associated with the measurement locations at each site. Results will be given for the small turbine type (S1) followed by the micro turbine type (M1) (see Section 1.3 for a list of small and micro turbine types involved in the study). Finally, a short comparison of the results for the two turbine sizes will be given.

The key figures which illustrate the results will be shown in this Section. Further figures can be found in Appendix C.

2.3.2.1 Small Turbine Type (S1)

In this Section, results from the measurements of noise associated with the small wind turbine type S1 at installations (a), (b) and (c) will be presented. The overall sound pressure levels at each of the measurement locations will be considered and the spectral analysis will also be discussed. The small wind turbine type S1, as shown in Section 1.3 is a 5kW turbine with a rated rotational speed of 200rpm and a 5m rotor diameter. The hub height can vary between 12m and 15m. Although this is a small turbine compared to a megawatt machine, it can be sited very close to where individuals live and work (for example at installation (c), the closest dwelling is only just over 100m from the turbine). The rated sound power level and immision levels at 25m and 60m stated by the manufacturer are of a low level ($L_{W,8m/s}$ is 89dBA at the hub at 8m/s wind speed with the sound pressure level at 25m due to the turbine $L_{p,25m}$ equal to 53dBA and at 60m $L_{p,60m}$ equal to 45.5dBA). The fact that turbine type S1 could be sited in close proximity to domestic dwellings means the turbine sounds are likely to be audible, particularly when background noise is of a low level.

Overall Sound Pressure Levels The overall sound pressure level at each of the measurement locations at each small turbine installation for each visit was plotted against the reference wind speed to identify how the environmental noise changes as the reference wind speed increases. Each point on a scatter plot represents a single measurement (see Table 2.2.2 in Section 2.2.1.3 for a list of measurement visit dates for each installation). Several measurements may have been taken from a particular measurement location on a single visit. If any increases in environmental noise levels with increasing reference wind speed are attributed to the turbine it would be expected that locations closer to the turbines would record higher sound pressure levels at a given reference wind speed, reducing the further from the turbine the measurements are taken.

The measurement locations at each installation which best capture the changes in wind turbine noise at increasing distances from and varying locations around the turbine at different reference wind speeds are plotted on scatter charts. Figure 2.2.1 in Section 2.2.1.1 shows a map of the measurement locations at each small wind turbine installation as well as the code associated with each measurement location. These codes are used as the legend for each scatter plot. The reader is reminded that the letter M in the code refers to the fact it is denoting a measurement location (and not the turbine location), the second letter denotes the installation code and the number indicates which measurement location for that installation the data is representing. A separate scatter chart has been drawn for each installation and all unusual background noise has been removed from each measurement (Section 2.3.1 describes the process for removing unusual background noise from a measurement). The scatter plots for installation (a), (b) and (c) are shown in Figures 2.3.2, 2.3.3 and 2.3.4 respectively (further scatter charts to illustrate the results are available in Appendix C, Sections C.1, C.2 and C.3 respectively).

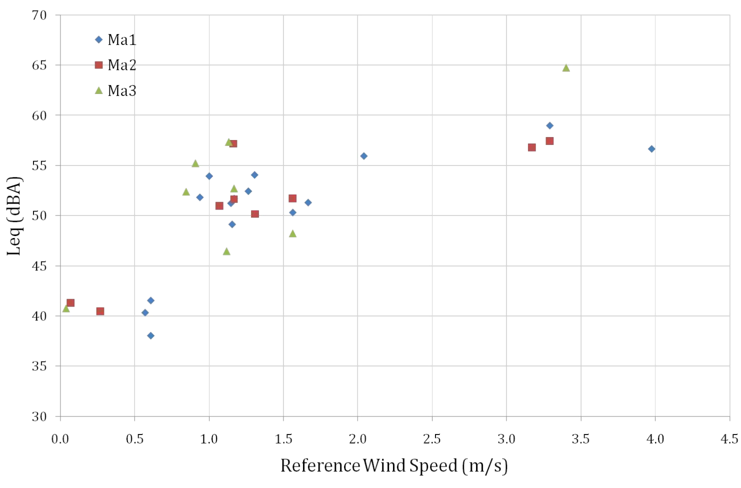

Figure 2.3.2: Scatter chart showing how noise levels vary with wind speed for measurement locations at installation (a)

The scatter plots show that for all small turbine installations the environmental noise measurements generally increase when reference wind speed increases. Scatter plot installation (a) in Figure 2.3.2 represents measurements taken at locations closest to the turbine, (Ma1 is 17m, Ma2 is 17m and Ma3 13m from the turbine hub). From the scatter plot it is clear that as reference wind speed increases so does the measured sound pressure level. However there is no clear difference between the measurement locations. It might be expected that measurement location Ma3 would experience higher environmental noise levels due to its closer proximity to the turbine. However, the sounds generated by the turbine are subject to directionality due to their nature. This will be discussed in more detail later. Therefore the measurements taken at the three measurement locations are roughly equal in magnitude. At higher wind speeds the maximum measured sound pressure level is at Ma3 and is approximately 65dBA. The lowest sound pressure levels measured were 38dBA at Ma1.

The correlation between reference wind speed and sound pressure level from the scatter plots has also been calculated (for a full description of the method for calculating correlation values, the reader is referred to Appendix E, Section E.8). If the background noise (not including the turbine noise) at a particular installation is high over and above the turbine noise, the correlation between reference wind speed and A-weighted sound pressure level would be expected to be low. The correlation would also be expected to be lower for measurement locations furthest from the turbines at each installation. The background noise is generally low compared to the turbine noise at all small turbine installations used for the study so high positive correlations are expected between the reference wind speeds and the sound pressure levels of the measurements, particularly for locations close to the turbine. The sound pressure levels measured at each location for installation (a) shown in the scatter plot in Figure 2.3.2 are highly correlated to the reference wind speed, all with correlation values above 0.71. There is some scatter on the results but this is expected due to changing conditions between each measurement visit, such as weather, season, wind direction and level of background noise. The scatter on the plots for each installation varies but it is still considered that this scatter is due to the changing conditions which occur as measurement visits took place over a period of 19 months. Table 2.2.2 in Section 2.2.1.3 shows a list of measurement visit dates for each installation.

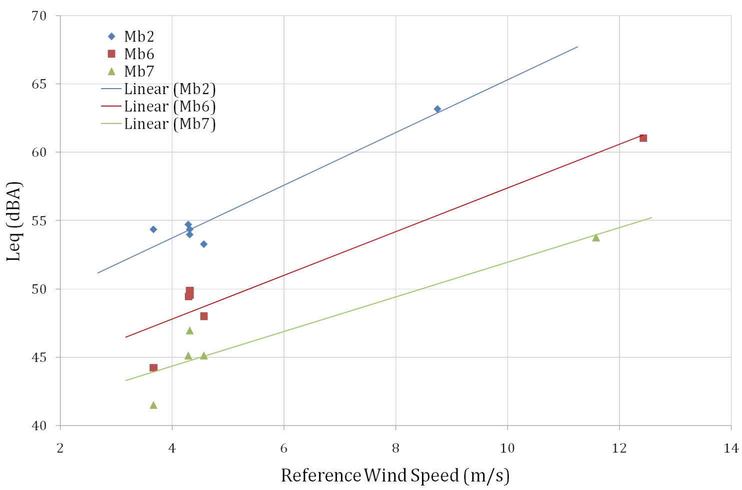

Figure 2.3.3: Scatter chart showing how noise levels vary with wind speed for measurement locations at installation (b)

At installation (b) the background noise is of a very low level, the scatter plot for this installation in Figure 2.3.3 shows measurement locations at increasing distances from the turbines. Mb2, at approximately 17m from the turbines; Mb6, at 43m from the turbines and Mb7, at 127m from the turbines. The correlations between the reference wind speed and the sound pressure level measurements for each location are extremely highly correlated with correlation values greater than 0.93. At location Mb7, the noise levels due to the turbines is low. The reason for the correlation at this location is that as wind speed increases, background noise is expected to increase due to wind noise and the presence of a large number of trees close to the measurement location. This is also indicated by the trend line for Mb7. The environmental noise levels increase the closer to the turbines measurements are taken indicating that closer to the turbine environmental noise is dominated by the turbines. The ranges for sound pressure levels measured at each of the locations is 41.5dBA to 54dBA at Mb7, 44dBA to 61dBA at Mb6 and 53dBA to 63dBA at Mb2. The trend lines diverge at higher reference wind speeds showing that the turbine noise is much louder in higher winds compared to the background noise levels. Measurements at high reference wind speeds were only available for a small number of measurement visits. Therefore points covering the whole wind speed range are not available and the trend lines in Figure 2.3.3 serve to give an indication of how noise associated with the wind turbines increase as wind speed increases. It is expected that if more measurement data were available over the whole range of reference wind speeds, the trend lines shown would follow a similar path.

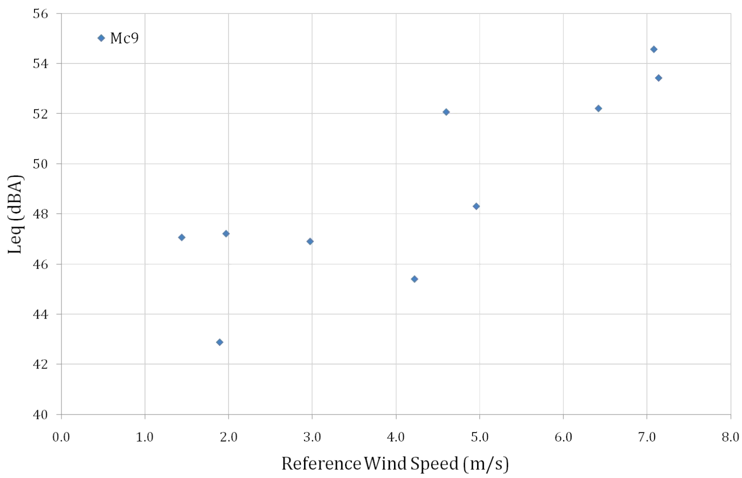

Figure 2.3.4: Scatter chart showing how noise levels vary with wind speed for measurement location Mc9 at installation (c)

Figure 2.3.4 shows noise measurements taken at installation (c) at location Mc9. At this measurement location, there is low background and wind noise due to the sheltered position of the location. Mc9 is 36m from the turbine and is far enough from the turbine so that any building reflections are unlikely to influence the data. The correlation between environmental noise levels and reference wind speed at Mc9 is 0.84 so as wind speed increases so does the measured sound pressure level. Even at 36m from the hub, the turbine noise contributes highly to the overall environmental noise levels measured as it is easily audible in the sound recordings taken simultaneously with the data collection. As background noise is extremely low at this location the increase in noise with increasing wind levels is assumed to be attributed to the turbine and the range of measured noise levels is from 43dBA to 55dBA.

As has been shown from the scatter plots, the environmental sound levels at each location do vary as a function of the reference wind speed, increasing as the wind speed increases. However, the magnitude of all sound pressure levels recorded are low, with a maximum value of 65dBA, the equivalent to general speech. However, as has been observed in the literature, it is likely that it is the characteristics of the turbine noise in addition to the absolute level that cause annoyance to individuals and is therefore of particular interest for the research. Hence, in the following Section spectral analyses of the environmental noise levels measured at all small wind turbine installations will be given.

Spectral Analysis In this Section the results of the spectral analysis for the small turbine type will be given. As discussed previously, the small turbine installations included in this study are located in areas with low background noise. Therefore it is expected that analysis of the frequency spectra for the measurement data collected will represent well the characteristics of the noise attributed to the small turbine type. In this Section, the types of sounds the spectra represent will be examined. These included sounds such as swooshing and humming, for a detailed description of the noise mechanisms and sounds associated with wind turbines see Section 1.2.

A selection of the results are discussed in this Section. Further charts showing the frequency spectra for the small turbine installations are available in Appendix C, Sections C.1, C.2 and C.3. As with the scatter plots showing the overall sound pressure levels, each line on a spectra plot in this Section represents a single measurement period with any unusual background noise removed using the method described in Section 2.3.1. Several measurements may have been taken from a particular measurement location on a single visit. The legend on each spectra plot shows which measurement locations are represented in the figure. Figure 2.2.1 in Section 2.2.1.1 shows a map of the measurement locations at each small wind turbine installation as well as the code associated with each measurement location. The reader is reminded that the letter M in the code refers to the fact it is denoting a measurement location (and not the turbine location), the second letter denotes the installation code and the number indicates which measurement location for that installation the data is representing.

The frequency plot in Figure 2.3.5 shows measurements taken at installation (a) at increasing distances from the turbine, Ma3 is 13m from the turbine, Ma2 17m from the turbine, Ma6 37m from the turbine and Ma5 is 85m from the turbine, all at low reference wind speeds up to 1.07m/s. Figure 2.3.5 shows that below 100Hz there are no significant differences between the sound pressure levels measured at each location because noise at these low frequencies is largely due to wind noise over the microphone. This factor is represented in all frequency spectra given in this Section and any variation is due to the differing reference wind speeds for each measurement. The values for A-weighting at lower frequencies are large. This is due to the way the human ear detects sound, i.e. the ear is more sensitive to mid-range and higher frequency sounds (A-weighting correction values are given in Appendix B). Therefore the low frequency wind noise provides a negligible contribution to the overall equivalent sound level. This means the low frequency noise seen in the measurement data would not be audible and is not discussed further in the following results.

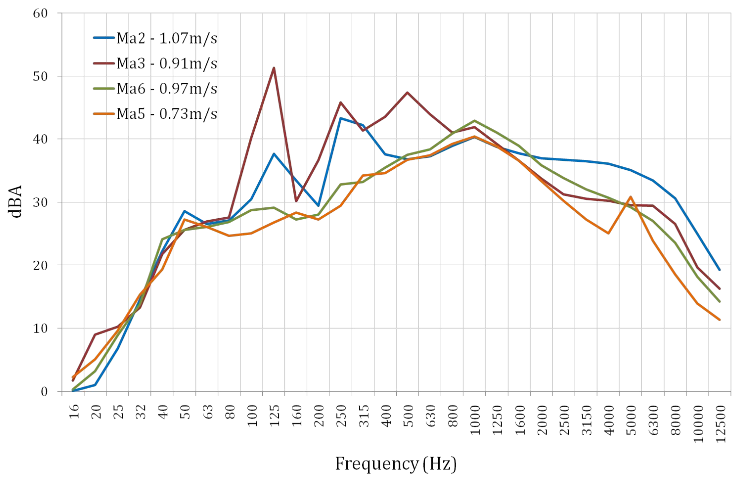

Figure 2.3.5: Measurements at increasing distances from the turbine with low reference wind speeds up to 1.07m/s

Swooshing is audible in the recording associated with Figure 2.3.5 at Ma2 but not at Ma3, a measurement location directly under the turbine rotor next to the mast and closer to the turbine hub than Ma2. This is due to the directionality of the noise mechanism, and the fact that measurements are taken directly under the turbine hub. The noise mechanism does not appear to travel vertically downwards at low wind speeds. The magnitude of the sound due to the swooshing noise mechanism reduces the further from the turbine the measurements are taken with a maximum difference of 10dB between Ma2 and Ma5 measurements. The mechanism can be seen in the spectra in Figure 2.3.5 above 1600Hz peaking between 3150Hz and 4000Hz up to a level of 37dBA at Ma2. The swooshing noise mechanism is broadband in nature, which is also represented in the frequency spectrum.

In Figure 2.3.5 two peaks in the spectrum are visible at 100Hz-125Hz and at 200-630Hz. These peaks are due to the humming and buzzing sound mechanisms from the electromechanical parts of the turbine and are tonal in nature. It was clear during measurements that the source of the humming and buzzing mechanisms was from the electromechanical workings of the small turbine type S1. This was because the noise was heard to be emitted from the the tower, in particular the base of the tower. The exact frequency at which the peaks occur depends on the rotational speed of the turbine and hence the rotational speed of the generating mechanisms within the turbine at the base of the turbine mast. The magnitude of the peaks are highest for measurements taken at Ma3, closest to the turbine at up 51.5dBA. The humming and buzzing sounds are also audible at Ma2 because this location is in an enclosed space where building reflections are likely to play a role in the measured data. The peaks and hence the humming and buzzing sound mechanisms are not audible or represented in the spectrum further from the turbine. This is because there is a small plant building near the turbine, between the base of the mast and the measurement locations at increasing distances from the turbine. The building is not shown on the map of the installation (a). Because the humming sound originates from the base of the turbine mast, this building obstruction is sufficient to cause attenuation of the humming noise mechanism and it is not audible further from the turbine. In contrast to this the aerodynamic noise mechanisms are radiated from the rotor at hub height, hence low obstructions do not cause attenuation of the turbine aerodynamic sounds and attenuation occurs over an increased distance. As the reference wind speed and hence rotational speed of the rotor increases the humming and buzzing tonal peaks shift further up the frequency spectrum. This is shown in Figure 2.3.6, where the peaks occur at 160Hz-200Hz and 315Hz-500Hz, with a maximum magnitude up to 59.5dBA. The frequency plot in this figure shows measurements taken at installation (a) at increasing distances from the turbine, Ma3 is 13m from the turbine, Ma1 17m from the turbine, Ma4 36m from the turbine and Ma5 is 85m from the turbine at reference wind speeds up to 3.98m/s. In these spectra, the peaks are not detected as clearly in the data at measurement location Ma1 as they are at Ma2, even though both locations are the same distance from the turbine hub. Ma1 is not in an enclosed space so there are no building reflections affecting the measurements as there are for Ma2. The swooshing noise mechanism is also represented in the frequency spectrum and occurs for a wide range of frequencies from 800Hz onwards. As with humming and buzzing, when the reference wind speed increases the magnitude of the noise due to the swooshing mechanism also increases with values up to 50dBA. Swooshing is also less audible the further from the turbine the measurements are taken. However the difference between measurements taken closest to and furthest from the turbine is smaller at higher wind speeds.

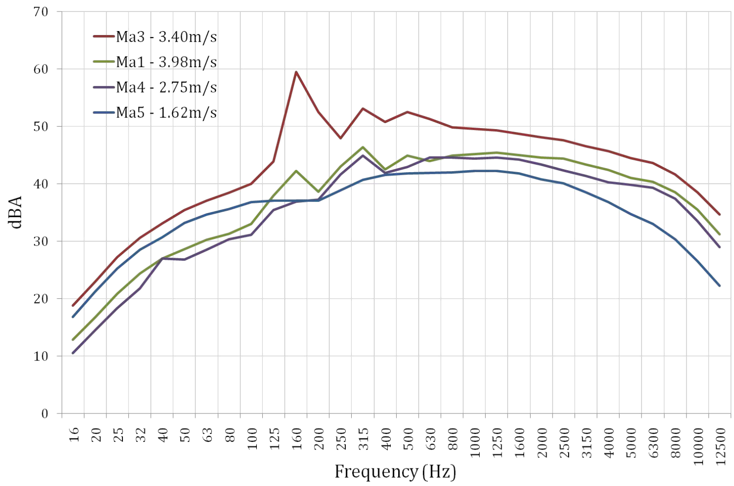

Figure 2.3.6: Measurements at increasing distances from the turbine with high reference wind speeds up to 3.98m/s

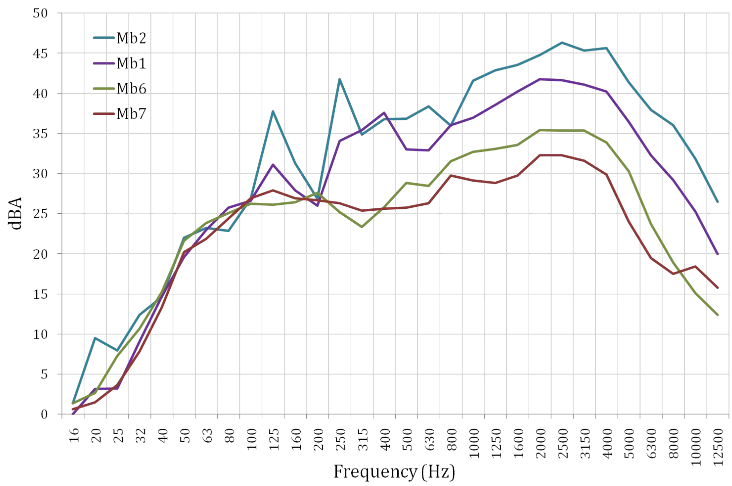

Figure 2.3.7: Measurements at increasing distances from the turbines with low reference wind speeds approximately 1.33m/s

The humming, buzzing and swooshing sounds are also observed from the spectral results of installation (b) at similar wind speeds to those in Figure 2.3.5 for installation (a) at frequencies in agreement with the results for the other small turbine installations. These observations are illustrated in Figure 2.3.7 where measurements taken at installation (b) at increasing distances from the turbines are shown. The shape of the spectra are very similar to those in Figure 2.3.5 (at installation (a)), however the magnitude of each of the noise mechanisms represented in the spectra are different. This is firstly because the reference wind speeds for each of the spectra in Figure 2.3.7 are approximately 0.3m/s higher than for Figure 2.3.5 (at hub height this increase in wind speed will be significantly larger), therefore the peak magnitude of sound from the broadband swooshing mechanism is 46dBA compared to 37dBA in Figure 2.3.5, decreasing the further from the turbines measurements are taken. Secondly, at installation (b) two turbines are sited, meaning the magnitude of the sound at each measurement location is expected to be up to 3dBA higher compared to measurements taken the same distances from a turbine at an installation where only one is sited at similar reference wind speeds. When there are two sound sources with equal sound power level, the combined sound power level is 3dB higher than if there were only one sound source. In contrast to the higher magnitude of the swooshing mechanism sound, the magnitude of the humming noise mechanism is lower at installation (b) compared to installation (a). This is because the closest measurement location to the turbine is 17m from the turbines compared to only 13m at installation (a). In addition to this, the results for installation (a) have shown that the humming mechanism attenuates quicker than the aerodynamic sounds as it is more prone to attenuation due to obstructions such as the fence and small building around the base of where the turbines are sited at installation (b). A full discussion describing the reason the attenuation of the humming and buzzing noise mechanisms occurs over a shorter distance than the aerodynamic noise mechanisms is given earlier in this Section for Figure 2.3.5. To complete the picture for low to mid wind speeds, Figure 2.3.8 shows measurements taken at increasing distances from the turbine at installation (c) at reference wind speeds up to 2.09m/s. Humming, buzzing and swooshing are all represented in the spectra, and in the same frequency ranges with similar magnitudes to the other small wind installations.

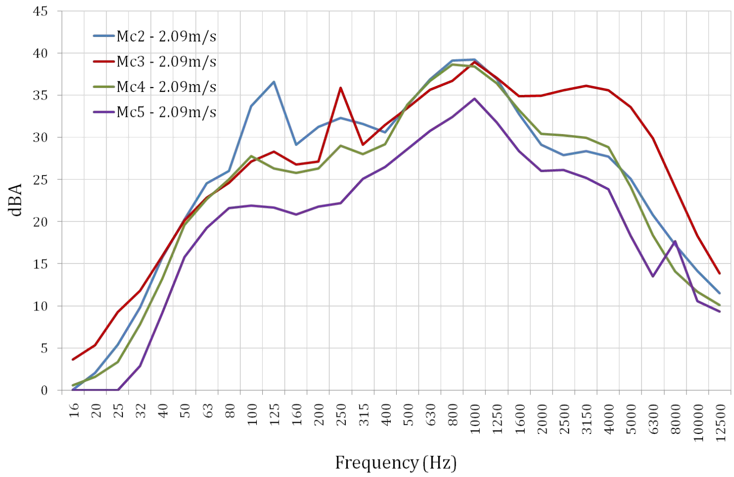

Figure 2.3.8: Measurements at increasing distances from the turbine with mid reference wind speeds approximately 2.09m/s

Measurements taken at installation (b) at high reference wind speeds up to 4.63m/s at increasing distances from the turbines are represented in Figure 2.3.9. The shape of this spectrum agrees very well with the spectrum in Figure 2.3.6 (installation (a) measurements at higher wind speeds). The wind speeds for measurements taken at installation (b) are slightly higher than at installation (a) so although the shape of the spectra are similar the magnitudes of the three sound mechanisms are higher but occur at frequencies in agreement with those for installation (a).

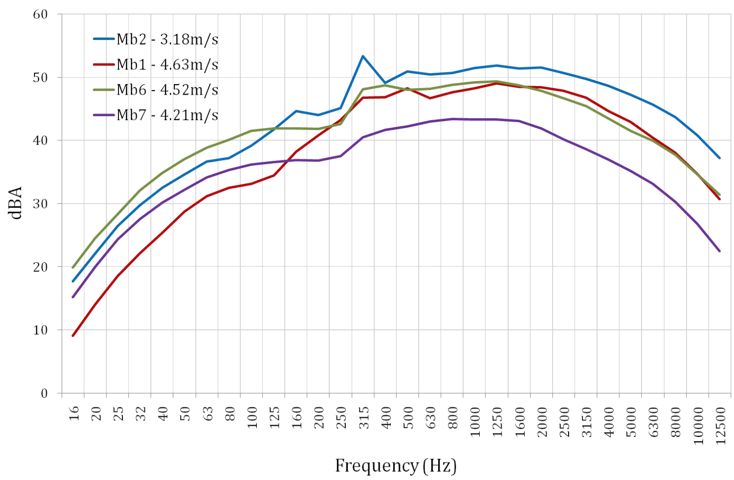

Figure 2.3.9: Measurements at increasing distances from the turbines with high reference wind speeds up to approximately 4.63m/s

The frequency plot in Figure 2.3.10 shows measurements all taken at location Ma3 with low reference wind speeds up to 1.17m/s. Specific sounds were picked out of the sound signal recorded in parallel to the collection of the data. The method for picking out the specific sounds from the sound recordings and hence the corresponding measurement data from the sound analyser has been described in Section 2.3.1. The corresponding measurement data were investigated to analyse how the frequency spectrum changes for the different noise mechanisms selected, these were humming, chopping and swooshing. Two peaks are clearly visible in the spectra for the humming noise mechanism at 125Hz to 160Hz with a magnitude of 46dBA, and 250Hz to 630Hz with a magnitude of 42dBA. These values are in agreement with the peaks seen in Figures 2.3.5 and 2.3.7 associated with the humming and buzzing mechanism at similar wind speeds. The chopping noise mechanism in Figure 2.3.10 is similar in nature to swooshing and occurs as a broadband aerodynamic sound the blades make when the rotor is turning fast slightly out of the wind direction. The magnitude of the sound is however much higher than for the swooshing mechanism, particularly above 1600Hz and peaking at a maximum magnitude of 46.5dBA at 3150Hz.

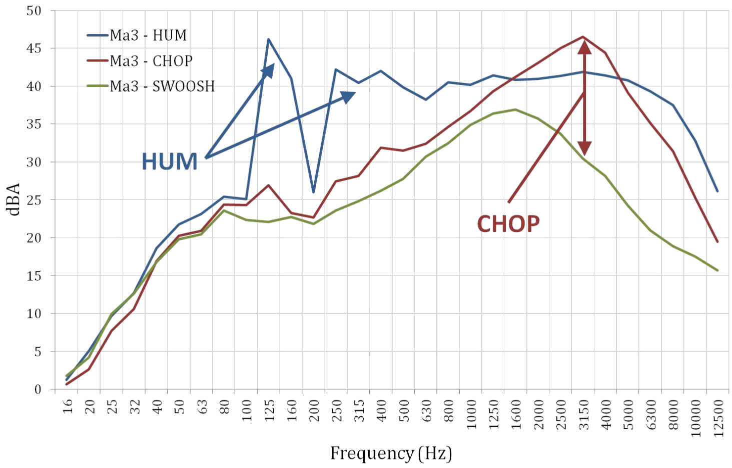

Figure 2.3.10: Comparison of different turbine sounds with low reference wind speeds approximately 1.17m/s

A similar plot to Figure 2.3.10 is given in Figure 2.3.11 but for installation (c). The measurements taken here are all at the same location, Mc9, 36m from the turbine hub with increasing wind speeds where, at the lowest wind speeds the rotor is not turning. The measurement location at installation (c) features very little background and wind noise as it is sheltered and far from any traffic or trees so the data represented in Figure 2.3.11 give a clear example of the sounds the turbine makes over and above the background noise. The humming and buzzing mechanism is not represented in these spectra because measurements are taken sufficiently far from the turbine so that the humming noise has attenuated to such a level as to be inaudible. The key point to take from the spectra in Figure 2.3.11 is that as the reference wind speed increases, the magnitude of the swooshing sound mechanism increases and there is a large difference between values when the rotor is not turning at the lowest wind speeds. However, the broadband frequency range of the swooshing sound does not vary with increasing wind speeds except at the highest wind speeds (above 3m/s) when the swooshing sound begins to change to the chopping sound and occurs over a larger range of the high end of the frequency spectrum.

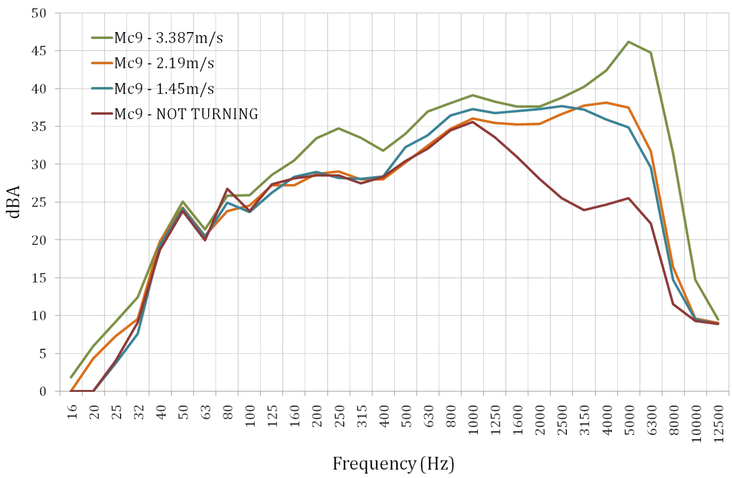

Figure 2.3.11: Comparison of different turbine sounds measured at the same location with varying reference wind speeds up to 3.39m/s

Finally, Figure 2.3.12 shows measurements taken at installation (a) at the three measurement locations closest to the turbine at reference wind speeds up to 1.67m/s. The humming mechanism is again represented by two peaks at 100Hz to 160Hz and 250Hz to 315Hz at location Ma3 directly under the turbine hub. These mechanisms are also represented in the measurement taken at Ma2 but not at Ma1 even though the reference wind speed during the measurement at Ma1 was higher. This is due to the fact that the measurements at Ma2 are in an enclosed space so building reflections magnify the humming noise mechanism. Above 1600Hz the swooshing mechanism is more audible at Ma1 than Ma2 due to the higher reference wind speeds. These findings support earlier discussed findings for the directionality of the sound, and how the reference wind speeds have a higher influence on the magnitude of the swooshing noise mechanism than the humming and buzzing sound mechanisms.

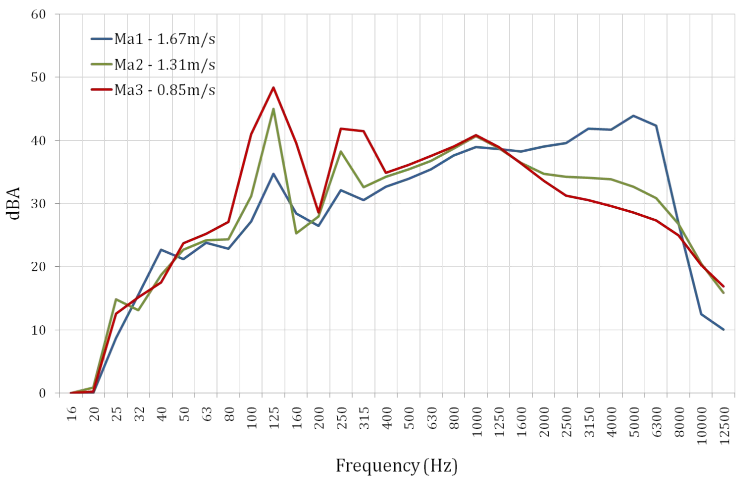

Figure 2.3.12: Measurements showing directionality of the noise close to the turbine with low reference wind speeds up to 1.67m/s

Further frequency spectra plots for each small wind installation are found in Appendix C. The plots in the appendix are for measurements taken at mid range wind speeds not discussed in this Section but which further support the findings discussed. In the following Section, results from the same method of analyses for the small wind turbine installation will be given for the micro turbine installations involved in this study.

2.3.2.2 Micro Turbine Type (M1)

In this Section, results from the measurements of noise associated with the micro wind turbine type M1 at installations (d), (e), (f) and (g) will be presented. The overall sound pressure levels at each of the measurement locations will be considered and the spectral analysis will also be discussed. The micro wind turbine type M1, as shown in Section 1.3 is a 0.6kW turbine with a rated rotational speed of 1000rpm and a 1.2m rotor diameter. The hub height can vary dramatically for this turbine as it can be either mast or building mounted. This turbine has the potential to be sited even closer to where people live and work due to this ability to roof mount this turbine type. Indeed at installations (d) and (e), the turbines are roof mounted. The rated sound power level as quoted by the manufacturer for the micro turbine type M1 is 89.5dBA at the hub at 8m/s wind speeds. The sound pressure level due to the turbine at 25m is 54dBA and at 60m is 46dBA. Although this micro turbine type is much smaller than the small turbine type S1 the sound levels are actually certified to be marginally higher. In the following Sections, first the overall sound pressure levels displayed on scatter plots will be given followed by a spectral analysis of the turbine sounds.

Overall Sound Pressure Levels All measurement data from the four sites with a micro turbine type M1 installed and used for the study were examined and the same analyses were carried out as for the small turbine type in Section 2.3.2.1. The measurement locations at each installation which best capture the changes in wind turbine noise at increasing distances from and varying locations around the turbine at different reference wind speeds are plotted on scatter charts. Figure 2.2.2 in Section 2.2.1.1 shows a map of the measurement locations at each micro turbine installation as well as the code associated with each measurement location. These codes are used as the legend for each scatter plot. The reader is reminded that the letter M in the code refers to the fact it is denoting a measurement location (and not the turbine location), the second letter denotes the installation code and the number indicates which measurement location for that installation the data is representing. A separate scatter chart has been drawn for each installation and all unusual background noise has been removed from each measurement (Section 2.3.1 describes the process for removing unusual background noise from a measurement). The scatter plots for installation (d), (e), (f) and (g) are shown in Figures 2.3.13, 2.3.15, 2.3.14 and 2.3.16 respectively (further scatter charts to illustrate the results for installation (e) and (f) are available in Appendix C, Sections C.5 and C.6 respectively).

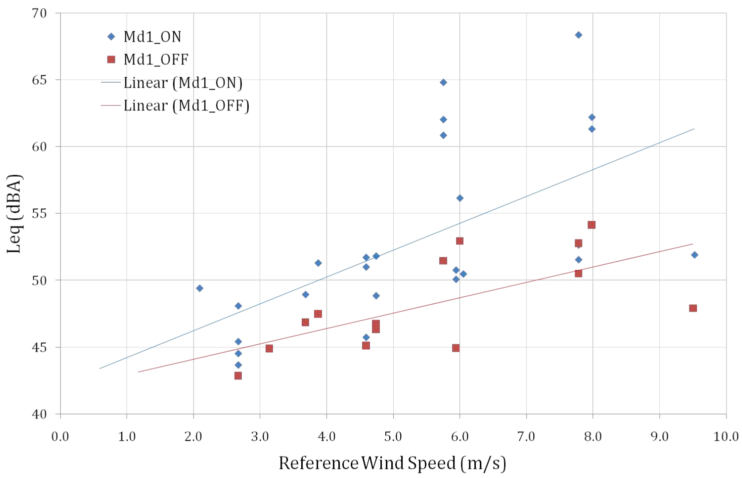

Figure 2.3.13: Scatter chart showing how noise levels vary with wind speed for measurement locations at installation (d)

Installation (e) and installation (g) both have high background noise in comparison to the noise from the turbine and the background noise is principally from traffic. In contrast to this, installation (f) and (d) have comparatively low background noise. The background noise is especially low at installation (d) for measurements taken on the roof of the tower block on which the turbines are mounted. At installation (d) it was also possible to switch the turbines on and off as there was access to the isolator switches for the turbines on the roof of the building. When the turbines were switched off, the rotors were stationary. The scatter plot in Figure 2.3.13 for installation (d) clearly shows that as the wind speed increases the measured noise also increases and that the measured noise is much higher when the turbines are switched on compared to when they are switched off. The range of sound pressure levels measured when the turbines are switched on is approximately 43.5dBA to 68dBA compared to much lower measured sound pressure levels of between 43dBA and 54dBA with the turbines switched off. The increases in noise levels at increasing wind speeds with the turbines off are due to the conditions and wind noise occurring over the microphone, the scatter around the measurements can also be attributed to these factors. The trend lines in Figure 2.3.13 show that the lines for the measurements with the turbines on and off diverge at higher wind speeds. This is as expected as at higher wind speeds the contribution to the overall sound levels from the turbines is much higher and the measurements are dominated by turbine noise. A linear correlation is therefore assumed between reference wind speeds and noise levels. The correlation is 0.75 with the turbines on compared to only 0.67 when the turbines are off, showing that the relationship between environmental noise and reference wind speed is stronger when the turbines are switched on and hence the turbine noise is captured well in the sound pressure levels measured.

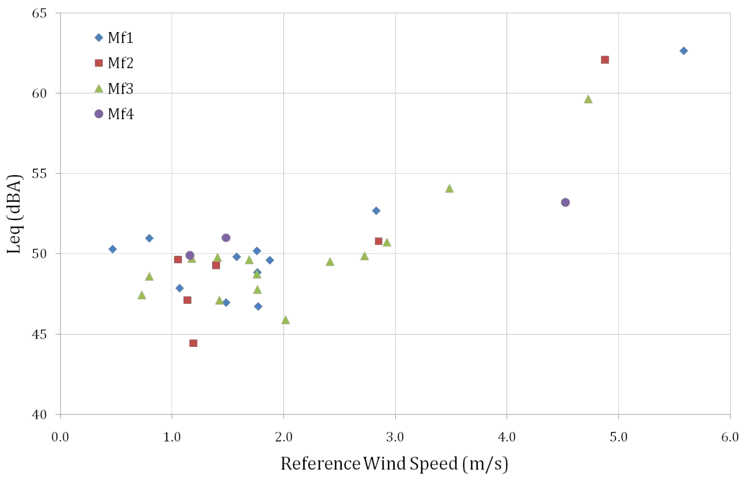

Figure 2.3.14: Scatter chart showing how noise levels vary with wind speed for measurement locations at installation (f)

The scatter plot in Figure 2.3.14 represents measurement locations Mf1, Mf2, Mf3 and Mf4 at installation (f), these are the measurement locations closest to the turbine at a maximum of 11m from the hub. The background noise at this installation is low so the increases in measured noise as the reference wind speed increases are expected to be due to the turbine noise. The scatter plot clearly shows that there is strong relationship between the reference wind speed and the measured noise levels with a range of measured sound levels between 44.5dBA at lower wind speeds and 63dBA for the highest reference wind speeds. The correlation values support this observation, with values of 0.86 for Mf1, 0.93 for Mf2, 0.83 for Mf3 and 0.97 for Mf4. As a result of the observations in the scatter plots and from the correlation values it is expected that the spectral analysis of the results at installation (f) will represent well the characteristics of the micro turbine noise.

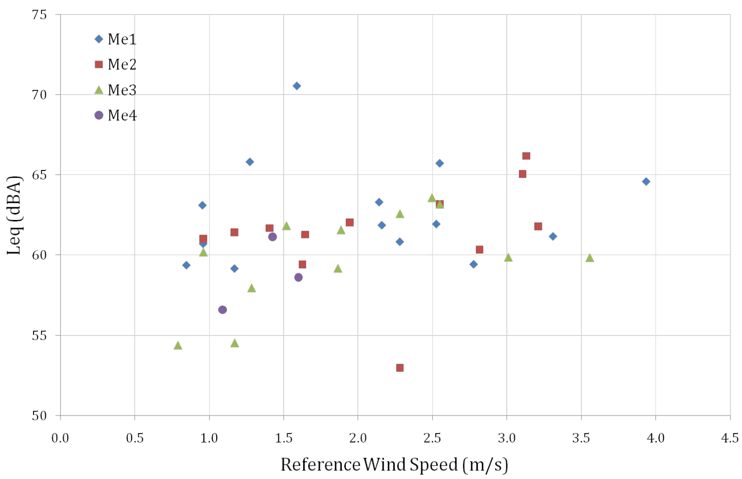

Figure 2.3.15: Scatter chart showing how noise levels vary with wind speed for measurement locations at installation (e)

At installation (e) where the background noise due to traffic is very high, the turbine noise is very rarely audible over this background traffic noise, this is represented in the scatter plot in Figure 2.3.15.

A relationship between the measured noise levels and the reference wind speed is not obvious from the plot, the correlation values also indicate this. The correlations values are 0.07 for measurement location Me1, -0.04 at location Me2, 0.54 at location Me4 and 0.60 at location Me4. These values are not high enough to show that the measurements taken at installation (e) are capturing the turbine noise over and above the background noise. It is also likely that the spectral analyses of the noise measurements will not represent the characteristics of the turbine noise. The problems with background noise also feature for installation (g) where the background noise from passing traffic is relatively high. The scatter chart in Figure 2.3.16 does not show a relationship between the measured noise levels and the reference wind speed and the correlation values also reflect this at 0.41 for location Mg1, -0.38 at Mg2 and -0.21 at Mg3.

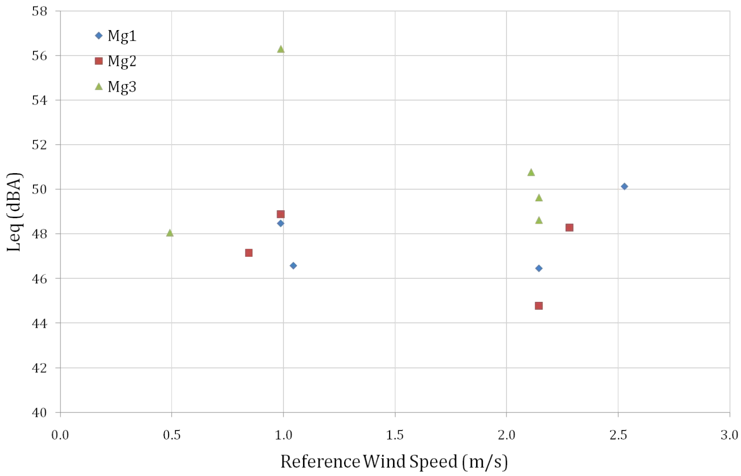

Figure 2.3.16: Scatter chart showing how noise levels vary with wind speed for measurement locations at installation (g)

In the next Section the results of the spectral analysis for the micro turbine type will be given, followed by a comparison between the results for the micro turbine type and the small turbine type.

Spectral Analysis In this Section the results of the spectral analysis for the micro turbine type M1 will be given. As discussed in the previous Section micro turbine installations (d) and (f) have low background noise and it is expected that analysis of the full frequency spectra for the measurements taken at these installations will represent well the characteristics of the noise due to the micro turbine type. In this Section, the types of sounds the spectra represent will be examined. These included sounds such as swooshing and humming, for a detailed description of the noise mechanisms and sounds associated with wind turbines see Section 1.2.

A selection of the results are discussed in this Section. Further figures showing the frequency spectra for the micro turbine installations are available in Appendix C, Sections C.5, C.5, C.6 and C.7. As with the scatter plots showing the overall sound pressure levels, each line on a spectra plot in this Section represents a single measurement period with any unusual background noise removed using the method described in Section 2.3.1. Several measurements may have been taken from a particular measurement location on a single visit. The legend on each spectra plot shows which measurement locations are represented in the figure. Figure 2.2.2 in Section 2.2.1.1 shows a map of the measurement locations at each micro wind turbine installation as well as the code associated with each measurement location. The reader is reminded that the letter M in the code refers to the fact it is denoting a measurement location (and not the turbine location), the second letter denotes the installation code and the number indicates which measurement location for that installation the data is representing.

As installations (e) and (g) suffer from very high background traffic noise it was not easy to extract turbine noise from either the measurement data or the sound signals recorded in parallel to the data collection. For this reason, spectra plots for these two installation are not presented in this Section. For completeness, spectra plots are available in Appendix C, Sections C.5 and C.7 respectively. At installation (e) however, it was possible to take measurements inside the building the turbine is mounted on in the room directly below the turbine mounting position. The sound the turbine makes inside the building is a humming, or whirring type noise which travels through the structure of the building. Aerodynamic noise from the turbine is not audible inside the building. The frequency spectrum in Figure 2.3.17 represents these measurements taken inside at installation (e) at mid-range reference wind speeds of 2.48m/s. There is a clear peak in the frequency spectrum from 160Hz to 315Hz. The magnitude of this peak is only 30dBA. This is of a very low level but in a quiet room the humming sound associated with this peak is easily audible. This could cause annoyance to individuals living in a building with a micro turbine mounted on the roof.

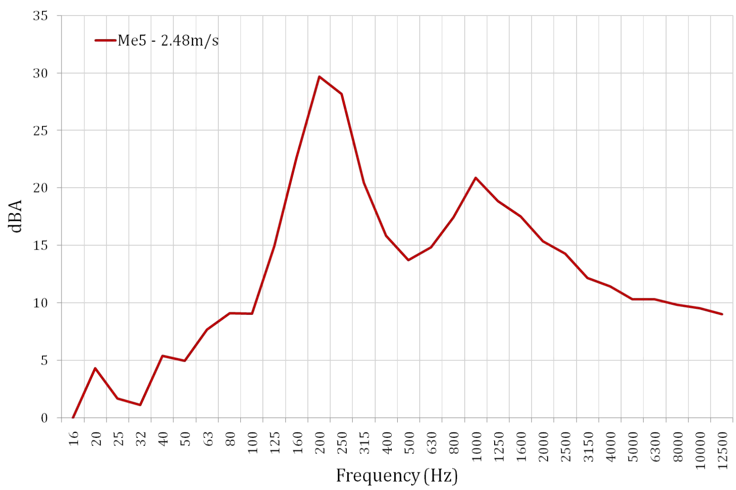

Figure 2.3.17: Measurement taken inside the building with a reference wind speed of 2.48m/s

At installation (d) it was also possible to take measurements inside the building the turbines are mounted on. However the measurements were not taken directly below the turbine mounting positions but inside the building at the same level the turbines are positioned. The micro turbines at installation (d) make a swooshing sound and due to the characteristics of the small rotor, the turbines also make a squeaking type sound as the rotor turns. The swooshing sound is not audible inside the building at installation (d), but, the aerodynamic squeaking sound is, as is a humming sound, which is transmitted through the building structure. Figure 2.3.18 shows frequency spectra for measurements taken inside the building at installation (d) with the turbines on and off at low wind speeds up to 1.69m/s. The humming sound audible from the turbines inside the building can be seen in the spectrum of noise data with the turbines switched on in the range 200Hz to 315Hz. The squeaking sound can be seen within the range 1600Hz to 4000Hz. The magnitude of the humming sound is only 23dBA and the squeaking magnitude is only just over 25dBA. These sounds are of a very low magnitude and are only audible inside the building when there is no background noise. It should be noted however that the measurements represented in Figure 2.3.18 are for low reference wind speeds and it is likely that for higher wind speeds the magnitude of the sounds would be higher, particularly in the case of the humming sound and hence could cause annoyance in higher wind conditions.

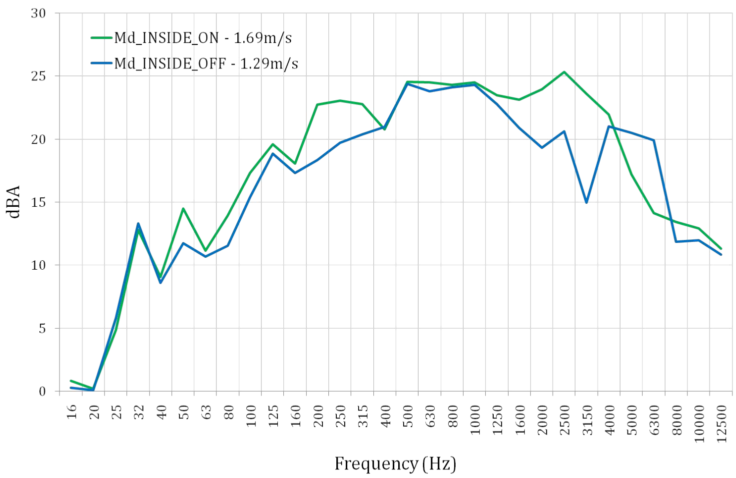

Figure 2.3.18: Measurements taken inside the building with the turbines on and off with low reference wind speeds up to 1.69m/s

Two separate plots are shown in Figures 2.3.19 and 2.3.20 both representing measurement data collected at installation (d) at measurement location Md1 on the roof of the building where the turbines are mounted. Measurements were taken with the turbines on and with the turbines off. Figure 2.3.19 shows two separate measurements with the turbines switched on compared to one measurement with the turbines switched off, all for for reference wind speeds of approximately 2.38m/s. Figure 2.3.20 also shows two separate measurements with the turbines switched on. One at reference wind speeds of 2.78m/s and one at very high reference wind speeds of 6.10m/s. The measurement shown in Figure 2.3.20 with the turbines switched off is for reference wind speeds of 4.63m/s.

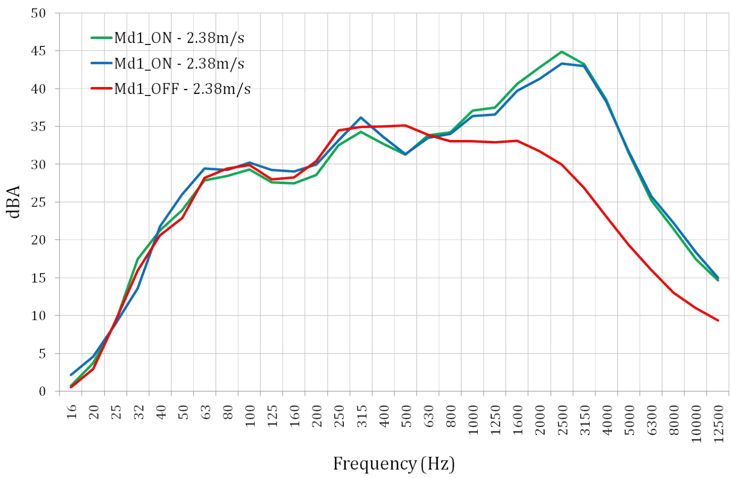

Figure 2.3.19: Measurements with the turbines on and off with reference wind speeds approximately 2.38m/s

The spectra plots in Figure 2.3.19 show that at reference wind speeds of 2.38m/s below 800Hz there are no significant differences between the magnitudes of the the noise for each of the 1/3rd octave frequency bands with the turbines on compared to with them off. Therefore, turbine noise is not significant below 800Hz. Above 1000Hz the turbine noise is however, clearly visible in the frequency spectra as the magnitude of the noise in 1/3rd octave frequency bands from 1000Hz upwards are significantly higher for measurements with the turbines on than for the measurements taken with the turbines switched off. The noise in this range is due to the clear swooshing sound the turbines make at these reference wind speeds in the form of a broadband sound across the highest parts of the frequency spectrum. As discussed previously and seen from the frequency spectra of measurements taken inside at installation (d) in Figure 2.3.18, the micro turbine type also makes a very distinctive squeaking sound as the turbine rotates. This sound was audible from the turbines inside the building where the swooshing sound was not. For the measurement taken inside, this squeaking sound occurred between 1600Hz and 4000Hz. Although much of the magnitude of the sound above 1000Hz from measurements taken at Md1 in Figure 2.3.19 is attributable to the swooshing sound, there is a clear and significant increase in the magnitude of the sound between 1600Hz and 4000Hz, up to 45dBA at 2500Hz. This is an increase in magnitude of up to 15dB compared to measurements taken with the turbines off at the same wind speed and is attributable to the squeaking sound heard. The frequency range for the squeaking sound is therefore in agreement with the range for the measurements taken inside the building. At higher wind speeds, when the rotors of the turbines are rotating at up to 1200rpm the squeaking sound no longer becomes perceptible from the sound recordings taken in parallel with the collection of the measurement data. Based on a subjective interpretation of the recordings taken simultaneously to collection of the noise data, at these fast rotational speeds the swooshing sound turns into an aerodynamic sound similar to the sound a fan makes.

Figure 2.3.20 shows frequency spectra for measurements taken when the turbine rotors were turning with high rotational speeds up to 1200rpm. Spectra are presented both with the turbines on and with them off.

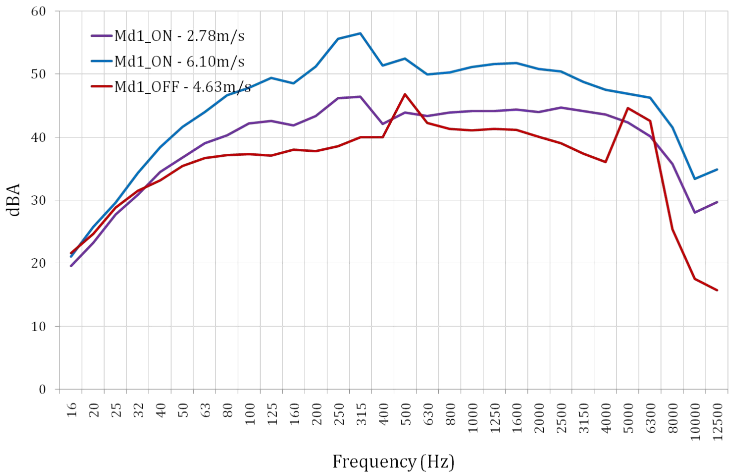

Figure 2.3.20: Measurements with the turbines on and off with very high reference wind speeds up to 6.10m/s

The significant observations to take from Figure 2.3.20 are as follows:

- Background noise occurs at very low frequencies below 100Hz;
- Increases in the sound levels with the turbines turning compared to data collected when they are not occur over the whole of the frequency spectrum due to the swooshing noise mechanism.
- At very high rotational speeds up to 1200rpm the swooshing noise mechanism changes to the noise similar to that of a fan and is represented over a larger portion of the frequency spectrum;
- The peak in the spectrum from 200-400Hz for very high reference wind speeds (6.10m/s) is heard as a humming sound with a magnitude up to 56.5dBA a margin of over 15dB compared to measurements with the turbines off;
- The magnitude of the swooshing noise mechanism occurring at the higher end of the frequency spectrum is approximately 52dBA compared to up to a magnitude of 41dBA with the turbines off;
- When the turbines are switched on at lower reference wind speeds, the magnitude of the turbine sounds across the spectrum are also lower.

Figure 2.3.21 also shows frequency spectra for data collected at installation (d) but compares measurements taken at location Md1 with the turbines off with measurements taken at location Md3 with the turbines on, both at 5.75m/s. This gives a clear indication of how the turbine noise attenuates to location Md3, approximately 64m from the turbines at ground level rather than on the roof. There are no significant differences below 800Hz between measurements taken with the turbines off at Md1 and measurements taken with the turbines on at Md3, showing that the background and wind noise is roughly equal for both measurements. Above 800Hz, the magnitude of the sound is higher further from the turbine mounting positions showing that the swooshing and fan type noise mechanism at these high reference wind speeds can be heard at distances of 64m from the turbines over and above any wind and background noise. However, the magnitude of the fan type sound and the swooshing noise mechanism has attenuated to a maximum of 45dBA reducing down to 30dBA at the highest frequencies. Although turbine noise is clearly audible and visible in the frequency spectrum at Md3, the magnitude of the sound pressure levels at the high end of the frequency spectrum are lower than for measurements taken on the roof at Md1 with the turbines switched on at similar wind speeds (see Figure 2.3.20). This means that the sound from the turbines has attenuated, and further from the turbines where building obstructions will cause further attenuation of the noise it is unlikely that the turbine noise would be audible.

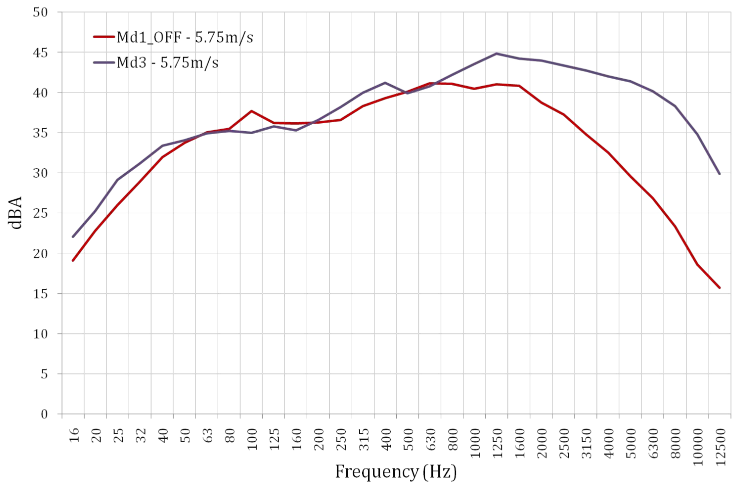

Figure 2.3.21: Measurements at increasing distances from the turbines with high reference wind speeds approximately 5.75m/s

The final two frequency plots to be given in this Section to represent the noise from the micro wind turbine type are given in Figures 2.3.22 and 2.3.23. Both Figures represent data collected at installation (f). Figure 2.3.22 shows measurements taken at increasing distances from the turbine to give an indication of how the turbine sounds attenuate and Figure 2.3.23 shows data from four measurements taken at location Mf4, 9m from the turbine hub at increasing wind speeds, where at the lowest wind speeds the rotor of the turbine was not turning.

The frequency spectra in Figure 2.3.22 shows measurements taken at increasing distances from the turbine at low reference wind speeds up to 1.52m/s. Mf1 is 11m from the turbine, Mf3 also 11m from the turbine, Mf6 22m from the turbine and Mf7 56m from the turbine. Below 100Hz any differences in the sound levels are due to the changes in background wind noise because the higher reference wind speeds have the highest magnitude of sound for 1/3rd octave bands below 100Hz due to increased wind noise over the microphone. Above 100Hz the closer the measurement locations are to the turbine, the higher the magnitude of the sound for each of the 1/3rd octave bands is, showing that the turbine sounds attenuate through the air, so the further from the turbine hub, the less turbine noise is audible. Figure 2.3.22 also shows that the sounds at the highest frequencies attenuate over a much shorter distance as the differences seen between measurements taken at subsequently increasing distances are much lower, particularly between Mf6 and Mf7 above 4000Hz. It would be expected that measurements taken at Mf1 and Mf3 would be equal in magnitude as both locations are the same distance from the turbine hub however the magnitude of the 1/3rd octave bands is significantly higher for Mf1 than Mf3, particularly above 2500Hz. This is because although the wind speeds are roughly equal for the two measurement locations it was noted during data collection that the turbine was not turning consistently during the data collection at Mf3 and was not making the swooshing sound this micro turbine type typically makes. This confirms that the swooshing noise mechanism occurs above 1000Hz supporting the observations made from data collected at installation (d). The turbine was not rotating fast enough during any of the measurements in Figure 2.3.22 to make the squeaking noise mechanism observed from the data at installation (d) to be apparent.

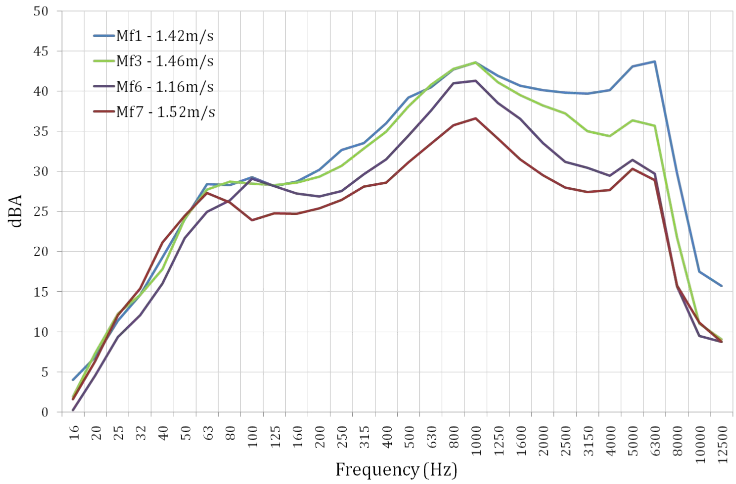

Figure 2.3.22: Measurements at increasing distances from the turbine with reference wind speeds up to 1.52m/s

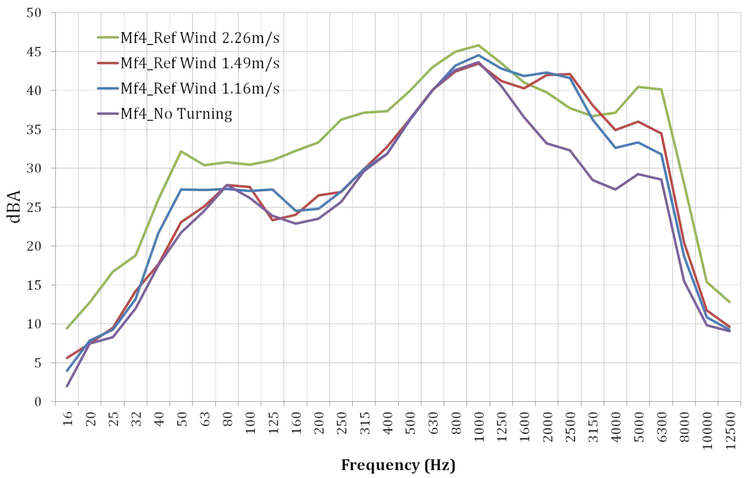

Figure 2.3.23: Measurements taken in the same location with increasing reference wind speeds up to 2.26m/s

The final spectra plot in Figure 2.3.23 supports the observations made from the data collected at installation (d) comparing measurements with the turbines switched on and switched off. This is because the frequency spectra in Figure 2.3.23 compares data collected at installation (f) at measurement location Mf4 at increasing reference wind speeds, where the rotor was not turning at the lowest wind speeds. Below 1250Hz, there are no differences between measurements taken when the turbine is not turning compared to increasing wind speeds except for the highest reference wind speeds used for the comparisons. When the turbine is turning well at 2.26m/s reference wind speeds the magnitude of the sound over the whole frequency spectrum increases. Above 1250Hz there is a sudden increase in sound for each of the 1/3rd octave bands for all measurements where the rotor was turning peaking at 42dBA at between 2000Hz and 2500Hz for data collected at reference wind speeds of 1.49m/s and 1.16m/s. In the sound recording taken in parallel to this data collection swooshing is audible at these reference wind speeds. When the reference wind speed increases to 2.26m/s, the squeaking noise mechanism becomes audible and the sound levels peaks at 40dBA between 4000Hz and 6300Hz. This is a higher frequency than observed at installation (d), potentially because there is only one turbine sited at installation (f) compared to two at installation (d).

Overall the key noise mechanisms the micro turbine type makes are squeaking at mid reference wind speeds when the rotor is turning well but not at the highest reference wind speeds. Swooshing occurs for all winds speeds at the higher end of the frequency spectrum, however when the reference wind speeds are high and the rotor turns at up to 1200rpm the swooshing sound turns to a fan type sound and occurs over a larger range of the frequency spectrum. A humming sound can be audible from the turbines when measurements are taken inside the building where a turbine is mounted on the roof. This is not an aerodynamic sound but a sound that is transmitted structurally. This means the humming sound is not effectively radiated to the external environment but is easily audible inside the building when background noise is low. Further frequency spectra plots for each micro wind installation to support the observations made in this Section are found in Appendix C. The spectra in the appendix are for measurements taken at mid range wind speeds not discussed in this Section. In the following Section, a brief comparison of the micro and small wind turbine types will be given with a more detailed conclusion in Section 2.4.

2.3.2.3 Comparison of Micro and Small Turbine Types

In the previous Sections of the Thesis a full analysis of the measurement data collected at all installations of the small turbine type S1 and the micro turbine type M1 has been given. This included an analysis of the overall sound levels and how these increase with increasing reference wind speed and an analysis of the frequency spectra collected with the data. In this Section an outline of the important comparison between the two turbine types will be given, with a full conclusion of the noise measurement results in Section 2.4.

- From the scatter plots of the measured overall sound pressure levels against reference wind speeds, the highest measured sound pressure levels are 65dBA for both turbine types at the highest reference wind speeds. As reference wind speed increases so does the measured sound pressure level;

- Sound levels for frequencies below 100Hz are due to wind noise over the microphone. This is true for both turbine types;
- The swooshing noise mechanism is audible from both the micro and small turbine types. For both turbines it is broadband in nature and occurs above 1000Hz for low to mid reference wind speeds and over an increased range of the spectrum for higher reference wind speeds;
- The magnitude of the swooshing noise mechanism is higher for higher reference wind speeds up to 50dBA for both the micro and small turbine types;
- The humming and buzzing noise mechanisms audible from measurement data taken at locations closest to the hub of the small turbine type occurs at two tonal peaks in the spectrum from 100Hz to 125Hz and 200Hz to 400Hz. The frequency ranges of these two peaks are higher as the reference wind speed and rotational speed of the turbine increases. The humming noise mechanism is not audible from the micro turbine type, except when measurements are taken inside;
- For both turbine types, the further measurement data is collected from the turbine hubs, the less audible the turbine sounds are. This is particularly the case for the tonal noise mechanisms of humming from the small turbine type and the highest frequency sounds from the micro turbine types;
- A squeaking aerodynamic noise mechanism occurs from the micro turbine type when the rotor is turning well and is associated with the rotational speed of the turbine. The range of frequencies for the squeaking noise mechanism is from 1600Hz to 4000Hz. This squeaking noise mechanism does not occur from the small turbine type;
- The chopping noise mechanism the small turbine makes at high reference wind speeds does not occur for the micro turbine type, however the swooshing noise mechanism from the micro turbine type turns to a noise similar to the noise a fan would typically make at the highest reference wind speeds. This is due to the very high rotational speeds of up to 1200rpm for the micro turbine type compared to only 230rpm for the small turbine type.

In the following and final Section of the noise measurement results Section an analysis of the results from the sound maps created with the noise mapping software CadnaA will be given. The sound maps will serve to give an indication of how the small wind system noise attenuates at each installation and how this compares to the measurements taken.

2.3.3 Graphical Noise Software

In this Section of the Thesis, the results of the analysis carried out using the CadnaA sound mapping software will be given. Sound maps from one small and one micro turbine installation will be used to illustrate the results. Sound maps for all other installations are given in Appendix D, Section D.2. The sound mapping software CadnaA was used to create sound maps for each of the installations where measurements were taken. For an outline of the methodology for this work see Section 2.2.2. The sound maps were calculated over the topography maps at each of the installations and the turbines were set as a point source of sound to look at how the sound attenuates over the map area rather than the absolute levels of sound due to the turbines. This is because the noise small and micro turbines generate is dynamic and is dependent on factors such as wind speed (hence how fast the rotor rotates) and the direction the rotor is facing relative to the wind speed (small wind systems are much more dynamic in yaw than large turbines). Factors such as the level of background noise and wind noise will also play a role. To get an accurate representation of how noise from small wind systems attenuates, a separate sound map would have to be generated for a full range of wind speeds at a variety of wind directions. The sound maps would also be required at each possible small wind system sound power level at each key frequency. This is possible but is outside the scope of the current research.

2.3.3.1 Sound Maps

First it was necessary to check that the reduction in sound is linear over the range of frequencies, i.e. is the level of attenuation of the sound the same over a range of magnitudes for a given frequency. The turbines at each installation were set as a point source of sound of 30dB, 50dB, 70dB and 100dB at frequencies of 500Hz and 2000Hz. The amount the sound attenuated over the map for each installation at each sound level and frequency was then investigated. The facade values of selected buildings at each installation were also examined. The sound maps for this analysis will not be shown here but it can be confirmed that the attenuation of sound was linear for both frequencies at each installation. The colour palettes showing the magnitude of sound each colour on the sound map represents for each magnitude sound power level are given in Appendix D, Section D.1.

For the final analysis of the attenuation of the sound at each installation, the turbines were set as a 50dB point source of sound at 12.5Hz, 25Hz, 50Hz, 100Hz, 200Hz, 400Hz, 800Hz, 1600Hz, 3150Hz, 6300Hz and 12500Hz. A separate sound map was created for each frequency with the grid spacing set as described in Section 2.2.2. The sound maps and the facade sound pressure levels of selected buildings at each installation were investigated. The important frequencies associated with the turbine noise mechanisms observed from the spectral analysis of the measurement data at each installation were investigated in more detail.

From the analysis of the spectra in Section 2.3.2.1, for the small turbine type S1, there are two peaks in the frequency spectrum due to the humming noise mechanism in the frequency ranges of 100Hz-125Hz and 200-630Hz. The sound maps at small turbine installation (a) for a 50dB turbine sound power level at 100Hz and 200Hz are shown in Figure 2.3.24 to reflect this. The swooshing noise mechanism for the small turbine type occurs between 1000Hz and 12.5kHz and peaking at 3150H. Therefore, sound maps at 3150Hz and 12.5kHz are also shown in Figure 2.3.24. Figure 2.3.25 shows building facade values at installation (a) with the turbine set as 50dB point source of sound at a frequency of 3150Hz.

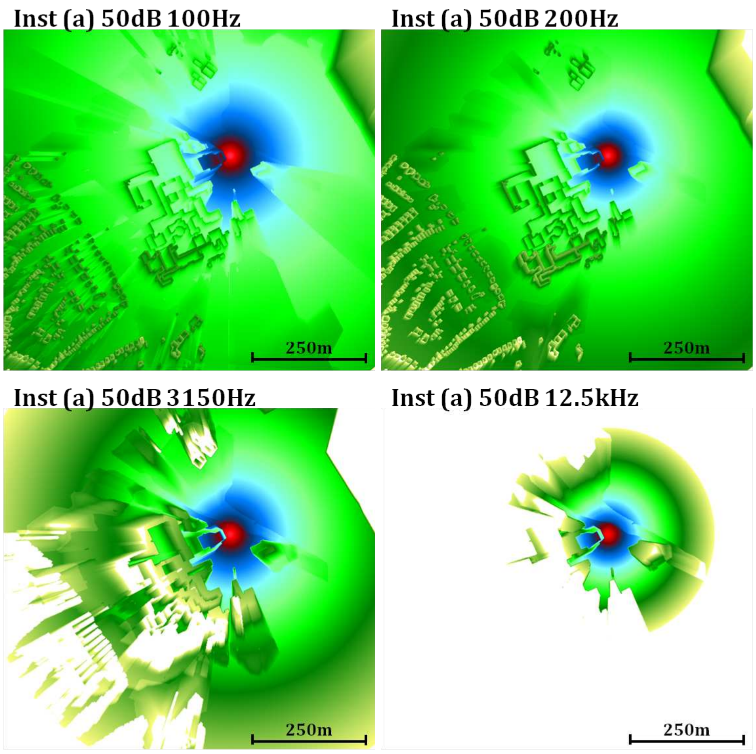

Figure 2.3.24: Sound maps for installation (a) with a point sound source at the turbine hub with a sound power of 50dB at 100Hz, 200Hz, 3150Hz and 12.5kHz

Figure 2.3.25: Map of installation (a) showing sound pressure levels at building facades close to the turbine

From the analysis of the spectra in Section 2.3.2.2, the micro turbine type M1 does not make the humming noise mechanism which is audible from the small turbine type. The swooshing mechanism does occur above 1000Hz and a squeaking noise mechanism occurs between 1600Hz and 4000Hz. At higher wind speeds, the micro turbine type makes a noise similar to that a fan makes occurring over a larger range of the frequency spectrum. Therefore Figure 2.3.26 shows sound maps at installation

(d) at 200Hz, 1600Hz, 3150Hz and 12.5kHz. Figure 2.3.27 shows building facade values at installation (d) with the turbines set as 50dB point sources of sound at 3150Hz.

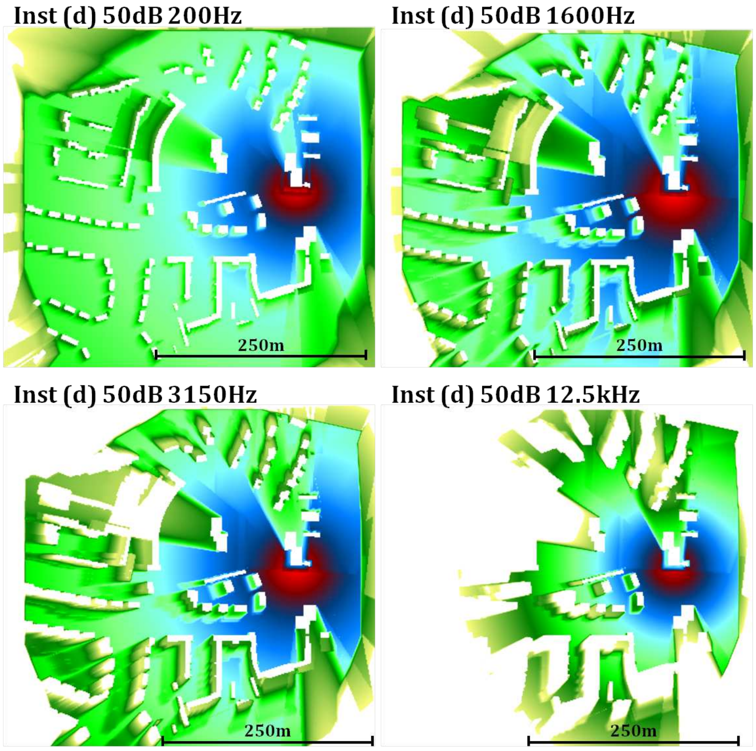

Figure 2.3.26: Sound maps for installation (d) with a point sound source at each of the turbine hubs with a sound power of 50dB at 200Hz, 1600Hz, 3150Hz and 12.5kHz

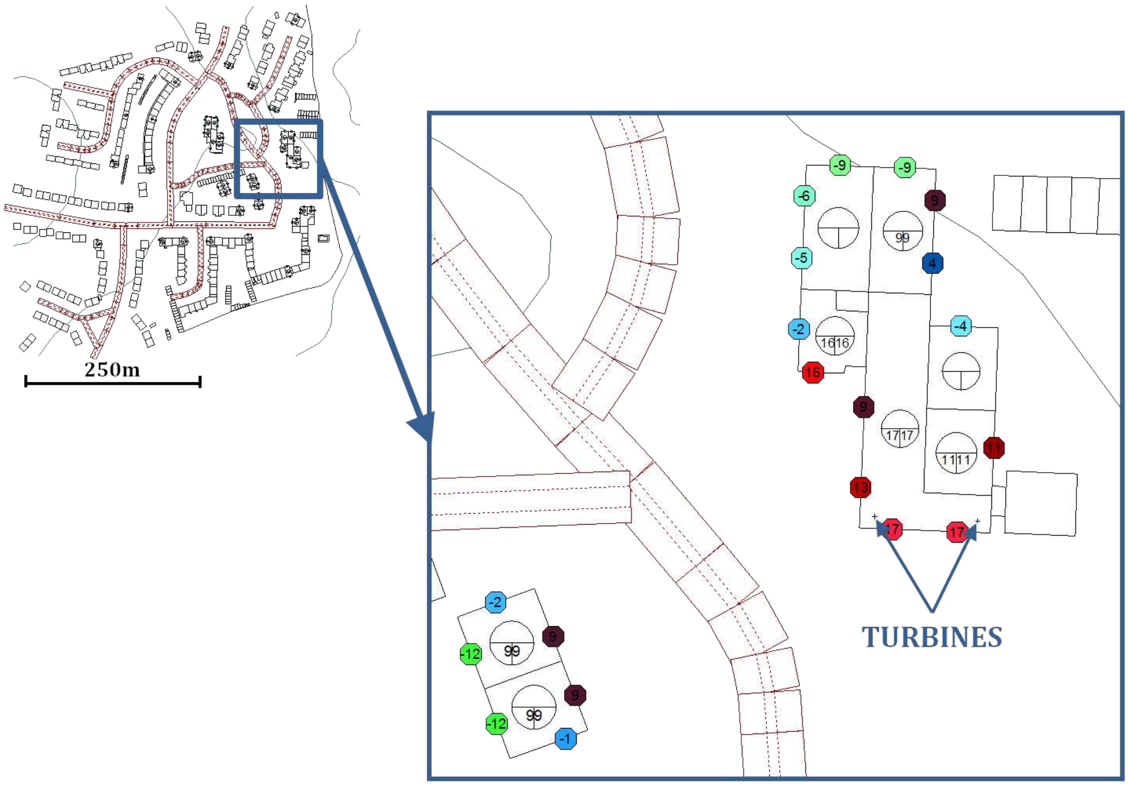

Figure 2.3.27: Map of installation (d) showing area topography and sound pressure levels at building facades close to the turbines

The sound maps for installation (a) and installation (d) show that as expected higher frequency sounds attenuate over a shorter distance compared to the the lower frequency sounds. The atmospheric air has an attenuation factor which removes a proportion of the acoustic energy each time the sound wave undergoes a cycle. As high frequencies have shorter wavelengths, the attenuation per meter is much higher than for low frequencies. This is illustrated by looking at the facade values closest to the turbines in Figure 2.3.25 for installation (a) and Figure 2.3.27 for installation (d). The 3150Hz, 50dB point source of sound at installation (a) has attenuated by 34dB to the closest building facade approximately 17m from the turbine. At installation (d) the two 50dB point source sounds from the turbines have attenuated by 33dB to the nearest building facade approximately 16m from the turbine hubs. The building facade values and the sound maps given can be used to develop a general relationship for how a point source of sound due to the turbines at different frequencies will attenuate at each installation. The rated sound power levels as quoted by the manufacturers of the small and micro turbine types are approximately 89dBA. The attenuation of the sound observed from the sound maps and building facade values are in line with the sound pressure levels quoted by the manufacturers of the micro and small turbine types 25m and 60m from the turbines. For the small turbine type the quoted values are $L_{p,25m}$ equal to 53dBA and $L_{p,60m}$ equal to 45.5dBA and for the micro turbine type $L_{p,25m}$ equal to 54dBA and $L_{p,60m}$ equal to 46dBA.

The attenuation maps will be used in more detail in the Noise Measurement Conclusion in Section 2.4 where the attenuation level indicated by the sound map will be compared to the levels as seen from the spectral analysis of the noise measurement data.

2.3.3.2 The Influence of Road Noise

The results of the measurement data showed that at installation (e) the background traffic noise is sufficiently high so the turbine is rarely audible over and above the background noise. To verify this finding sound maps with traffic noise were examined for installation (e). The major road settings were 6000 vehicles in an 18hr period (i.e. 1 car every 10 seconds) at a speed of 30mph (50kph). Minor roads were set with 200 vehicles in an 18hr period (i.e. 5 cars in a 30 minute period) at a speed of 20mph (30kph). Figure 2.3.28 shows sound maps for installation (e), both with traffic noise but with and without turbine noise set (a sound power level of 50dB). Figure 2.3.28 shows that the sound maps are identical with and without the turbine noise, confirming that the turbine noise would not be audible over and above the background traffic noise as this is the dominating source of sound. This would be the same for all turbine installations with a large volume of passing traffic.

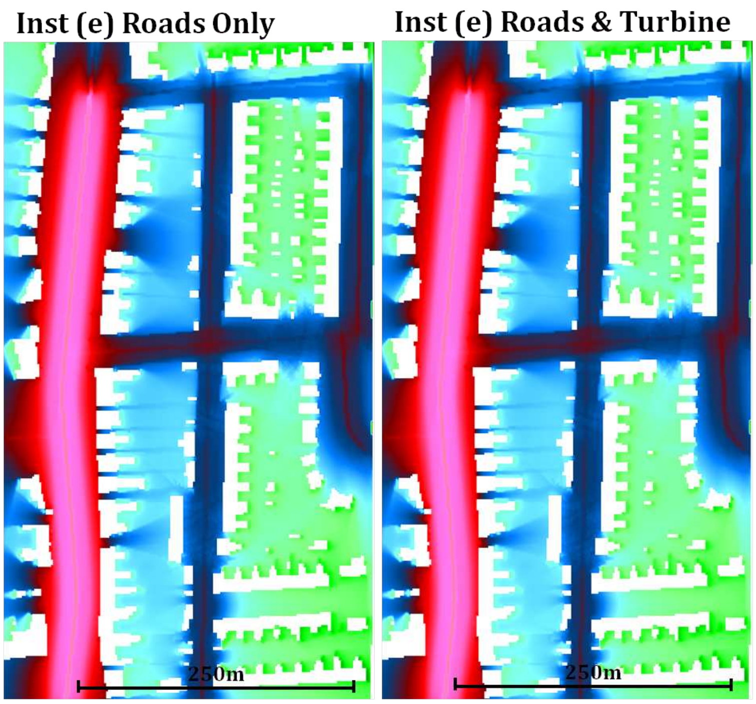

Figure 2.3.28: Sound maps for installation (e) showing road noise with and without turbine noise.

2.3.3.3 The Effect of Wind Speed and Directionality on Sound Levels

It was also important to investigate how the wind affects how noise attenuates. This was done by setting a point source of sound of 50dBA and applying a southerly wind of 0m/s, 1m/s and 12m/s at 12.5Hz, 500Hz, 2000Hz and 12500Hz. The results for the 500Hz and 2000Hz analysis will be given here and are presented in Figures 2.3.29 and 2.3.30 as these frequencies are the most representative of the turbine noise. Maps for the other two frequencies are given in Appendix D, Section D.2. As has been seen in the sound maps for each installation presented in Section 2.3.3.1, higher frequency sounds attenuate quicker than lower frequency sounds. This phenomenon can also be seen in Figures 2.3.29 and 2.3.30. The magnitude of micro and small turbine noise sound power levels are sufficiently low so that for distances over 100m from a turbine hub, little noise should be experienced, except in high winds or when background noise levels are very low. As is shown in Figures 2.3.29 and 2.3.30, faster wind speeds do not affect how the noise attenuates any more than lower wind speeds and only a sound which has attenuated to a low level is affected by the wind. As a rule of thumb, additional attenuation due to wind effects only becomes noticeable at distances remote from the source. Close to the source the effects are negligible. If the source is loud, this can mean the effect is quite marked at distant observation points. If the source is weak, inverse square law attenuates the source to the point where it is inaudible at distant observation points and a listener would not notice the sound. When considering this for the turbine sounds from the results of the measurement data collected it has been seen that the turbine noise should be sufficiently low far from the turbine so that wind magnitude and direction should not affect the level of turbine noise experienced, and any effects of the wind on noise levels would not be noticeable. It is more likely that the level of wind noise and increases in background noise due to the effect of the wind (i.e. such as increased tree noise) are more likely to affect how the turbine noise is perceived.

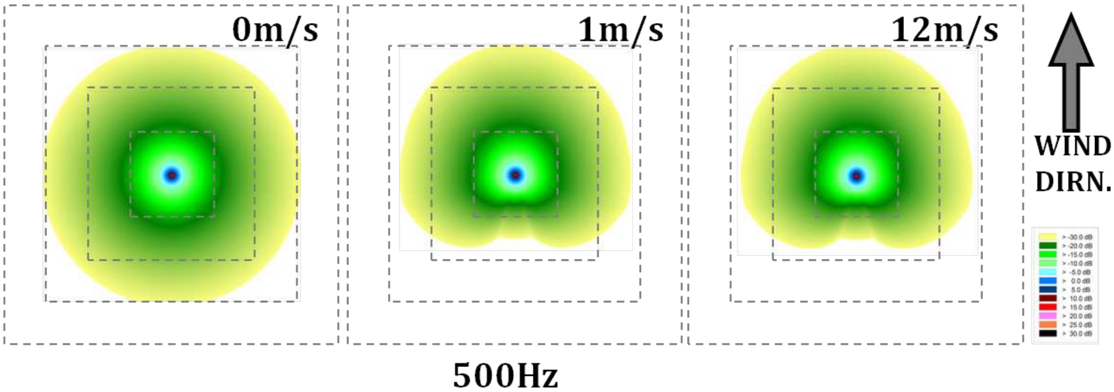

Figure 2.3.29: Sound map showing the effect of wind speed on a 50dB point source of sound at 500Hz

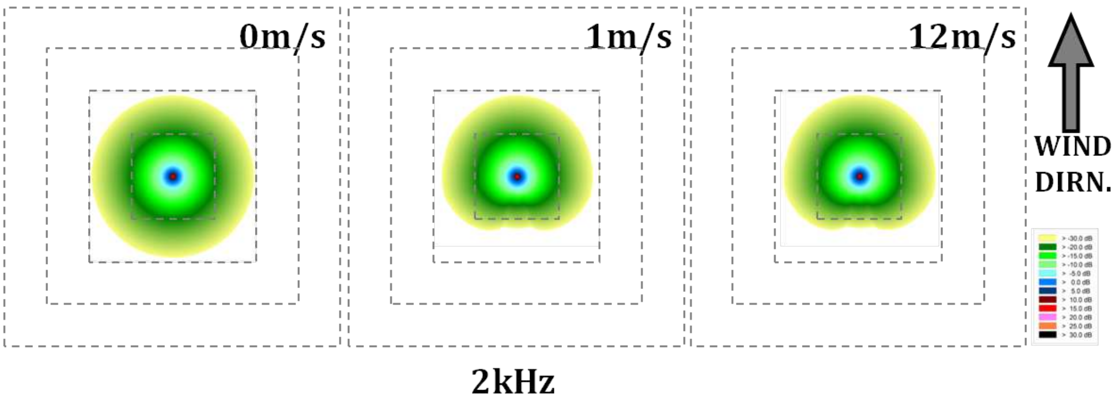

Figure 2.3.30: Sound map showing the effect of wind speed on a 50dB point source of sound at 2kHz

Temperature effects will also play a role in how the wind turbine sound propagates and attenuates through the atmosphere. One reason for this is that the speed of sound is dependent on temperature and at higher temperatures, the speed of sound increases. Another reason is that temperature gradients change how sound waves refract through air. When the temperature is the same at all elevations, the propagation of sound waves occurs in straight lines emanating from the sound source. At different times of the day, temperature gradients occur. During the day, the sun heats the ground and hence the air temperature close to the ground is warmer than at higher elevations and the speed of sound further from the ground is also lower. At night, as cooling of the ground occurs, the air close to the ground is cooler than at higher elevations and the speed of sound increases with elevation. This means that during the day, sound rays refract and curve upward. Therefore, sound levels close to the ground due the sound source are lower than when the sound propagates in a straight line. At night the opposite is true and downward refraction occurs. Therefore, sound levels close to the ground at a certain distance from the source are higher than normal. More complex refraction patterns occur if the temperature gradients are not uniform and/or the wind speed and direction plays a role. These temperature effects have been acknowledged but a full analysis of them on wind turbine sound attenuation is outside the scope of this research. For this reason, the temperature has been set as dry air at $20^{o}C$ for all sound map calculations where the corresponding speed of sound is $343.2m/s$.

In this Section, an analysis of the noise maps generated using the sound mapping software CadnaA has been given. In the following Section a conclusion of all the noise measurement data will be given including recommendations for future work.

2.4 Conclusions of the Noise Measurement Work

The aims and objectives of the noise measurement work have been achieved. The noise levels from real small and micro wind turbine installations have been measured and the noise characterised. A spectral analysis of the noise has been carried out as well as an investigation of the attenuation of the sound at each installation. Together, the results have given an indication of the noise likely to be experienced at real micro and small turbine installations. This information can be fed back to planners and policy makers as well as small wind system manufacturers and individuals living close to a proposed small wind system site to satisfy the drivers of the research.

It has been found that the measured sound pressure levels at all installations are not high. For the micro turbine type, the maximum A-weighted L_{eq} values measured in high reference wind speeds were 68.35dBA at installation (d) and 62.63dBA at installation (f) at 12 metres and 11 metres from the turbines respectively. At low reference wind speeds at the same measurement locations and installations the equivalent A-weighted sound pressure levels are measured between 45dBA and 50dBA. The rated sound power level quoted by the micro turbine manufacturer at 8m/s wind speeds is 89.5dBA. It is quoted that 25m from the turbine, the noise has attenuated by 35.5dB [49].

The measured values for the small turbine type are similar to the micro turbine type. For example, at installation (b) in high reference wind speeds, 14 metres from the turbines the maximum measured

A-weighted L_{eq} level is 63.17dBA. 122 metres from the turbines at the same reference wind speeds the A-weighted L_{eq} level implied by the trend line is 51dBA. This suggests an attenuation of over 12dB. At low reference wind speeds, these levels are 53.28dBA and 45.14dBA, 14 metres and 122 metres from the turbine respectively; an attenuation of 7dB. However, attenuation values for noise only attributable to the turbines are likely to be higher as all measured sound pressure levels include background noise. The rated sound power level quoted by the small turbine manufacturer at 8m/s wind speeds is 89dBA. It is quoted that 25m from the turbine, the noise has attenuated by 36dB [50]. All measured values for both the micro and small turbine types appear to be in agreement with these values, particularly as the sound pressure levels measured include background noise. At installations with high traffic noise, the levels from the turbines have been shown to be sufficiently low so the turbine noise is not audible or visible in the analysis of the L_{eq} sound levels or frequency spectra.

Even though the environmental sound pressure levels measured are low and equivalent to general conversation levels, a full spectral analysis has been carried out. This is because it has been suggested by Waye and Ohrstrom [51] that it is the characteristics of the turbine noise and not the absolute levels which may affect individuals living close to turbine installations.

The sounds typically heard from the micro turbine type are swooshing in all reference wind speeds, squeaking at low to mid reference wind speeds and at high reference wind speeds the swooshing sound turns in to a fan sound due to the very high rotational speeds of the rotor. Sound is transmitted through the building structure a micro turbine is mounted on and is audible inside as a humming sound. Swooshing is also heard from the small turbine type at all wind speeds and as the wind speeds increase the swooshing aerodynamic sound can change to a chopping sound if the rotor is oriented slightly out of the wind direction. Humming is heard from the tower base close to the turbine, this sound however attenuates quickly as its source is close to the ground and obstructions have a large effect on the attenuation. Aerodynamic sounds are emitted from the rotor hub so are able to travel further without obstructions causing attenuation. These descriptions of the sounds heard during collection of the noise measurement data from both the micro and small turbine types are subjective and the frequencies associated with the sounds have been established from analysis of the frequency spectra.

The swooshing noise heard is a broadband sound typically occurring above 1000Hz peaking at around 3150Hz. From this it can be deduced that the swooshing noise heard from the turbine is associated with inflow turbulence and turbulent boundary layer trailing edge noise. Wagner [17] stated that inflow turbulence noise occurs as a swooshing sound up to 1000Hz for large scale turbines and turbulent boundary layer trailing edge noise occurs up to 1500Hz. Due to the increased rotational speeds of micro and small turbines compared to large scale turbines, these noise mechanisms present themselves at higher frequencies. At increased rotational speeds the broadband chopping and fan sounds heard from the small and micro turbine types respectively typically occur over a larger portion of the frequency spectrum and are still associated with inflow turbulence and turbulent boundary layer trailing edge noise.

The humming and buzzing noise mechanisms heard from the small turbine type are tonal in nature and occur in the frequency spectra analysed at 100Hz to 125Hz and 200Hz to 400Hz. These noise mechanisms are not aerodynamic sound sources but due to the electro-mechanical workings of the turbine at the hub.

The squeaking noise mechanism from the micro turbine type occurs between 1600Hz and 4000Hz and is therefore tonal in nature. The exact frequency depends on the wind speed and hence rotational speed of the rotor. The squeaking noise mechanism only occurs at low to mid reference wind speeds and is heard cyclically as the turbine rotates. As a tonal sound, the squeaking could be due to tip noise interacting with the turbine mast. Possible other noise mechanisms creating such a tonal source of sound could be blunt trailing edge noise or laminar boundary layer trailing edge noise. However, Wagner [17] also stated that these noise mechanisms can be eliminated with careful design. Further analysis is required to determine the exact noise mechanism associated with the squeaking sound and whether the design of the micro turbine type could generate the squeaking sound.

The magnitude of all the sounds audible at the key frequencies decrease the further from the turbines measurements are taken, and the exact frequencies at which the sounds occur vary depending on the wind speed and hence the rotor rotational speeds. For example, at higher reference wind speeds the squeaking sound occurs at a higher frequency and at fast rotational speeds, broadband sounds occur over a larger portion of the high end of the frequency spectrum. The frequency spectra analysed show that higher frequency sounds attenuate at a faster rate. This is confirmed by looking at the attenuation of a 50dB point source of sound at a range of frequencies at each installation from the sound maps created using CadnaA software.

From the spectra in Figure 2.3.22, it is seen that at Mf1, 11 metres from the turbine, the magnitude of the sound at 6300Hz is approximately 43dBA. At Mf7, 56 metres from the turbine the measured sound pressure level was approximately 30dBA, an attenuation of 13dBA. The sound map created for installation (f) shows that the attenuation between Mf1 and Mf7 is approximately 20dBA due to the colours of the regions on the sound map corresponding to where these measurements took place (see Appendix D for colour palettes). It can be assumed that these values are in agreement with each other as the measurement data collected for spectral analysis includes background noise and attenuation levels on the sound maps do not. These attenuation levels are also in agreement with values quoted by the manufacturer.

The conclusions given here are a snapshot of the key findings of the research. This work is the first of its kind for small wind systems and can be considered as a starting point for future work. In Section 5, comparisons will be made between the results of the noise measurement analysis and analysis of the data collected for the studies of the psychological and health impacts of small wind systems and the noise modelling results.

There are limitations to the noise measurement work. Measurements taken are environmental noise measurements and no attempt has been made to mathematically remove the turbine noise from the background noise, i.e. the turbine noise has been identified by listening to sound signals recorded during collection of the data. In addition to this, wind speed measurements taken for the current research act as a reference only as it was not possible to take measurements at the hub. Further work could include taking continuous noise measurements over a number of weeks and conditions. Continuous wind speed measurements at hub height could also be taken simultaneously with noise data collection. This would allow quantification of sound power levels in all conditions and at a full range of wind speeds. With detailed continuous noise measurements a full assessment of the attenuation of the turbine noise to various locations around the turbines and whether this agrees with the inverse power law would also be possible.

The focus of the current research has been on aerodynamic noise, however the results suggest that mechanical noise is present at the base of a small turbine tower. The results also suggest that if a micro turbine is building mounted, noise is transmitted through the structure of the building and is audible inside. For this reason, future work could include full assessment of vibration and mechanical noise.

It would be advantageous for future work to compare to measured manufacturers' data and include more turbine types in the analysis to get a more complete picture of small wind system noise.

More sophisticated methods for measuring aerodynamic noise from small and micro wind turbine aerofoils as outlined in Section 2.1 could be considered for further work if the resource were available. These include, the use of a wind tunnel or PIV. New methods are also becoming available such as the use of an acoustic camera. These methods would in future allow confirmation of the noise mechanisms associated with the sounds heard from the small and micro wind turbines included in the study. This would be of particular importance to assess whether blunt trailing edge noise causes the squeaking sound for example.

In the following Chapter full details of the studies of psychological and health impacts of small and micro wind systems will be given.

Chapter 3

Psychological and Health Impacts

There is little understanding of how individuals are likely to be affected by small wind system noise. An introduction to the research and drivers for the current research has been given in Chapter 1. It is important to identify the types of noises individuals perceive from small wind systems sited close to where they live in order to have an idea of the level of noise experienced at real turbine installations and the noise mechanisms associated with the turbines (see Section 1.2 for a review of wind turbine noise mechanisms). However, there is likely to be between-individual differences in the way that this noise is perceived. An investigation of how these effects of between-individual differences on the perception of noise affect general health should also be carried out. This would give (i) a picture of whether small wind system noise is a problem in built up areas and (ii) for whom is this noise likely to be more of a problem.

This Chapter of the research serves to achieve the objective of the study of the psychological and health effects of small wind systems included in this research:

- To survey individuals living close to small and micro wind turbine installations, to investigate the level and type of noise perceived and to link this to individuals attitudes towards wind turbines and personality and temperamental characteristics.
- To confirm the results with an experimental recordings study and compare the results of the two studies to the results of the noise measurements and noise modelling.

Two separated studies will be carried out, the first, a domestic study will be sent to individuals living close to a real small or micro wind turbine installation, the second is an experimental recordings study where individuals are played recordings of small wind system noise which have been chosen by the researcher.

In this Chapter the current relevant literature associated with the psychological and health impacts of small wind systems will be reviewed. Next, the methodology and results of the statistical analyses of the data for both a domestic questionnaire and an experimental recordings questionnaire will be given. Finally conclusions and comparisons of the two questionnaire studies will be given including recommendations for future work.

The relevant theory for the statistical tests used to analyse the data is given as a reference in Appendix E.

Statistical Terms

A	intercept values of the regression equation
α	Cronbach's alpha
$\hat{b_1}$,$\hat{b_2}$,$\hat{b_3}$	simple slopes regression coefficients
B	gradient of the slope of the regression equation / unstandardised regression coefficient
β_i	standardised regression coefficient for the ith IV
CI	confidence interval
df	degrees of freedom
DV	dependent variable
F	F-statistic from ANOVA test
IV	independent variable
k	number of independent variables in the regression equation
N	Number of values in a sample
p	probability
pr^2	partial correlation
r	Pearson r
r_s	Spearman's rank order correlation
r_{yi}	correlation between the DV and the ith IV
R	multiple correlation
R^2	squared multiple correlation
sr^2	semi-partial correlation
SD	standard deviation
SE	standard error
SS	sum of squares
t	t-score
$\hat{\omega}$	simple slope
x	simple slopes predictor variable
xz	simple slopes interaction effect
X	value of a score in a sample / independent variable

$\overline{X}$	mean of a sample of scores with X values
$\hat{y}$	simple slopes model implied value of Y
Y	dependent variable
Y'	predicted values of Y
z	simple slopes moderator / z-score / standard score

Abbreviations

The abbreviations used within this Chapter of the Thesis for the measures described in Sections 3.2.1.2 and 3.3.1.2 are as below. These abbreviations shall also be used when presenting the results in Sections 3.2.2 and 3.3.2.

NOP = negative oriented personality; **NSS** = non-specific symptoms; **ATT** = attitude to wind turbines; **ACTUAL** = typical noise level rating; **LOUD** = perceived noise loudness; **OCCUR** = perceived noise occurrence; **SYMP** = symptom reporting score; **PA** = positive affect; **NA** = negative affect; **N** = neuroticism; **FD** = trait frustration discomfort; **F-disc** = discomfort intolerance; **F-emot** = emotional intolerance.

The following abbreviations shall only be used when describing the measures and results of the recordings study in Section 3.3.

LOUDx = perceived noise loudness from each recording (x - denotes which recording the score refers to); **ANNOYx** = the annoyance rating of each recording (x - denotes which recording the score refers to); **LENGTHx** = the length of time to switch off rating for each recording (x - denotes which recording the score refers to); **ALL** = scores for all recordings; **ALLT** = scores for all recordings with turbine noise; **SOUND** = scores for all sound recordings with turbine noise; **VIDEO** = scores for all video recordings with turbine noise.

3.1 Literature Review

3.1.1 Introduction

Recent evidence suggests that the public are increasingly turning to environmental causes for symptoms and malaise when medicine cannot offer satisfactory explanations [52]. For example, individuals will point to a nearby mobile phone mast or radio transmitter to make sense of broad symptoms of ill health [53]. Similarly, increases in perceptions of ill health at a time when general health is improving (known as the paradox of health) demonstrate that other potentially psychological factors may be at play when understanding people's willingness to report feeling unwell. Concern about invisible environmental agents especially those from new technologies, such as radiation, radio-waves, and odours, appear to act as a trigger for such reports of ill health [53]. Indeed, it has been argued that a rise in green politics and environmental consciousness may contribute towards these effects [52]. However, there is emerging evidence to suggest that this may not be the case. Wind-turbines are an archetypal green technology, so with the rise in green politics it would be expected that public support for wind-turbines would be high. However, wind turbines are often accused as a new possible culprit in the explanations of medically unexplained symptoms [54]. In addition, while psychological distress [55], the presence of a monotonous environment [56] and heightened awareness of environmental hazards [57] have all been shown to increase symptom reporting due to environmental factors, the role of individual differences in negative oriented personality (NOP) (i.e. those with an increased level of negative personality traits such as high neuroticism or an inability to cope with negative thoughts or feelings) is also a possible exacerbating factor [58]. This Chapter of the Thesis therefore examines the influence of negative orientated personality in influencing the link between exposure to a 'green' new technology – micro and small sized wind turbines and symptom reporting. By relating the sound measurements taken during the study (see Section 2) and people's reactions in a rigorous manner the much debated 'wind turbine syndrome' [54] can be systematically investigated.

Research has shown that while there is general public support for renewable energy, when faced with having structures to produce this energy sited within their community e.g. wind turbines, individuals are often more negative [59, 9, 10]. This research finds that negative responses are typically related to anticipated or experienced noise, and the anticipation of negative health effects of living close to wind turbines. Installation of small turbines usually requires planning permission, where the potential negative impacts of any new building or structure on the surrounding community are taken into account, and can potentially result in the cancellation of schemes. While noise levels for small wind turbines are expected to be much lower than for large wind turbines, the closer proximity to domestic dwellings and business properties may increase the likelihood of noise annoyance and the possibility of detrimental effects on physical and psychological health [60, 61]. As increased symptom reporting is one of the main determinants of contact with health services [62], it is important to know whether there is a link between noise from small wind systems and symptom reporting. This study examines the extent to which small wind system noise influences symptoms of ill health – focusing on the role of individual differences on (i) attitudes to wind turbines, (ii) perceived noise, (iii) the link between attitudes to wind turbines and perceived noise, and (iv) the link between perceived noise and reported symptoms of ill-health.

3.1.2 Wind Power and Noise Annoyance

Very little work has been done looking at reactions and perceptions to small and micro wind turbines in environments close to where people live. The literature that does exist, examining the psychological impact of wind turbines typically assesses a straightforward link between noise sensitivity and sound pressure levels with annoyance and not personality traits. These studies are also usually related to either large scale isolated wind turbines or those situated within wind farms in rural areas in Sweden. The relevant literature is summarised in this Section of the Thesis.

Waye and Ohrstrom [51] evaluated annoyance due to different types of sounds from five different wind turbines ranging from 250kW to 600kW rated power. They stated that previous research into the perception of, and annoyance due to wind turbine noise was limited, however, they suggested that individual differences in sensitivity to noise, assessed using Weinstein's [63] Sensitivity to Noise scale, predicted annoyance from noise. Specifically those sensitive to noise experienced the most annoyance from noise in their community. In their study, Persson Waye exposed 25 individuals to five different wind turbine sounds with an equal LA_{eq} of 40dBA for 3 and 10 minute intervals in a controlled environment. It was found that the perception and annoyance levels due to the different sounds varied across the range. In this study, the individuals were exposed in a sound insulated room furnished to resemble an outdoor environment. It is suggested here that the relevance of the results in this study to real life situations is limited since it is believed that an annoyance level due to noise may be increased by a prolonged exposure intruding into an individual's everyday life and true annoyance cannot be measured from short exposures to noise. In their work it was hypothesised that the different wind turbine noise mechanisms may provoke different levels of noise annoyance depending on their characteristics. This is an important point to consider because, as suggested by Waye and Ohrstrom when speculating on the broader implications of their work, it might be expected that the spectral and temporal noise characteristics of small wind turbines will vary considerably depending on the turbine type. More details investigating this observation for small and micro turbines has been given in the Noise Measurement Chapter of the Thesis (Chapter 2). Waye and Ohrstrom suggested that a tonal or a high frequency noise may be considered more annoying than a broadband sound and the sounds which were perceived more readily were also considered the most annoying; these were 'lapping', 'swishing' and 'whistling'. 'Low-frequency' and 'grinding' sounds were considered to be less obtrusive. These finding were supported in a later paper by Pederson and Halmstad [64] who reviewed the knowledge to date on noise perception and annoyance from large wind turbines. In this paper it was also found that the proportion of individuals annoyed by wind turbine noise is higher than for other community noise sources with the same sound levels and that people who were annoyed by the noise were also found to be annoyed the most often. This introduces the fact that personality may play a key role in noise perception and annoyance from small wind systems. Individuals' responses to different sounds potentially relating to wind turbine noise will be investigated in the the current study. Interestingly a more recent study by Pedersen [14] found that the highest non-acoustical impact factor on noise annoyance from wind turbines was economic benefit. Individuals profiting from a local wind turbine are less likely to be annoyed by the noise it produces, showing that those who install a small or micro turbine themselves may perceive less noise.

The noise attributed to micro and small wind turbines is likely to be of a low level compared to large scale turbines and should therefore cause a low level of annoyance but additional work is needed to quantify the noise levels from turbines of this size. Pederson [65] states that:

> 'In a society where people are being exposed to an increasing noise load, moderate and low level noise sources may also be perceived as annoying'

In Pedersen's work [65] it was observed that respondents who were annoyed by the wind turbine noise in their area, also did not consider it a place for health recovery and mental restoration, thus impacting on health and resulting in an inability to overcome the stresses caused by the noise and also stresses from everyday working life. This finding shows that wind turbine noise could have a potential impact on individuals' health over and above the noise annoyance. It is also important to consider different living environments when analysing an individual's perception and annoyance due to wind turbine noise. Pedersen [66] found that the living environment has a direct influence on the effects of wind turbine noise. The importance of environmental noise measurements taken in the field at real turbine installations is evident from Pedersen's research. Quantifying the actual noise levels and associated frequency characteristics of small and micro turbines provides a context against which to compare the responses of subjects. Measurement provides an objective description to both inform the methodology for exploring the subjective response of participants in the survey and interpreting the subsequent results (more details on noise measurements in the field has been given in Chapter 2).

3.1.3 Personality and Perception of Turbine Noise

Individual differences play a key role in assessing whether individuals are likely to be annoyed by a noise source over and above noise sensitivity and sound levels. Little research exists linking individual differences to the perception of wind turbine noise but research has been carried out linking personality traits to noise sources other than wind turbines, these include individual differences to noise in a college dormitory [63], and annoyance due to tape recorded noise [67]. Some of the findings in this research could apply to reactions to wind turbine noise but specific work is necessary in the area. In addition, there have been studies exploring community noise levels, which have examined individual differences in terms of stress and coping [68] as well as the long term health effects of environmental noise sources. Stansfeld, Sharp et al. [69] demonstrated that both Negative Affectivity (NA) – the general trait or disposition to experience negative emotions - and Neuroticism (N) are strongly associated with noise sensitivity and may play a role in the relationship between wind turbine noise and annoyance levels. Similarly, according to the stress perception hypothesis: compared to those who are low in N, higher N individuals perceived the same events to be more stressful, and were more emotionally reactive to stressors [70, 71, 72]. Therefore, as uncontrollable wind turbine noise could be conceptualised as an environmental stressor [73], it is expected that those in the current study with higher levels of negatively orientated personality (i.e. higher N, NA FD - frustration discomfort) will report the noise from wind turbines to be louder and more frequent than those lower in these traits. Belojevic et al. investigated subjective reactions to traffic noise with regard to personality traits [60]. It was found that noise sensitivity and neuroticism significantly and positively influenced the extent to which participants found traffic noise annoying. This conclusion is supported by other work, such as that by Weinstein who investigated the role of individual differences and personality on noise annoyance [74]. Weinstein found that people who tend to be consistently negative were typically more annoyed by a new source of noise. This statement is particularly applicable for small wind systems as they have the potential to be a new noise source in many communities if the Government's renewable targets are to be met. Therefore in the current study it is important that personality characteristics which would indicate a negative oriented personality are recorded when surveying for reaction to noise.

3.1.4 Personality, Perceived Noise and Symptom Reporting

No studies to date have examined the influence of personality and perceived turbine noise on perceived physical health as indexed by symptom reporting. Looking at the literature on general environmental noise, Lercher [68] reviewed a number of concepts for the link between environmental noise and health effects and suggested the possibility that personality factors such as negative affectivity and neuroticism may be influential on different health outcomes. Similarly, Belojevic, Jakovljevic et al. [60] found that individual differences in noise sensitivity and Neuroticism significantly and positively influenced the effect of traffic noise on individuals in terms of their sleep patterns, psychological disturbances and behavioural effects such as intention to change place of living, interpersonal relationships between dwellers and closing the windows facing the street. Belojevic also found significant correlations between Neuroticism and noise related psychological disturbances such as depression, nervousness and headache frequency.

The presence of uncontrollable noise has been previously established as a potential stressor which can affect learning and task performance, and one which has the potential to increase feelings of negativity and aggression [75]. However, most work examining the impact of noise on motivational experiences such as feelings of helplessness and depression have examined acute noise during experimental tasks (see Evans and Stecker [76] for a review). Far fewer have examined effects of chronic uncontrollable noise, of which wind turbine noise would be an example. One notable exception [77] demonstrated that it is the uncontrollable nature of noise (rather than the volume of the noise per se) which can produce the negative effects of noise such as poorer general health. Examining wind turbine noise specifically, Pedersen and Waye [65] observed that residents who were annoyed by the wind turbine noise in their area, also considered the turbines to negatively impact on health recovery and mental restoration, thus impacting on health and resulting in an inability to overcome the stresses caused by the noise and also stresses from everyday working life. Therefore the conceptualisation of wind turbine noise as a stressor can be seen within the literature examining the effects of stress on health, however, more recent reviews of this literature, particularly relating to work-related stressors has shown that it is the role of negative orientated personality on health outcomes which may be responsible for this link [58]. According to the Ferguson et al's review, the existing data is best represented by a positive association between negative oriented personality (NOP) and perception of negative job characteristics, with a greater relationship between NOP and health (especially physical health) than between perceived job characteristics and health. As perceived negative job characteristics are essentially a negative response to the demands of the environment, it is reasonable to use this model to anticipate that NOP and perceived wind turbine noise should be positively associated. It is therefore likely that any effects of noise perception on reported health may be moderated by these individual differences and negative oriented personality, specifically Negative Affectivity and Frustration Discomfort. However, the effect of perceived noise on symptom reporting may be due to the fact that those who perceive more noise are actually experiencing more actual noise from the turbine. If this is the case, it is important to also examine the effect of actual noise experienced on reported symptoms. If this association is non-significant, then this would further support the symptom perception model, rather than the impact of hearing noise from the turbine on health.

3.1.5 Individual Differences and Attitudes to Wind Turbines

No existing work has examined how or whether personality is associated with attitudes to energy production, specifically wind turbines. However, those with negative orientated personality (NOP: for example, Neuroticism, Negative Affectivity) [58] are more likely to hold a more negative attitude to wind turbines in general, as those with NOP generally experience more negative affect [78], and negative evaluations to aspects of their environment [58]. For example, according to David, Green, et al.[79], those scoring high in N and NA are more easily frustrated and hypersensitive to negative events, such as the uncontrollable noise generated by a wind turbine. In addition, trait Frustration Discomfort (FD) [80] is the propensity to be generally unable to cope with or 'bear' negative emotions, thoughts, and events. Specifically, this personality trait has four subscales: Emotional intolerance, discomfort intolerance, entitlement and achievement. Most relevant here are the subscales discomfort intolerance - the ability to bear any experience of discomfort (which uncontrollable noise could hypothetically generate) and emotional intolerance – the inability to bear negative affect. It is anticipated that individuals scoring higher in N, NA and both measures of Frustration Discomfort would have a more negative attitude to wind turbines due to a general negative cognition set and the propensity for wind turbine noise to generate negative affect. Finally, Pedersen et al. [14] and Wolsink, et al. [13] demonstrated that attitudes to wind turbines strongly correlated with experience of noise annoyance. Pedersen's study emphasised that initial attitudes to wind turbines affected noise annoyance and those with negative attitudes towards the impact of wind turbines were more annoyed by their noise levels. Therefore attitude to wind turbines in general will also be measured in the current study to examine its influence on perceived noise. The extent to which attitudes to wind turbines vary as a function of the probability of being able to actually hear the noise from the turbine is also examined in order to assess whether it is real or perceived noise that is related to attitude to wind turbines.

3.1.6 Summary

It is clear from the literature that personality and mood play a significant role in the link between external stresses and self reported health, particularly the NA and neuroticism personality traits which are associated with higher symptom reporting. Noise from small wind systems may be considered to be an external stressor so the relevance for individual differences on the health effects due to wind turbine noise are apparent. It has also been shown that individual differences also play a role in the perception of nuisance or noise sources. Such studies as these have not often been applied to wind turbine noise and in particular micro and small wind turbines in built environments so there is a research gap in this field. These findings highlight the importance of exploring the role of individual differences when discussing noise perception and the potential effects and underline the fact that the effect of personality factors and attitudes on noise perception and the effects of this noise for small wind systems are still not well known.

This study examines the extent to which wind turbines influence symptoms of ill health – but crucially, it focuses on the role of individual differences on (i) attitudes to wind turbines, (ii) perceived noise from small wind turbines, (iii) the link between attitude and perceived noise and (iv) the link between perceived noise and symptom reporting.

Two studies will be carried out to assess the psychological and health impacts of small wind systems, a questionnaire sent to individuals living close to small or micro turbine installations (the domestic study) and a questionnaire will be given to individuals who will be played recordings of wind turbine noise (experimental recordings study). This will test whether it is the characteristics of the turbine noise itself or prolonged exposure to turbine noise which is the key stressor. For the domestic study, individuals report the type of sounds they hear from the turbines close to their domestic dwelling. An analysis of whether personality affects this noise perception will be carried out. However, the researcher does not know exactly which turbine sounds the respondents have heard. In the experimental recordings study, the researcher will control the turbine sounds the individuals hear. It will then be possible to see directly how personality affects the perception of turbine noise. This type of study is similar to the experimental study carried out by Persson Waye [51]. The detailed hypotheses for both studies are given in the following Section.

3.1.7 Hypotheses

Having considered the review of the current literature and the aims of the Thesis, the hypotheses for the research are therefore as follows:

1. Individuals scoring high in NOP (N, NA and FD) will:
   (a) have a more negative general attitude to wind turbines,
   (b) report greater perception of small wind turbine noise from the nearby small or micro turbine; and
   (c) demonstrate greater symptom reporting.
2. Those with a negative general attitude to wind turbines will report:
   (a) greater perception of wind turbine noise (loudness and occurrence) from the nearby turbine; and
   (b) NOP will moderate these relationships.

3. Individuals who perceive greater noise (loudness and occurrence) from the nearby turbine will:
   (a) report more symptoms of general ill health; and
   (b) NOP will moderate these relationships.
4. To test whether the effect of NOP on attitude to wind turbine noise, perceived noise and symptom reporting is due to the actual sound emitted by the nearby turbine, the following hypotheses are tested: Greater probability of hearing noise from the turbine (calculated from actual sound levels) will be associated with:
   (a) a more negative attitude to wind turbines;
   (b) a greater perception of wind turbine noise from the nearby turbine; and
   (c) a greater reporting of symptoms. The moderating influence of NOP on these relationships will also be examined where significant relationships occur.
5. A questionnaire will also be given to students who are asked to evaluate four sound recordings of wind turbines, two video recordings of wind turbines and a sound recording from a turbine site when the turbine is switched off. Those perceiving increased noise levels in the recordings will:
   (a) rate the turbine sounds in the recordings as more annoying and will report not being able to tolerate the recordings for as long before wanting to switch them off;
   (b) will report more symptoms of general ill health; and
   (c) NOP will moderate these relationships.
6. Individuals scoring high in NOP (N, NA and FD) will:
   (a) have a more negative general attitude to wind turbines;
   (b) report greater perception of wind turbine noise in the recordings;
   (c) report higher levels of turbine noise in the sound recording which does not contain any turbine noise;
   (d) find the recordings to be more annoying in terms of their sound;
   (e) not be able to listen to the recordings for as long before having to switch them off; and
   (f) demonstrate greater symptom reporting.
7. Those with a negative general attitude to wind turbines from the recordings study will report:
   (a) greater perception of wind turbine noise in the recordings;
   (b) turbine sounds in the sound recording which does not contain any turbine noise;
   (c) the recordings to be more annoying and will not be able to tolerate recordings for as long before having to switch off; and
   (d) NOP will moderate these relationships.

Hypotheses 1 to 4 are related to the domestic study and hypotheses 5 to 7 to the recordings study.

3.2 Domestic Study

In this Section the methodology and results of the domestic questionnaire sent out to individuals living close to each wind turbine installation as outlined in Section 1.3 will be detailed. This part of the study contributes to achieving the aims of the Thesis with the analysis of the data designed to answer the hypothesis questions given in Section 3.1.7.

3.2.1 Methodology

The measures included in the domestic questionnaire are described in detail in the following Sections as well as the procedure for collecting the data. The questionnaire was split into three parts as follows:

1. Questions about the wind turbine close to each respondent's dwelling,
2. Questions regarding particular personality traits of each respondent,
3. Questions to explore the demographics of the sample population e.g. age, sex, occupations etc.

The full questionnaire is available in Appendix F.

3.2.1.1 Participants and procedure

Households living within 500m of eight 0.6kW micro turbine installations and within 1km of four 5kW small wind turbine installations were contacted to participate in the survey (details of these installations are given in Section 1.3). All households (N contacted = 1327) were sent a survey by postal mail. Any member of each household over the age of 18 could anonymously complete the survey; with the choice to complete the survey by pre-paid postal mail or via the Internet (57 were returned due to incorrect address details).

3.2.1.2 Measures

In the following Sections more details about the measures included in each of the three parts of the domestic questionnaire will be given.

Sample Population Demographics One hundred and thirty eight completed surveys were returned (age range of respondents = 20-95; mean age = 53.80, SD = 15.59; 1.4% were aged between 18-25, 12.3% between 26-35, 15.9% between 36-45, 23.2% between 46-55, 22.5% between 56-65, 12.3% between 66-75, 7.3% between 76-85 and 5.1% between 86-95) resulting in a response rate of 10.86%, 54.4% were male. The occupations of the sample population are shown in Table 3.2.1. The split of the type of dwellings that respondents live in was as follows; 40.0% in detached, 22.8% in semi-detached, 7.4% in terraced, 28.7% in flats with 0.7% stating other type of dwelling. 82.5% of participants reported that they do have an outside space available for their use at their dwelling.

Occupation	% Participants
Management	13.5
Professional	25.4
Skilled/Administrative	11.9
Unskilled	6.3
Retired	29.4
Unemployed	4.8
Not seeking employment	8.7

Figure 3.2.1: Split of occupations of the sample population

The data were checked to determine whether there were any differences between male and female responses, no significant differences were found, therefore, the data were analysed as one group. The completed questionnaires were checked to determine whether missing data were systematic (e.g. to check whether a large percentage of participants did not give a blank answer for one particular question), it was verified that data was missing at random and not systematically.

Wind Turbine Measures

General Respondents were asked whether they could see a turbine from their domestic dwelling and whether there is a small or micro wind turbine attached to the building they live in. The majority of respondents (64.8%) could see a turbine from their dwelling, and 14% had a turbine attached to the building they live in.

Attitude to Wind Power Participant's attitudes to wind turbines in general (ATT) was measured using a single item "Please rate how you feel about wind power in general". Participants responded using a 7 point Likert type scale (1 = very positive to 7 = very negative). Respondents reported a reasonably positive attitude to wind turbines (mean attitude = 2.33, SD = 1.76).

Typical Turbine Sound Level The typical sound level from the turbine per household (ACTUAL) was determined using sound maps. Analysis of how the sound from the turbine at each installation attenuates across the surrounding geographical area was calculated using a series of geographical 'sound maps' generated (see Figure 3.2.2 for an example sound map) with the DataKustik CadnaA software package. CadnaA uses the ISO 9613-1 [31] and ISO 9613-2 [32] standards to map how sound attenuates over a land area based on its topography. More details about how the sound maps were created and used within this research are given in Sections 2.2.2 and 2.3.3. The probability of sound from the wind turbine being heard at specific locations away from the turbine is shown in the associated sound map (Figure 3.2.2) based on the colour of the locations. As would be expected, households close to the turbine typically experience a higher probability of hearing the noise from the turbine and this reduces as a function of distance and prevailing landscape (e.g. presence of tall buildings). Households closer to the turbine are also likely to experience the turbine's sound as louder than households living further from the turbine; this is due to the attenuation of the turbine's sound power level at increasing distances from the turbine. It was possible to identify three zones at each installation at increasing distances from each turbine using the sound maps on a three point scale: high probability of noise heard (rated 2 - red regions of the map), moderate probability of noise heard (rated 1 - blue regions of the map) and low to zero probability of turbine noise heard (rated 0 - green and yellow regions of the map).

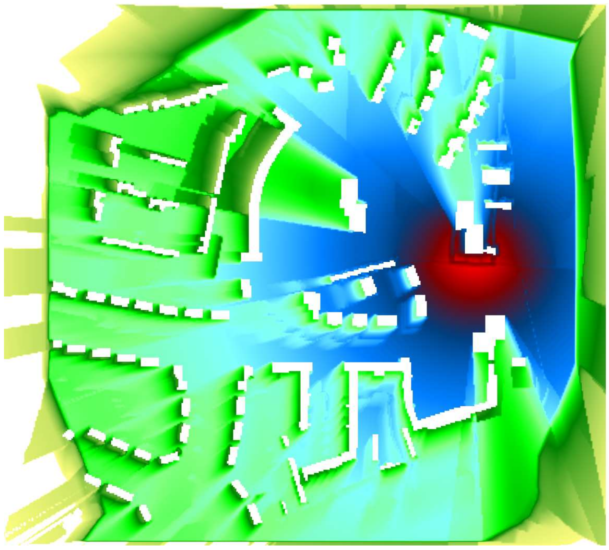

Figure 3.2.2: An example sound map used to determine typical noise levels at each household

Perceived Noise from the Turbine Participants rated a) how often they had heard ten sounds (swooshing, screeching, whistling, humming, throbbing, thumping, scratching, high frequency, low frequency and buzzing) from the micro or small turbine close to their dwelling (OCCUR) and b) how loud each sound was when it was heard (LOUD). Both occurrence and loudness ratings were given on a five point Likert type scale. For occurrence, 0 = 'never noticed' and 4 = 'notice continuously' and for loudness, 0 = and 'never heard' and 4 = 'extremely loud'. A mean score was calculated for both the occurrence and loudness scales for each participant by taking the mean of scores for the ten sounds rated. The ten sounds were selected following pilot studies and those identified by Pedersen[14].

Time and Weather Participants were asked at what times of the day and in which weather conditions they typically noticed each of the ten sounds from the turbine close to their dwelling. When entering this data from the returned completed questionnaires it was inconsistent and it appeared that a number of the participants had not fully understood the question (for example, a participant might have reported that they never noticed humming sounds from the turbine but then reported that they did hear this sound at particular times of the day or in a particular weather condition. Or participants reported that a certain sound from the turbine was loud but did not comment at what times or in which weather conditions the sound was heard). For this reason, no further analysis including the time of day and in which weather conditions the sounds from the turbine was heard is included as it was believed that any analysis would not be a true representation for how the sample population perceive the noise from the turbine close to their dwelling and may give misleading conclusions.

Personality Measures A number of personality measures have been used in many contexts to assess and describe personality traits in individuals such as frustration discomfort [80], individual responses to aggression [75], positive and negative affectivity [81] and neuroticism [82]. Modified versions of four of these measures will be used in the current research. The modified versions are shorter and some terms have been removed to make them more applicable to wind turbine noise.

Positive and Negative Affectivity Watson et al. [81] developed and validated the positive and negative affectivity (PANAS) scale, for a full development methodology the reader is referred to the original text.

Positive affect (PA) refers to the extent to which a person feels enthusiastic, active and alert where a high positive affectivity is a state of high energy, full concentration and pleasurable engagement. Negative affect (NA) is in contrast to this and is a general measure of subjective distress and un-pleasurable engagement, where high negative affectivity causes feelings such as anger, contempt, and nervousness. Low negative affectivity is characterised by a state of calm and serenity. The PANAS scale can be used to assess an individual's tendency towards a positive or negative affectivity. Individuals must rate how often they have felt various feelings over a given time period.

An example of a PA and NA adjective from the PANAS scale is:

> Indicate to what extent you have felt the following over the last month,
> Interested (PA)/Nervous (NA)
> A little 1 2 3 4 Most of the time

To restrict the length of the survey sent to households, 12 items from the 20-item Positive and Negative Affectivity scales were used [81]. In this shortened version, six items assessed positive affect (PA) and six items assessed negative affect (NA). Items were scored using a Likert-type scale where 1 =very slightly or not at all to 5 = extremely. The six PA and six NA items were selected by using six items from the original 20 item PANAS PA and NA scales which were the most statistically affiliated with each scale.

Neuroticism The IPIP (International Personality Item Pool) [82] website is intended as an international effort to develop and continually refine a set of personality inventories, whose items are in the public domain, and whose scales can be used for both scientific and commercial purposes. The creator of this website states that "No one investigator alone has access to many diverse criterion settings; but the international scientific community has such access, and by pooling their findings we should be able to devise instruments over the next decade that make our present ones seem like ancient relics." It is from this website that the scale for neuroticism is drawn. For details on how the different personality scales have been developed and verified, the reader is referred to the IPIP website.

Neuroticism (N) was assessed using the 10-item IPIP Neuroticism scale [82]. The neuroticism scale can be used to evaluate an individual's tendency to experience negative emotional states. The scale is split into positive and negative statements where the individual will be asked to rate how well each statement applies to them. Items were scored using a Likert-type scale where 1 = very inaccurate for me to 5 = very accurate for me.

An example statement from the neuroticism scale is:

> I rarely get irritated.
>
> Very inaccurate 1 2 3 4 5 Very accurate

Frustration intolerance Harrington [80] developed and validated the frustration discomfort scale. For a full development methodology of the scale the reader is referred to the original text. The frustration discomfort scale is a self rated scale and can be used to determine an individual's capacity to cope with situations where they do not feel comfortable or cannot control. Individuals must rate how well a set of statements applies to them.

An example statement from the frustration discomfort scale is:

> Listed below are a number of common thoughts and beliefs that people may have when they are distressed or frustrated. Please read each statement and decide how well this usually describes your own beliefs. Circle the number that best indicates the strength of this belief.
>
> I can't stand to lose control of my feelings
>
> Absent 1 2 3 4 5 Very Strong

Frustration intolerance was assessed using two sub-scales of the Frustration Discomfort scale [80]; Emotional Intolerance (F-emot) (7 items e.g. 'I can't bear disturbing feelings') and Discomfort Intolerance (F-disc) (7 items e.g. 'I can't stand doing tasks that seem too difficult'). Participants responded to both sub-scales using a 5 point Likert scale with the following anchors: (1) absent, (2) mild, (3) moderate, (4) strong, (5) very strong.

Symptoms Non-specific somatic symptoms (SYMP) over the preceding 6 months were assessed with 12 common symptoms (e.g. headache, fatigue) each rated on a five point scale (0 = did not experience the symptom, with 1 to 4 indicating the severity of any experienced symptom) [83].

For all measures, higher scores indicate higher levels of the measure itself, except for attitude, where a higher score indicates a more negative attitude.

The full results and analysis of the data collected from the domestic study responses are given in the the following Section. A conclusion of the key findings will be given in Section 3.4.

3.2.2 Results

3.2.2.1 Descriptive statistics

Descriptive statistics and scale reliabilities (α) for all measures are shown in Table 3.2.1. Zero-order correlations for all measures are shown in Table 3.2.2. All scales were reliable showing that all items in each scale were internally consistent, i.e. the set of items measure the same thing.

	α	Mean	SD
ATT		2.33	1.76
ACTUAL		.620	.776
LOUD	.90	.225	.551
OCCUR	.89	.225	.505
SYMP	.85	8.49	6.87
PA	.93	2.56	1.14
NA	.85	1.76	0.90
N	.84	2.59	0.76
F-disc	.85	2.29	0.77
F-emot	.86	2.33	0.88

Note: ATT = attitude to wind turbines; ACTUAL = actual noise level rating; LOUD = perceived noise loudness; OCCUR = perceived noise occurrence; SYMP = symptom reporting score; PA = positive affect; NA = negative affect; N = neuroticism; F-disc = discomfort intolerance; F-emot = emotional intolerance

Table 3.2.1: Descriptive statistics and reliability for all measures

	1	2	3	4	5	6	7	8	9
ATT (1)									
ACTUAL (2)	.015								
LOUD (3)	.279**	.332**							
OCCUR (4)	.284**	.363**	.951**						
SYMP (5)	.023	-.029	.228*	.213*					
PA (6)	-.283**	-.312**	-.159	-.166	-.015				
NA (7)	.219*	.036	.399**	.400**	.346**	.272**			
N (8)	.081	.146	.163	.216*	.441*	-.269**	.323**		
F-disc (9)	.236*	-.134	.054	.053	.373*	.076	.191*	.226*	
F-emot (10)	.139	-.027	.261**	.243**	.391**	.104	.379**	.493**	.766**

*p<.05; **p<.01

Note: ATT = attitude to wind turbines; ACTUAL = actual noise level rating; LOUD = perceived noise loudness; OCCUR = perceived noise occurrence; SYMP = symptom reporting score; PA = positive affect; NA = negative affect; N = neuroticism; F-disc = discomfort intolerance; F-emot = emotional intolerance

Table 3.2.2: Zero-order correlations for all measures

The zero-order correlations in Table 3.2.2 give an early indication of the relationships between measures. As expected, the reported loudness of wind turbine noise is positively correlated with the reported occurrence of the wind turbine noise. And both the LOUD and OCCUR scores are also positively correlated with the amount of noise an individual is expected to perceive based on the ACTUAL rating. Although the correlation is significant, the correlation value is not high. This implies that other measures will also play a role in the relationship. The same is true for all other significant correlations between measures shown in Table 3.2.2. However, the significant correlations show the following:

- All personality measures are correlated, except PA with F-disc or F-emot;
- PA is negatively correlated with attitudes to wind turbines, NA and F-disc are positively correlated with attitudes;
- And attitudes to wind turbines are positively correlated with noise perception;
- All negative personality measures (measure of NOP) are positively correlated with symptom reporting;
- And symptom reporting is positively correlated with perceived noise;
- Finally NA, neuroticism and F-emot are positively correlation with noise perception.

The significant correlations discussed require further investigation to determine the direction of the relationship and how the measures interact with other relationships between measures. Further investigations will be carried out using regression statistical tests and moderation analyses. Results of these further investigations are given in the following sections.

3.2.2.2 Occupation Effect

The postal method used to collect data from participants meant that the sample population was self selecting. It was therefore necessary to check the sample population were not all from the same societal demographic. The best method to do this with the data available was to compare how participants from each occupation group perceived wind turbine noise, their attitudes to wind turbines and their symptom reporting. If the mean values of attitudes (ATT), noise perception (LOUD and OCCUR scores) and symptom reporting (SYMP) between each occupational group are not significantly different, then the sample population is a valid representation of the overall population and the data can be analysed as one group. Three one-way between-groups ANOVA (analysis of variance) tests were conducted and the results are given in Table 3.2.3. An ANOVA compares the mean scores of a dependent variable for more than two groups; in this case occupation, and is so called because it does this by comparing the variance in the dependent variable between the groups with the variance within each of the groups. This is done by calculating the F ratio (see Appendix E, Section E.9.26 for the method to do this). A large F ratio indicates that there is more variability in the dependent variable between groups (due to the independent variable), rather than within the groups. In this case a non-significant effect and low F ratio are required to prove that there are no differences between the occupational groups and all participants can be analysed as one group.

Dependent Variable	F statistic	p
ATT	$F_{6,110} = 1.104$	.365
LOUD	$F_{6,116} = .733$	.624
OCCUR	$F_{6,115} = .839$	.542
SYMP	$F_{6,104} = 1.003$	.427

Note: ATT = attitude to wind turbines; LOUD = perceived noise loudness; OCCUR = perceived noise occurrence; SYMP = symptom reporting score

Table 3.2.3: Results of three one-way between-groups ANOVA tests investigating the effects of participants' occupation

The data show that all three statistical tests fail to reach statistical significance (i.e. $p > 0.05$ for each test). Hence those in a particular occupational group did not have more negative attitudes to wind turbines, perceive increased noise levels or report increased symptoms of ill health. For this reason the data can be analysed as one group.

3.2.2.3 Perceived Sounds

In order to investigate the sounds which are most commonly perceived from the small and micro wind turbines in this study the mean loudness and occurrence scores for each of the ten sounds listed in the questionnaire were calculated on the same rating scale as in the questionnaire, for occurrence, 0 = 'never noticed' and 4 = 'notice continuously' and for loudness, 0 = 'never heard' and 4 = 'extremely loud'. To compare the sounds individuals perceive from small or micro wind turbines with the results of the noise measurement and noise modelling parts of the Thesis, the mean scores were split into the different turbine types involved in the study (see Table 1.3.1 in Section 1.3). The mean loudness and occurrence ratings for the small turbine types are shown in Table 3.2.4, for the micro turbine types in Table 3.2.5 with a comparison between the small, micro and all turbine types in Table 3.2.6.

	Small Type S2 n=3		Small Type S1 n=37		All Small Types n=40	
	LOUD	OCCUR	LOUD	OCCUR	LOUD	OCCUR
Swooshing	0.00	0.00	0.25(2)	0.38(1)	0.23(1)	0.35(1)
Screeching	0.00	0.00	0.08(7=)	0.08(6=)	0.07(6=)	0.07(7=)
Buzzing	0.67(3=)	0.67(1=)	0.00	0.00	0.05(8=)	0.05(9)
Whistling	0.00	0.00	0.10(6)	0.13(4=)	0.10(5)	0.12(4=)
Humming	1.33(1=)	0.67(1=)	0.13(3=)	0.16(3)	0.21(2)	0.20(3)
Throbbing	0.00	0.00	0.08(7=)	0.13(4=)	0.07(6=)	0.12(4=)
Thumping	0.00	0.00	0.13(3=)	0.00	0.00	0.00
Scratching	0.00	0.00	0.38(1)	0.08(6=)	0.05(8=)	0.07(7=)
High Freq.	1.33(1=)	0.67(1=)	0.08(7=)	0.08(6=)	0.17(3=)	0.12(4=)
Low Freq.	0.67(3=)	0.67(1=)	0.13(3=)	0.18(2)	0.17(3=)	0.22(2)
Mean All	0.400	0.267	0.088	0.120	0.109	0.130

Table 3.2.4: Mean Loudness (LOUD) and Occurrence (OCCUR) scores for the Small Turbine Types

	Micro Type M3 n=13		Micro Type M2 n=9		Micro Type M1 n=65		All Micro Types n=87	
	LOUD	OCCUR	LOUD	OCCUR	LOUD	OCCUR	LOUD	OCCUR
Swooshing	0.46(1)	0.69(1)	0.00	0.00	0.59(2)	0.63(1)	0.51(2)	0.57(1)
Screeching	0.00	0.00	0.00	0.00	0.13(9)	0.15(9)	0.10(9)	0.11(9)
Buzzing	0.08(4=)	0.15(3=)	0.00	0.00	0.31(4)	0.28(4)	0.24(4)	0.24(4)
Whistling	0.15(2=)	0.15(3=)	0.00	0.20(4)	0.39(3)	0.37(3)	0.31(3)	0.32(3)
Humming	0.15(2=)	0.31(2)	0.50(2)	0.60(1)	0.60(1)	0.57(2)	0.53(1)	0.53(2)
Throbbing	0.00	0.00	0.00	0.00	0.27(5)	0.22(7)	0.20(6)	0.17(7=)
Thumping	0.00	0.00	0.00	0.30(2)	0.18(8)	0.18(8)	0.13(8)	0.17(7=)
Scratching	0.00	0.00	0.00	0.10(5)	0.07(10)	0.07(10)	0.06(10)	0.07(10)
High Freq.	0.00	0.00	0.00	0.00	0.25(6)	0.27(5)	0.19(7)	0.20(6)
Low Freq.	0.08(4=)	0.08(5)	0.60(1)	0.22(3)	0.19(7)	0.24(6)	0.22(5)	0.22(5)
Mean All	0.092	0.139	0.390	0.240	0.299	0.299	0.279	0.269

Table 3.2.5: Mean Loudness (LOUD) and Occurrence (OCCUR) scores for the Micro Turbine Types

	All Small Types n=40		All Micro Types n=87		All Types n=127	
	LOUD	OCCUR	LOUD	OCCUR	LOUD	OCCUR
Swooshing	0.23(1)	0.35(1)	0.51(2)	0.57(1)	0.42(2)	0.50(1)
Screeching	0.07(6=)	0.07(7=)	0.10(9)	0.11(9)	0.09(8=)	0.10(9)
Buzzing	0.05(8=)	0.05(9)	0.24(4)	0.24(4)	0.18(5=)	0.18(5=)
Whistling	0.10(5)	0.12(4=)	0.31(3)	0.32(3)	0.24(3)	0.26(3)
Humming	0.21(2)	0.20(3)	0.53(1)	0.53(2)	0.43(1)	0.43(2)
Throbbing	0.07(6=)	0.12(4=)	0.20(6)	0.17(7=)	0.16(7)	0.15(7)
Thumping	0.00	0.00	0.13(8)	0.17(7=)	0.09(8=)	0.11(8)
Scratching	0.05(8=)	0.07(7=)	0.06(10)	0.07(10)	0.05(10)	0.07(10)
High Freq.	0.17(3=)	0.12(4=)	0.19(7)	0.20(6)	0.18(5=)	0.18(5=)
Low Freq.	0.17(3=)	0.22(2)	0.22(5)	0.22(5)	0.20(4)	0.22(4)
Mean All	0.109	0.130	0.279	0.269	0.225	0.225

Table 3.2.6: Mean Loudness (LOUD) and Occurrence (OCCUR) scores for the Micro, Small and All Turbine Types

In general, the mean ratings for all of the turbine types are low (all scores < 1.5), therefore individuals do not report small and micro turbine sounds to be either loud or occurring often. The tables show a ranking number next to the ratings for each sound. Swooshing and humming are the loudest and most commonly occurring sounds for all micro turbine types, however for the small turbine types, low frequency noise is also ranked highly, second for occurrence and third for loudness. From the results in the tables, it appears that sounds which are likely to occur higher in the frequency spectrum are more commonly associated with the micro turbine types than for the small turbine types. A comparison of how these reported sounds compare to those measured and modelled from the noise measurement (Section 2) and noise modelling (Section 4) parts of the research respectively will be given in the concluding remarks of the Thesis in Chapter 5.

3.2.2.4 The Influence of Visibility of the Turbine on Noise Perception

The effect of seeing a turbine from the property on perceived noise, symptom reporting and attitude to wind power was examined using three independent samples t-tests. The results are shown in Table 3.2.7. It is shown that those who are able to see a turbine from their dwelling do experience more noise, but do not have a more negative attitude towards wind turbines or report increased general symptoms. There could be two reasons for respondents who can see a wind turbine reporting increased noise levels from the turbine; the first reason is that the respondents who can see a turbine are those living closest to the turbine installation so are more likely to perceive the noise as there are fewer barrier objects between the source and the receiver. However, secondly, there have been studies [84] suggesting that the visibility of a noise source increases the likelihood of reporting noise from that noise source compared to not being able to see the noise source at the same sound pressure levels.

Dependent Variable	t	p
Noise Perception	-3.583	.001
Symptom Reporting	-0.411	.682
Attitude	0.009	.993

Table 3.2.7: Results of three independent samples t-tests investigating the effects of visibility of a turbine

Further statistical tests were carried out to determine which of the two reasons better explain the results. The data was split into three depending on the ACTUAL noise rating, as in general those with a higher ACTUAL rating live closer to the turbine near their dwelling. A regression analysis was carried out for each zone to examine the effect of being able to see a turbine on the scores LOUD, OCCUR and SYMP. Results of the three analyses for each zone are shown in Table 3.2.8. Results show that participants with an ACTUAL rating of zero, (more specifically, generally furthest from the turbine with least likelihood of experience noise from the turbine) who could see the turbine did experience louder noise than those who could not. Those participants with an ACTUAL rating of two (i.e. closest to the turbine and more likely to experience noise) reported decreased symptoms if they could not see the turbine. However the sample sizes for groups with ACTUAL rating 1 and 2 are small and therefore the results should be treated with caution.

Results for Responses in ACTUAL region	N Participants		IV: Visibility DV: LOUD			IV: Visibility DV: OCCUR			IV: Visibility DV: SYMP		
	Can't See	Can See	B	SE	β	B	SE	β	B	R	β
0	37	34	.065	.031	.250*	.049	.035	.169	2.142	1.819	.153
1	1	32	.465	.763	.109	.393	.604	.116	2.926	7.877	.070
2	6	15	.488	.378	.284	.429	.405	.242	-5.220	2.706	-.405*

*p<.05; **p<.01

Note: ACTUAL = actual noise level rating; LOUD = perceived noise loudness; OCCUR = perceived noise occurrence; SYMP = symptom reporting score

Table 3.2.8: Comparison of the link between turbine visibility with noise perception and symptom reporting for the three ACTUAL noise regions

The data were then split into two depending on whether participants could or could not see the turbine from their dwelling. Then for each of the two groups a regression analysis was carried out to examine the effect of ACTUAL sound rating on the scores LOUD, OCCUR AND SYMP. Results of the three analyses for each group are shown in Table 3.2.9 and show that participants in both groups do report more frequent and louder noise from the turbine the higher the ACTUAL rating, (more specifically, the more noise the participant should experience from the turbine the more noise they do report). However the ability to see the turbine does not affect symptom reporting for either of the two groups.

Results for Responses with Visibility	N Participants			IV: Visibility DV: LOUD			IV: Visibility DV: OCCUR			IV: Visibility DV: SYMP		
	Zone 0	Zone 1	Zone 2	B	SE	β	B	SE	β	B	R	β
Can't See	37	1	6	.047	.017	.404**	.072	.029	.362*	1.598	1.315	.193
Can See	34	32	15	.268	.080	.354**	.268	.082	.350**	-1.777	1.119	-.188

*p<.05; **p<.01

Note: ACTUAL = actual noise level rating; LOUD = perceived noise loudness; OCCUR = perceived noise occurrence; SYMP = symptom reporting score

Table 3.2.9: Comparison of the link between ACTUAL noise level with noise perception and symptom reporting for those who can and cannot see a turbine

When exploring the two reasons why those who are able to see the turbine close to their dwelling report increased noise levels from the turbine, it would be expected that if the reason why increased noise levels is due to the visibility effects from the turbine, the relationship between visibility and noise reporting would only be significant for those who can see the turbine. Table 3.2.9 shows that this is not the case when LOUD score is the dependent variable. However, when OCCUR rating is the dependent variable the relationship is slightly more significant for those who can see the turbines suggesting that individuals report more frequent noise because they are able to see the turbine and not necessarily just because they live in a zone closer to the turbine.

3.2.2.5 Attitudes to Wind Turbines, Typical Noise, Noise Perception and General Health

Regression analyses were conducted to examine the effect of individuals' general attitudes towards wind turbines on their perception of turbine noise and the effect of participants' noise perception on their symptom reporting. The results of the regression analyses in Table 3.2.10 show that attitude to wind power significantly predicted perceived loudness and occurrence of turbine noise (supporting hypothesis 2a). Those with a more negative attitude towards wind turbines reported increased perceived noise levels from the turbine (supporting Hypothesis 1b) and those perceiving greater noise levels reported greater symptoms of ill health (supporting Hypothesis 3a). To examine whether the association between an individual's attitude to wind turbines on perceived noise was due to individuals typically being exposed to greater noise from the turbine, the relationship between attitude to wind turbines and typical noise experienced was examined using regression analyses. If this relationship was non-significant, it would indicate that the relationship between attitude to wind turbines and perceived noise was not due to typical noise experienced. The relationships between typical noise experienced and perceived noise, and typical noise experienced and reported symptoms were also examined using regression analyses. The results displayed in Table 3.2.10 demonstrate that the typical noise experienced does not predict general attitude to wind turbines (not supporting Hypothesis 4a). The typical noise experienced does however, predict the perceived loudness and frequency of noise from the turbines near to their dwelling (supporting Hypothesis 4b). Therefore, an individual living in a household with a higher probability of experiencing noise from the turbine does indeed perceive increased noise levels from that turbine. Importantly, typical noise experienced does not predict individuals' symptom reporting (not supporting Hypothesis 4c). To summarise, typical noise experienced from the turbine is not associated with a more negative attitude to wind turbines or symptoms of ill health reported, although it is associated with individuals' reported frequency and loudness of wind turbine noise. Conversely, increased perceived noise from the turbine is associated with greater symptom reporting, and a negative general attitude to wind turbines predicts increased loudness and frequency of noise from the turbine.

Independent Variable	Dependent Variable	β	t	p
ATT	LOUD	.279	3.197	.002
ATT	OCCUR	.284	3.244	.002
LOUD	SYMP	.228	2.543	.012
OCCUR	SYMP	.213	2.354	.020
ACTUAL	ATT	.015	.167	.867
ACTUAL	LOUD	.332	4.050	.000
ACTUAL	OCCUR	.363	4.457	.000
ACTUAL	SYMP	-.029	-.315	.753

Note: ACTUAL = actual noise level rating; ATT = attitude to wind turbines; LOUD = perceived noise loudness; OCCUR = perceived noise occurrence; SYMP = symptom reporting score

Table 3.2.10: Relationships between typical noise levels, attitude to wind turbines, noise perception scores and symptom reporting

3.2.2.6 The Role of Personality in Predicting Attitude to Wind Power, Turbine Noise Perception and Symptom Reporting

Two-step hierarchical linear regression analyses were conducted to examine whether NOP predicts attitude to wind power (Table 3.2.11), perceived turbine noise (Table 3.2.12) and reported symptoms (Table 3.2.13) over and above the effect of age and sex. Age and sex were entered into step 1 of the regression with all NOP measures entered at step 2. In all analyses neither age nor sex significantly predicted attitudes to wind power, perceived noise or reported symptoms. However, adding the NOP measures at step 2 revealed that, those with low positive affect, high negative affect and those who were intolerant of discomfort had a more negative attitude to wind power (supporting Hypothesis 1a). Those with lower positive affect, higher emotional intolerance and higher discomfort intolerance perceived turbine noise to be both louder and more frequent (supporting Hypothesis 1b). Finally, those with higher levels of negative affect, neuroticism and discomfort intolerance reported increased symptoms of ill-health (supporting Hypothesis 1c).

		B	*SE*	*β*
Step 1	Age	.026	.011	.232*
	Sex	.072	.341	.020
Step 2	Age	*.021*	.010	.185*
	Sex	..065	.305	.018
	PA	-.659	.153	-.427**
	NA	.742	.198	.378**
	N	-.277	.275	-.119
	F-disc	.695	.325	.302*
	F-emot	-.290	.328	-.145
Step 1 R		.231 (p = .060)		
Step 2 R^2 Change		.234 (p < .001)		

*p<.05; **p<.01

Note: PA = positive affect; NA = negative affect; N = neuroticism; F-disc = discomfort intolerance; F-emot = emotional intolerance

Table 3.2.11: Hierarchical regression analyses of personality on attitude to wind turbines

		Perceived Noise Loudness			Perceived Noise Occurrence		
		B	*SE*	*β*	*B*	*SE*	*β*
Step 1	Age	-.005	.003	-.147	-.004	.003	-.136
	Sex	-.051	.106	-.046	-.020	.097	-.020
Step 2	Age	-.006	.003	-.163	-.004	.003	-.134
	Sex	-.087	.089	-.079	-.047	.084	-.047
	PA	-.193	0.45	-.401**	-.161	.042	-.364**
	NA	.286	.058	.468**	.255	.055	.455**
	N	-.234	.080	-.321*	-.132	.076	-.198
	F-disc	-.231	.095	-.322*	-.167	.090	-.254
	F-emot	.336	.096	.538**	.234	.091	.408*
Step 1 R		.151 (p = .290)			.136 (p = .366)		
Step 2 R^2 Change		.325 (p< .001)			.285 (p < .001)		

*p<.05; **p<.01

Note: PA = positive affect; NA = negative affect; N = neuroticism; F-disc = discomfort intolerance; F-emot = emotional intolerance

Table 3.2.12: Hierarchical regression analyses of personality on perceived turbine noise (loudness and occurrence)

		B	*SE*	*β*
Step 1	Age	.024	.043	.054
	Sex	.826	1.327	.060
Step 2	Age	.037	.038	.084
	Sex	1.085	1.128	.079
	PA	.140	.568	.023
	NA	1.537	.732	.201*
	N	3.625	1.016	.399**
	F-disc	3.191	1.204	.356**
	F-emot	-1.250	1.215	-.160
Step 1 R		.078 (p = .720)		
Step 2 R^2 Change		.318 (p < .001)		

*p<.05; **p<.01

Note: PA = positive affect; NA = negative affect; N = neuroticism; F-disc = discomfort intolerance; F-emot = emotional intolerance

Table 3.2.13: Hierarchical regression analyses of personality on reported symptoms

3.2.2.7 Moderation Analyses

Moderation analyses were carried out to determine which personality variables influence the relationships between attitudes to wind turbines, noise perception and symptom reporting. For the theory behind moderation analysis and the reason why it is carried out see Appendix E, Section E.10.

The Role of NOP in Moderating the Wind Turbine Attitude – Noise Perception Association The potential moderating impact of NOP on the attitude to wind turbine - perceived noise relationship was examined. A two-step hierarchical regression analysis[1] was carried out for the attitude – perceived loudness relationship. Attitude to wind power, and NOP variables were entered at step 1 and interaction terms at step 2. All predictor variables were based on mean centred scores. Simple slopes analyses[2] were carried out 1 SD above and below the moderator variable where a moderating effect was found, and all values entered into the simple slopes analyses were standardised. A moderating effect is present if the interaction term introduced at step 2 is significant (i.e.$p < 0.05$). Results from the analyses in Table 3.2.14 show that the link between attitude to wind turbines and perceived noise loudness was moderated by NA, discomfort intolerance and emotional intolerance.

[1]See Appendix E, Section E.9.2 for the theory behind hierarchical linear regression.
[2]See Appendix E, Section E.10.2 for the theory behind simple slopes.

Interaction Term	Step 1: ATT and Moderator	Step 2: Interaction Term
ATT × PA	R = .291; $F_{2,107}$ = 4.966; p = .009 β: ATT = -.254*; PA = .08	ΔR^2 = .000; $F_{1,106}$ = .016; p = .898 β: ATT×PA = .013
ATT × NA	R = .445; $F_{2,105}$ = 12.951; p < .001 β: ATT = -.201*; NA = -.355**	ΔR^2 = .061; $F_{1,104}$ = 8.526; p = .004 β: ATT×NA = .281**
ATT × N	R = .313; $F_{2,108}$ = 5.855; p =.004 β: ATT = -.268**; N = -.142	ΔR^2 = .022; $F_{1,107}$ =2.664; p =.106 β: ATT×N = .149
ATT × F-disc	R = .279; $F_{2,101}$ = 4.275; p =.017 β: ATT = -.282**; F-disc = .012	ΔR^2 = .047; $F_{1,100}$ =5.366; p =.023 β: ATT×F-disc = .233*
ATT × F-emot	R = .358; $F_{2,100}$ = 7.370; p =.001 β: ATT = -.248*; F-emot = -.227*	ΔR^2 = .112; $F_{1,99}$ = 14.595; p <.001 β: ATT×F-emot = .339**
For β values *p<.05; **p<.01		

Note: ATT = attitude to wind turbines; PA = positive affect; NA = negative affect; N = neuroticism; F-disc = discomfort intolerance; F-emot = emotional intolerance

Table 3.2.14: Moderation results for attitude – loudness of noise link with NOP measures as moderator

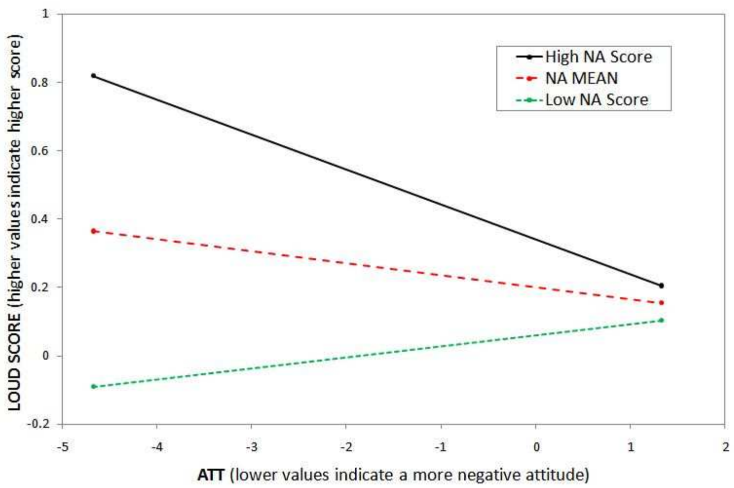

Figure 3.2.3: Simple slopes for the attitude – loudness of noise link with NA as moderator

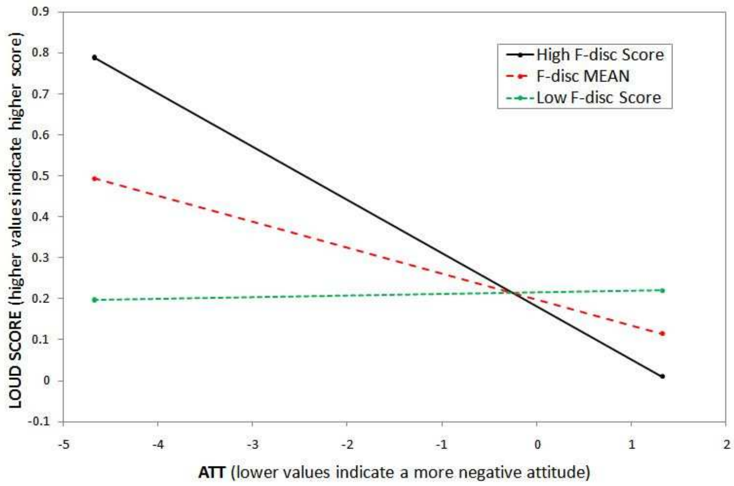

Figure 3.2.4: Simple slopes for the attitude – loudness of noise link with F-disc as moderator

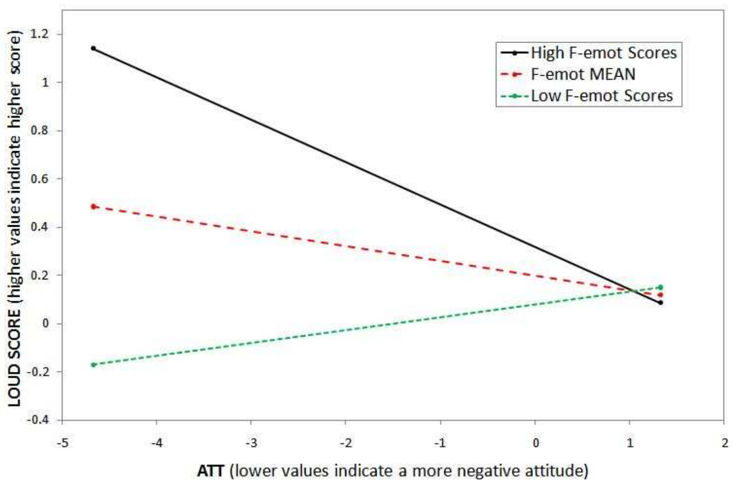

Figure 3.2.5: Simple slopes for the attitude – loudness of noise link with F-emot as moderator

The same analyses were carried out for the attitude – perceived noise occurrence relationship. Results in Table 3.2.15 show again that, the relationship between attitude to turbines and perceived noise occurrence was moderated by NA, and emotional intolerance, supporting Hypothesis 2b.

Interaction Term	Step 1: ATT and Moderator	Step 2: Interaction Term
ATT × PA	R = .298; $F_{2,106}$ = 5.153; p = .007 β: ATT = -.258**; PA = .093	ΔR^2 = .001; $F_{1,105}$ = .063; p = .803 β: ATT×PA = .025
ATT × NA	R = .448; $F_{2,104}$ = 13.057; p < .001 β: ATT = -.206*; NA = -.355**	ΔR^2 = .042; $F_{1,103}$ = 5.722; p = .019 β: ATT×NA = .234*
ATT × N	R = .344; $F_{2,107}$ = 7.170; p =.001 β: ATT = -.268**; N = -.194*	ΔR^2 = .027; $F_{1,106}$ =3.375; p =.069 β: ATT×N =.166
ATT × F-disc	R = .284; $F_{2,100}$ = 4.397; p =.015 β: ATT = -.287**; F-disc = .015	ΔR^2 = .034; $F_{1,99}$ =3.843; p =.053 β: ATT×F-disc = .199
ATT × F-emot	R = .351; $F_{2,99}$ = 6.938; p =.002 β: ATT = -.255**; F-emot = -.208*	ΔR^2 = .100; $F_{1,98}$ = 12.561; p <.001 β: ATT×F-emot = .320**

For β values *p<.05; **p<.01

Note: ATT = attitude to wind turbines; PA = positive affect; NA = negative affect; N= neuroticism; F-disc = discomfort intolerance; F-emot = emotional intolerance

Table 3.2.15: Moderation results for attitude – occurrence of noise link with NOP measures as moderator

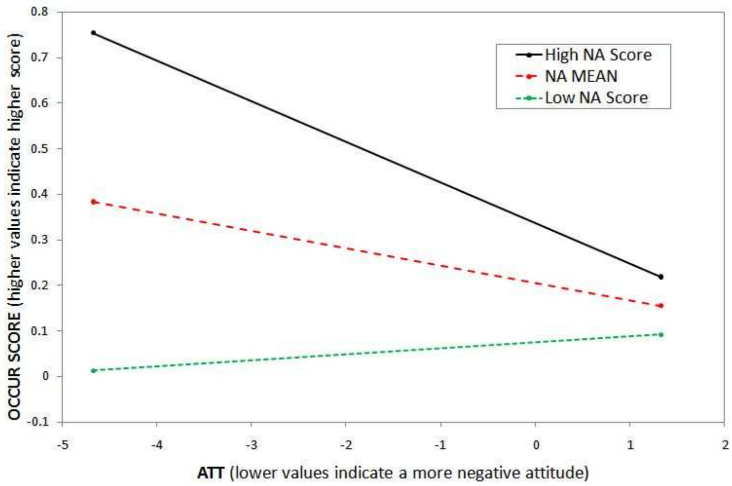

Figure 3.2.6: Simple slopes for the attitude – occurrence of noise link with NA as moderator

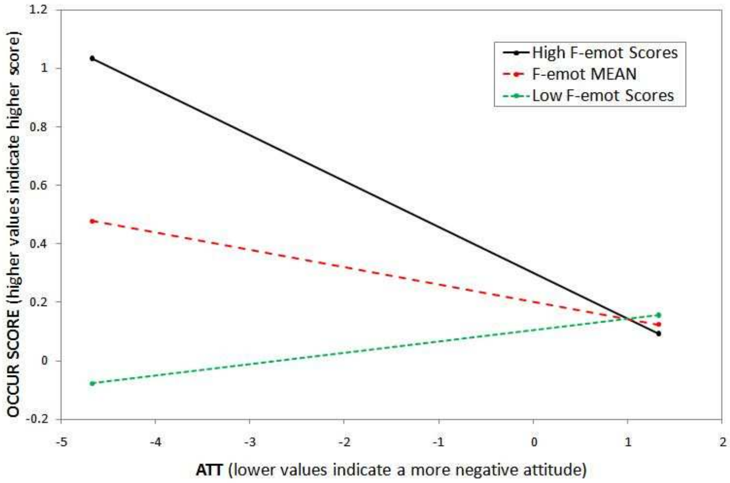

Figure 3.2.7: Simple slopes for the attitude – occurrence of noise link with F-emot as moderator

The simple slope analyses show that the relationships between attitude and both loudness and occurrence of noise perception only occurs at high levels of NA (β=-0.1024, t=-2.9755, p=.004 Figure 3.2.3, and β=-0.0893, t=-2.686, p=.008 Figure 3.2.6 respectively) and emotional intolerance (β=-0.1756, t=-4.2187, p<.001 Figure 3.2.5 and β=-0.1568, t=-3.9778, p<.001 Figure 3.2.7 respectively). The relationship between attitude and loudness of noise occurs at high levels of discomfort intolerance (β=-0.1297, t=-2.99, p=.004 Figure 3.2.4).

The Role of NOP in Moderating of the Noise Perception – Reported Symptom Association The moderating impact of NOP on the effect of perceived noise on reported symptoms was examined. Two two-step hierarchical regression analyses were carried out to examine the moderating impact of NOP on the perceived noise loudness - symptom and the perceived noise occurrence - symptom relationships.

Interaction Term	Step 1: LOUD and Moderator	Step 2: Interaction Term
LOUD × PA	R = .229; $F_{2, 112}$ = 3.098; p = .049 β: LOUD = .231*; PA = -.022	ΔR^2 = .003; $F_{1, 111}$ = .344; p = .559 β: LOUD×PA = -.055
LOUD × NA	R = .359; $F_{2, 111}$ = 8.235; p < .001 β: LOUD = .107; NA = -.303**	ΔR^2 = .038; $F_{1, 110}$ = 4.995; p = .027 β: LOUD×NA = -.390*
LOUD × N	R = .469; $F_{2, 115}$ = 16.186; p <.001 β: LOUD = .160; N = -.415**	ΔR^2 = .016; $F_{1, 114}$ =2.416; p =.123 β: LOUD×N = -.135
LOUD × F-disc	R = .427; $F_{2, 108}$ = 12.057; p <.001 β: LOUD = .208*; F-disc = -.362**	ΔR^2 = .039; $F_{1, 107}$ =5.319; p =.023 β: LOUD×F-disc = -.230*
LOUD × F-emot	R = .412; $F_{2, 109}$ = 11.140; p <.001 β: LOUD = .135; F-emot = -.355**	ΔR^2 = .041; $F_{1, 108}$ = 5.617; p =.020 β: LOUD×F-emot = -.338*

For β values *p<.05; **p<.01

Note: LOUD = perceived noise loudness; PA = positive affect; NA = negative affect; N = neuroticism; F-disc = discomfort intolerance; F-emot = emotional intolerance

Table 3.2.16: Moderation results for loudness of noise – symptom link with NOP measures as moderators

Interaction Term	Step 1: OCCUR and Moderator	Step 2: Interaction Term
OCCUR × PA	R = .214; $F_{2, 111}$ = 2.655; p = .075 β: OCCUR = .216*; PA = .827	ΔR^2 = .003; $F_{1, 110}$ = .337; p = .563 OCCUR×PA = -.055
OCCUR × NA	R = .355; $F_{2, 110}$ = 7.940; p = .001 β: OCCUR = .088; NA = -.310**	ΔR^2 = .051; $F_{1, 109}$ = 6.694; p = .011 OCCUR×NA = -.409*
OCCUR × N	R = .457; $F_{2, 114}$ = 15.072; p <.001 β: OCCUR = .123; N = -.415**	ΔR^2 = .015; $F_{1, 113}$ =2.194; p =.141 OCCUR×N = -.140
OCCUR × F-disc	R = .420; $F_{2, 107}$ = 11.471; p <.001 β: OCCUR = .194*; F-disc = -.363**	ΔR^2 = .044; $F_{1, 106}$ =5.996; p =.016 OCCUR×F-disc = -.264*
OCCUR × F-emot	R = .409; $F_{2, 108}$ = 10.860; p <.001 β: OCCUR = .125; F-emot = -.360**	ΔR^2 = .047; $F_{1, 107}$ = 6.470; p =.012 OCCUR×F-emot = -.332*

For β values *p<.05; **p<.01

Note: OCCUR = perceived noise occurrence; PA = positive affect; NA = negative affect; N = neuroticism; F-disc = discomfort intolerance; F-emot = emotional intolerance

Table 3.2.17: Moderation results for occurrence of noise – symptom link with NOP measures as moderator

Table 3.2.16 and Table 3.2.17 show that NA, discomfort intolerance and emotional intolerance moderate both the relationships between perceived noise loudness and perceived noise occurrence on symptom reporting (supporting Hypothesis 3b).

The simple slope analyses show that the link between both loudness and occurrence of noise perception and symptom reporting only occurs at high levels of discomfort intolerance (β=3.954, t=3.4815, p<.001

Figure 3.2.8, and β=3.784, t=3.148, p=.002 Figure 3.2.10 respectively) and emotional intolerance (β=1.921, t=1.677, p=.096 Figure 3.2.9 and β=2.158, t=1.756, p=.082 Figure 3.2.11 respectively). However, the link between both perceived loudness and occurrence with symptom reporting does not reach significance at any level of NA.

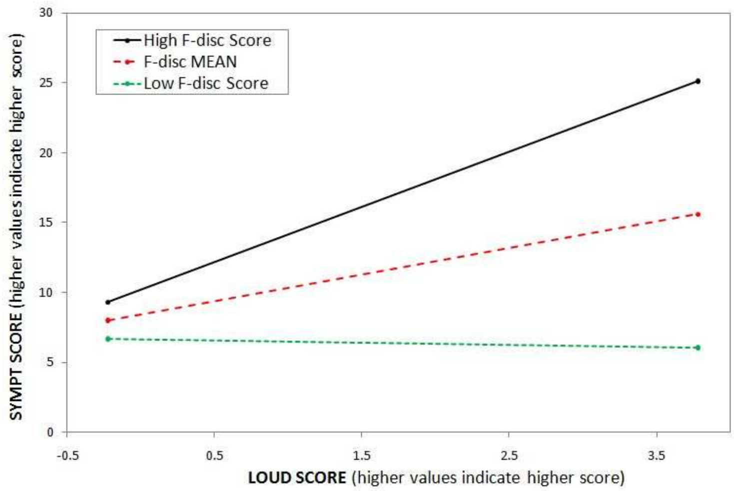

Figure 3.2.8: Simple slopes for the loudness of noise - symptoms link with F-disc as moderator

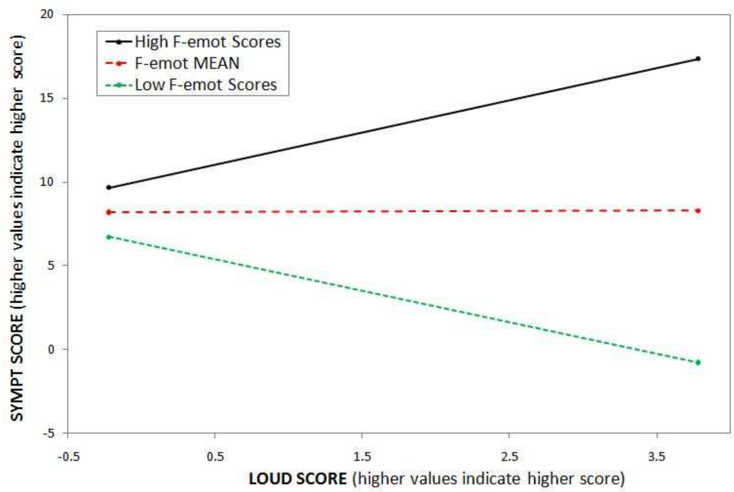

Figure 3.2.9: Simple slopes for the loudness of noise - symptoms link with F-emot as moderator

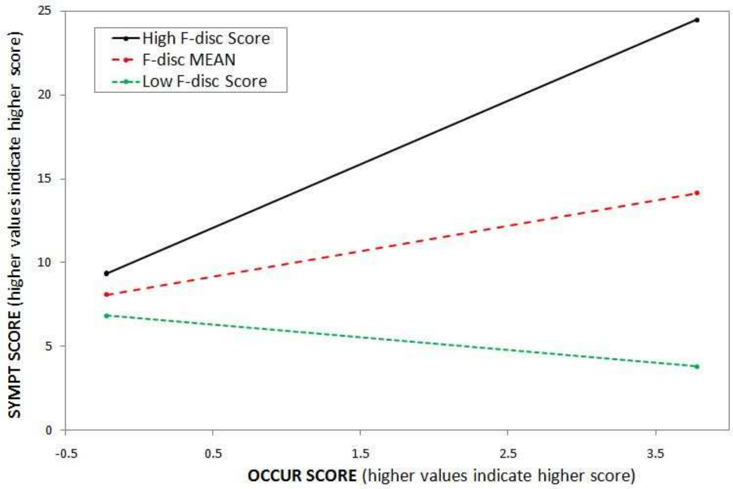

Figure 3.2.10: Simple slopes for the occurrence of noise - symptoms link with F-disc as moderator

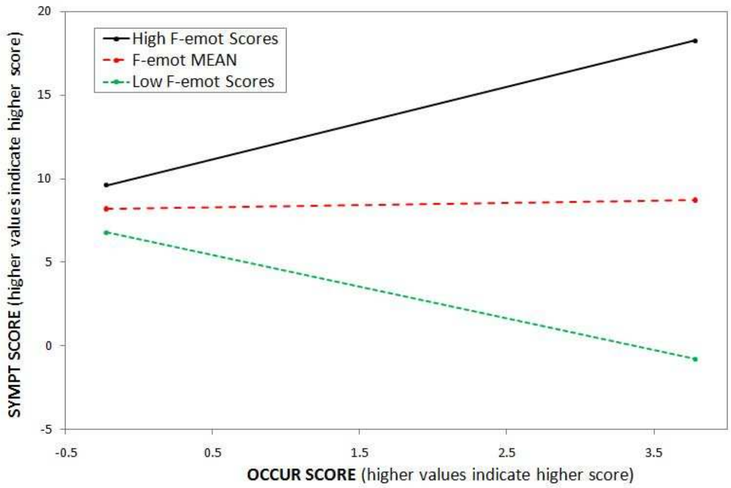

Figure 3.2.11: Simple slopes for the occurrence of noise - symptoms link with F-emot as moderator

3.2.2.8 Participant Comments

There were a number of interesting comments voluntarily left by the respondents in response to an optional free response section, where participants were asked to make any further comments. The comments given widely ranged from comments about the turbine close to the dwelling to comments about the survey itself. Interestingly a number of participants commented that they did not have a turbine close to their dwelling. It was known that each household sent a survey did in fact live close to a small or micro turbine. It is possible that this is due to the perception of what a wind turbine is and that when talking about wind turbines, some people associate the term only with large scale turbines and do not understand what small or micro turbines really are.

Some respondents stated that they were aware of the turbine, but could not hear it and that it is not a problem to their everyday life. Some of the comments of this type are shown below (the participant numbers are given after each quote):

> *"Although visible, the small wind turbine is some distance away, so I would not expect to hear it. Were I to live closer, my attitude may be different!"* - D11.3

> *"I have seen the turbine but never experienced noise from it."* - D14.109

> *"I can't hear the wind turbine and the sight of it doesn't bother me."* - D5.7

> *"My daughter's school has recently put up a wind turbine close to my house, and I find it to be of no distraction."* - D8.47

Some commented that they could hear the turbine, but that they liked the noise or that the noise did not bother them as follows:

> *"Not sure how I would feel if I were closer and could hear (the turbine). Whenever I walk past I rather like the noise it makes."* - D7.104

> *"I can only see the turbine when the leaves are off the trees. I quite like it, especially if it is going round. I'm close enough to hear it."* - D8.20

> *"The turbine is purely noticeable when the wind is blowing - it gets louder as the wind gets stronger and becomes integrated with the windy noises. It is a noise that you gradually get used to."* - D9.88

> *"I think the turbines are a great idea to save money and love to hear them humming/throbbing along with the strong wind."* - D15.274

> *"Although when windy it can be loud, it is by no means irritating."* - D2.53

> *"Much quieter than was expected."* - D5.5

However, others commented that they were able to hear the noise and in addition to this, experience the noise as a negative. Some even commenting that this affects their moods as follows:

> *"The small wind turbine make a BIG NOISE. We can't sleep and take rest out from the terrible noise."* - D15.283

> *"While the wind turbine is switched on, it is very noisy. At night time I am not able to sleep. I have to work and the lack of sleep causes me mood swings."* - D15.33

> *"Not only noisy but very ugly which depresses me."* - D9.63

The differences in attitudes by individuals about the noise emphasises the fact that the perception of the noise has been shown to be personality driven because some people experience the noise and like it but others absolutely can not bear it. The findings from regression analyses demonstrate differences in attitudes may be due to other factors than the noise itself.

Some general statements about wind turbines were left by individuals, on the whole these were positive comments and reinforced the notion that the mean attitude to wind turbines reported by all respondents was positive (mean attitude = 2.33):

> *"I generally agree with wind power - if it is positioned sensitively and with agreement of the community."* - D13.108

> *"We need more-many more. Personally I would like one on every house next to a solar panel."* - D14.95

> *"I am bothered that the school might decide to expand the project, also it is so near my property and there have been no assurances as the the safety of these masts."* - D8.73

3.3 Recordings Study

In this Chapter the methodology and results of the recordings study given to students of the University of Nottingham will be detailed. In this version of the questionnaire, sound and video recordings of micro and small turbine noise plus one recording with only ambient noise at one of the installations were played to the participants. They were asked to complete measures relating to the recordings as well as personality measures so their perceptions of the turbine noise could be assessed. This part of the study contributes to achieving the objectives of the Thesis with the analysis of the data designed to answer the hypothesis questions 5 to 7 given in Section 3.1.7. It also serves to further confirm the results from the domestic study to identify whether noise perception of wind turbine noise depends largely on whether the noise is an intrusion on everyday life or simply due to the characteristics of the noise. In this experimental study it was possible to control the turbine noises the individuals were hearing. Therefore it is known what they should have heard and the issue of personality on the perceptions of the noise can be seen directly.

3.3.1 Methodology

The measures included in the recordings study are described in detail in the following Sections as well as the procedure for collecting the data. The questionnaire was split into three parts as follows:

1. Questions regarding particular personality traits of each respondent, age and sex and attitude to wind turbines,

2. Questions relating to each turbine recording,
3. Questions about non-specific symptoms of each participant.

The full questionnaire is available in Appendix G.

3.3.1.1 Participants and Procedure

Students at the University of Nottingham were asked to complete this recordings version of the questionnaire. Participation was voluntary and the questionnaire was carried out during a lecture. Students completed questions concerning six recordings of wind turbine noise and one recording with only ambient noise at one installation. Each recording was thirty seconds in length, four sound recordings were included, two were video recordings and one was a sound recording which did not feature any wind turbine noise. The video recordings were included to investigate whether the visibility of the turbines increases the perception of noise from the recordings. Each of the seven recordings were taken at one of the turbine installations included in the noise measurement part of the research (see Section 2.2.1.1). The recordings were chosen to give a good range of the sounds typically heard from the small and micro wind turbine types S1 and M1 respectively. Recordings in a low and high wind speeds were selected.

One hundred and twelve students participated in the questionnaire, (age range of respondents = 18-32; mean age = 20.02, SD = 1.902) 86% were female. As analysis from the domestic study data showed that there were no significant differences in the results depending on age or sex, the high percentage of females and small range of ages of students participating in the study was not considered as a concern. There were no significant differences between male and female responses, therefore, the data were analysed as one group.

3.3.1.2 Measures

In the following Sections more details about the measures included in each of the three parts of the recordings questionnaire are given.

Wind Turbine Measures

Attitude to Wind Power Attitude to wind power was measured using a single item "Please rate how you feel about wind power in general". Participants responded using a 7 point Likert type scale (1 = very positive to 7 = very negative).

Recordings Included A description of the seven recordings included in the study are as follows and the sound recordings used for the study are available on the CD found at the back of the Thesis:

- Recording 1 - a sound recording of two micro turbines of type M1 at installation (d) in moderate wind speeds. The loudest noises in this recording are expected to be perceived as high frequency squeaking, whistling and swooshing. There is some wind noise over the microphone at the end of the recording (may be perceived as low frequency).
- Recording 2 - a sound recording of a small turbine type S1 at installation (a) at moderate wind speeds. The main noises in this recording are expected to be perceived as swooshing, humming and buzzing.
- Recording 3 - a video recording of two small turbines of type S1 at installation (b) at moderate wind speeds. The most predominant noises expected to be perceived in this recording are swooshing and humming with some wind noise.
- Recording 4 - this is a sound recording taken at installation (d) in the same wind conditions as recording 1 but with the two micro turbines switched off. There should therefore be no noise from the turbine perceived from this recording.
- Recording 5 - a sound recording of one small turbine type S1 taken at installation (c) in very high wind speeds. There is some wind noise during the recording however the key noise perceived from the turbine are expected to be swooshing, thumping, humming, throbbing and low frequency sounds. It may be expected that participants might also report chopping as a sound that is not listed but that they perceive.
- Recording 6 - a sound recording taken at installation (d) with the two micro turbines of type M1 but at very high wind speeds where the turbines are both rotating extremely fast at approximately 1000rpm. The predominant sounds in this recording are expected to be perceived as humming, buzzing, whistling, low frequency and thumping.
- Recording 7 - a video recording of one small turbine type S1 at installation (a) at low to moderate wind speeds where the turbine is slowly turning to face the wind direction and increasing in rotational speed. The main sounds expected to be perceived from this recording are swooshing, screeching, thumping and low frequency sounds.

Perceived Noise from each Turbine Recording Participants rated how loud they perceived each of ten given sounds to be. The sounds included were the same as those in the domestic survey (swooshing, screeching, whistling, humming, throbbing, thumping, scratching, high frequency, low frequency and buzzing). The rating was given on a five point Likert type scale where 0 = ‘cannot hear’ and 4 = ‘extremely loud’. A mean score was calculated for the perception of sound in each separate recording for each participant by taking the mean of scores for the ten sounds rated. A mean noise perception score was also calculated for each participant for the following:

- A mean noise perception score for all six recordings with turbine sounds present calculated as the mean of each recording noise perception score for each participant (LOUD_ALLT).

- A mean noise perception score for all four sound recordings calculated as the mean of each sound recording noise perception score for each participant (LOUD_SOUND).
- A mean noise perception score for the two video recordings calculated as the mean of each video recording noise perception score for each participant (LOUD_VIDEO).
- A noise change score calculated as the loudness score for the recording with no turbine noise present subtracted from the loudness rating score for all six recordings with turbine noise present (LOUD_CHANGE).

Annoyance of each Turbine Recording Each participant was asked to answer the following two questions to rate how annoying they considered each recording to be:

1. "Please rate how annoying you find the sounds in this recording" - participants answered on a 5 point Likert type scale where 1 = not at all annoying and 5 = extremely annoying
2. "How long do you feel you could put up with the sounds in this recording before you would have to switch it off?" Participants had to choose one of five answers; "seconds", "minutes", "hours", "days" and "wouldn't have to switch off". The answers were converted to a Likert type scale to give a rating score where 1 = "seconds" and 5 = "wouldn't have to switch off".

A mean annoyance and length of time rating was also calculated for each participant for the following:

- A mean annoyance and length of time rating for all six recordings with turbine sounds present calculated as the mean of each annoyance and length of time score for each participant for all recordings (ANNOY_ALLT and LENGTH_ALLT).
- A mean annoyance and length of time rating for all four sound recordings calculated as the mean of each annoyance and length of time score for each participant for the sound recordings (ANNOY_SOUND and LENGTH_SOUND).
- A mean annoyance and length of time rating for the two video recordings calculated as the mean of each annoyance and length of time score for each participant for the video recordings (ANNOY_VIDEO and ANNOY_SOUND).

Personality Measures The personality measures included in the recordings version of the questionnaire were the positive and negative affectivity scale, the neuroticism scale and both sub-scales of the frustration discomfort scale and the symptom reporting scale.

For all measures, higher scores indicate higher levels of the measure itself, except for attitude, where a higher score indicates a more negative attitude and length of time to switch off, where a higher score indicates that the time the participant could listen to the recording before it would have to be switched off is longer (i.e. less intrusive).

The full results and analysis of the data collected from the recordings study responses are given in the the following Section and a conclusion of the key findings will be given in Section 3.4. The conclusion will also include a comparison of the results from both the domestic and recordings studies.

3.3.2 Results

3.3.2.1 Descriptive statistics

Descriptive statistics and scale reliabilities for attitude to wind turbines and all personality measures are shown in Table 3.3.1. Descriptive statistics for all noise perceptions scores, annoyance ratings and time to switch off the recording ratings are shown in Table 3.3.2 along with the scale reliabilities for the loud scores for each recording. All scales were reliable with Cronbach's alphas all >0.7 showing that all items in each scale were internally consistent i.e. the set of items measure the same thing. The data was checked to verify that any missing responses were random and not systematic and this was found to be the case.

Zero-order correlations are shown in Table 3.3.3. Correlations are given with the mean score of all the noise perception, annoyance rating and time to switch off ratings only as these scores for the individual recordings are all highly correlated to one another. In addition to this the correlations between individual recordings are not meaningful as the recordings are all of different turbines in different wind conditions.

	α	Mean	SD
ATT		2.61	1.254
SYMP	.786	.78	.338
PA	.812	2.28	.432
NA	.805	1.55	.266
N	.858	2.77	.412
F-disc	.764	2.67	.480
F-emot	.805	2.89	.371

Note: ATT = attitude to wind turbines; SYMP = symptom reporting score; PA = positive affect; NA = negative affect; N = neuroticism; F-disc = discomfort intolerance; F-emot = emotional intolerance

Table 3.3.1: Descriptive statistics for attitudes and personality measures

	LOUDx			ANNOYx		LENGTHx	
	α	Mean	SD	Mean	SD	Mean	SD
RECORDING 1	.778	1.08	.572	2.71	1.021	2.52	.881
RECORDING 2	.605	1.05	.472	2.96	.967	2.32	.812
RECORDING 3	.731	1.00	.936	2.80	1.030	2.59	.899
RECORDING 4	.761	.60	.478	1.75	.913	3.51	1.131
RECORDING 5	.775	1.24	.673	3.75	.872	2.02	.786
RECORDING 6	.745	1.03	.932	2.66	.968	2.68	.983
RECORDING 7	.735	.64	.448	1.96	1.004	3.44	1.165
ALLT		1.01	.497	2.81	.685	2.59	.719
SOUND		1.10	.530	3.01	.688	2.38	.695
VIDEO		.82	.586	2.37	.851	3.00	.897

Note: LOUDx = perceived noise loudness from each recording; ANNOYx = the annoyance rating of each recording; LENGTHx = the length of time to switch off rating for each recording (x - denotes which recording the score refers to)

Table 3.3.2: Descriptive statistics for LOUD, ANNOY and LENGTH measures for each recording

The zero-order correlation table shows that noise perception scores are correlated with how annoying the recordings are and also with how long respondents could tolerate the recordings before switching them off, LOUD scores are also correlated with symptom reporting scores. The louder the turbine noises in the recording are perceived to be the more annoying they are considered and shorter the length of time individuals can tolerate the recording before having to switch it off. Attitudes to wind turbines also show a correlation with noise perception scores, annoyance ratings and the length of time to switch off where those with a more negative attitude to wind turbines find the turbine noises in the recordings to be louder, more annoying and would have to switch off the recording sooner than respondents with a positive attitude to wind turbines. These correlations are investigated in more detail in the following Sections as well as the correlations showing links with personality traits. These early correlation results are similar to the results seen for the domestic study where individuals with a more negative attitude to wind turbines perceived more noise from the turbines close to their dwellings and in turn reported higher general symptom levels.

	1	2	3	4	5	6	7	8	9
ATT (1)									
PA (2)	.073								
NA (3)	.046	.018							
N (4)	-.181	-.206*	.519**						
F-disc (5)	-.026	-.123	.196	.065					
F-emot (6)	-.175	.016	.287**	.291**	.502**				
SYMP (7)	-.031	-.120	.395**	.435**	.153	.183			
LOUD_ALLT (8)	.324**	.160	.175	.064	.406**	.208*	.112		
ANNOY_ALLT (9)	.268**	.057	.231*	.192	.222*	.127	.157	.484**	
LENGTH_ALLT (10)	-.286**	.097	-.248*	-.170	-.181	.052	-.108	-.319**	-.559**

*p<.05; **p<.01

Note: ATT = attitude to wind turbines; PA = positive affect; NA = negative affect; N = neuroticism; F-disc = discomfort intolerance; F-emot = emotional intolerance; SYMP = symptom reporting score; LOUD_ALLT = mean perceived noise loudness for all recordings; ANNOY_ALLT = the annoyance rating for all recordings; LENGTH_ALLT = the length of time to switch off rating for all recordings

Table 3.3.3: Zero-order correlations for personality measures and mean turbine measure scores for all recordings

3.3.2.2 Perceived Sounds

Respondents were asked to rate how loud each of ten sounds were in the seven recordings. A description of the seven recordings is given in Section 3.3.1.2.

The mean perception score for the ten sounds for each of the seven recordings is shown in Table 3.3.4. The mean LOUD noise perception score for each recording, as well as the mean annoyance rating and the mean length of time the respondents could tolerate the sound before having to switch it off is also shown in the table. The top five perceived sounds for each recording are ranked in superscript. The recordings are also ranked in terms of their LOUD, ANNOY and LENGTH ratings (in superscript next to the mean scores).

	LOUD1	LOUD2	LOUD3	LOUD4	LOUD5	LOUD6	LOUD7	Average
Swooshing	1.66 (2)	1.30 (4)	1.60 (1)	0.96 (3)	1.94 (1)	1.23 (3)	1.41 (1)	1.44 (1)
Screeching	1.04 (4)	0.24	0.37	0.12	0.70	0.44	0.32	0.46
Buzzing	0.59	1.97 (1)	1.10 (4)	0.44	1.05	1.14 (4=)	0.38	0.95 (4)
Whistling	1.82 (1)	0.64	0.65	0.40	0.85	0.67	0.75 (4)	0.83
Humming	1.01 (5)	1.83 (2)	1.44 (2)	1.03 (2)	1.13 (5=)	1.45 (2)	0.59 (5=)	1.21 (3)
Throbbing	0.70	0.78	0.57	0.85 (4)	1.26 (4)	1.14 (4=)	0.45	0.82
Thumping	0.67	0.41	0.40	0.48 (5)	1.13 (5=)	0.90	0.27 (5=)	0.61
Scratching	0.77	0.99 (5)	0.97 (5)	0.13	1.69 (2)	0.62	0.90 (2)	0.87 (5)
High Freq.	1.59 (3)	0.67	0.72	0.17	0.98	0.51	0.59	0.75
Low Freq.	0.94	1.60 (3)	1.33 (3)	1.41 (1)	1.56 (3)	1.50 (1)	0.76 (3)	1.30 (2)
Mean All	1.08 (2)	1.05 (3)	1.00 (5)	0.61 (7)	1.24 (1)	1.03 (4)	0.64 (6)	0.95
ANNOY	2.71 (4)	2.96 (2)	2.80 (3)	1.75 (7)	3.75 (1)	2.66 (5)	1.96 (6)	2.66
LENGTH	2.52 (3)	2.32 (2)	2.59 (4)	3.51 (7)	2.02 (1)	2.68 (5)	3.44 (6)	2.73

Table 3.3.4: Scores for each sound for each recording with mean ANNOY and LENGTH ratings with rankings

The results in Table 3.3.4 show that generally the more turbine noise from the recordings the more annoying they are and the shorter the length of time they could be tolerated before having to be switched off. The individual turbine sounds also match up well with the expected ranking of sounds in each recordings given in Section 3.3.1.2. The most commonly reported sounds from the turbines in the recordings were swooshing, humming, scratching and low frequency sounds. Turbine sounds were reported from recording 4 (the recording without turbine sound) but as expected this ranked as having the least turbine noise and the least annoying. From the results of which sounds were reported in a recording and how annoying that recording was, it is inferred that the turbine sounds which are the most annoying are swooshing, humming and scratching.

3.3.2.3 Attitudes to Wind Turbines, Noise Perception and General Health

Regression analyses were conducted to examine the effect of an individual's general attitude towards wind turbines on their perception of turbine noise in the recordings and the effect of participant's noise perception on their symptom reporting. Regression analyses were also carried out to determine whether attitude has an effect on a respondent's annoyance rating of the turbine noise in the recordings and the length of time the respondents are able to tolerate the recordings before they would have to switch them off. The results of the regression analyses with attitude set as the independent variable are shown in Table 3.3.5. The results show that all results are significant and individuals who have a more negative attitude to wind turbines perceive the turbine noises as louder in the recordings (supporting Hypothesis 7a). They also observe the recordings as more annoying and could not tolerate them for as long before having to switch off (supporting Hypothesis 7c).

Independent Variable	Dependent Variable	β	t	p
ATT	LOUD1	.203	2.079	.040
ATT	LOUD2	.242	2.503	.014
ATT	LOUD3	.181	1.847	.068
ATT	LOUD4	.284	2.976	.004
ATT	LOUD5	.282	2.953	.004
ATT	LOUD6	.284	2.971	.004
ATT	LOUD7	.237	2.451	.016
ATT	LOUD_ALLT	.324	3.443	.001
ATT	LOUD_SOUND	.324	3.443	.001
ATT	LOUD_VIDEO	.235	2.430	.017
ATT	ANNOY_ALLT	.268	2.797	.006
ATT	ANNOY_SOUND	.261	2.716	.008
ATT	ANNOY_VIDEO	.226	2.331	.022
ATT	ANNOY4	.353	3.769	.000
ATT	LENGTH_ALLT	-.286	-2.996	.003
ATT	LENGTH_SOUND	-.229	-2.366	.020
ATT	LENGTH_VIDEO	-.331	-3.528	.001
ATT	LENGTH4	-.358	-3.836	.000

Note: ATT = attitude to wind; LOUDx = perceived noise loudness from each recording; ANNOYx = the annoyance rating of each recording; LENGTHx = the length of time to switch off rating for each recording (x - denotes which recording the score refers to)

Table 3.3.5: Relationships between attitude to wind turbines with noise perception scores, annoyance and length of time to switch off

Results of the regression analyses to investigate the effect of the perceived loudness of the turbine sounds in the recordings on symptom reporting is shown in Table 3.3.6. Results are non-significant showing that the perceived loudness of the turbine sounds in the recordings does not affect symptom reporting (not supporting Hypothesis 5b) except for in the cases of the video recordings where results were significant. Therefore, respondents perceiving the turbine sounds as louder in the video recordings are reporting increased general symptom levels (supporting Hypothesis 5b). This finding implies that there is something about the visual nature of the recording which is linked to increased symptom levels. It is unlikely in this case that the sounds in the recordings are having an influence on each individual's symptom reporting level as the respondents are only exposed to the noise for the duration of the questionnaire. It is more likely in this instance that the level of symptoms an individual is experiencing at the time of the questionnaire will have an effect on how they perceive the noise from the recordings. Further investigation of this observation is given in Section 3.3.2.6.

Independent Variable	Dependent Variable	β	t	p
LOUD1	SYMP	.061	.637	.525
LOUD2	SYMP	.083	.866	.388
LOUD3	SYMP	.195	2.055	.042
LOUD4	SYMP	.080	.828	.409
LOUD5	SYMP	-.149	-1.559	.122
LOUD6	SYMP	.131	1.369	.174
LOUD7	SYMP	.189	1.996	.049
LOUD_ALLT	SYMP	.112	1.167	.246
LOUD_SOUND	SYMP	.025	.262	.794
LOUD_VIDEO	SYMP	.227	2.410	.018

Note: SYMP = symptom reporting score; LOUDx = perceived noise loudness from each recording (x - denotes which recording the score refers to)

Table 3.3.6: Relationships between loud scores and symptom reporting

Regression analyses were also carried out to investigate any effect the perceived loudness ratings have on the annoyance rating and the length of time respondents could tolerate the recordings before having to switch them off. The results of these analyses shown in Table 3.3.7 show all relationships as significant. The louder the turbine sounds are perceived to be the more annoying they are and the shorter the time the recordings could be tolerated before having to be switched off (supporting Hypothesis 5a).

Independent Variable	Dependent Variable	β	t	p
LOUD_ALLT	ANNOY_ALLT	.484	5.805	.000
LOUD_SOUND	ANNOY_SOUND	.513	6.262	.000
LOUD_VIDEO	ANNOY_VIDEO	.281	3.069	.003
LOUD4	ANNOY4	.448	5.214	.000
LOUD_ALLT	LENGTH_ALLT	-.319	-3.535	.001
LOUD_SOUND	LENGTH_SOUND	-.287	-3.136	.002
LOUD_VIDEO	LENGTH_VIDEO	-.303	-3.334	.001
LOUD4	LENGTH4	-.429	-4.932	.000

Note: LOUDx = perceived noise loudness from each recording; ANNOYx = the annoyance rating of each recording; LENGTHx = the length of time to switch off rating for each recording (x - denotes which recording the score refers to)

Table 3.3.7: Relationships between loud scores with annoyance ratings and length of time to switch off

Results from these regression analyses support the findings from the correlation results as described in Section 3.3.2.1 as well as the results from the domestic study. In the following Section an investigation of how personality might affect these results is carried out.

3.3.2.4 The Role of Personality in Predicting Attitude to Wind Power, Turbine Noise Perception and Symptom Reporting

Two-step hierarchical linear regression analyses were conducted to examine whether personality predicts attitude to wind power and reported symptoms (Table 3.3.8) over and above the effect of age and sex. The same analysis was carried out to examine the effect of personality on the perceived turbine noise in the recordings, the annoyance ratings of the recordings and the length of time the recordings could be tolerated before they would have to be switched off (Table 3.3.9) over and above the effects of age and sex. These analyses were carried out on the average score when all recordings with turbine noise are taken into account as well as only for recording 4. This recording does not feature any turbine noise and will help to understand whether personality has an effect on whether turbine noise is perceived in a recording or not. Age and sex were entered into step 1 of the regression with all personality measures entered at step 2. In all the analyses neither age nor sex significantly predicted attitudes to wind power, perceived noise, annoyance ratings, length of time to switch off or reported symptoms. However, adding personality measures at step 2 revealed that those with a high negative affect and who were more neurotic reported increased symptoms (supporting Hypothesis 6f) and those who were intolerant to discomfort reported increased turbine noise levels from the recordings (supporting Hypothesis 6b). Those who were intolerant to discomfort and emotional frustrations stated that they could not tolerate the recordings very long before having to switch them off (supporting Hypothesis 6e). In contrast to these findings, personality does not predict whether individuals report noise from recording 4 (where turbine noise is not present), the annoyance rating of recording 4 or the length of time this recording could be tolerated before it would have to be switched off (results of the analyses are given in Table 3.3.10.

Personality measures did not affect respondents' attitudes to wind turbines (not supporting Hypothesis 6a) or the annoyance rating of the turbine sounds in the recordings (not supporting Hypothesis 6d). However, the results do show that generally individuals who have more negative personality tendencies do perceive increased turbine noise and that personality has a significant effect on symptom reporting.

		ATT			SYMP		
		B	*SE*	*β*	*B*	*SE*	*β*
Step 1	Age	-.030	.070	-.045	-.010	.028	-.038
	Sex	.335	.380	.094	-.071	.152	-.050
Step 2	Age	-.018	.071	-.027	.003	.026	.010
	Sex	.370	.379	.103	-.168	.137	-.117
	PA	.061	.202	.033	-.040	.073	-.054
	NA	.389	.248	.199	.184	.090	.236*
	N	-.412	.232	-.232	.218	.084	.307*
	F-disc	.071	.265	.034	.084	.096	.101
	F-emot	-.321	.216	-.192	-.008	.078	-.011
Step 1 R		.103 (p = .627)			.064 (p = .835)		
Step 2 R^2 Change		.086 (p = .173)			.248 (p < .001)		

*p<.05; **p<.01

Note: ATT = attitude to wind turbines; SYMP = symptom reporting score; PA = positive affect; NA = negative affect; N = neuroticism; F-disc = discomfort intolerance; F-emot = emotional intolerance

Table 3.3.8: Hierarchical regression analyses of personality on attitude to wind turbines and reported symptoms

		LOUD_ALLT			ANNOY_ALLT			LENGTH_ALLT		
		B	*SE*	*β*	*B*	*SE*	*β*	*B*	*SE*	*β*
Step 1	Age	-.036	.027	-.138	.008	.038	.023	.011	.040	.028
	Sex	-.014	.149	-.010	.101	.207	.052	-.111	.217	-.054
Step 2	Age	-.013	.026	-.051	.031	.038	.087	-.017	.039	-.045
	Sex	-.088	.138	-.062	.012	.204	.006	-.022	.211	-.011
	PA	.161	.074	.221*	.123	.109	.123	.040	.112	.038
	NA	.054	.090	.070	.134	.133	.125	-.246	.138	-.220
	N	.043	.085	.061	.158	.124	.163	-.116	.129	-.114
	F-disc	.360	.097	.437**	.296	.142	.261	-.330	.147	-.277*
	F-emot	-.030	.079	-.046	-.083	.116	-.091	.277	.120	.289*
Step 1 R		.139 (p = .420)			.057 (p = .863)			.060 (p = .850)		
Step 2 R^2 Change		.208 (p < .001)			.113 (p = .068)			.139 (p = .025)		

*p<.05; **p<.01

Note: LOUD_ALLT = perceived mean noise loudness for all recordings; ANNOY_ALLT = the mean annoyance rating for all recordings; LENGTH_ALLT = the mean length of time to switch off rating for all recordings; PA = positive affect; NA = negative affect; N = neuroticism; F-disc = discomfort intolerance; F-emot = emotional intolerance

Table 3.3.9: Hierarchical regression analyses of personality on LOUD scores, annoyance rating and length of time to switch off for all recordings with turbine noise present

		LOUD4			ANNOY4			LENGTH4		
		B	*SE*	*β*	*B*	*SE*	*β*	*B*	*SE*	*β*
Step 1	Age	-.031	.026	-.125	-.003	.050	-.007	.047	.063	.080
	Sex	.072	.144	.052	.406	.273	.156	-.163	.341	-.050
Step 2	Age	-.019	.026	-.075	.015	.052	.032	.022	.064	.036
	Sex	.039	.141	.029	.328	.278	.126	-.102	.341	-.032
	PA	.115	.075	.165	.058	.148	.044	.135	.182	.082
	NA	-.103	.092	-.139	.274	.181	.193	-.389	.223	-.221
	N	.077	.086	.114	.065	.170	.051	.063	.209	.039
	F-disc	.256	.099	.324	.157	.194	.104	-.252	.239	-.135
	F-emot	.004	.080	.006	-.112	.158	-.092	.398	.195	.264
Step 1 R		.134 (p = .448)			.156 (p = .336)			.093 (p = .680)		
Step 2 R^2 Change		.112 (p = .065)			.053 (p = .445)			.083 (p = .189)		

*p<.05; **p<.01

Note: LOUD4 = perceived mean noise loudness for recording 4 (no turbine); ANNOY4 = the mean annoyance rating for recording 4 (no turbine); LENGTH4 = the mean length of time to switch off rating for recording 4 (no turbine); PA = positive affect; NA = negative affect; N = neuroticism; F-disc = discomfort intolerance; F-emot = emotional intolerance

Table 3.3.10: Hierarchical regression analyses of personality on LOUD scores, annoyance rating and length of time to switch off recording 4 (no turbine noise present)

Analyses of whether personality moderates the relationships explored in Section 3.3.2.3 are given in Section 3.3.2.6.

3.3.2.5 The Role of the Change in the Perception of Noise Between when Turbine Noise is and is not Present

A score was calculated for each individual to determine how much louder they perceived the turbine noises in the recordings where turbine noise was present compared to recording 4 (which did not contain turbine noise). The score was calculated by subtracting the LOUD score for recording 4 from the LOUD score for all recordings with turbine noise. A low LOUD_CHANGE score indicates that individuals are not able to differentiate the turbine sounds as louder when they are present, or more significantly that they report turbine noise where there is none. It would therefore be expected that those with a lower LOUD_CHANGE score have a more negative attitude towards wind turbines and would report increased symptom levels. It is also expected that personality would predict an individual's LOUD_CHANGE score. Individual's with a high LOUD_CHANGE score would also be expected to perceive increased turbine noise levels in all the recordings with turbine noise.

Independent Variable	Dependent Variable	β	t	p
ATT	LOUD_CHANGE	.074	.746	.458
LOUD_CHANGE	LOUD_ALLT	.458	5.409	.000
LOUD_CHANGE	SYMP	.040	.418	.677

Note: ATT = attitude to wind turbines; LOUD_ALLT = mean LOUD score for all recordings with turbine noise; LOUD_CHANGE = change in LOUD score between LOUD_ALLT and LOUD4 (no turbine noise); SYMP = symptom reporting score

Table 3.3.11: Regression results examining the effect of the loud change score on noise perception and symptom reporting

Regression analyses were carried out to confirm these hypotheses and are presented in Table 3.3.11. The results show that the link between attitude to wind turbines and the LOUD_CHANGE score is not significant. Therefore, individuals who have a more negative attitude towards wind turbines do not perceive turbine noise where there is none (i.e. in recording 4) any more than individuals with a positive attitudes towards wind turbines. The results also show that the LOUD_CHANGE score does not predict symptom reporting. This means that those who cannot differentiate between the amount of turbine noise in the recording where there is none compared to the recordings where turbine noise is present do not suffer from increased symptoms of ill health. The relationship between the LOUD_CHANGE score and the LOUD score for all recordings where turbine noise is present is significant. Meaning that those who perceive more turbine noise in the recordings where turbine noise is present compared to the recording with no turbine noise do report the most turbine noise in general.

		LOUD_CHANGE		
		B	*SE*	*β*
Step 1	Age	-.005	.023	-.025
	Sex	-.085	.124	-.073
Step 2	Age	.005	.023	.023
	Sex	-.127	.124	-.109
	PA	.041	.066	.069
	NA	.161	.081	.253
	N	-.036	.076	-.063
	F-disc	.103	.087	.151
	F-emot	-.036	.071	-.065
Step 1 R		.078 (p = .763)		
Step 2 R^2 Change		.076 (p = .236)		

*p<.05; **p<.01

Note: LOUD_CHANGE = change in LOUD score between LOUD_ALLT and LOUD4 (no turbine noise); PA = positive affect; NA = negative affect; N = neuroticism; F-disc = discomfort intolerance; F-emot = emotional intolerance

Table 3.3.12: Results of the a multiple regression examining the effects of personality on the change in loudness score

A hierarchical linear regression analysis was carried out to determine whether personality predicts the LOUD_CHANGE score over and above the effect of age and sex, the results are presented in Table 3.3.12. The results show that personality does not predict how much more turbine noise individuals perceive in recordings where turbine noise is present compared to when turbine noise is not present.

In the following and final results Section results of the analyses exploring where personality plays a role moderating the attitude, turbine noise and symptom reporting links are given.

3.3.2.6 Moderation Analyses

In this Section first results of the moderation and simple slopes analyses for the wind turbine attitude - noise perception link are given. Following this, results for the symptom perception - noise perception link are given. Moderation analyses are carried out to determine which personality variables influence the relationships investigated. For the theory behind moderation analysis and the reason why it is carried out see Appendix E, Section E.10.

The Role of NOP in Moderating the Wind Turbine Attitude – Noise Perception Association The potential moderating impact of personality on the attitude to wind turbine - perceived noise relationship was examined. Two-step hierarchical regression analyses were carried out for the attitude – perceived loudness relationship, the attitude - annoyance rating link and the attitude - length of time to switch off rating. Analyses were carried out with the following as the dependent variable: scores for all recordings with turbine noise present (ALLT), recording 4 (4 - no turbine noise), all sound recordings with turbine noise (SOUND) and all video recordings (VID) with turbine noise. Attitude to wind power, and personality variables were entered at step 1 and interaction terms at step 2. All predictor variables were based on mean centred scores. Simple slopes analyses were carried out 1 SD above and below the moderator variable where a moderating effect was found, and all values entered into the simple slopes analyses were standardised. A moderating effect is present if the interaction term introduced at step 2 is significant (i.e.$p < 0.05$). Results are presented for analyses for ALLT scores and recording 4 scores as the dependent variables, results for SOUND and VID scores as the dependent variables are not present, unless results were different from ALLT and recording 4 results, in these cases, simple slope results are given.

Results in Tables 3.3.13 and 3.3.14 show that the link between attitude to wind turbines and perceived noise loudness in the recordings with turbine noise was moderated by discomfort intolerance and emotional intolerance. For recording 4 (no turbine noise) the link was only moderated by emotional intolerance.

The simple slope analyses for this link show that the relationship between attitude and loudness of noise in all recordings with turbine noise and for recording 4 only (with no turbine noise) only occurs at high level of F-emot ($\beta=0.238$, $t=4.495$, $p<.001$ Figure 3.3.2, and $\beta=0.200$, $t=3.853$, $p<.001$ Figure 3.3.4 respectively). Simple slopes results show that this link is also moderated by and only occurs for high levels of F-disc for all recordings with turbine noise ($\beta=0.219$, $t=4.040$, $p<.001$ Figure 3.3.1) and recording 4 ($\beta=0.169$, $t=3.006$, $p=.003$ Figure 3.3.3). Even though the statistics in Table 3.3.14 show that F-disc does not moderate the link for recordings 4, a simple slope analysis was carried out as the interaction term in the moderation analysis was close to significance. This approach will be adopted for other relationships where the interaction term for moderators is close to significance, i.e. $p < .10$.

	Dependent Variable: LOUD_ALLT	
Interaction Term	Step 1: ATT and Moderator	Step 2: Interaction Term
ATT × PA	R = .352; $F_{2, 97}$ = 6.842; p = .002 β: ATT = .314*; PA = .137	ΔR^2 = .355; $F_{1, 96}$ = .274; p = .602 β: ATT × PA = -.050
ATT × NA	R = .361; $F_{2, 97}$ = 7.289; p = .001 β: ATT = .317**; NA = .160	ΔR^2 = .010; $F_{1, 96}$ = 1.131; p = .290 β: ATT × NA = .101
ATT × N	R = .347; $F_{2, 96}$ = 6.574; p = .002 β: ATT = .347**; N = .126	ΔR^2 = .011; $F_{1, 95}$ = 1.152; p =.286 β: ATT × N = .103
ATT × F-disc	R = .526; $F_{2, 89}$ = 17.027; p <.001 β: ATT = .335**; F-disc = .415**	ΔR^2 = .031; $F_{1, 88}$ = 3.970; p =.049 β: ATT × F-disc = .187*
ATT × F-emot	R = .421; $F_{2, 88}$ = 9.481; p <.001 β: ATT = .372**; F-emot = .273**	ΔR^2 = .059; $F_{1, 87}$ = 6.782; p =.011 β: ATT × F-emot = .245*

For β values *p<.05; **p<.01

Note: LOUD_ALLT = perceived noise loudness for all recordings with turbine noise; ATT = attitude to wind turbines; PA = positive affect; NA = negative affect; N = neuroticism; F-disc = discomfort intolerance; F-emot = emotional intolerance

Table 3.3.13: Moderation results for attitude – loudness of noise for all recordings with turbine noise link with NOP measures as moderator

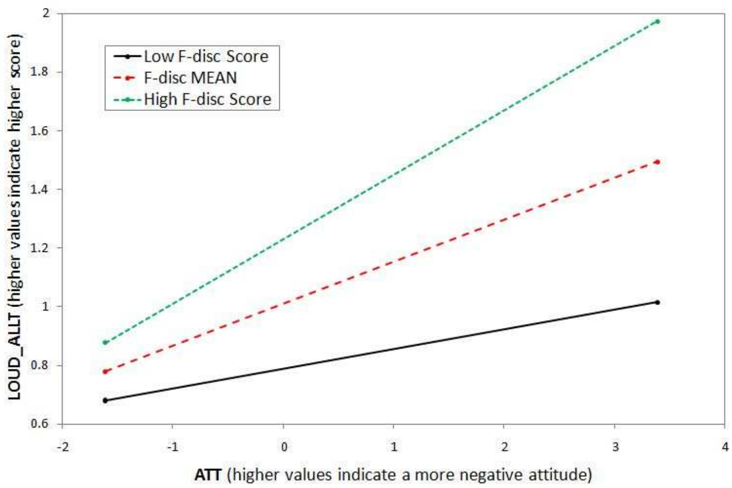

Figure 3.3.1: Simple slopes for the attitude – loudness of noise in all recordings with turbine noise link with F-disc as moderator

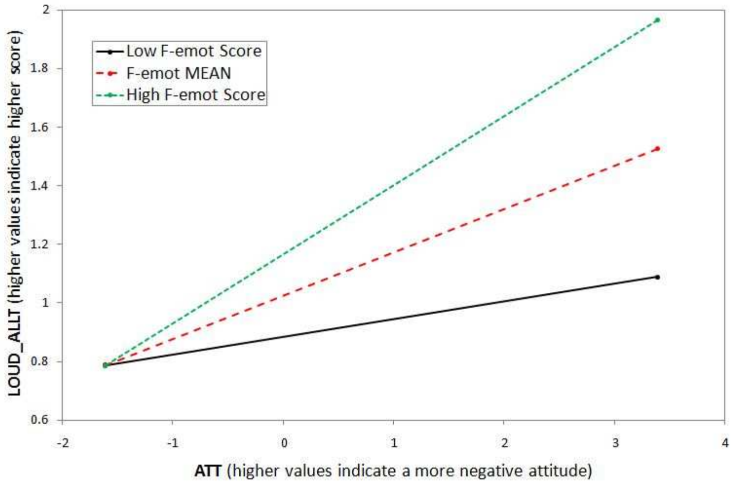

Figure 3.3.2: Simple slopes for the attitude – loudness of noise in all recordings with turbine noise link with F-emot as moderator

	Dependent Variable: LOUD4	
Interaction Term	Step 1: ATT and Moderator	Step 2: Interaction Term
ATT × PA	R = .294; $F_{2, 97}$ = 4.605; p = .012 β: ATT = .278**; PA = .078	ΔR^2 = .000; $F_{1, 96}$ = .040; p = .842 β: ATT × PA = .020
ATT × NA	R = .284; $F_{2, 97}$ = 4.266; p = .017 β: ATT = .285**; NA = -.015	ΔR^2 = .007; $F_{1, 96}$ = .726; p = .396 β: ATT × NA = .084
ATT × N	R = .297; $F_{2, 96}$ = 4.647; p = .012 β: ATT = .300**; N = .089	ΔR^2 = .002; $F_{1, 95}$ = .186; p = .667 β: ATT × N = .042
ATT × F-disc	R = .421; $F_{2, 89}$ = 9.567; p < .001 β: ATT = .292**; F-disc = .310**	ΔR^2 = .014; $F_{1, 88}$ = 1.539; p = .218 β: ATT × F-disc = .126
ATT × F-emot	R = .359; $F_{2, 88}$ = 6.502; p = .002 β: ATT = .323**; F-emot = .223*	ΔR^2 = .042; $F_{1, 87}$ = 4.383; p = .039 β: ATT × F-emot = .205*
For β values *p<.05; **p<.01		

Note: LOUD4 = perceived noise loudness for recording 4 (no turbine noise);
ATT = attitude to wind turbines; PA = positive affect; NA = negative affect; N = neuroticism;
F-disc = discomfort intolerance; F-emot = emotional intolerance

Table 3.3.14: Moderation results for attitude – loudness of noise for recording 4 (no turbine noise) link with NOP measures as moderator

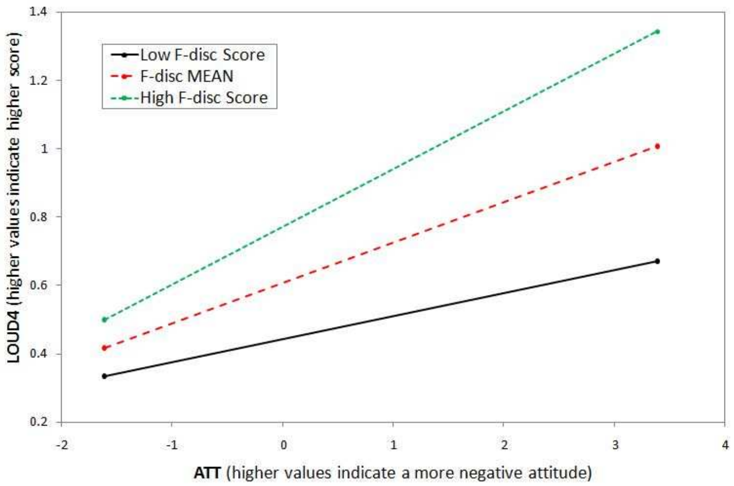

Figure 3.3.3: Simple slopes for the attitude – loudness of noise in recording 4 (no turbine noise) link with F-disc as moderator

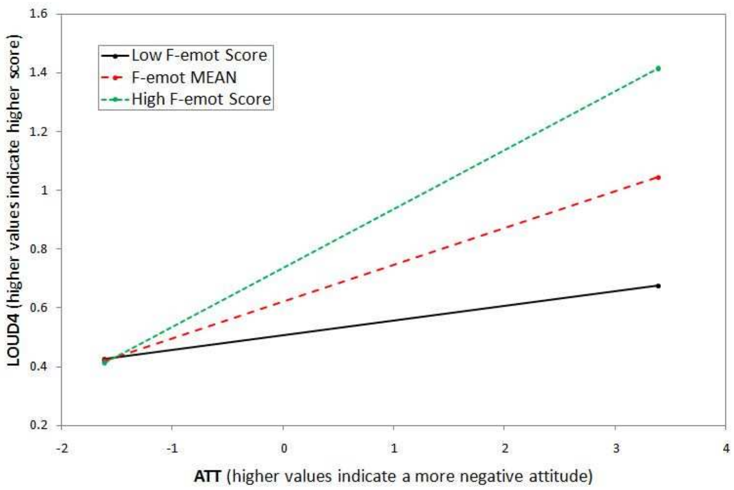

Figure 3.3.4: Simple slopes for the attitude – loudness of noise in recording 4 (no turbine noise) link with F-emot as moderator

Results in Tables 3.3.15 and 3.3.16 show that the link between attitude to wind turbines and perceived annoyance rating of the recordings with turbine noise was moderated by neuroticism only. None of the personality measures moderated this link for recording 4 (no turbine noise).

The simple slope analyses for this link show that the relationship between attitude and annoyance rating of all recordings with turbine noise and of recording 4 only (with no turbine noise) only occurs at high levels of neuroticism (β=0.264, t=4.151, p<.001 Figure 3.3.5, and β=0.362, t=4.089, p<.001 Figure 3.3.7 respectively). Interestingly, when analysing whether personality measures moderate the relationship between attitude and annoyance rating of only sound recordings with turbine noise, the statistics show that PA moderates the relationship and the relationship is only significant for individuals with a low level of positive affect (β=.229, t=2.952, p=.004 Figure 3.3.6).

	Dependent Variable: ANNOY_ALLT	
Interaction Term	Step 1: ATT and Moderator	Step 2: Interaction Term
ATT × PA	R = .271; $F_{2,97}$ = 3.835; p = .025 β: ATT = .265**; PA = .038	ΔR^2 = .025; $F_{1,96}$ = 2.709; p = .103 β: ATT × PA = -.161
ATT × NA	R = .346; $F_{2,97}$ = 6.602; p = .002 β: ATT = .258**; NA = .102*	ΔR^2 = .009; $F_{1,96}$ = .982; p = .324 β: ATT × NA = .095
ATT × N	R = .362; $F_{2,96}$ = 7.262; p = .001 β: ATT = .313**; N = .248*	ΔR^2 = .054; $F_{1,95}$ = 6.236; p =.014 β: ATT × N = .232*
ATT × F-disc	R = .352; $F_{2,89}$ = 6.310; p = .003 β: ATT = .274**; F-disc = .229*	ΔR^2 = .006; $F_{1,88}$ = .639; p =.426 β: ATT × F-disc = .084
ATT × F-emot	R = .321; $F_{2,88}$ = 5.061; p = .008 β: ATT = .299**; F-emot = .180	ΔR^2 = .000; $F_{1,87}$ = .030; p =.862 β: ATT × F-emot = .018
For β values *p<.05; **p<.01		

Note: ANNOY_ALLT = the mean annoyance rating for all recordings with turbine noise; ATT = attitude to wind turbines; PA = positive affect; NA = negative affect; N = neuroticism; F-disc = discomfort intolerance; F-emot = emotional intolerance

Table 3.3.15: Moderation results for attitude – annoyance rating of noise for all recordings with turbine noise link with NOP measures as moderator

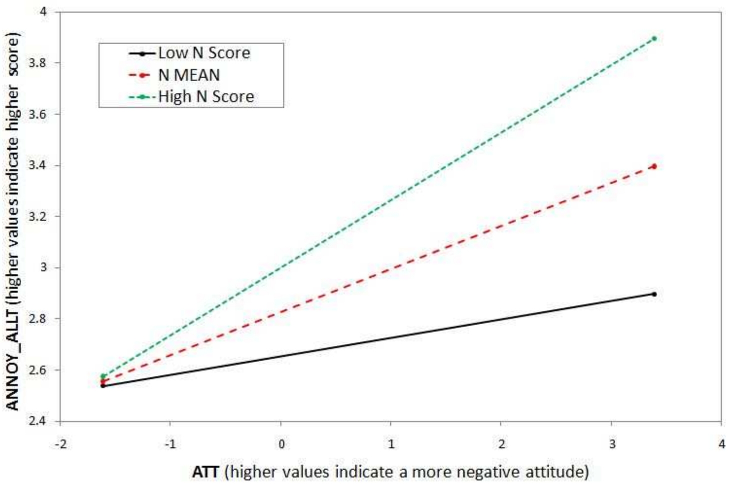

Figure 3.3.5: Simple slopes for the attitude – annoyance of noise in all recordings with turbine noise link with N as moderator

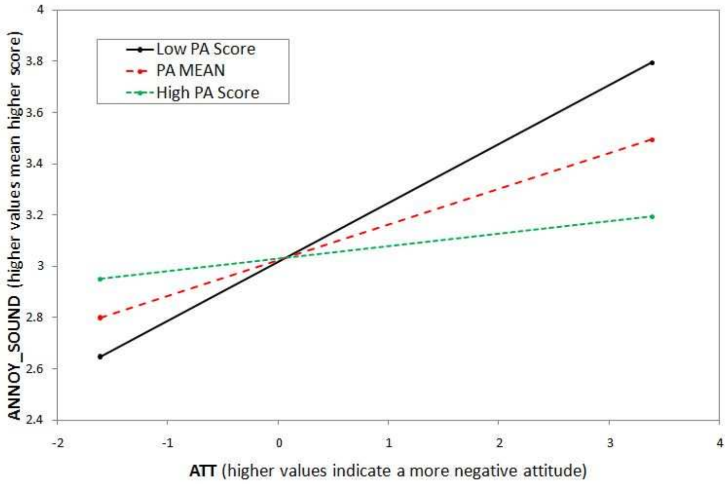

Figure 3.3.6: Simple slopes for the attitude – annoyance of noise in all sound recordings with turbine noise link with PA as moderator

	Dependent Variable: ANNOY4	
Interaction Term	Step 1: ATT and Moderator	Step 2: Interaction Term
ATT × PA	R = .353; $F_{2,96}$ = 6.826; p = .002 β: ATT = .353**; PA = -.010	ΔR^2 = .000; $F_{1,95}$ = .023; p = .879 β: ATT × PA = .015
ATT × NA	R = .411; $F_{2,96}$ = 9.752; p < .001 β: ATT = .343**; NA = .211*	ΔR^2 = .012; $F_{1,95}$ = 1.352; p = .248 β: ATT × NA = .109
ATT × N	R = .404; $F_{2,96}$ = 9.376; p < .001 β: ATT = .389**; N = .201*	ΔR^2 = .028; $F_{1,95}$ = 3.271; p =.074 β: ATT × N = .167
ATT × F-disc	R = .370; $F_{2,89}$ = 7.060; p = .001 β: ATT = .356**; F-disc = .112	ΔR^2 = .005; $F_{1,88}$ = .500; p =.481 β: ATT × F-disc = .074
ATT × F-emot	R = .369; $F_{2,88}$ = 6.925; p = .002 β: ATT = .372**; F-emot = .109	ΔR^2 = .000; $F_{1,87}$ = .034; p =.853 β: ATT × F-emot = -.019

For β values *p<.05; **p<.01

Note: ANNOY4 = the mean annoyance rating for recording 4 (no turbine noise); ATT = attitude to wind turbines; PA = positive affect; NA = negative affect; N = neuroticism; F-disc = discomfort intolerance; F-emot = emotional intolerance

Table 3.3.16: Moderation results for attitude – annoyance rating of noise for all recording 4 (no turbine noise) link with NOP measures as moderator

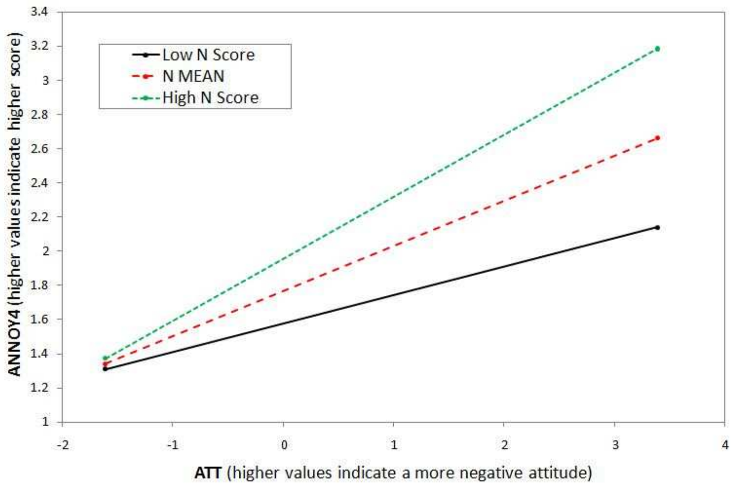

Figure 3.3.7: Simple slopes for the attitude – annoyance of noise in recording 4 (no turbine noise) link with N as moderator

Results in Tables 3.3.17 and 3.3.18 show that personality measures did not moderate the link between attitude to wind turbines and the length of time the recordings could be tolerated before they would have to be switched off for any of the recordings.

	Dependent Variable: LENGTH_ALLT	
Interaction Term	Step 1: ATT and Moderator	Step 2: Interaction Term
ATT × PA	R = .309; $F_{2, 97}$ = 5.124; p = .008 β: ATT = -.294**; PA = .118	ΔR^2 = .011; $F_{1, 96}$ = .1.196; p = .277 β: ATT × PA = .107
ATT × NA	R = .370; $F_{2, 97}$ = 7.693; p = .001 β: ATT = -.275**; NA = -.235*	ΔR^2 = .001; $F_{1, 96}$ = .060; p = .808 β: ATT × NA = .023
ATT × N	R = .364; $F_{2, 96}$ = 7.332; p = .001 β: ATT = -.327**; N = -.229*	ΔR^2 = .002; $F_{1, 95}$ = .223; p =.638 β: ATT × N = -.045
ATT × F-disc	R = .342; $F_{2, 89}$ = 5.899; p = .004 β: ATT = -.291**; F-disc = -.188	ΔR^2 = .003; $F_{1, 88}$ = .276; p =.601 β: ATT × F-disc = -.056
ATT × F-emot	R = .286; $F_{2, 88}$ = 3.911; p = .024 β: ATT = -.285**; F-emot = .002	ΔR^2 = .003; $F_{1, 87}$ = .330; p = .567 β: ATT × F-emot = .059
For β values *p<.05; **p<.01		

Note: LENGTH_ALLT = the mean length of time to switch off rating for all recordings with turbine noise; ATT = attitude to wind turbines; PA = positive affect; NA = negative affect; N = neuroticism; F-disc = discomfort intolerance; F-emot = emotional intolerance

Table 3.3.17: Moderation results for attitude – length of time rating for all recordings with turbine noise link with NOP measures as moderator

	Dependent Variable: LENGTH4	
Interaction Term	Step 1: ATT and Moderator	Step 2: Interaction Term
ATT × PA	R = .377; $F_{2, 96}$ = 7.950; p = .001 β: ATT = -.367**; PA = .118	ΔR^2 = .001; $F_{1, 95}$ = .111; p = .740 β: ATT × PA = -.032
ATT × NA	R = .385; $F_{2, 96}$ = 8.335; p < .001 β: ATT = -.352**; NA = -.140	ΔR^2 = .000; $F_{1, 95}$ = .012; p = .913 β: ATT × NA = -.010
ATT × N	R = .370; $F_{2, 96}$ = 7.627; p = .001 β: ATT = -.375**; N = -.096	ΔR^2 = .001; $F_{1, 95}$ = .079; p =.780 β: ATT × N = .027
ATT × F-disc	R = .365; $F_{2, 89}$ = 6.853; p = .002 β: ATT = -.360**; F-disc = -.072	ΔR^2 = .002; $F_{1, 88}$ = .219; p =.641 β: ATT × F-disc = -.049
ATT × F-emot	R = .367; $F_{2, 88}$ = 6.861; p = .002 β: ATT = -.344**; F-emot = .083	ΔR^2 = .007; $F_{1, 87}$ = .670; p = .415 β: ATT × F-emot = .082

For β values *p<.05; **p<.01

Note: LENGTH4 = the mean length of time to switch off rating for recording 4 (no turbine noise); ATT = attitude to wind turbines; PA = positive affect; NA = negative affect; N = neuroticism; F-disc = discomfort intolerance; F-emot = emotional intolerance

Table 3.3.18: Moderation results for attitude – length of time rating for recording 4 (no turbine noise) link with NOP measures as moderator

These findings support Hypothesis 7d showing that negative personality traits do moderate the link between attitude to wind turbines and annoyance and noise perception due to turbine sounds in the recordings.

The Role of NOP in Moderating of the Reported Symptom - Noise Perception Association The potential moderating impact of personality on the symptom perception - perceived noise relationship was examined. Two-step hierarchical regression analyses were carried out for the symptom perception – perceived loudness relationship, the symptom perception - annoyance rating link and the symptom perception - length of time to switch off rating. Analyses were carried out with the following as the dependent variable; scores for all recordings with turbine noise present (ALLT), recording 4 (4 - no turbine noise), all sound recordings with turbine noise (SOUND) and all video recordings (VID) with turbine noise. Symptom perception, and personality variables were entered at step 1 and interaction terms at step 2. All predictor variables were based on mean centred scores. Simple slope analyses were carried out 1 SD above and below the moderator variable where a moderating effect was found, and all values entered into the simple slope analyses were standardised. A moderating effect is present if the interaction term introduced at step 2 is significant (i.e.$p < 0.05$). Results are presented for analyses for ALLT scores and recording 4 scores as the dependent variables, results for SOUND and VID scores as the dependent variables are not present, unless results were different from ALLT and recording 4 results, in these cases, simple slope results are given.

Results in Table 3.3.19 shows that the link between symptom reporting and perceived noise loudness in the recordings with turbine noise was moderated by positive affect. However, Table 3.3.20 shows that the link between symptom perception and perceived noise loudness in recording 4 was not moderated by any personality variables.

Interestingly, the simple slope analyses for this link show that the relationship between symptom perception and loudness of noise in all recordings with turbine noise only occurs at high levels of PA (β=0.340, t=2.376, p=.019 Figure 3.3.8). When analysing whether personality measures moderate the relationship between symptom perception and perceived turbine noise in only the video recordings with turbine noise, the statistics show that neuroticism moderates the relationship and the relationship is only significant for individuals with a low level of neuroticism (β=.491, t=2.996, p=.004 Figure 3.3.9). These results are in contrast to what is predicted by Hypothesis 5c.

	Dependent Variable: LOUD_ALLT	
Interaction Term	Step 1: SYMP and Moderator	Step 2: Interaction Term
SYMP × PA	R = .207; $F_{2,99}$ = 2.219; p = .114 β: SYMP = .133; PA = .175	ΔR^2 = .045; $F_{1,98}$ = 4.838; p = .030 β: SYMP × PA = .215*
SYMP × NA	R = .181; $F_{2,99}$ = 1.676; p = .192 β: SYMP = .051; NA = .155	ΔR^2 = .006; $F_{1,98}$ = .629; p = .430 β: SYMP × NA = .087
SYMP × N	R = .113; $F_{2,99}$ = .644; p = .528 β: SYMP = .104; N = .018	ΔR^2 = .012; $F_{1,98}$ = 1.242; p =.268 β: SYMP × N = -.121
SYMP × F-disc	R = .409; $F_{2,92}$ = 9.243; p < .001 β: SYMP = .051; F-disc = .398**	ΔR^2 = .000; $F_{1,91}$ = .002; p =.969 β: SYMP × F-disc = -.004
SYMP × F-emot	R = .221; $F_{2,91}$ = 2.341; p = .102 β: SYMP = .076; F-emot = .194	ΔR^2 = .002; $F_{1,90}$ = .181; p =.672 β: SYMP × F-emot = -.044
For β values *p<.05; **p<.01		

Note: LOUD_ALLT = perceived noise loudness for all recordings with turbine noise;
SYMP = symptom reporting score; PA = positive affect; NA = negative affect; N = neuroticism;
F-disc = discomfort intolerance; F-emot = emotional intolerance

Table 3.3.19: Moderation results for symptom – loudness of noise for all recordings with turbine noise link with NOP measures as moderator

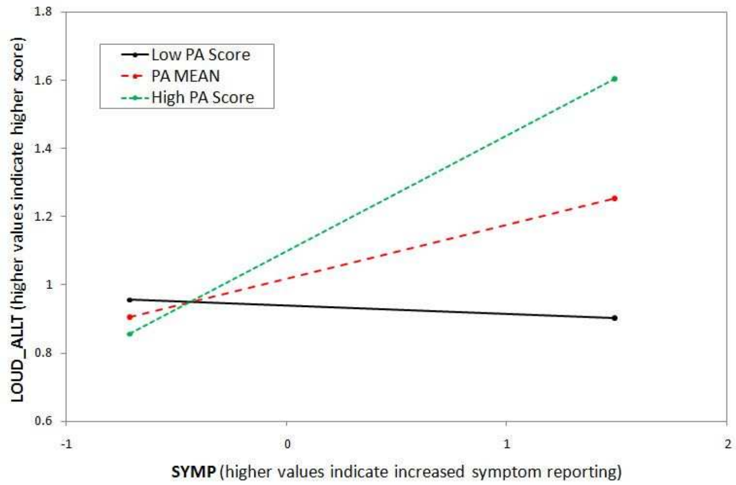

Figure 3.3.8: Simple slopes for the symptom – loudness of noise in all recordings with turbine noise link with PA as moderator

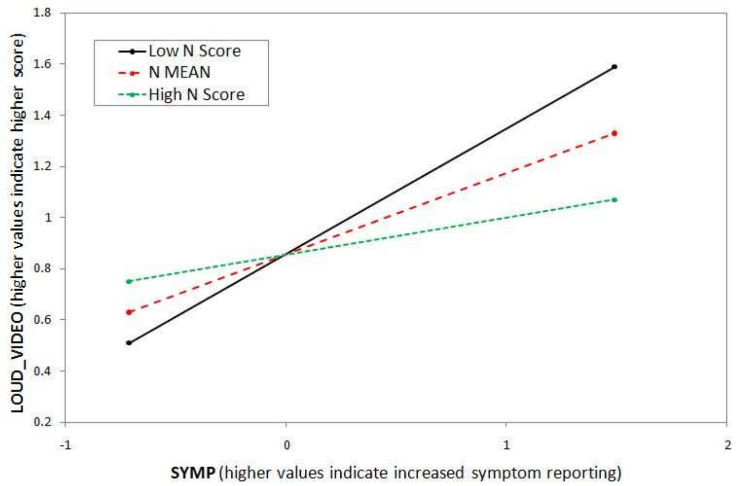

Figure 3.3.9: Simple slopes for the symptom – loudness of noise in all video recordings link with N as moderator

	Dependent Variable: LOUD4	
Interaction Term	Step 1: SYMP and Moderator	Step 2: Interaction Term
SYMP × PA	R = .135; $F_{2, 99}$ = .919; p = .402 β: SYMP = .093; PA = .110	ΔR^2 = .004; $F_{1, 98}$ = .400; p = .529 β: SYMP × PA = .064
SYMP × NA	R = .088; $F_{2, 99}$ = .384; p = .682 β: SYMP = .095; NA = -.040	ΔR^2 = .018; $F_{1, 98}$ = 1.859; p = .176 β: SYMP × NA = .151
SYMP × N	R = .080; $F_{2, 99}$ = .317; p = .729 β: SYMP = .080; N = .000	ΔR^2 = .009; $F_{1, 98}$ = .889; p = .348 β: SYMP × N = -.103
SYMP × F-disc	R = .305; $F_{2, 92}$ = 4.713; p = .011 β: SYMP = .034; F-disc = .298**	ΔR^2 = .003; $F_{1, 91}$ = .314; p = .577 β: SYMP × F-disc = -.056
SYMP × F-emot	R = .174; $F_{2, 91}$ = 1.417; p = .248 β: SYMP = .051; F-emot = .157	ΔR^2 = .001; $F_{1, 90}$ = .106; p = .745 β: SYMP × F-emot = -.034
For β values *p<.05; **p<.01		

Note: LOUD4 = perceived noise loudness for recording 4 (no turbine noise);
SYMP = symptom reporting score; PA = positive affect; NA = negative affect; N = neuroticism;
F-disc = discomfort intolerance; F-emot = emotional intolerance

Table 3.3.20: Moderation results for symptom – loudness of noise for recording 4 (no turbine noise) link with NOP measures as moderator

Results in Tables 3.3.21 and 3.3.22 show that personality measures did not moderate the link between symptom perception and the annoyance rating of any of the recordings.

	Dependent Variable: ANNOY_ALLT	
Interaction Term	Step 1: SYMP and Moderator	Step 2: Interaction Term
SYMP × PA	R = .175; $F_{2,99}$ = 1.557; p = .216 β: SYMP = .166; PA = .077	ΔR^2 = .000; $F_{1,98}$ = .005; p = .944 β: SYMP × PA = -.007
SYMP × NA	R = .242; $F_{2,99}$ = 3.077; p = .051 β: SYMP = .078; NA = .200	ΔR^2 = .032; $F_{1,98}$ = 3.455; p = .066 β: SYMP × NA = .198
SYMP × N	R = .208; $F_{2,99}$ = 2.247; p = .111 β: SYMP = .091; N = .152	ΔR^2 = .012; $F_{1,98}$ = 1.241; p =.268 β: SYMP × N = .119
SYMP × F-disc	R = .254; $F_{2,92}$ = 3.184; p = .046 β: SYMP = .126; F-disc = .203*	ΔR^2 = .019; $F_{1,91}$ = 1.867; p =.175 β: SYMP × F-disc = .137
SYMP × F-emot	R = .186; $F_{2,91}$ = 1.637; p = .200 β: SYMP = .138; F-emot = .102	ΔR^2 = .001; $F_{1,90}$ = .107; p =.744 β: SYMP × F-emot = .034
For β values *p<.05; **p<.01		

Note: ANNOY_ALLT = the mean annoyance rating for all recordings with turbine noise; SYMP = symptom reporting score; PA = positive affect; NA = negative affect; N = neuroticism; F-disc = discomfort intolerance; F-emot = emotional intolerance

Table 3.3.21: Moderation results for symptom – annoyance rating of noise for all recordings with turbine noise link with NOP measures as moderator

	Dependent Variable: ANNOY4	
Interaction Term	Step 1: SYMP and Moderator	Step 2: Interaction Term
SYMP × PA	R = .115; $F_{2,99}$ = .668; p = .515 β: SYMP = .115; PA = .030	ΔR^2 = .005; $F_{1,98}$ = .508; p = .478 β: SYMP × PA = -.072
SYMP × NA	R = .228; $F_{2,99}$ = 2.717; p = .071 β: SYMP = .026; NA = .217*	ΔR^2 = .013; $F_{1,98}$ = 1.345; p = .249 β: SYMP × NA = .125
SYMP × N	R = .144; $F_{2,99}$ = 1.049; p = .354 β: SYMP = .068; N = .101	ΔR^2 = .001; $F_{1,98}$ = .097; p = .756 β: SYMP × N = .034
SYMP × F-disc	R = .141; $F_{2,92}$ = .938; p = .395 β: SYMP = .098; F-disc = .088	ΔR^2 = .002; $F_{1,91}$ = .214; p = .645 β: SYMP × F-disc = .048
SYMP × F-emot	R = .114; $F_{2,91}$ = .601; p = .550 β: SYMP = .107; F-emot = .025	ΔR^2 = .002; $F_{1,90}$ = .203; p = .653 β: SYMP × F-emot = .047
For β values *p<.05; **p<.01		

Note: ANNOY4 = the mean annoyance rating for recording 4 (no turbine noise); SYMP = symptom reporting score; PA = positive affect; NA = negative affect; N = neuroticism; F-disc = discomfort intolerance; F-emot = emotional intolerance

Table 3.3.22: Moderation results for symptom – annoyance rating of noise for all recording 4 (no turbine noise) link with NOP measures as moderator

Results in Table 3.3.23 show that the link between symptom reporting and length rating for all recordings with turbine noise was moderated by intolerance to discomfort only; the simple slopes show that this moderation was only significant at high levels of F-disc (β=-.400, t=-2.061, p=.042 Figure 3.3.10). The moderation analysis for the symptom reporting and length rating for only video recordings with turbine noise was moderated by and significant only at low levels of positive affect (β=-.494, t=-2.234, p=.028 Figure 3.3.11).

	Dependent Variable: LENGTH_ALLT	
Interaction Term	Step 1: SYMP and Moderator	Step 2: Interaction Term
SYMP × PA	R = .137; $F_{2,99}$ = .952; p = .389 β: SYMP = -.098; PA = .085	ΔR^2 = .025; $F_{1,98}$ = 2.524; p = .115 β: SYMP × PA = .159
SYMP × NA	R = .248; $F_{2,99}$ = 3.251; p = .043 β: SYMP = -.012; NA = -.243*	ΔR^2 = .028; $F_{1,98}$ = 3.009; p = .086 β: SYMP × NA = -.185
SYMP × N	R = .174; $F_{2,99}$ = 1.554; p = .217 β: SYMP = -.042; N = -.152	ΔR^2 = .002; $F_{1,98}$ = .246; p =.621 β: SYMP × N = -.054
SYMP × F-disc	R = .198; $F_{2,92}$ = 1.884; p = .158 β: SYMP = -.083; F-disc = -.168	ΔR^2 = .051; $F_{1,91}$ = 5.099; p =.026 β: SYMP × F-disc = -.226*
SYMP × F-emot	R = .131; $F_{2,91}$ = .789; p = .457 β: SYMP = -.122; F-emot = .074	ΔR^2 = .023; $F_{1,90}$ = 2.196; p =.142 β: SYMP × F-emot = -.154
For β values *p<.05; **p<.01		

Note: LENGTH_ALLT = the mean length of time to switch off rating for all recordings with turbine noise; SYMP = symptom reporting score; PA = positive affect; NA = negative affect; N = neuroticism; F-disc = discomfort intolerance; F-emot = emotional intolerance

Table 3.3.23: Moderation results for symptom – length of time rating for all recordings with turbine noise link with NOP measures as moderator

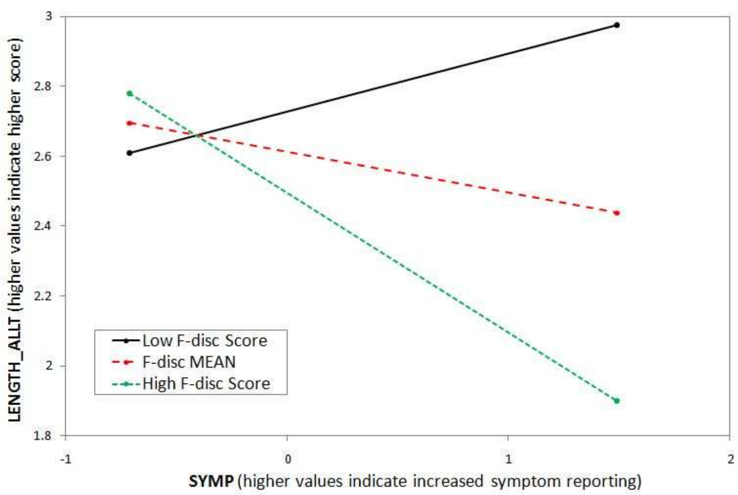

Figure 3.3.10: Simple slopes for the symptom – LENGTH rating for noise in all recordings with turbine noise link with F-disc as moderator

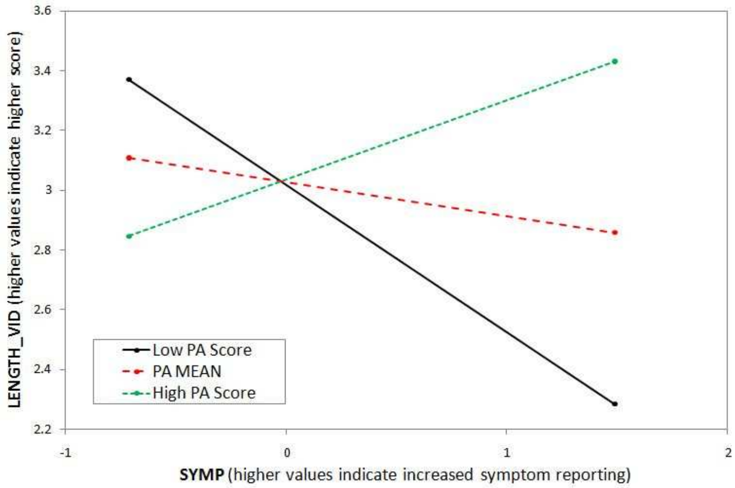

Figure 3.3.11: Simple slopes for the symptom – LENGTH rating for noise in all video recordings link with PA as moderator

Table 3.3.24 shows that this link for only recording 4 (no turbine noise) was moderated by and significant at low levels of positive affect (β=-.400, t=-2.061, p=.042 Figure 3.3.13). Simple slopes analysis show that this link was also moderated by and significant at high levels of negative affect (β=-.609, t=-2.155, p=.034 Figure 3.3.12).

	Dependent Variable: LENGTH4	
Interaction Term	Step 1: SYMP and Moderator	Step 2: Interaction Term
SYMP × PA	R = .205; $F_{2, 99}$ = 2.163; p = .120 β: SYMP = -.184; PA = .069	ΔR^2 = .045; $F_{1, 98}$ = 4.774; p = .031 β: SYMP × PA = .214*
SYMP × NA	R = .212; $F_{2, 99}$ = 2.323; p = .103 β: SYMP = -.155; NA = -.095	ΔR^2 = .029; $F_{1, 98}$ = 3.099; p = .081 β: SYMP × NA = -.190
SYMP × N	R = .202; $F_{2, 99}$ = 2.116; p = .126 β: SYMP = -.223*; N = .069	ΔR^2 = .001; $F_{1, 98}$ = .092; p = .762 β: SYMP × N = -.033
SYMP × F-disc	R = .196; $F_{2, 92}$ = 1.831; p = .166 β: SYMP = -.188; F-disc = -.034	ΔR^2 = .019; $F_{1, 91}$ = 1.794; p = .184 β: SYMP × F-disc = -.136
SYMP × F-emot	R = .265; $F_{2, 91}$ = 3.423; p = .037 β: SYMP = -.227*; F-emot = .184	ΔR^2 = .006; $F_{1, 90}$ = .543; p = .463 β: SYMP × F-emot = -.075
For β values *p<.05; **p<.01		

Note: LENGTH4 = the mean length of time to switch off rating for recording 4 (no turbine noise); SYMP = symptom reporting score; PA = positive affect; NA = negative affect; N = neuroticism; F-disc = discomfort intolerance; F-emot = emotional intolerance

Table 3.3.24: Moderation results for symptom – length of time rating for recording 4 (no turbine noise) link with NOP measures as moderator

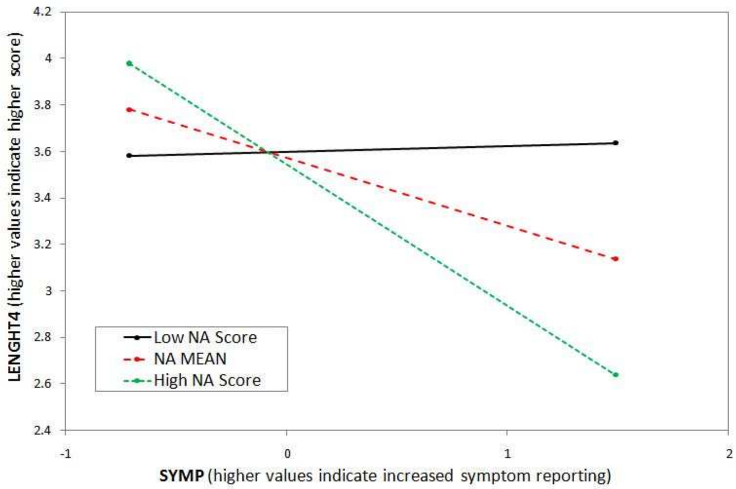

Figure 3.3.12: Simple slopes for the symptom – LENGTH rating for noise in recording 4 (no turbine noise) link with NA as moderator

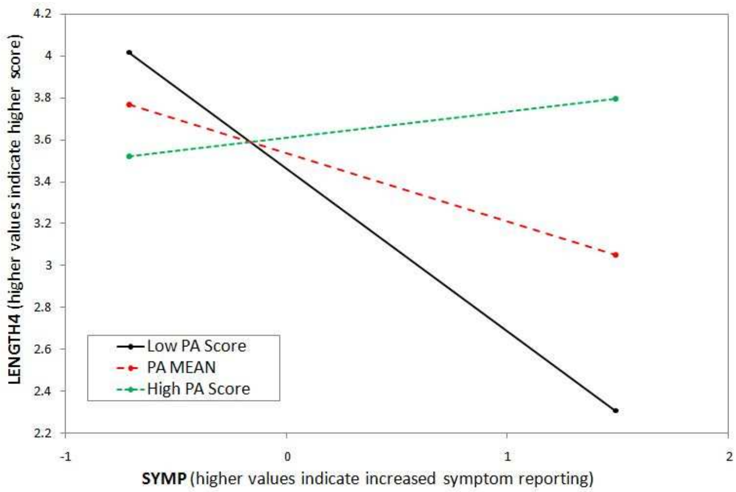

Figure 3.3.13: Simple slopes for the symptom – LENGTH rating for noise in recording 4 (no turbine noise) link with PA as moderator

All the findings in this Section support Hypothesis 5c, except for the symptom reporting - perceived loudness of turbine noise in the recordings link, where the relationship is moderated by low levels of negative personality traits rather than high levels.

In the following Section, concluding remarks for both the domestic and recordings studies will be given. These results will be compared to the noise measurement and noise modelling methods also adopted for the research in Chapter 5.

3.4 Conclusions of the Psychological and Health Impacts Studies

The objectives of the psychological and health impacts studies of small wind systems have been achieved. A survey has been carried out on individuals living close to small and micro wind turbine installations to investigate the level and type of noise perceived. This noise perception has been linked to individuals' attitudes towards wind turbines as well as their personality and temperamental characteristics and hence the effects on general health. In addition to the domestic survey an experimental recordings study has been carried out to confirm the results of the domestic survey by controlling the sounds the participants hear and linking this directly to the personality traits and attitudes measured. The methods adopted for this part of the research have enabled the hypotheses questions given in Section 3.1.7 to be answered.

It has been important to consider the sounds most frequently reported from the turbines for both the domestic and recordings surveys to compare later (in Chapter 5) to results of the noise measurement and noise modelling work. From the domestic study, the loudness and occurrence scores for all the turbine sounds was low indicating that the levels of noise experienced from small wind systems is of a low level. This further supports the assumption that it is the characteristics of the noise which are likely to cause annoyance. From the domestic study, the sounds most frequently reported from small turbines were swooshing and humming. Of particular interest are the sounds reported from the small wind turbine type S1 as this is the turbine that has been used for the noise measurement work. The top five reported sounds from turbine S1 were scratching, swooshing, humming, thumping and low frequency sounds. The most commonly reported sounds from the micro turbine types were humming, swooshing, whistling and buzzing and of particular interest is the micro turbine type M1 as again, this is the micro turbine used for the noise measurement work as well as the noise modelling work. The most common sounds reported from the turbine M1 are the same as those for all the micro turbine types.

For the recordings study, individuals were played sound and video recordings of small turbine type S1 and micro turbine type M1. The turbine sounds perceived by respondents from each recording match well to the expected perceived sounds. The purpose of the recordings study was to control the sounds the respondents heard by using recordings representative of the range of sounds heard from the two turbine types in different wind speeds at real turbine installations. As expected, the recording that did not contain any wind turbine noise was reported as having the least turbine noise by the participants. It was however expected that recordings taken in the highest wind speeds would be reported as containing the loudest turbine sounds compared to recordings at lower wind speeds, this was not always the case. This further supports the assumption that it is the characteristics of the noise the turbines make which influences the level of noise perceived and the turbines make different sounds depending on the wind speed. For the sound recording of turbine M1 in moderate wind speeds (recording 1) the sounds reported were whistling, swooshing, high frequency and screeching. For the sound recording of M1 taken at very high wind speeds (recording 6) the sounds reported were low frequency, humming, swooshing and buzzing or throbbing.

From the video recording of turbine S1 taken in very low wind speeds (recording 7), the sounds reported were swooshing, scratching, low frequency and whistling. For the video recording at moderate wind speeds (recording 3) the sounds were low frequency, humming, swooshing and throbbing. For the sound recording of turbine S1 at moderate wind speeds (recording 2), participants perceived low frequency, humming, swooshing and throbbing sounds the most. For the sound recording at very high wind speeds (recording 5), participants reported swooshing, scratching, low frequency and throbbing.

These findings show that the range of sounds perceived for the micro turbine type are similar to the sounds perceived from the small turbine types. However, sounds associated with higher frequencies such as screeching are perceived more readily from the micro turbine type and lower frequency sounds are heard more readily from the small turbine type. The sounds perceived by respondents of the domestic survey are very similar to the sounds reported by the participants of the controlled recordings study.

The domestic study is the first study to investigate the effect of typical and perceived noise from small wind turbines on reported symptoms. While typical small wind system noise did not predict reported symptoms, the perceived loudness and occurrence of noise did. Following the symptom perception model [58, 78], this link between perceived noise and symptom reporting was moderated by negative oriented personality (NOP). Specifically, for those higher in NOP traits; i.e. high negative affect and a high discomfort and emotional intolerance, there was a stronger link between perceived noise and symptom reporting. In addition, the effect of NOP was direct such that higher NOP was associated with more negative attitudes to wind turbines, greater and more frequent perceived noise from nearby small wind turbines and increased symptom reporting. NOP also significantly moderated the relationships between attitude to turbines and both perceived occurrence and loudness of noise (i.e. the link between attitudes to turbines and perceived noise was only significant for individuals with a high negative affect and those unable to cope with emotional frustrations or discomfort) and between perceived noise and symptom reporting, thus supporting the Symptom Perception model [58, 78]. There was, however, no relationship between typical noise from the turbine and participants' attitude to wind turbines. This means that those who had a more negative attitude to wind turbines were more likely to hear louder and more frequent noise from the turbine, but this effect was not simply due to individuals being able to hear the noise more. Thus, the notion that turbine noise is linked to increased symptoms per se is simplifying the reality. This study demonstrates that individual differences play a key role in the link between perceived noise and symptom reporting, but that there is no relationship between typical noise and reported symptoms, nor any link between NOP and typical noise. These findings suggest that perceived rather than typical noise is more important in predicting symptoms of ill-health. The fact that these perceptions are influenced partly by typical noise means that these perceptions are based not only on typical noise experienced, but also on individuals' environmental perception. NOP has been demonstrated elsewhere to be associated with negative and threatening evaluations of events and ambiguous environmental stimuli [71, 72, 70] and these results confirm that for individuals low in NOP – especially Frustration Intolerance, the link between noise perception and symptoms is dramatically attenuated.

The second study, the recordings study, seeked to confirm the findings from the domestic survey by controlling the noise inputs the participants heard and directly comparing the noise perception with attitudes, personality traits and symptom reporting. As expected, the recordings reported as containing the most turbine noise were also reported as the most annoying and the least tolerable and individuals with the most negative attitudes to wind turbines reported increased turbine noise levels in the recordings. This is in agreement with findings from the domestic study where individuals with the most negative attitude to wind turbine reported the most noise from the small or micro turbine installed close to their domestic dwelling. The level of perceived noise from the recordings did not predict symptom reporting in all but the video recordings. This implies that the visibility of the turbines has an effect on the relationship. It is unlikely that the turbine noise in the recordings is influencing the participants' general health as exposure to the sounds was only for the duration of the questionnaire (specifically 30 seconds for each of the seven recordings), it is more likely that the general health of the participants influenced the level of perceived noise. For example, those experiencing frequent symptoms of ill health may be more sensitive to stressors such as the sounds in the small wind system recordings. The recordings study has strengthened the findings of the domestic study by proving that even for short exposures to the turbine noise, attitudes and personality traits play an important role in predicting the amount of small wind system noise that is likely to be perceived.

The results of the recordings study also confirm that personality plays a role in turbine noise perception. Those with higher NOP traits did indeed report increased noise levels from the recordings and describe the recordings as the least tolerable, these respondents also reported increased levels of ill-health. The relationships were further examined by assessing whether NOP traits moderate the attitudes-noise perception and symptom reporting-noise perception links. The attitudes-noise perception and attitudes-annoyance due to the recordings links were significant only for those with high NOP, specifically high neuroticism and high emotional intolerance and intolerance to frustrations. It was also shown that for the recording which did not contain any turbine noise, it was individuals with high NOP who reported the recording as containing the most wind turbine noise and as the most annoying even though the recording only contained ambient noise.

The relationship between symptom reporting and the length of time the recordings could be tolerated before having to be switched off was only significant for those with higher NOP. However, interesting results were seen for the symptom reporting-noise perception link, the relationship was only significant for those with high levels of positive affect and low levels of neuroticism. Specifically, individuals reporting increased levels of ill health report increased noise levels but only for individuals with high positive affect and those who experience less neuroticism. This finding is in contrast to all other findings from both the domestic and recordings studies and could be explained because those experiencing frequent symptoms of ill health may be more sensitive to stressors such as the sounds in the small wind system recordings. This effect could be increased for those with high positive affect and low neuroticism as they are more alert to their surroundings. Further work would be required to confirm whether symptoms of ill health increase turbine noise perception levels for short exposure times and for whom this relationship would occur.

To summarise, while some work has associated turbine noise with increased symptoms of ill health for those living close to wind turbines [54], the current study suggests that this approach may be too simplistic, and any model aiming to examine the effects of turbine installations more fully should assess the role of individual differences and differential effects of perceived and typical noise on symptoms including the level of exposure. The role of NOP is therefore potentially key in understanding how perception of environmental negative characteristics (such as noise from small wind systems) may be translated into symptoms of ill health. In Chapter 5, comparisons will be made between the results of the data collected for the studies of the psychological and health impacts of small wind systems with the noise modelling analysis as well as with the noise measurement results.

The studies of the psychological and health impacts of small winds systems have contributed towards satisfying the drivers of the research. By understanding the type of individual who is likely to perceive small wind turbine noise as a negative environmental stressor, it will be possible to engage with these individuals in the most efficient manner to help aid understanding of the likely real noise levels which will be experienced at proposed small wind system installations. The work has also shown that an individual's attitude to wind turbines plays a key role in the level of noise they are likely to experience from a small wind system. By changing attitudes through educating individuals with a true understanding of small wind system noise levels and characteristics it will be possible to reduce oppositions to new small wind system installations.

The key limitation of the domestic study is that it was cross-sectional. As a result, it may be the case that individuals who have a negative attitude to turbines have so because they perceive greater noise (not the other way around). This is the reason the recordings study was carried out so that it was possible to see how attitudes predict the noise perception. Future research focusing on the noise perception at real small wind installation should still seek to implement a longitudinal design, commencing prior to turbine installation, to assess the causal direction of attitudes on noise perception more directly. A longitudinal study would also allow an assessment of whether symptom reporting and attitudes change before and after the implementation of a new small wind system installation.

In the following Chapter full details of the noise modelling part of the research will be given.

Chapter 4

Noise Modelling

There is little understanding of the characteristics of noise from small wind systems. An introduction to the research and drivers for the current research has been given in Chapter 1. It is important to attempt to model the noise attributed to small wind systems in order to have an idea of why the noise occurs and the likely important noise mechanism associated with them (see Section 1.2 for a review of aerofoil noise mechanisms). It is not the intention of the noise modelling part of this research to develop methods for predicting and modelling wind turbine noise but to assess the best tool which could be used by small wind system manufacturers for assessing likely small wind system noise mechanisms. It is also the intention to give a starting point for modelling the noise for further development and to compare with results of the noise measurement and questionnaire methods also adopted within the research. This Chapter of the research serves to achieve the noise modelling objectives of the research:

> To identify the noise mechanisms associated with small wind systems by modelling the turbulent flow and hence noise around a turbine blade to compare to the noise measurement results.

In this Chapter noise modelling tools currently available in the literature will be reviewed, focusing on how well they could achieve the objectives of the research given the constraints and merits of the different methods. The literature review will be followed by the methodology chosen for the current research. The results of the analysis using the chosen method will then be given. Finally, the conclusions and the recommendations for future work will follow the results Section.

Noise Modelling Nomenclature

A	surface area of the body (m)
b	semi-chord (m)
c, c_0	speed of sound (m/s)
C_v	specific heat (J/kgK)
CV	control volume (m^3)
d	semi-span (m)
f	function for the description of a surface according to FW-H
h	hub height (m)
i	internal energy (J)
k	turbulent kinetic energy (m^2/s^2)
k_x,k_y	chord-wise and spanwise wave number of turbulence $(1/m)$
K_A	A-weighting filter (dB)
K_x	particular value of $k_x = -\omega/U$ $(1/m)$
$l_y(\omega)$	frequency dependent wave length scale of turbulence (m)
L	turbulence length scale (m)
M,M_r	free stream Mach number and relative Mach number
$\mathbf{n}$	vector normal to surface
p,p_0	fluid pressure and pressure of undisturbed medium (Pa)
p_{ij}	stress tensor
r	radius, distance from source to receiver (m)
R	gas constant (J/kgK)
$R_{uu}(x)$	axial cross correlation of u, (u = axial velocity fluctuation of turbulence m/s)
$R_{ww}(k_x, y)$	spanwise cross-correlation of w, (v = velocity fluctuations of turbulence normal to aerofoil m/s)
S	surface (m^2)
S_i	internal energy source term
S_M	momentum source term
S_{PP}	surface pressure spectrum of blade boundary layer (dB)
$S_{ww}(\omega)$	spectrum of z velocity fluctuations of the turbulence
t	time (s)
T	temperature (K)
T_{ij}	Lighthill tensor (kg/ms^2)
u_τ	friction velocity (m/s)

u, v, w	velocity components (m/s)
u^+	dimensionless velocity (CFD)
U	free stream velocity (m/s)
V	volume (m^3)
x, y, z	coordinates
y^+	dimensionless distance from wall (CFD)
β	$\sqrt{1-M^2}$
δ	boundary layer thickness (m)
ε	rate of change of k
μ	dynamic viscosity ($N\ s/m^2$)
ρ, ρ_0	fluid density and density of undisturbed medium (kg/m^3)
σ	$\sigma = \sqrt{x^2 + \beta^2(y^2 + z^2)}$
τ_w	wall shear stress (N/m^2)
ϕ	general variable
ω,ω_w,ω^+	specific dissipation rate (m^2/s^3), $_w$ denotes at the wall, $^+$ denotes dimensionless
Λ	$\Lambda = MK_x d$
Γ	diffusion coefficient
Φ	dissipation function
Φ_{ww}	energy spectrum of turbulence
$\mathcal{L}$	integral of aerofoil pressure distribution

4.1 Available Noise Modelling Tools

In this Section, methods for modelling noise as seen in the available literature will be discussed. First the fundamentals of modelling noise will be given, followed by how these methods have been developed. Finally a discussion of CFD methods used in the literature as well as the tools available in commercial CFD packages will be given. The relative merits and drawbacks of each method in terms of their use for this research is essential in order to identify the best method for achieving the objectives of the overall research as outlined in Section 1.1.1.

4.1.1 Fundamentals of Noise Prediction

In order to fully understand available noise modelling tools, it is important to be familiar with the fundamentals of noise prediction. These fundamentals as originally developed by Lighthill [85, 86] in the 1950s will be discussed in the following Sections. Development of Lighthill's work by Ffowcs-Williams and Hawkings [87] and Amiet [88] will also be briefly described since their work is also essential for noise prediction tools available today.

4.1.1.1 Lighthill's Acoustic Analogy

The question of how precisely to identify the real origins of a sound wave was addressed by Lighthill in the papers 'On Sound Generated Aerodynamically I/II' [85, 86]. It is not advantageous to give complete details of the mathematics. For a complete derivation of the acoustic analogy the reader is referred to the original texts. Some essential elements of the formulation will be described in this Section as the understanding of the physics is fundamental to the understanding of all wind turbine noise mechanisms. A general description of the physical issues revealed by the maths will also be given.

Lighthill's derivation is based on the Navier-Stokes equations and can be described by the propagation of sound in a uniform medium, without sources of matter or external forces.

The Lighthill equation is:

$$\frac{\partial^2 \rho'}{\partial t^2} - c_0^2 \frac{\partial^2 \rho'}{\partial x_i^2} = \frac{\partial^2 T_{ij}}{\partial x_i \partial x_j} \tag{4.1.1}$$

Where T_{ij} is the Lighthill tensor.

$$T_{ij} = \rho u_i u_j + \left(p - p_0 - c_0^2(\rho - \rho_0)\right) \delta_{ij} + \mu \left[-\frac{\partial u_i}{\partial x_j} - \frac{\partial u_j}{\partial x_i} + \frac{2}{3} \left(\frac{\partial u_k}{\partial x_k} \right) \delta_{ij} \right]$$

For a full derivation of the Lighthill equation and definition of the Lighthill tensor the reader is referred to the original texts [85, 86].

The Lighthill equation is similar to the inhomogeneous wave equation and is derived from rearrangement of the continuity and momentum equations (the Navier-Stokes equations).

On the left hand side of the Lighthill equation is the wave equation, which describes three dimensional sound radiation in air. It is linear and has an exact solution if the source is known. On the right hand side of the equation are the source terms which describe all of the aerodynamics. The source terms include:

- A double differential (first term) which describes a quadrupole source
- A forcing term (second term) which results in a monopole source field
- And a forcing term differential which results in a dipole source field

The last two terms can be described in terms of the local velocity and pressure at the surface. For a definition of monopole, dipole and quadrupole sound sources see Appendix A.

The important conclusion of Lighthill's theory is that the sound field radiated by a bounded region for turbulent flow can be calculated as long as the flow is known. This is Lighthill's acoustic analogy. Although Lighthill's equation gives an exact solution, many assumptions need to be made in order to achieve useful solutions; however it is well suited as a basis for wind turbine noise prediction.

There have been several extensions to Lighthill's acoustic analogy which are widely used today to predict noise from wind turbines. The most commonly used versions of these will be discussed in the following Sections.

4.1.1.2 Ffowcs Williams and Hawkings

The theory of aerodynamic sound is built upon the equations of mass and momentum conservation of a compressible fluid, combined to give an inhomogeneous equation such as that derived by Lighthill and discussed earlier. This equation is valid in the region exterior to any closed internal surfaces.

A more general solution is derived by Ffowcs Williams and Hawkings [87] for an unbounded fluid which is partitioned into regions by mathematical surfaces that correspond to real surfaces. The motion of the new fluid in and outside the mathematical surfaces is completely identical to the real motion and the interior flow can be specified arbitrarily. Mass and momentum sources must be introduced to maintain these discontinuities which act as sound generators.

Ffowcs Williams and Hawkings derived the following governing equations (for a full derivation the reader is referred to the original text [87])

For mass:

$$\frac{\partial \rho}{\partial t} + \frac{\partial}{\partial x_i}(\rho u_i) = \rho_0 u_i \delta(f) \frac{\partial f}{\partial x_i} \tag{4.1.2}$$

For momentum:

$$\frac{\partial}{\partial t}(\rho u_i) + \frac{\partial}{\partial x_j}(\rho u_i u_j + p_{ij}) = p_{ij} \delta(f) \frac{\partial f}{\partial x_i} \tag{4.1.3}$$

To obtain an inhomogeneous wave equation governing the equation and propagation of sound ρu_i is eliminated to give:

$$\frac{\partial^2 \rho'}{\partial t^2} - c_0^2 \frac{\partial^2 \rho'}{\partial x_i^2} = \frac{\partial^2 T_{ij}}{\partial x_i x_j} - \frac{\partial}{\partial x_i}\left(p_{ij}\delta(f)\frac{\partial f}{\partial x_i}\right) + \frac{\partial}{\partial t}\left(\rho_0 u_i \delta(f) \frac{\partial f}{\partial x_i}\right) \tag{4.1.4}$$

This equation is referred to by many as the Ffowcs Williams and Hawkings (FW-H) equation and shows that in general, sound is generated by three source distributions. The first term on the RHS is identical to Lighthill's term, representing a sound of quadrupole nature in the region exterior to the surfaces with strength denoted by the Lighthill tensor. The second term denotes surface distributions of acoustic dipoles proportional to the stress tensor with strength given by the force vector acting on the fluid by the surfaces. The third term applies if the surfaces are moving and relates to monopole sources.

There are a number of general solutions to the FW-H equation depending on the exact formula chosen. For wind turbine noise prediction models, when the FW-H equation is used it is often presented in the most general form given here as a basis for further development taking into account any assumptions made about the flow.

$$4\pi p = \int_S \left[\frac{\rho_0}{r\left(1-M_r\right)}\frac{\partial}{\partial t}\left(\frac{u_i n_i}{1-M_r}\right)\right]_{ret} dS + \int_S \left[\frac{r_i}{c_0 r^2\left(1-M_r\right)}\frac{\partial}{\partial t}\left(\frac{p_{ij} n_j}{1-M_r}\right)\right]_{ret} dS + ...$$

$$... \int_V \left[\frac{r_i r_j}{c_0^2 r^3\left(1-M_r\right)}\frac{\partial}{\partial t}\left\{\frac{1}{1-M_r}\frac{\partial}{\partial t}\left(\frac{T_{ij}}{1-M_r}\right)\right\}\right]_{ret} dV \tag{4.1.5}$$

The first term is due to the blade thickness, the second term is due to the local forces on the blade and the third term is a volume integral of the remaining quadrupole terms.

4.1.1.3 Amiet

Amiet [88] presented a paper in 1975 which described acoustic radiation from an aerofoil in a turbulent stream. He derived an expression for the far field acoustic power spectral density produced by an aerofoil in a subsonic turbulent stream in terms of quantities characteristic of the turbulence.

Amiet stated that if the unsteady loading at each point on an aerofoil were known as a function of time, then the noise at any point in the far field can be calculated exactly. However, the unsteady loading on an aerofoil is due to turbulence in the atmosphere and is very difficult to quantify mathematically. Amiet describes turbulence in the atmosphere as a series of parallel and skewed gusts of different magnitude in relation to the aerofoil.

For a full derivation of the final solutions the reader is referred to the original text. Amiet described the aerofoil using the 2D linearised aerofoil theory and derived the acoustic expressions by considering the sectional lift at each point on the aerofoil. Amiet used the theories developed by Kirchhoff [89] and Curle [90] who state that the acoustic response of the aerofoil can be determined by distributing dipoles over the surface equal to the strength of the force on the surface, to relate the surface pressure distribution to the far field sound.

The basic result for sound produced by an aerofoil in turbulence for an observer in the $y = 0$ plane is as follows:

$$S_{PP}\left(x,0,z,\omega\right) \rightarrow \left(\frac{\omega z \rho_0 b}{c_0 \sigma^2}\right)^2 \pi U d \left|\mathcal{L}\left(x,K_x,0\right)\right|^2 \Phi_{ww}\left(K_x,0\right) \ as\ d \rightarrow \infty \tag{4.1.6}$$

When $y \neq 0$:

$$S_{PP}\left(x,y,z,\omega\right) \rightarrow \left(\frac{\omega z \rho_0 b}{c_0 \sigma^2}\right)^2 \pi U d \left|\mathcal{L}\left(x,K_x,\frac{\omega y}{c_0\sigma}\right)\right|^2 \Phi_{ww}\left(K_x,\frac{\omega y}{c_0\sigma}\right) \ as\ \Lambda \rightarrow \infty \tag{4.1.7}$$

The introduction of the cross correlation length ($l_y(\omega)$) puts equation 4.1.6 in a more intuitive form:

$$l_y(\omega) = \frac{1}{R_{ww}\left(K_x,0\right)}\int_0^\infty R_{ww}\left(K_x,y\right) dy = \pi\Phi_{ww}\left(K_x,0\right)/R_{ww}\left(K_x,0\right) \tag{4.1.8}$$

The second equality occurs due to the Fourier transform relation of Φ_{ww} and R_{ww}, hence equation 4.1.6 can be written as:

$$S_{PP}\left(x,0,z,\omega\right) \rightarrow \left(\frac{\omega z \rho_0 b M}{\sigma^2}\right)^2 d\left|\mathcal{L}\left(x,K_x,0\right)\right|^2 l_y(\omega) S_{ww}(\omega) \; as \; \Lambda \rightarrow \infty \tag{4.1.9}$$

And $S_{ww}(\omega) = R_{ww}\left(K_x,0\right)/U$ is the spectrum of the vertical velocity fluctuations of the turbulence.

The theory becomes vigorous when $\Lambda \equiv MK_xd \rightarrow \infty$ (the expression used to check applicability of the solution).

For values of the Mach number which are not too small, this theory should give a valid expression for the overall sound levels when the integral length scale of the turbulence, $L = \int_0^\infty R_{uu}(x)dx$ of the turbulence is significantly smaller than the aerofoil span.

A comparison of the theory with experimental acoustic and lift measurements available in the literature at the time showed good agreement and is applicable particularly when $\Lambda \equiv MK_xd > 1$.

4.1.2 Noise Prediction Models

There is limited work in the literature which has been done to predict noise from small wind systems. The majority of literature available predicts noise based on large scale wind turbines for isolated use or within wind parks, rotors such as helicopter rotors or simple aerofoils. It is not possible to apply noise prediction models such as these directly to small wind systems because they face different noise issues. For example, small wind systems rotate up to 75 times faster than large scale turbines; therefore the low frequency noise issue that occurs for large turbines may not apply.

The earlier models tend to apply empirical approaches to predict noise levels. A key example of one such approach is the work of Grosveld [18]. More recent models are steering towards the use of computational fluid dynamics (CFD) approaches which take advantage of the increasing availability of large computer processing power, an example of this type of model is that of Fleig [91] who uses large eddy simulation to predict noise from large scale horizontal axis wind turbines. A considerable proportion of new prediction models available today use a combination of empirical and CFD approaches [92].

The range of wind turbine noise prediction models available today are based on a number of early key research papers which provided the basis for the models which have been developed. These include Ffowcs-Williams and Hawkings [87] who developed an acoustic analogy, which is now used to describe the far field noise by many researchers and Amiet [88], who described the acoustic radiation for an aerofoil in a turbulent stream. Both of which are outlined previously in Section 4.1.1. Brooks, Pope and Marcolini [19] used extensive experimental results from a number of research projects to develop semi-empirical relationships for the noise mechanisms associated with aerofoil "self-noise" and combined these relationships into a prediction model written as a computer code. The majority of new prediction models use the underlying theory behind these semi-empirical models to some extent.

As advancements occur in available computing power and understanding of the noise mechanisms associated with wind turbines, models become progressively more sophisticated. Lowson [16] proposed a classification for the prediction methods available, class I, class II and class III. A description of each classification can be found in Table 4.1.1.

Type of Code	*Description*
Class I	Predictions giving an estimate of overall level as a simple algebraic function of basic wind turbine parameters
Class II	Predictions based on separate consideration of the various mechanisms causing wind turbine noise, using selected wind turbine parameters.
Class III	Predictions utilising complete information about the noise mechanisms related to a detailed description of the rotor geometry, and aerodynamics.

Table 4.1.1: Classification of Noise Prediction Codes according to Lowson [16]

An outline of each of the key papers for wind turbine noise prediction to date can be found in the following Sections.

4.1.2.1 Empirical Noise Prediction Models

In this Section, available empirical modelling methods for predicting noise will be discussed. An outline of each relevant model will be given here, however the reader is referred to the original texts for derivations, scaling laws and details of the equations associated with each model. These models are based on the fundamentals of noise prediction as discussed in Section 4.1.1 and a knowledge of noise mechanisms associated with wind turbines (see Section 1.2). The positive and negative aspects towards their usage will be discussed in terms of their applicability to achieving the aims and objectives of this research.

Grosveld's Model (1985) Grosveld [18] formulated a model which predicts broadband noise from horizontal axis wind turbines and was compared to results of measured data from four popular wind turbines at the time, one upwind machine (the MOD-2) and three downwind machines (a MOD-OA, a WTS-4 and a Windpower Inc. turbine). The Grosveld model can be considered as an incomplete class II model.

The noise mechanisms modelled are as follows:

- Inflow turbulence noise
- Boundary layer trailing edge noise
- Trailing edge bluntness noise

For prediction of inflow turbulence noise Grosveld used a derived turbulence spectrum assuming the turbulence to be isotropic together with a negative temperature gradient as a function of height above the ground to predict the fluctuating forces on an aerofoil. He then used the relationship developed by Lighthill which relates the calculated fluctuating forces to sound pressure. In order to calculate the far field noise, the wind turbine rotor is modelled as a dipole point source located at the hub.

Grosveld used the Schlinker and Amiet [93] prediction model for turbulent boundary layer trailing edge noise which predicts the noise due to this mechanism from a local blade segment using first principles theory, which includes local Mach number, boundary-layer thickness, length of the blade segment and observer position. The noise prediction was achieved using a scaling law approach and the overall noise at the receiver location is calculated by integrating individual contributions from each blade segment over the blade. This noise mechanism is assumed to be a dipole radiator with a directivity pattern as proposed by Fink [94].

The prediction model for trailing edge bluntness noise uses the same calculation method as for turbulent boundary layer trailing edge noise but uses a separate set of equations which have been scaled by Grosveld and follow the directivity pattern of Howe [95]. The blunt trailing edge noise model contains two different flow conditions which are characterised by the trailing edge thickness and the displacement thickness of the boundary layer. Separate sound pressure level equations are used depending on whether this ratio is greater or smaller than 1.3.

For the trailing edge bluntness prediction, a peak in measured noise spectrum for the Windpower turbine with blunt trailing edged aerofoils of about 2000Hz is well predicted by the model. When the aerofoils are sharpened, there is reasonable agreement between measurements and prediction. Grosveld concluded that, in general, predictions were within 4dB of the measured data.

However, the predictions are limited to the acoustic far field, on axis and without distinction between upwind and downwind directions as no propagation effects are incorporated. The model also has an inconsistent prediction method. The trailing edge bluntness and turbulent boundary layer trailing edge noise mechanisms are predicted by integrating over the blade but the inflow turbulence noise is estimated for the whole rotor. It has also been suggested that estimates for inflow turbulence are not correct [16].

Glegg's Model (1987) Glegg [22] described a computational method to predict rotor broadband noise based on general theoretical formulations. The results are then compared to detailed measurements from a 20m diameter WEG wind turbine.

The noise mechanisms included in Glegg's prediction model are:

- Unsteady lift noise (inflow turbulence noise)
- Unsteady thickness noise (inflow turbulence noise)
- Trailing edge noise
- Noise from separated flow

For the inflow turbulence model, Glegg used the formulations derived by Amiet [88] for the acoustic radiation of an aerofoil in a turbulent stream which describes the noise radiated from an aerofoil due to the interaction of the blade with oncoming harmonic gusts. The trailing edge model is also based on results by Amiet and the noise from separated flow i.e. around bluff bodies, fairings etc is based on the work by Nelson and Morfey [96] who related the steady forces of a bluff body to the acoustic pressures.

The study also includes a detailed model of the atmospheric boundary layer which is compared to anemometer measurements with good agreement for a number of conditions. Glegg then assessed the formulations to obtain correction formulae which account for the effect on the radiated sound field due to blade rotation.

The study is limited to upwind rotor wind turbines only, however; Glegg did assess the effect of the presence of the tower for an upwind rotor on noise scattering and it was concluded that scattering effects were not important. The tower scattering can cause significant increases in noise levels but only for very short periods of time. These peaks in noise levels therefore do not have a considerable effect on the average noise level over several rotor rotations.

The formulations and findings for each noise mechanism were written into a computer program for an HP9485B desktop computer which computes the A-weighted one third octave spectrum for wind turbine noise.

Noise predictions were found to be around 10dB below measured levels. It was found that the most likely cause of this was an incorrect modelling of the inflow turbulence. To overcome this it was concluded that for machines with an advance ratio [1] of ≈ 0.15, a turbulence length scale equal to one blade chord length would give best fit results. Comparisons were also made with two 80m diameter turbine measurements with good agreement.

A drawback to the Glegg model is that the assumptions depend on the aerodynamic design of the wind turbine and may not apply in situations other than that used in the model.

The BPM Model (1989) The purpose of the BPM model [19] was to document the development of an aerofoil self-noise prediction method and to verify its accuracy for a range of applications. This was done using a semi-empirical approach based on previous theoretical studies and data from a series of tests on isolated aerofoils. The noise mechanisms included in the BPM prediction model are:

- Trailing edge noise
- Separation stall noise
- Laminar boundary layer vortex shedding noise
- Tip vortex formation noise

[1] The advance ratio is the ratio of the diameter of the rotor multiplied by it's rotational speed in rpm, with with incoming wind speed

- Trailing edge bluntness noise

Acoustic measurements were taken experimentally on various NACA aerofoils 2D and 3D models to form a database of results: 6 2D NACA 0012 aerofoil models with a span of 45.72cm and chord lengths of 2.54, 5.08, 10.16, 15.24, 22.86, and 30.48cm; 5 3D aerofoil models each with a span of 30.48cm and chord lengths equal to the five largest 2D models. All aerofoil models had a very sharp trailing edge. One NACA 0012 aerofoil model had a blunt trailing edge with a chord length of 60.96cm. All the models were tested in the low-turbulence potential core of a free jet located in an anechoic chamber. For the acoustic tests an array of 8 $\frac{1}{2}$" free-field response microphones were mounted on the plane perpendicular to the models and for the aerodynamic tests the microphones were replaced with hot wire probes. The models were tested in free stream velocities up to 71.3m/s, this corresponds to Mach numbers up 0.208 and Reynolds numbers up to 1.5×10^6. Six angles of attack were tested between 0 $^\circ$ and 25.2 $^\circ$; the larger angles of attack were not tested for the larger models. In some tests the blades were untripped (clean and smooth surfaces) and in some cases the models were tripped to provide a turbulent boundary layer (grit strip at 20% chord from the leading edge).

Boundary layer thickness and integral parameters were measured in order to normalise the aerofoil noise data. The spectral shape, level and frequencies of the noise were then examined for their dependency on various parameters such as geometry and Mach number. The results were used to develop scaling laws for each of the five self noise mechanisms and the resulting predictions (determined by implementing the spectral scaling laws into a FORTRAN 77 computer code) of aerofoil self noise were tested against results found in three studies [93, 97, 98].

Conclusions were drawn regarding each noise mechanism:

- Trailing Edge Noise and Separation Stall – accurate and generally applicable, particularly at high Reynolds numbers and low to moderate angles of attack.
- Laminar Boundary Layer Vortex Shedding – found to be dominant at low Reynolds numbers with a good predictability, however there are some issues regarding how best to apply the formulations to different aerofoil geometries.
- Tip Vortex Formation – appears well predicted but as it was found not to be an important mechanism. The full accuracy cannot be properly assessed.
- Trailing Edge Bluntness – Very important mechanism and predictable using methods applied.

The full prediction code was found to be particularly good for aerofoils in low to moderate flow speeds and good as a basis for future research. In fact Lowson [16] stated that "the BPM data is thought to provide good basis for an initial prediction of wind turbine noise, providing that the limitations are properly recognised." The main limitation of the BPM model is that the scaling laws are heavily based on one aerofoil shape and as a consequence it may not be applicable for other aerofoil shapes.

The BPM model is an important one as much subsequent research has used the scaling laws Brooks, Pope and Marcolini developed as a basis for their work and extensions of it. Examples of such more recent prediction models who discuss the BPM model are [16, 21].

Lowson's Model (1992) Lowson's work [16] aimed to develop a full class III prediction model which could be implemented in a simple manner for noise prediction via basic wind turbine data. Blunt trailing edge noise and laminar boundary layer vortex shedding noise can be readily controlled at source so it would be more useful to identify means for elimination of these noise sources than predict them. For this reason they are not included in the model. Separation stall noise and tip noise are also not included as they require a detailed prediction of local aerodynamic parameters. Therefore Lowson's work includes self noise due to the attached boundary layer and inflow turbulence noise.

Lowson assumed that on average the sound from each element of the turbine has a uniform distribution of noise radiation due to a high frequency of shifts in wind direction; this assumption greatly simplified the prediction formulae.

For the Lowson trailing edge model, the BPM data is used to develop a simpler prediction scheme, closely related to the known physics of the turbulent boundary layer and specifically aimed at the wind turbine case. Lowson stated that there are three main issues when predicting trailing edge noise, these are:

- Prediction of the boundary layer thickness - For the Lowson model, the boundary layer thickness is established using the empirical prediction for that of a flat plate.
- Prediction of the scaled overall level – The empirical value used here to scale the relationship developed by BPM for the peak 1/3rd octave band to other conditions is 128.5.
- Prediction of the spectral shape – this gives the level or 1/3rd octave bands away from the peak. Lowson uses a simplified version of BPM's complex formula for this shape and prediction of the peak frequency is done using the formula developed in BPM.

Lowson found that his model for trailing edge noise gave good agreement to the BPM model and data. To apply the trailing edge model to wind turbines is simply a matter of integrating the prediction formula over the whole blade length (similar to the approach taken by Grosveld [18]).

For the inflow turbulence model Lowson uses the model developed by Amiet [88] which is based on a flat plate response to turbulence. Amiet gives two formulae which apply to the low and high frequency regimes due to different sized turbulent eddies as described in Section 1.2. Amiet gave no recommendations for prediction of noise in the transition region between low and high frequencies. However Lowson developed an empirical formula which gives a smooth transition between the two and showed encouraging agreement with experimental results.

Lowson stated that the turbulence parameters which must be included in the turbulence model are those listed below. Lowson sought to develop a prediction model which captured the leading features of the practical problem without undue complication and modified a prediction model to achieve this.

- Wind speed as a function of height
- Turbulence level
- Turbulence scale
- Turbulence spectrum

Using the relationships developed, a BASIC program was written and compared to noise data for two wind turbines (a MOD2 and a VESTAS 39) with reasonable agreement.

The Lowson model discussed did not require detail of geometry and aerodynamics, as it was thought such methods were best undertaken after a very basic model was developed and compared with experimental data. A refined version of this noise prediction code has since been published incorporating a detailed description of the flow at the trailing edge of an aerofoil.

Empirical Models 1997 - Present After the work of Lowson in 1993 there was a slow down in research in the area. This was particularly the case for wind turbine noise. This slow down could be due to the fact that during this time there was a respite in renewable energy research in general. From around 1997, papers started to be published again and since then much research was carried out in the area. In this Section a brief overview of research carried out to present will be given.

During this time period, a shift towards computational based prediction has been seen; this has likely been due to the huge increase in computational processing power available. However, semi-empirical research has still continued to be carried out. Examples of such empirical research during this time is that of Fuglsang [99], Moriarty [21, 92, 100, 101] and Burley [102]. These semi-empirical models were based on previous semi-empirical research as discussed in the previous Sections and predicted wind turbine noise with emphasis on turbulence inflow noise and aerofoil self noise split into the individual noise mechanisms. An example of an improvement in semi-empirical modelling which takes advantage of available computer programs is that of Moriarty in 2004 [92] who replaced the assumptions made previously to determine the boundary layer properties of an aerofoil with a more detailed description calculated using the XFOIL software available [103]. Other improvements in semi-empirical modelling include using numerical optimisation [99] and writing semi-empirical relationships using more powerful coding compilers.

Zhu's work in 2005 [104] aimed to model aerodynamically generated noise from wind turbines using a semi-empirical coupled aerodynamic and aero-acoustic model (hybrid model). The modelling of inflow turbulence noise is based on the work of Lowson [16] and the aerofoil self-noise description is based on the BPM model [19]. A Blade-Element Momentum method (BEM) is used to describe the aerodynamic properties. A development in this paper compared to Zhu's previous work is that a tip correction has been implemented in the model. The viscous-inviscid interactive aerofoil XFOIL [103] code is used to determine the boundary layer properties as input into the prediction model.

The noise mechanisms predicted in this research are:

- Inflow turbulence noise
- Turbulent boundary layer trailing edge noise
- Separation stall noise
- Tip vortex formation noise
- Trailing edge bluntness vortex shedding noise

The aerofoils are divided into a number of aerofoil sections (blade elements) refined at the tip. The sound pressure levels are then calculated for each noise source as using the Lowson and BPM models. The total noise is then determined by summing all contributions from each noise source:

$$SPL^{i}_{Total} = 10log_{10}\left(\sum_{j} 10^{0.1(SPL_j+K_A)}\right) \tag{4.1.10}$$

And then by summing this value over all blade elements:

$$SPL_{Total} = 10log_{10}\left(\sum_{i} 10^{0.1SPL^{i}_{total}}\right) \tag{4.1.11}$$

The prediction results are compared to measurement results from a Bonus 3 bladed, upwind, 300kW turbine with a rotor radius of 15.5m and rotor angular speed of 35.2RPM. Two comparisons are offered. Corrected measurement values are compared to predictions for a NACA 0012 aerofoil. The computed noise spectrum based on this aerofoil illustrates that the model captures the basic features of the noise levels. The second validation case predicts noise levels for a NACA 632xx aerofoil (that which is used on the Bonus 3 wind turbine) and the predicted noise spectra are much closer to the measured levels. Future work will take into account separation and rotational effects of the turbine.

The empirical models discussed are an overview of those which are currently available in the literature for predicting wind turbine noise. There are key drawbacks to the empirical approach for modelling noise, particularly when considering how they might be used by small wind turbine manufacturers. The empirical models may not be applicable to wind turbines and aerofoils other than those on which the original research was carried out and most are specifically designed for large scale wind turbines. Many of the models only predict certain noise mechanisms and do not give an overview of how small and micro turbines and aerofoils generate noise. A full understanding of detailed coding and complicated noise equations is required to implement and develop the models to make them applicable to this research and small wind systems. It is unlikely that small wind system manufacturers would have access to this resource and therefore the empirical noise modelling approach will not be used for the current research. In the following Section computational fluid dynamics methods will be considered.

4.1.2.2 Computational Fluid Dynamics in the Literature

As seen in Section 4.1.2.1, earlier noise predicting models tend to apply empirical approaches to predict noise levels. However, more recent models are steering towards the use of computational fluid dynamics (CFD) approaches which take advantage of the increasing availability of large computing power. A considerable proportion of new prediction models available today use a combination of empirical and CFD methods.

In this Section, a discussion will be given of current work in the literature that uses CFD or a combination of methods to predict and model noise levels from aerofoils or wind turbines.

Doolan [105] wrote a review paper of aerofoil trailing edge prediction models in 2008. In this paper it was written that trailing edge prediction models can be categorised into three classifications as follows:

- Empirical prediction models – derived from anechoic wind tunnel experimental results. The works of Schlinker [93] and Brooks, Pope and Marcolini [19] as discussed in Section 4.1.2.1 are categorised as this type of model.
- Direct prediction models – computational method which computes the turbulent flow around the aerofoil and noise in a single step. There have been limited applications of this type of model in the literature due to the extremely high computational cost. One example of a direct model is that of Sandberg [106] who modelled a low Reynolds number flow. Direct models will not be considered as the computational resource available is not sufficient for the current research to use this method.
- Hybrid models – the flow and noise calculations are decoupled and the flow pattern is calculated first which is then used as an input for the noise calculation.

These classifications are in contrast to those by Lowson [16] as outlined in Section 4.1.2, and are able to accommodate more readily the advances in computational power available today. This classification code should not be restricted to only trailing edge models and could also be applied to all wind turbine noise prediction models which use CFD.

It is suggested by Doolan that hybrid models which use CFD in part are currently the most commonly available tools for predicting noise. They can be subdivided into further categories by considering how the air flow around the aerofoil can be calculated and the noise predicted. These methods are the most common as they have a reduced computational cost compared to direct prediction models.

Hybrid models can be further categorised as follows:

- Synthesised turbulence methods – a method which produces a flow field using a model to estimate the effects of turbulence. This method is often referred to as RANS (Reynolds averaged Navier Stokes). An important example of a recent prediction model which uses RANS is Mathey's research [107], however this research uses a zonal RANS-LES approach where RANS simulations are performed over the whole aerofoil and flow region and a refined LES simulation is performed in the trailing edge area of the aerofoil where better accuracy is required.

- Simulated turbulence using LES (Large eddy simulation) - LES is a more accurate method than RANS but has a higher computational cost because the turbulence length scales are resolved with no assumptions. The grid size must be small enough to resolve the smallest eddies of interest. Manoha [108] developed a model that uses LES along with acoustic analogy.

Iida [109] and Fleig's [110, 111, 91] research emphasis was on aerofoil tip noise, a likely reason for this is that many consider it to be an important noise source due to high flow speeds at the outer sections of a wind turbine blade. Their tip noise models use Large Eddy Simulation (LES) to predict the flow fields and noise around a turbine blade by assessing the surface pressure fluctuations on the blade; some of these LES models use a direct computation of the noise levels, where the calculations for the flow field and noise are performed in one step [109], however LES is a very expensive method (Fleig's research in 2005 [91] required the use of the Earth Simulator [2] in order to carry out these computations) so further improvements in this technique are needed in order to make it viable for general use. LES was used as early as 2000 by Wang [112] who attempted to predict the trailing edge noise from an aerofoil using LES to predict the noise in the near field and then the acoustic analogy developed by Ffowcs Williams to calculate the far field noise. Wang's work is an example of a hybrid prediction model where the flow field and noise are calculated in two steps using separate methods which are then coupled together. There has been a shift towards hybrid type models as they are able to produce refined predictions in the cheapest possible way. Hybrid methods show great promise, however there is a great need for further validation with experimental results and more efficient optimisation routines.

Hybrid Methods with Simulated Turbulence In 2007 Shen and Sørensen [113] presented a paper for aero-acoustic modelling using large eddy simulation (LES). The model discussed in this paper is one which solves the 3D compressible Euler/Navier-Stokes equations using LES and is developed in order to solve the problem of applicability to different situations of semi-empirical models. LES is becoming increasingly possible with the advancements of computer technology. Shen and Sørensen's computational aero-acoustic (CAA) model is a developed splitting technique, where the flow and acoustic equations are solved separately with two different discretised meshes and time steps. This is a hybrid method that is a much faster technique than the alternative direct method of solving the compressible Euler/Navier Stokes equations.

The steps involved in computing the noise with this model are:

- Step 1 – Obtain the flow solution by solving the incompressible Navier-Stokes equations with a suitable grid to capture the turbulence of interest in the flow.

- Step 2 – Solve the compressible equations for noise levels once the flow has stabilised.

[2] The Earth Simulator is a Japanese supercomputer intended for running global climate models with 5120 processors and 10 terabytes of memory

The governing equation for the flow solution is the three-dimensional incompressible Navier-Stokes equations and solved using the EllipSys3D code developed at the Technical University of Denmark (DTU). The three-dimensional acoustic/compressible equations for turbulent flow were developed in previous work by Shen and Sørensen. For details of these equations the reader is referred to the original text [113]. The equations are discretised and solved with a predictor-corrector/finite volume method.

Two different flow patterns and meshes are considered and tested; both tests are on a NACA 0015 aerofoil with a Mach number of 0.2. The first test is a laminar flow at a Reynolds number of 800 and the second is a turbulent flow at a Reynolds number of 100000. Predictions of the numerical noise spectrum with experimental data from the BPM model show general agreement. Slight differences are seen between predicted and experimental results, but the likely cause of this is the differences between the aerofoil shapes.

An extension to this research would be to apply the model specifically to wind turbine noise rather than single aerofoils although this would be at a high computational cost and would require a much larger grid.

Moroianu [114] presented a paper to predict wind turbine noise generation and propagation based on an acoustic analogy. This hybrid method comprises two steps. The flow solution and hence noise sources are computed using the LES solution of incompressible flow. The propagation of the noise and far-field values are calculated using the acoustic analogy developed by Ffowcs-Williams [87].

In this paper the noise considered is that for a complete turbine. The noise predicted using the LES solution of incompressible flow is due to blade velocity variations and forces by the blades on the fluid. To predict the propagation of the noise, the noise predicted using the LES solution is then considered as a point source at the turbine hub and the far-field values are calculated using Ffowcs-Williams' acoustic analogy. The definition of the problem used to predict the noise is a 26m diameter rotor with a rotational speed of 60rpm at a wind speed of 10m/s. The blade profile considered is that of NACA 4415 twisted blade with a constant angle of attack of 7°. The computational domain for the calculations is a box with dimensions much larger than the rotor diameter and the domain for the acoustical problem is much larger than that for the flow problem.

Moroianu found that vortices are produced by the blade due to the differences in pressure on the suction and pressure sides of the blades, and these vortices extend backwards transported by the induced flow. In the near field, the spectrum of turbulent kinetic energy generated by these vortices is dominated by the turbine's blade passing frequency. The spectra of acoustic density fluctuation show that in the near field, the frequency range is broader and shrinks towards smaller values with the distance from the rotor. In the far field the SPL intensity decreases as if the wind turbine is a point source and the isocontours become almost spherical far from the turbine. At this distance the spectrum is influenced by ground effects and noise signals from neighbouring turbines.

Further work is required to assess the influence of terrain irregularities or air dissipation. This method would not be applicable to the current research as the specific regions of the aerofoil where noise is generated are of interest. Therefore modelling the noise as a point source would not give enough detail, however the manner in which the vortices propagate downstream of the turbine could be of interest.

Mathey's [107] zonal RANS-LES approach, is another example of a hybrid method using turbulence modelling in the near field of the aerofoil and Ffowcs-Williams' acoustic analogy to assess the frequency spectra of the noise. However, in order to model the turbulence Mathey used a RANS-LES approach, with a sub-domain of LES at the trailing edge and the synthesised turbulence RANS method near the rest of the aerofoil wall region. The acoustic noise sources were then resolved from the LES results. Runs were carried out for flows with high Reynold's numbers over a flat aerofoil in 3D. The CFD model represented well the flow separation occurring at the aerofoil trailing edge. The zonal RANS-LES acoustic noise sources matched well the frequency spectrum predicted using acoustic analogy, matching the broadband noise, and two tonal peaks at 220Hz and 1000Hz, but it was noted in the paper that the turbulence must be modelled fully to achieve accuracy of the results. The computational cost of the zonal method is low as LES is only used in the area of key interest but the cost would be significantly higher for a full wind turbine or aerofoil with a more complicated geometry. Mathey's method bridges the gap between simulated and synthesised turbulence methods as it uses aspects from both for different regions of the domain.

Hybrid Methods with Synthesised Turbulence Humpf's [115] research presents an assessment of two different approaches to predict trailing edge noise; the semi-empirical noise prediction model NAFNoise developed by Moriarty [100] and a hybrid approach, which calculates the aerodynamic and aero-acoustic calculations performed with the Navier-Stokes CFD code FLUENT and a synthesised turbulence method for modelling the noise.

As stated on the prediction tool website homepage, NAFNoise, which stands for NREL (National Renewable Energy Laboratory) AirFoil Noise, is a program that predicts the noise of any aerofoil shape for all five different noise mechanisms related to an aerofoil. The models in the program are based on the work of others (primarily using the semi-empirical models developed by BPM as discussed earlier) and research performed at NREL. The XFOIL routine is used within the program to calculate the boundary layer properties for aerofoils other than the NACA 0012 evaluated in the BPM paper. Several options of summing the distinct noise mechanisms (turbulent boundary layer trailing edge; suction and pressure side, blunt trailing edge noise and separation noise) are considered.

For the CFD method, the scattering effect created at the trailing edge which turns an inefficient quadrupole noise in the surface boundary layer into a more efficient dipole noise source at the trailing edge is determined by calculating the effect of the two different noise sources (quadrupole and dipole) and summing the results. The Proudman formula which the CFD method uses to calculated the broadband noise sources is based on Lighthill's acoustic analogy and is used to calculate the quadrupole source terms and the boundary layer noise source model is used to calculate the dipole source terms. Each of these broadband noise source models use the RANS simulation results as the input and are available in FLUENT. FLUENT's internal post processor to calculate the Acoustic Power from the RANS aerodynamic simulations. Circular regions of varying radii about the trailing edge were evaluated so the total scattering effect could be captured and the full 'surface acoustic power' and 'acoustic power' (L_{Wtotal}) could be computed using the summing relationship:

$$L_{Wtotal} = 10log\left(\frac{\sum L_{W_i}}{1 \times 10^{-12}}\right) \tag{4.1.12}$$

These sound power levels are then converted to sound pressure levels (L_P) using the formula:

$$L_P = L_W - 20log10(r) - 10log\left(\frac{1}{2\pi rh}\right) \tag{4.1.13}$$

Comparisons of the two approaches were made with experimental measurement conducted at IAG (Institute of Aerodynamics and Gas Dynamics). Comparisons refer to a tripped aerofoil at 2.7° angle of attack, Reynolds number of 3×10^6 and an inflow Mach number of 0.178. The chord length is 0.8m; the span of the aerofoil is 0.73m with a trailing edge thickness of 1mm.

The short computation time of the semi-empirical models by BPM is an attraction for design purposes and in the future it would be advantageous to develop a deeper knowledge of the functionality of the models. However, when comparing the FLUENT results to predictions from the NAFNoise program, there are deviations up to 29dB over the whole frequency range. The RANS model predicted the aerodynamic properties and hence turbulence in the flow well. It is assumed that the acoustic post processor in FLUENT is the source of the deviations as the broadband noise sources model is a relatively new tool available within CFD and therefore requires further investigation.

Tadamasa and Zangeneh [116] used the RANS $k - \omega$ SST turbulence based model within the solver ANSYS CFX 11.0 to calculate the inputs to the Ffowcs Williams-Hawkings (FW-H) equations for noise prediction of wind turbines. Thickness and loading types of noise were obtained using original FW-H code. In Tadamasa's paper, the use of LES methods was considered as a method to calculate wind turbine noise. However, the LES method was ruled out due to the inaccessible computational cost. Tadamasa compared computational simulations of the flow field around a NREL Phase VI HAWT wind turbine blade with experimental results. An NREL Phase VI HAWT wind turbine has a 10.06m diameter with a power rating of 20kW, a 0.737m chord length at the blade root section and a 0.356m chord length at the blade tip section. Simulations were carried out at wind speeds of 7m/s, 9m/s, 11m/s, 13m/s, and 15 m/s at five blade spanwise sections at 30%, 46.6%, 63.3%, 80% and 95% of the blade span. Tadamasa concluded that although with the current turbulence models available within CFD solvers it is still difficult to accurately simulate the highly separated flow field; CFD simulation, and more specifically RANS methods, can predict fairly well the flow field around a wind turbine blade. The RANS results were then used as the input to the FW-H codes to calculate the thickness and loading types of noise. It was found that using the RANS inputs and the original FW-H code gave good results and that in future these codes can be used for designing acoustically improved wind turbine blades.

The RANS method of modelling the turbulence of the flow and hence potential wind turbine noise mechanisms has shown promise by Humpf [115] and Tadamasa [116]. Other researchers have also used the RANS synthesised turbulence methods to model the aerodynamics of aerofoils and wind turbines [117, 118, 119, 120]. However, modelling aerodynamic noise was not the focus of their research. It has been shown in the literature and with a knowledge of aerofoil noise mechanisms that turbulence is directly related to noise generation, so an analysis of the turbulence could be a feasible method for estimating noise sources from a small wind system aerofoil, particularly when available computational power is a concern.

Lin and Sheih [117] used the SST $k-\omega$ RANS method to model the turbulence and interference between the rotor and tower of a large scale upwind wind turbine. The 3D domain was modelled with two regions, a stationary zone for the tower and a sliding mesh for the rotor and periodic boundaries. Contours of the velocity magnitude were examined, but results of the turbulence were not. Although the method of observing velocity magnitudes of a sliding mesh with periodic boundaries is not appropriate to achieve the aims of the current research, Lin's work shows that the SST $k-\omega$ would be appropriate for this type of problem.

Campobasso [118], addressed modelling aspects of wind turbine aerofoil aerodynamics based on the RANS methods and also included a comparison of the solutions obtained using the different turbulence modelling methods. Campobasso also used the XFOIL code as used by Drela [103] and Humpf [115] to further verify the results. The RANS turbulence models compared for a 2D aerofoil blade section were the $k-\varepsilon$, the $k-\varepsilon$ ASM (algebraic stress model), the $k-\omega$ and the $k-\omega$ ASM models. Campobasso's research showed that the RANS model gave the best comparison with the XFOIL modelling by investigating total pressure values with the $k-\omega$ ASM model. Although aerodynamic noise and turbulence were not investigated directly, the low computational cost of using the RANS method to model turbulence makes it an attractive method for the current research.

Finally, synthesised RANS methods are starting to be implemented in the literature to investigate the aerodynamics around micro turbines, Monteiro [119] computed the turbulent flow around a micro turbine blade with a rotor diameter of 2.2m to support development of a micro turbine which could be available for mass production and implementation. The RANS model used in this research was the $k-\varepsilon$ model. This has been shown by Campobasso to show less accurate results than the $k-\omega$ method. However, Monteiro's work highlights the fact that the RANS method for modelling turbulence is a feasible method for analysing the aerodynamics and hence potential noise sources around a small wind system, particularly when considering small wind system manufacturers as the end user.

As seen in the literature, commercial CFD packages have been used extensively to model aerodynamics, turbulence and noise from wind turbines and aerofoils. Direct numerical simulation of noise and turbulence and LES methods will describe most accurately turbulence and noise but this comes at a very high computational cost, still not available to most. Hybrid methods which used a combination of LES and RANS methods are a more attractive method and are more accessible, however a high level of expertise is still required for these methods and they are not recommended for flows with high Reynolds numbers. Although RANS methods have not been used extensively in the literature to model noise, aerodynamics of wind turbines have been investigated using RANS and to estimate broadband noise sources using the results of RANS simulations. It is considered that RANS methods to estimate the turbulence around aerofoil blade sections would be the most appropriate technique for the current research. An idea of the aerodynamics around small wind system blade sections will show the regions of high turbulence and hence noise levels. RANS methods are the most achievable given the computational resource available.

4.1.2.3 Summary and Noise Modelling Tool Chosen

In order to make a final decision about which noise modelling tool to use to achieve the objectives of the research summarised in the Introduction to the Thesis in Section 1.1.1, it is essential to consider how small turbine manufacturers could use the tools available to them in industry. Use of empirical approaches requires an advanced understanding of the background theory and computer programming in order to implement the methods, whereas the use of LES and direct and integral method noise modelling within CFD requires a huge amount of computer processing power. Small turbine manufacturers are unlikely to have these resources available to them due to the high cost.

A more realistic option would be to use a commercial CFD package to identify high turbulence regions around designed wind turbine blades using RANS methods as this requires a small amount of computing power compared to LES and direct or integral method noise modelling. Desktop computers are also rapidly becoming able to handle the necessary processing power needed to model turbulence using RANS methods. In addition to using the RANS method the broadband noise source model is also a feasible possibility because it also does not require a large computer processing power.

Having considered the literature review in this Chapter and the aims and objectives of the research it has been decided that the RANS turbulence modelling option within the commercial package Ansys Fluent will be used. This will be done by using the package to give an indication of noise mechanisms present around an aerofoil based on the regions of high turbulence in the airflow.

The specific aims of the noise modelling part of the research are as follows:

- To understand why a small wind system's aerofoil produces noise
- To verify that the majority of noise from a small wind system is due to aerodynamic noise sources
- To identify regions of high noise on a small wind system's aerofoil
- Allow comparisons between questionnaire data and environmental noise measurement data

In the following Section details of the methodology for the CFD work will be given, followed by results of the CFD analysis and a conclusion of the findings.

4.2 CFD Methodology

CFD is used within this research as a tool to identify why aerodynamic noise around a turbine blade might occur and further work would be needed to develop the findings of the CFD modelling, Ansys Fluent is the solver that will be used for the CFD analysis. A brief outline of the capabilities of CFD relevant to this research is outlined in the following Sections. Further details about the methods outlined are available for the reader in textbooks [121, 122] and the Fluent User's Guide [123]. This will be followed by details of the model setup within Fluent. Finally the physical background of the model will be given in this Section, including the results of the mesh independence check.

4.2.1 CFD Theory

Computational Fluid Dynamics is a computational tool to solve the governing equations (a. the conservation of mass, b. Newton's second law and c. the conservation of energy) for fluid flow for a number of applications. In recent years, CFD methods have been greatly improved and the capabilities of the methods expanded. Fluent has the facility to model flow, turbulence and heat transfer with special models for combustion, aero-acoustics, turbo-machinery and multiphase systems. For this research turbulence modelling will be used because aerodynamic noise is directly related to turbulence. Acoustic methods are available within Fluent but these are still relatively new and not well established. The available acoustic modelling methods are the Ffowcs Williams and Hawkings (FW-H) method and the Broadband Noise Sources method. The FW-H method requires a full time dependent solution for each model before the noise sources can be calculated. This would require high computational power and high cost and is therefore not feasible for this research. The Broadband Noise Sources method uses results of the turbulence modelling using RANS methods to calculate the levels of aerodynamic noise in the flow and the magnitude of the broadband noise sources are directly related to the magnitude of the turbulence levels calculated using the RANS methods. For this reason, an analysis of the turbulence in the flow will be sufficient to give an indication of the aerodynamic noise mechanisms which occur in the flow field around aerofoil blade sections. It is not the intention of this research Thesis to develop or explain CFD methodologies.

CFD analysis requires three steps, pre processor, solver and post processor. The solver step is where the use of Ansys Fluent is required. The solver consists of three steps:

- Integration - of the governing equations of fluid flow over all control volumes of the domain (cells within the created mesh)
- Discretisation - conversion of the integral equations into a system of algebraic equations
- Solution - of the algebraic equations using an iterative method.

The fluid flows that CFD methods seek to solve are usually very complex and hence a number of assumptions must be made about the model in order to carry out the three steps above. The following

Sections will offer the reader a summary of the theory behind the governing equations in CFD and the model chosen to carry out the simulations. Details of the discretisation and solution schemes chosen will be given in Section 4.2.2 of the Thesis.

4.2.1.1 Complete Navier-Stokes Equations

The first step in carrying out CFD analysis is the integration step. The governing equations must be solved in order to reach a solution within CFD. They are then applied to a suitable model of the flow. The governing equations are:

- The conservation of mass (continuity)
- Newton's second law (momentum)
- The conservation of energy (energy)

These can be defined by the complete Navier-Stokes equations:

Continuity:

$$\frac{\partial \rho}{\partial t} + div(\rho \mathbf{u}) = 0 \tag{4.2.1}$$

x-momentum:

$$\frac{\partial(\rho u)}{\partial t} + div(\rho u \mathbf{u}) = -\frac{\partial p}{\partial x} + div(\mu grad\, u) + S_{Mx} \tag{4.2.2}$$

y-momentum:

$$\frac{\partial(\rho v)}{\partial t} + div(\rho v \mathbf{u}) = -\frac{\partial p}{\partial y} + div(\mu grad\, v) + S_{My} \tag{4.2.3}$$

z-momentum:

$$\frac{\partial(\rho w)}{\partial t} + div(\rho w \mathbf{u}) = -\frac{\partial p}{\partial z} + div(\mu grad\, w) + S_{Mz} \tag{4.2.4}$$

Energy:

$$\frac{\partial(\rho i)}{\partial t} + div(\rho i \mathbf{u}) = -p\, div\, \mathbf{u} + div(k\, grad\, T) + \Phi + S_i \tag{4.2.5}$$

These are a set of non-linear partial differential equations where $div\, \mathbf{u} = 0$ can be written in longhand notation as $\frac{\partial u}{\partial x} + \frac{\partial v}{\partial y} + \frac{\partial w}{\partial z} = 0$. S_{Mx}, S_{My}, S_{Mz} and S_i are the x, y, z momentum and internal energy source terms respectively, Φ is the dissipation function. There are 5 equations with six unknown flow field variables. In many aerodynamic cases the fluid is described as a perfect gas where $p = \rho RT$. This provides the sixth equation but introduces a seventh unknown T so $i = C_v T$ is required to compute the system of equations.

Due to the similarities in each of the governing equations the above can be written in the following general form:

$$\frac{\partial(\rho\phi)}{\partial t} + div(\rho\phi\mathbf{u}) = div(\Gamma\, grad\, \phi) + S_\phi \tag{4.2.6}$$

Where ϕ is a general term describing the conservation terms, and can be set as 1, u, v, w or i giving a special set of Equations 4.2.1 to 4.2.5. Γ is the diffusion coefficient. This general equation can be integrated over a three-dimensional control volume (CV):

$$\frac{\partial}{\partial t}\left(\int_{CV} \rho\phi dV\right) + \int_A \mathbf{n}\,.\,(\rho\phi\mathbf{u})dA = \int_A \mathbf{n}\,.\,(\Gamma\, grad\, \phi)dA + \int_{CV} S_\phi dV \tag{4.2.7}$$

n is a vector normal to the control volume surface.

The relationship in Equation 4.2.6 can be described in words as:

Rate of increase of ϕ inside the control volume + Net rate of decrease of ϕ due to convection across the control volume boundaries = Net rate of increase of ϕ due to diffusion about the control volume boundaries + Net rate of creation of ϕ inside the control volume.

The complete Navier-Stokes equations are used for all fluid flow in computational fluid dynamics, it is the boundary conditions applied which dictate what the final solution will be. The boundary conditions used for this research are described in more detail in Section 4.2.2.3.

4.2.1.2 Turbulence Modelling

In the majority of engineering applications, turbulence is of interest as there is a need to either encourage or reduce turbulent flows or simply analyse whether turbulence is present to identify the implications of any turbulence present in the flow. Turbulence modelling in CFD has been used in the literature to analyse noise from wind turbines or aerofoils and a summary of this work has been given in Section 4.1.2.2. Turbulence is of particular interest for the current research as it is directly related to any aerodynamic noise production. It will be used in this work for analysing where noise is likely to occur around 2D sections of a micro turbine blade. Results from the analysis will be compared to the noise measurements and results of the studies of the psychological and health impacts of small wind systems to achieve the objectives of the research.

Turbulence modelling in CFD can be split into four key methods and each has its own capabilities and limitations. When deciding which method to use several things must be considered, such as the physics encompassed in the flow, established practice for the type of problem, the level of accuracy required, the available computational resources and the time available for the simulation. For more information about the methods the reader is referred to the Fluent Theory Guide [124] and reference text books [121], for information they are outlined briefly below:

- Direct numerical simulation (DNS) - solving the complete Navier-Stokes equations directly, the whole turbulence spectrum is resolved so this method has a prohibitively high cost and will not be used for this research.
- Large eddy simulation (LES) - a portion of the turbulence scale is resolved. Any turbulent eddies larger than the smallest grid size will be resolved so the grid size must be sufficiently small to capture all the turbulence which is of interest. LES carries a high computational cost if the boundary layer must be fully resolved and therefore will not be used in the current research. LES is used widely in academia and a number of the current research papers in the literature have been outlined in Section 4.1.2.2.
- Detached eddy simulation (DES) - a hybrid model which compares the turbulence length scales with the grid size and switches between RANS and LES mode as required. The DES model still has a comparatively large computing cost compared to RANS methods so will not be used for this research.
- Reynolds-averaged-Navier-Stokes (RANS) - averaging procedures are applied to filter out the turbulence spectrum. RANS models simplify the problem by eliminating all turbulence structures in the flow. The velocity and pressure fields are also averaged. This requires additional equations because unknowns are introduced in the form of the Reynolds stresses. There are a number of RANS methods available, the k-ε model, the k-ω model and the Reynolds Stress Equation model. For more information about these methods the reader is referred to the Fluent Theory Guide [124] and reference textbooks [121]. It is important to choose the most practical option for the model.

Having considered all the turbulence modelling options available within Fluent, their relative merits and drawbacks, computational cost and relevance to the research in question, it has been decided that the SST k-ω (shear stress transport) model is the most applicable for modelling air-flow around a turbine blade section. The k-ω model is appropriate for the research because it is equipped to deal with flow separation and hence aerodynamic flows. However the solution of the standard k-ω model has a strong sensitivity to the free stream values of k and ω. The SST k-ω is recommended to overcome these sensitivities, it was developed to blend the accurate formulations of the standard k-ω model in the near wall region with the free-stream independence of the k-ε model in the far field. It is accurate in predicting the details of the wall boundary layer as it uses the enhanced wall treatment as default (for information on wall treatments for the SST k-ω model see Section 4.2.1.3). For more information on the k-ω SST model the reader is referred to Appendix H.

The k-ω SST model is the method which will be used for this research and any later description of the CFD theory and the model setup will be given in terms of this model.

4.2.1.3 Wall Functions

Turbulent flows are significantly affected by the presence of a wall; i.e. in the current research an aerofoil surface. The mean velocity field is affected by the no slip condition where the velocity is zero at the wall. The turbulence is also affected by factors such as the production of turbulent kinetic energy due to large gradients in the mean velocity at the outer parts of the near wall region. The near-wall region can be split into the viscous sublayer (closest to the wall) and a fully-turbulent layer furthest from the wall with an interim layer where the effects of molecular viscosity and turbulence are equally important, known as the buffer layer.

$$y^+ \equiv \rho u_\tau y/\mu \tag{4.2.8}$$

Where $u_\tau = \sqrt{\frac{\tau_w}{\rho}}$ and is the friction velocity, $y^+ = 5$ to the edge of the viscous sublayer and $y^+ = 60$ at the start of the outer fully turbulent region. The fully turbulent region is also known as the log-law region.

There are two approaches to modelling the near wall region, wall function approaches where a semi-empirical formula is used to bridge the region between the wall and the fully turbulent regions, and near-wall modelling approach where the near wall region is fully resolved to the wall. Wall functions are known to deteriorate under refinement of the grid in the normal wall direction and y^+ values below 15 will result in errors to the wall shear stress and heat transfer values. For this reason advanced y^+ independent formulations (Enhanced Wall Treatment) have been developed to overcome this.

The Enhanced Wall Treatment is the least sensitive to y^+ values and gives the most consistent wall shear stress and wall heat transfer predictions. It is automatically implemented at wall boundaries when using the SST k-ω model.

In Fluent, the value of ω at the wall is:

$$\omega_w = \frac{\rho(u*)^2}{\mu}\omega^+ \tag{4.2.9}$$

Where analytical solutions are available for both the laminar sublayer:

$$\omega^+ = \frac{6}{\beta_i (y^+)^2} \tag{4.2.10}$$

And in the logarithmic region:

$$\omega^+ = \frac{1}{\sqrt{\beta_\infty *}} \frac{du^+_{turb}}{dy^+} \tag{4.2.11}$$

The wall treatment is defined so the k-ω model switches automatically from the viscous sublayer formulation to the logarithmic layer formulation based on y^+ (depending on the grid), providing blending and a grid independent solution. Even with enhanced wall functions a sufficient number of cells must be used within the boundary layer rather than adhering to strict y^+ values.

4.2.2 Model Setup

In the following Sections the model setup within Fluent, the assumptions made, the boundary conditions as well as the discretisation and solution schemes chosen will be given.

4.2.2.1 Assumptions

In order to use CFD for the analysis of the airflow around a turbine blade it is always necessary to make a number of assumptions, this is because the theory behind CFD is based on the governing equations, where initial values must be set and the scheme for discretisation and solution of the model must be stated.

- Steady-state vs transient - initially steady-state cases will be run. If in any of the steady-state cases, there is an indication that transience is occurring, such as vortex shedding, all cases will be run as transient as well as steady-state, then comparisons between the cases will be made to identify any differences or similarities.
- Pressure-based vs density-based - the two solvers available in Fluent are the pressure-based and the density-based solvers. The pressure-solver has traditionally been used for incompressible or low compressibility flows whereas the density based for high speed compressible flows. As the flow around a turbine blade is incompressible the pressure-based solver will be used for the research. More details about the pressure-based solver will be given in Section 4.2.2.2.
- Turbulence model - there are a number of turbulence models within Fluent, each with its own merits and drawbacks, the SST k-ω model has been chosen for this research. Details of why this model has been chosen has been given in Section 4.2.1.2.
- Boundary conditions - all CFD problems are defined in terms of initial and boundary conditions. Details of the boundary conditions chosen for the current research are given in Section 4.2.2.3.
- Solution methods - there are a number of solution methods available for the pressure-velocity coupling, spatial discretisation and temporal discretisation (where transient cases are run). A detailed description of the methods available and those chosen for the current research as well as other important solution settings is given in Section 4.2.2.4.
- Grid - it is necessary to create a grid for simulations within Fluent. This is done with the meshing software Ansys ICEM. A full mesh independence check will be carried out to verify that mesh independence has been reached. Details about the grid and mesh independence check are given in Section 4.2.3.

- Verification vs. validation - verification is the process of determining that a model implementation accurately represents the developer's conceptual description of a model i.e. the governing equations are solved correctly. Validation is the process of determining the degree to which the model is accurate in its representation of the real world where full experimental results are available to compare with the CFD results. In this research, validation is not possible as detailed experimental results for the airflow around a turbine blade are not available for the aerofoil type in question. Therefore verification of the model will be carried out with a full mesh independence check, details of which are given in Section 4.2.3.4.

4.2.2.2 General Settings

The general settings for the CFD model within Fluent are as follows:

- The model is checked for anything which may cause problems in running the simulation and scaled so the units in Fluent correspond to those for which the mesh was created in ICEM.
- Gravity settings,
  - Gravity settings are based on the pitch angle of the blade section, the rotational speed and the wind speed for the case. Details of the gravity settings for each case and how these values are determined are given in Section 4.2.3.
- Pressure-based solver,
  - There are two algorithms available under the pressure-based solver within Fluent, these are the segregated solver and the coupled solver. For the segregated solver the governing equations are solved sequentially, in the coupled algorithm they are solved simultaneously. Although the coupled algorithm improves the convergence speed over the segregated algorithm it is also much more computationally expensive. For this reason the segregated solver will be used for this research.
- A steady-state or transient solver is selected depending on the simulations being run. Details of the calculation set up for steady-state and transient solutions are given in Section 4.2.2.4.

4.2.2.3 Boundary Conditions

It is necessary to define the boundary conditions and cell zones for the model. The cell zone condition for the entire domain is a fluid condition with the fluid as air. The options available within Fluent for the boundary conditions are inlets, outlets, walls, pressure, symmetry and periodic boundaries. In the domain created for this research, inlets and outlets at the domain boundaries are present and the surfaces of the aerofoil being modelled are treated as walls. There are a number options for each of these boundary types and those which should be used depends on the type of flow and the known values at the boundaries. The best options available for each boundary for the current model have been tested and based on the results the following boundary types will be used to run the mesh independence check and all subsequent models:

- All boundaries of the domain are treated as velocity-inlets because the aerofoil is considered as travelling through a region of air moving at a given velocity with the same turbulence throughout the region. Setting all boundaries as velocity-inlets eliminates any disturbances at the outer regions of the domain where the boundaries meet. The turbulence intensity for all boundaries is set as 10% with length scale 10mm. The length scale is chosen based on the size of micro and small wind turbine blade sections. The magnitude and direction of the velocity at the boundaries depends on the model. The specific values for each simulation are given in Tables 4.2.3 and 4.2.4 in Section 4.2.3.4. The other inlet/outlet boundary types available in Fluent are not suitable for open, incompressible flows where the magnitude of the static and total pressures are unknown and hence could not be used for this research.
- Aerofoil Walls- the aerofoil walls are set as stationary no slip walls, with wall roughness set with the default values. As the k-ω model is used for this research the Enhanced Wall Treatment is the default setting.

4.2.2.4 Solution Methods

In the following Sections the settings for running the simulations will be discussed. The choices for the pressure-velocity coupling method and spatial discretisation solution schemes will be given as well as the monitor settings and information about initialising the solution. The calculation settings will also be given.

Pressure-Velocity Coupling Method There are several algorithms available for solving the pressure-velocity coupling equation (for a full description of these algorithms and how they are implemented, the reader is referred to the Fluent User's Guide [123]). The SIMPLEC[3] algorithm with 0 skewness correction will be used for all steady-state simulations. This is because the mesh is not highly skewed and the SIMPLEC algorithm may help to achieve convergence quickly. The PISO[4] algorithm will be used for transient cases where necessary as this is the algorithm recommended for transience by the Fluent User's Guide [123] as it can maintain a stable calculation with a larger time step and an under-relaxation factor of 1.0 for both momentum and pressure.

Spatial Discretisation

[3] **S**emi-**I**mplicit **M**ethod for **P**ressure **L**inked **E**quations **C**onsistent
[4] **P**ressure-**I**mplicit with **S**plitting of **O**perators

Gradient There are three gradient options in Fluent, Green-Gauss cell based, Green-Gauss node based and Least squares cell based. The gradients are required to calculate values of the scalar ϕ at the cell faces and for computing secondary diffusion terms and velocity derivatives. The Green-Gauss cell based calculates the face values of a cell based on the average of the values at the neighbouring cell centre. The node based approach will calculate the face values based on the average of the nodal values on the face. While the node based method is more accurate it is much more computationally expensive. The least squares method assumes that solution values will vary linearly between cells. The accuracy of this method is comparable to the node based method but much less computationally expensive. It is therefore the default and the method which will be used for all simulations.

Pressure The default scheme in Fluent interpolates the pressure values at the faces of the mesh using the momentum equation coefficient. There are several pressure interpolation schemes available, however the "standard scheme" is acceptable for the current research and is the one which will be used for all simulations.

Momentum Fluent stores discrete values of the scalar ϕ at cell centres, however face values ϕ_f are required for convective terms and must be interpolated far from the cell centres. Upwinding means that the face values are derived from the quantities in the cell upstream. There are a number of methods available within Fluent to do this. The second-order upwind algorithm will be used for momentum spatial discretisation as there is increased accuracy with this scheme.

Turbulent Kinetic Energy As with the momentum spatial discretisation scheme, the second-order upwind algorithm will be used for turbulent kinetic energy spatial discretisation.

Specific Dissipation Rate As with the momentum spatial discretisation scheme, the second-order upwind algorithm will be used for specific dissipation rate spatial discretisation.

Transient Formulation For transient simulations, discretisation in both space and time is required. The second-order implicit scheme will be used as it provides improved accuracy and is suitable for the problem.

Monitors For the k-ω turbulence model, the usual scalars are monitored which are continuity, x-velocity, y-velocity, k and ω with a convergence criteria set equal to 10^{-6}, for transient cases the convergence criteria is set lower at 10^{-10}. A model is considered to be fully converged when the difference in the values of the monitored scalars between iterations is lower than the convergence criterion. The convergence criterion values are low enough so the solution converges to its final condition. The moment at the aerofoil wall as well as surface monitors of the sum of the wall shear stress at the wall are also monitored. This is another way to show that the solution has converged to its final condition.

Initialisation The solution is initialised to compute the solution from the values set at the velocity inlet. For example, to use the velocity magnitude and direction at the velocity inlet boundary as a starting point for the whole calculation. The specific values for each model are given in Tables 4.2.3 and 4.2.4 in Section 4.2.3.4.

Calculation Activities and Settings In order to run the calculations the calculation activities and settings must be defined. The settings for steady-state and transient cases are described below:

- Steady-state
  - All steady state cases are run for 50,000 iterations, this allows the solution to fully converge to its final condition and all steady state cases can be compared.
  - All data is saved every 250 iterations.
  - Images of the turbulent kinetic energy contours close to the aerofoil wall are saved every 200 iterations so an animation of the information can be saved during post processing.
- Transient - for transient cases a time step size and number of time steps must be specified.
  - The time step size is based on the velocity of the flow and the smallest cell size in the mesh in the x-direction as $time\ step\ size = \frac{velocity}{smallest\ cell\ size}$. Table 4.2.1 shows the values used to calculate the time step size.
  - The number of time steps required so that the flow passes through the domain 3 times is calculated as $time\ to\ pass\ domain = \frac{domain\ length}{x{-}velocity\ component}$, the number of time steps is then equal to $number\ of\ timesteps = \frac{time\ to\ pass\ domain}{time\ step\ size}$. Table 4.2.1 shows the values used to calculate the number of time steps.
  - 30 iterations per time step are carried out
  - The simulation is run for 2000 iterations steady state, then switched to the transient calculation settings
  - Data is saved every 5 time steps

Span (%)	x-vel. Rated (m/s)	x-vel. Cut-In (m/s)	Smallest Cell (mm)	Time Size Step Rated (s)	Time Size Step Cut-In (s)	Domain Length (m)	Time to Pass Domain Rated (s)	Time to Pass Domain Cut-In (s)	No. Time Steps for 3 Passes
15	25.820	7.569	1.00	3.87e-5	1.32e-4	4.26	0.17	0.56	12771
20	29.548	8.704	0.92	3.11e-5	1.06e-4	3.88	0.13	0.45	12647
25	33.319	9.851	0.86	2.58e-5	8.73e-5	3.53	0.11	0.36	12322
50	52.576	15.694	0.61	1.16e-5	3.89e-5	2.25	0.04	0.14	11039
90	84.149	25.210	0.46	5.47e-6	1.82e-5	1.39	0.02	0.06	9071

Table 4.2.1: Values used to calculate the time step size and number of time steps for transient simulations at rated and cut-in wind speeds

In the next and final part of the Methodology Section of this Chapter, full details of the physical background of the model will be given including details of the mesh independence check carried out to verify the model.

4.2.3 Physical Background of the Model

In the following Sections details of the physical background of the model will be described. This includes details of the wind turbine blade chosen for analysis, construction of the mesh, obtaining mesh independence and the final mesh choice.

4.2.3.1 Blade Selection

The blade of a micro turbine type M1 (see Table 1.3.1 in Section 1.3) was modelled in Fluent in 2D. This blade was chosen as it is the turbine type installed at all micro installation sites where environmental noise measurements have been taken. This means that comparisons can be made between results from the CFD modelling, the measured noise levels and the sounds identified from the micro installations by individuals living nearby as reported from the questionnaire results.

Micro Turbine M1 Blade Details Figure 4.2.1 shows the full 3D aerofoil as would be mounted on the micro turbine type M1 used for this research. The aerofoil is a standard Eppler E387 blade of length 767.5mm (875mm from origin when mounted on hub). The turbine rotates clockwise, hence in the negative y axis with a positive twist from root to tip. Figure 4.2.2 shows top, side and end views of the blade.

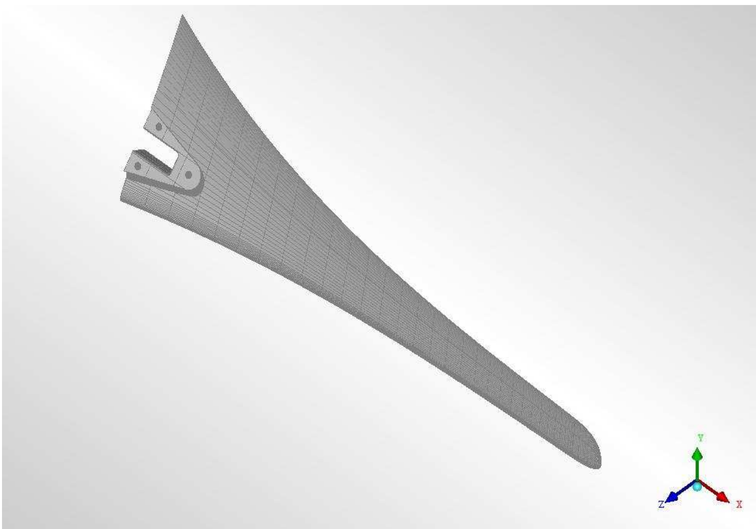

Figure 4.2.1: Full isometric A600 aerofoil

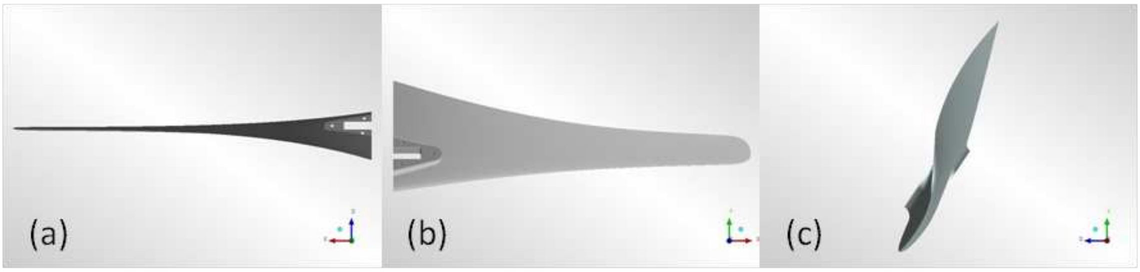

Figure 4.2.2: 2D views of A600 aerofoil; (a) Top (b) Front (c) End

4.2.3.2 Case Geometry

In order for the 2D computational fluid dynamics analysis to take place cut planes were extracted at various percentage spans. Figure 4.2.3 shows the cut planes at varying percentage spans of the aerofoil. Not all of the cut planes in the figure were used for the research. Details of the chord lengths and the pitch angle at each cut plane used is shown in Table 4.2.2. For each percentage span the cut plane was rotated and translated to be placed at a 0 degree angle of attack with the origin at the leading edge. This aids setup of the model in Fluent later where a resultant angle of attack can easily be applied taking into account the wind speed, rotational speed of the blade associated with this wind speed and the pitch angle at the percentage span of the cut plane so the resultant air flow acts in the +ve x-direction.

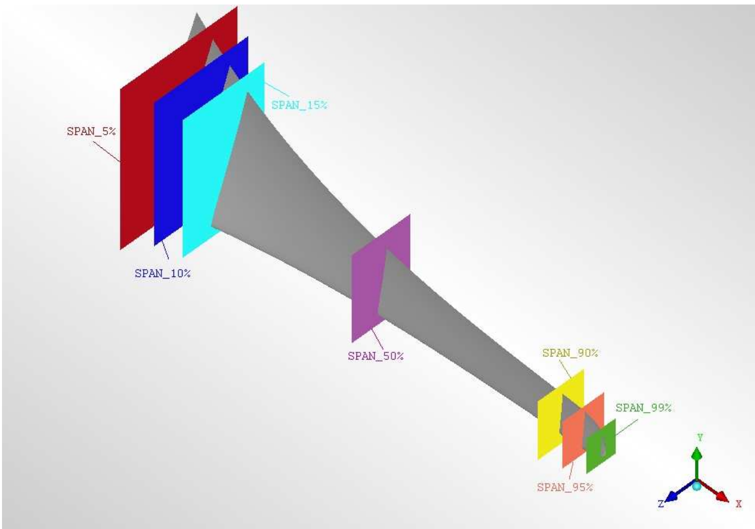

Figure 4.2.3: Cut Planes for the aerofoil geometry

% Span	Chord Length (mm)	Pitch Angle (degrees)	Span from Origin (mm)	Multiplier for Domain Size		Min (mm)		Max (mm)	
				Rad.	Down	X	Y	X	Y
15	197.91	17.21	222.625	7.5	15	-1287	-1485	2970	1485
20	180.39	15.54	261.000	7.5	15	-1173	-1353	2706	1353
25	164.29	13.96	299.375	7.5	15	-1068	-1232	2464	1232
50	104.40	7.57	491.250	7.5	15	-679	-783	1566	783
90	64.59	3.34	798.250	7.5	15	-420	-484	969	484

Table 4.2.2: Table showing % Span Mesh Domain Setups

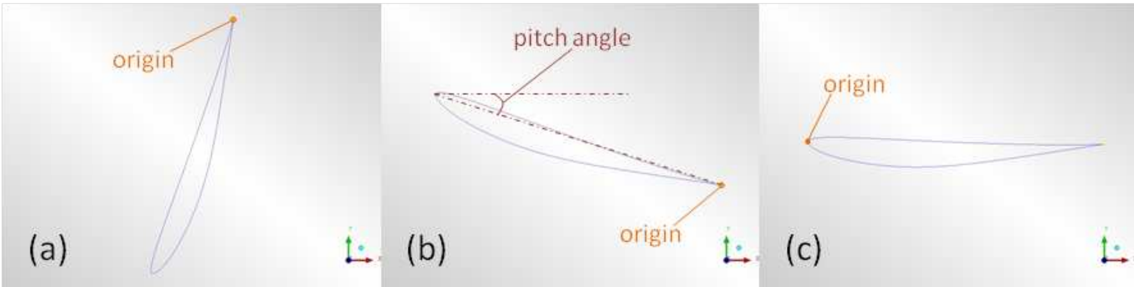

Figure 4.2.4: Cut plane: (a) Original (b) Rotated 90º (c) Rotated and translated to 0º with origin at leading edge

In order to work out the magnitude and the components of direction of the resultant air flow over the aerofoil cut planes, the resultant angle of attack must be determined based on the pitch angle of the 2D cut plane (see Figure 4.2.4(b) for definition of pitch angle), the rotational speed and the wind speed. A diagram showing how the magnitude and direction of the air flow is calculated is shown in Figures 4.2.5 and 4.2.6. Cases will be run for the wind turbine in two conditions, at cut-in wind speeds and rated wind speeds. The magnitude and direction for all cut planes at rated wind speed and rotational speed is shown in Table 4.2.3. Values for all cut planes at cut-in wind speed and rotational speed are shown in Table 4.2.4. The resultant magnitude and direction of the air flow over each cut plane will be used to set the boundary conditions at the domain boundaries for each case. For the remainder of this Chapter (the methodology, results and discussion Sections) each case will be referred to with a specific notation. For example, the 15% span rated case refers to the aerofoil section at 15% of the distance from the hub to the tip, at rated wind speeds. Similarly, the 15% span cutin case refers to the aerofoil section at 15% of the distance from the hub to the tip but at cut-in wind speeds. The same notation is used for all percentage distances from the hub to the tip (see Figure 4.2.3).

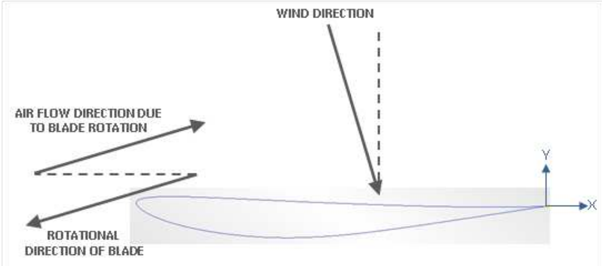

Figure 4.2.5: Diagram showing the wind and rotational directions of the blade based on the pitch angle of cut plane

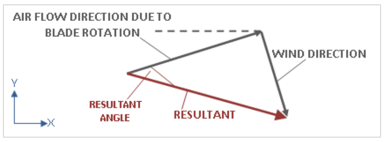

Figure 4.2.6: Diagram showing how magnitude and direction of air flow is determined

Span (%)	Dist. from Origin (m)	Circ. (m)	Blade Vel. (m/s)	Pitch Angle (º)	Resultant Air Speed (m/s)	Angle (º)	Total Angle (º)	Magnitude x	Magnitude y	Gravity (m/s^2) x	Gravity (m/s^2) y
15	0.223	1.399	23.313	17.21	26.220	27.24	-10.02	0.985	-0.174	9.66	-1.71
20	0.261	1.640	27.332	15.54	29.850	23.70	-8.16	0.990	-0.142	9.71	-1.39
25	0.299	1.881	31.350	13.96	33.569	20.95	-6.99	0.993	-0.122	9.74	-1.19
50	0.491	3.087	51.444	7.57	52.825	13.13	-5.56	0.995	-0.097	9.76	-0.95
90	0.798	5.016	83.593	3.34	84.449	8.17	-4.83	0.996	-0.084	9.78	-0.83

Table 4.2.3: Table showing magnitude and direction of air flow at rated 12m/s wind speed and 1000rpm rotational speed for all cut planes

Span (%)	Dist. from Origin (m)	Circ. (m)	Blade Vel. (m/s)	Pitch Angle (º)	Resultant Air Speed (m/s)	Angle (º)	Total Angle (º)	Magnitude x	Magnitude y	Gravity (m/s^2) x	Gravity (m/s^2) y
15	0.223	1.399	6.994	17.21	7.610	23.22	-6.00	0.995	-0.105	9.76	-1.03
20	0.261	1.640	8.200	15.54	8.731	20.10	-4.56	0.997	-0.079	9.78	-0.78
25	0.299	1.881	9.405	13.96	9.872	19.69	-3.73	0.998	-0.065	9.79	-0.64
50	0.491	3.087	15.433	7.57	15.722	11.00	-3.43	0.998	-0.060	9.79	-0.59
90	0.798	5.016	25.078	3.34	25.257	6.82	-3.49	0.998	-0.061	9.79	-0.60

Table 4.2.4: Table showing magnitude and direction of air flow at cut in 3m/s wind speed and 300rpm rotational speed for all cut planes

4.2.3.3 Mesh Development

A mesh for the 2D CFD analysis was developed and checked for mesh independence. In order to carry out this task, the 15% span section was chosen and a domain was built around the aerofoil where the mesh density was varied for each mesh created. Details of the cut plane sizes for the 15% span section is shown in Table 4.2.2. The domain size was based on the chord length of each cut plane. The distance the domain extends downwind from the blade trailing edge is 15 times the chord length, with a hemisphere upwind of the cut plane trailing edge which has a radial multiplier of 7.5 times the chord length. The minimum and maximum x and y points for the domain and the downwind and radial multipliers for each cut plane are also shown in Table 4.2.2.

Two domain shapes were considered: the first was based on well developed CFD aerofoil blade theory, the second domain shape was an egg shaped mesh. It was found with the standard domain that it was not possible to achieve a satisfactory mesh, because at the outer part of the domain there was a large change in adjacent cell sizes in the x-direction at the aerofoil trailing edge. This is not acceptable in Fluent as it can create convergence problems. It was therefore decided that the egg shaped domain in Figure 4.2.7 would be used. The Figure shows that cell size gradients are evenly spread throughout the domain, thus changes in adjacent cell sizes are kept to a minimum. The new domain geometry also means that a higher density of cells around the aerofoil can be achieved with no detrimental effect to the adjacent cell sizes at the outer regions of the domain.

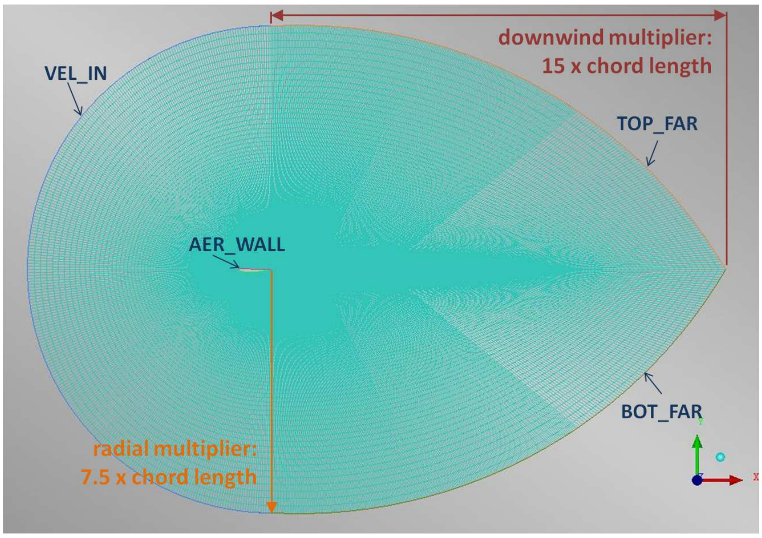

Figure 4.2.7: Egg Domain Shape for Mesh Development

4.2.3.4 Mesh Independence Check

A number of meshes were created with the egg shaped domain for the 15% span cut plane rated case in order to test for mesh independence. The node spacing along the boundaries and the cell densities for each mesh are shown in Table 4.2.5. Mesh independence checks were carried out and the best mesh for the final case was chosen. The node spacings of the final mesh choice were then applied to all percentage span 2D blade sections. Details for how the mesh independence check was carried out is found in this Section.

Mesh No.	Edge Counts				Total Elements	Edge Setup							
						Radial				Downwind Block Node Count			
	AER_ WALL	BOT _FAR	TOP _FAR	VEL _IN		Nodes	Type	Spacing	Ratio	1	2	3	4
1	225	197	197	224	46595	75	Exp2	1.500	2	75	75	50	75
2	285	272	272	284	124505	150	Exp2	0.750	2	100	100	75	150
3	404	347	347	404	165125	150	Exp2	0.750	2	125	125	100	150
4	285	272	272	284	124505	150	Exp2	0.250	2	100	100	75	150
5	285	272	272	284	124505	150	Exp2	0.100	2	100	100	75	150
6	285	397	397	284	162005	150	Exp2	0.100	2	150	150	100	150
7	285	272	272	284	124505	150	Exp2	0.075	2	100	100	75	150

Table 4.2.5: Table showing Egg Shape 2D Domain Mesh Setups

The 15% span cut plane rated case model was setup as described in Section 4.2.2, the boundary conditions at each of the domain boundaries were set as described in Section 4.2.2.3, the magnitude and direction of the air flow over the cut plane at the boundaries were set for the 15% span rated case as given in Table 4.2.3 in Section 4.2.3.2.

Each mesh model was run as a steady-state case for 25000 iterations. This allowed each case to converge to a satisfactory level, it also allowed comparisons between the meshes to identify whether mesh independence had been reached. The solver options were set as described in Section 4.2.2.4 and solution was initialised and monitored as also described in Section 4.2.2.4.

Once each of the mesh models had been run for 25000 iterations the following factors were examined to analyse whether mesh independence had been achieved:

- Contours examined for:
  - Pressure
  - Velocity
  - Turbulence
- Maximum and minimum values throughout the domain for:
  - Dynamic pressure
  - Velocity magnitude
  - Surface wall shear stress

  - Turbulence intensity

- Turbulent kinetic energy plotted along five lines in the aerofoil region (see Figure 4.2.8 for the locations of the lines in the domain)

  - The turbulent kinetic energy was plotted along the length of each of the lines, with the distance along the line on the x-axis and the magnitude of the turbulent kinetic energy on the y-axis. By plotting the results along the lines for different numbers of iterations, it has been possible to see whether the solution for each mesh is fully converged.

Although all of the contours and plots as above were investigated, only the contours and plots of the turbulence values will be given here as these are of most interest for the current research and are sufficient to ascertain whether mesh independence has been achieved.

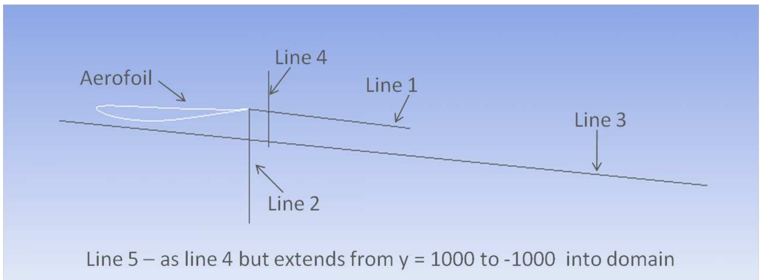

Figure 4.2.8: Lines for x-y plots in the domain

The ranges of values of dynamic pressure, velocity magnitude, surface wall shear stress and turbulence intensity are shown in Table 4.2.6. From the results it is evident that there is some variation in values for the different mesh densities. It can be seen from these values that the minimum and maximum values of dynamic pressure for meshes 1, 2 and 3 are vastly different than for the other meshes. These are the coarsest meshes in terms of the radial node spacing. Mesh 1 also has the least number of elements (see Table 4.2.5 for mesh densities). The maximum values for velocity magnitude and surface wall shear stress and the minimum values for turbulence intensity are also vastly different to those for the other meshes.

Mesh Number	Dynamic Pressure (Pa)		Velocity Magnitude (m/s)		Surface Wall Shear Stress (Pa)		Turbulence Intensity (%)	
	Min.	Max.	Min.	Max.	Min.	Max.	Min.	Max.
EM1	0.182	951.96	0	39.42	0	5.123	3.094	19.645
EM2	0.049	1080.75	0	42.00	0	7.302	2.907	18.099
EM3	0.038	1385.87	0	45.55	0	9.074	2.740	16.817
EM4	0.015	1129.64	0	42.94	0	11.290	0.228	19.061
EM5	0.005	1176.88	0	43.83	0	18.845	0.050	20.871
EM6	0.005	1167.39	0	43.66	0	18.694	0.050	18.801
EM7	0.004	1173.73	0	43.78	0	21.604	0.032	19.485

Table 4.2.6: Comparison of value ranges for each egg shaped mesh after 25,000 iterations

The contour plots showing the turbulence intensity for all the mesh densities examined for mesh independence are shown in Figure 4.2.9. It can be seen in Figure 4.2.9 that the region behind the trailing edge for meshes 1, 2 and 3 looks much different for those of the remaining meshes, and it looks like there is some instability in the wake region for the finer meshes 4 to 7.

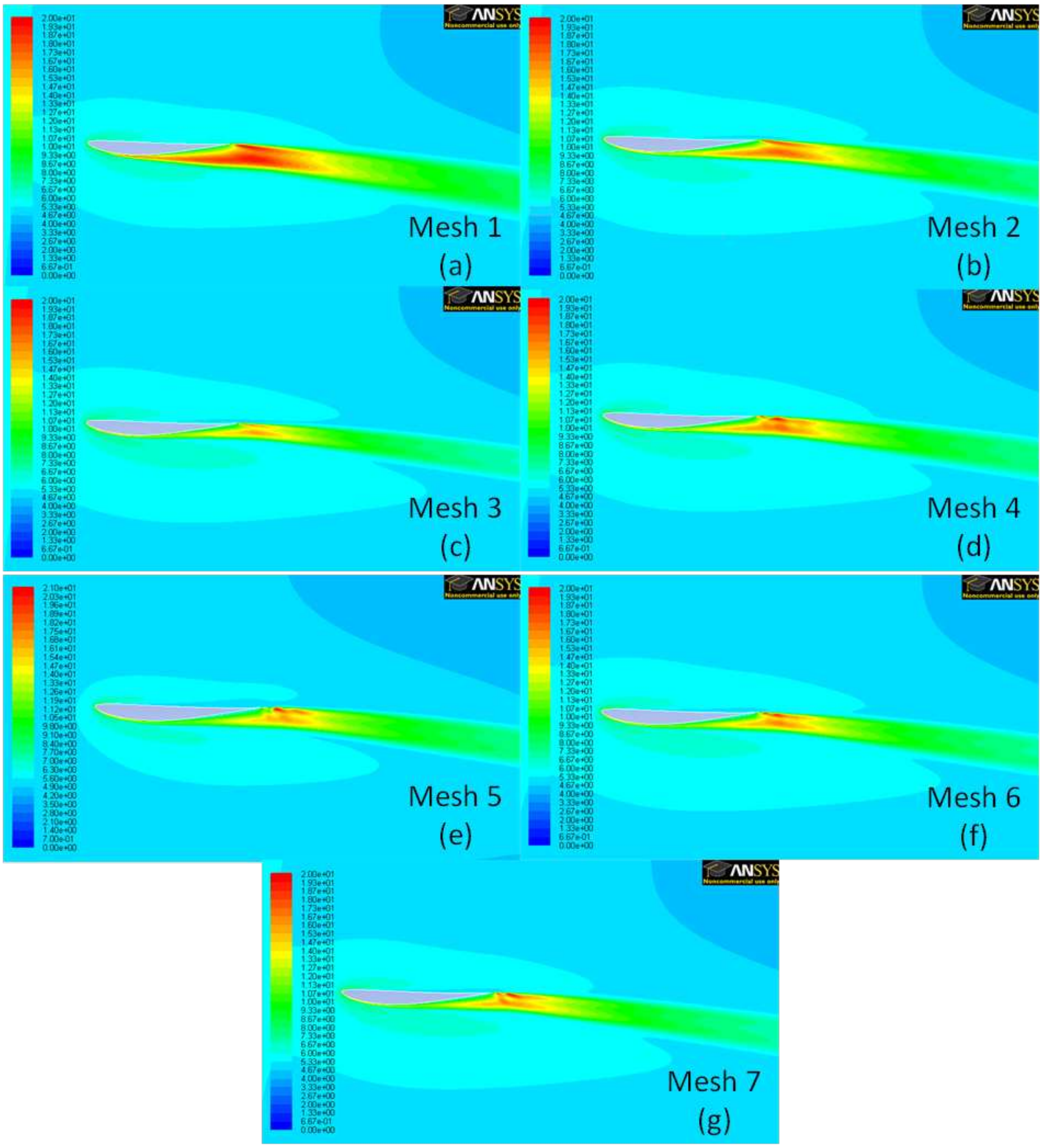

Figure 4.2.9: Contour plots showing turbulence intensity for all mesh densities

On examining the contours of the turbulence intensity and x-y plots of turbulent kinetic energy it is clear that vortex shedding occurs at the trailing edge for some of the meshes. Figure 4.2.10 shows contours of turbulent kinetic energy in the wake region for meshes 3 (a) and 7 (b). Figure 4.2.10 demonstrates that for the coarser meshes i.e. mesh 3 (a) vortex shedding does not occur, however for the finer meshes, i.e. mesh 7 (b) vortex shedding does occur at the trailing edge.

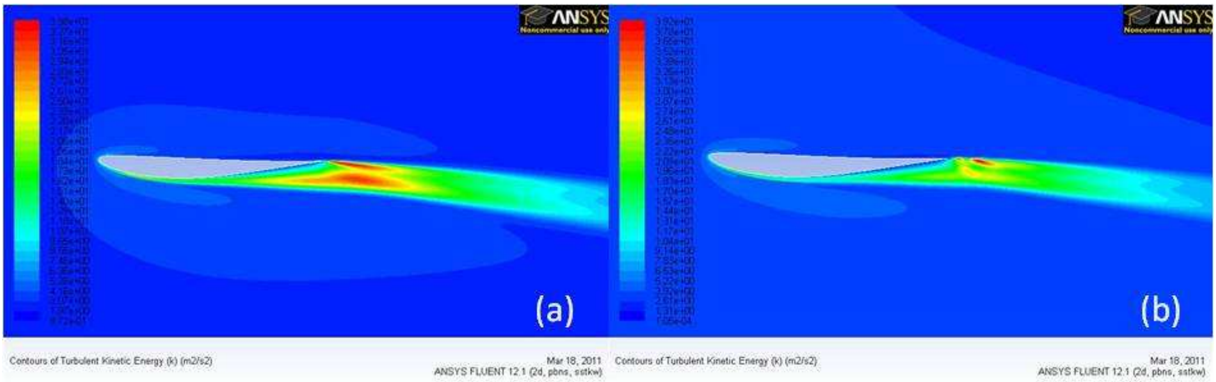

Figure 4.2.10: Comparison of turbulent kinetic energy contours for Mesh 3 (a) and Mesh 7 (b)

The x-y plots for turbulent kinetic energy reinforce this finding. Figure 4.2.11 (a-e) shows x-y plots of turbulent kinetic energy for each line in the domain for Mesh 3. The plots confirm that the solution is fully converged and that the data is the same for all the numbers of iterations plotted, i.e. shedding does not occur at the trailing edge.

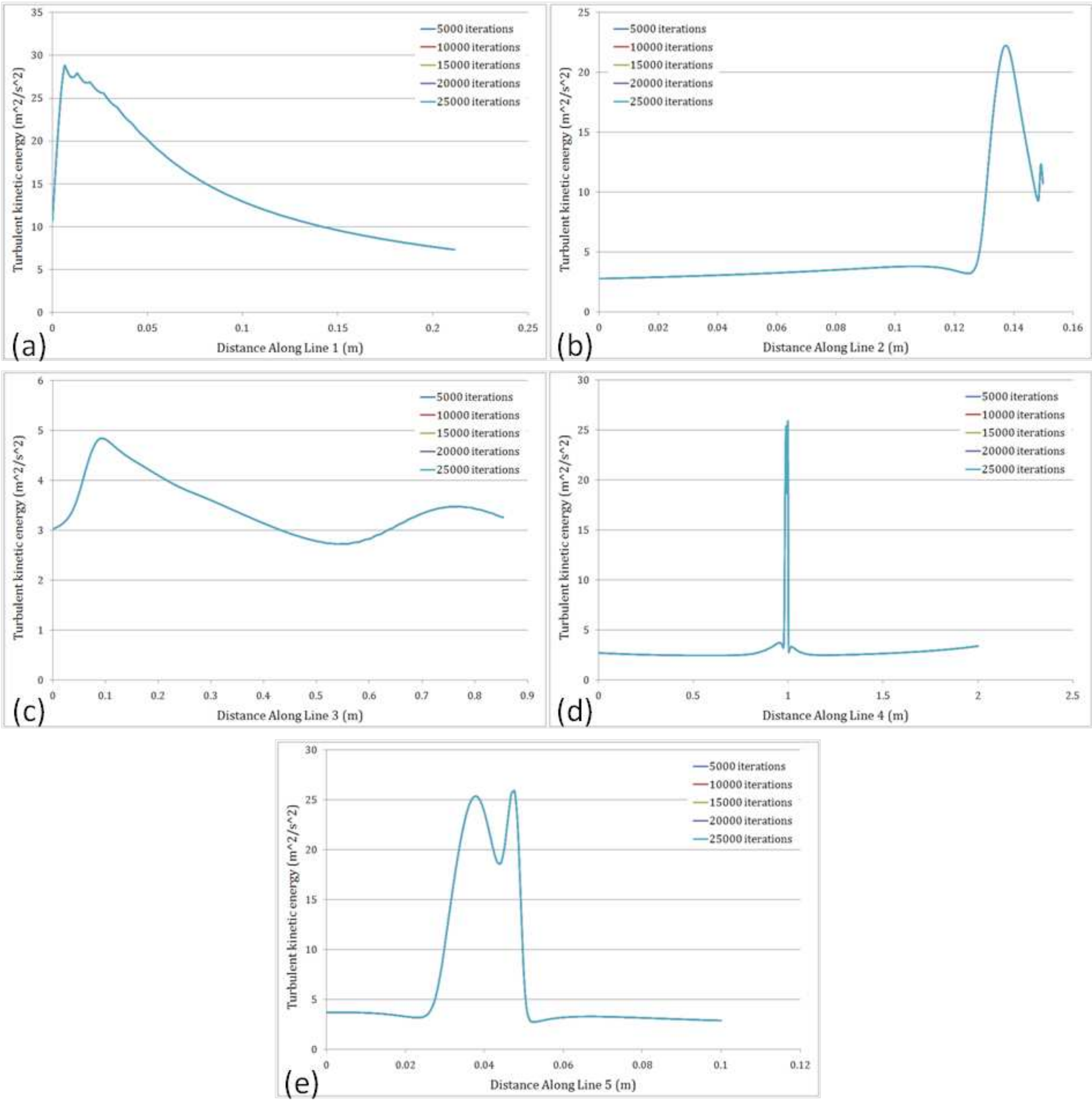

Figure 4.2.11: X-Y plots for each line in the domain for Mesh 3

Figure 4.2.12 (a-e) shows x-y plots of turbulent kinetic energy for each line in the domain for Mesh 7. Here, the data oscillates between maximum and minimum values for each iteration number plotted. This fact is especially clear looking at the x-y plots for line 1 and (Figure4.2.12a) line 5 (Figure 4.2.12e) as the turbulent kinetic energy values only vary close to the trailing edge within the wake where shedding is occurring. Away from the aerofoil wall, turbulent kinetic energy is the same for all iteration numbers, proving that although the magnitude of the turbulent kinetic energy oscillates close to the trailing edge, the solution is fully converged.

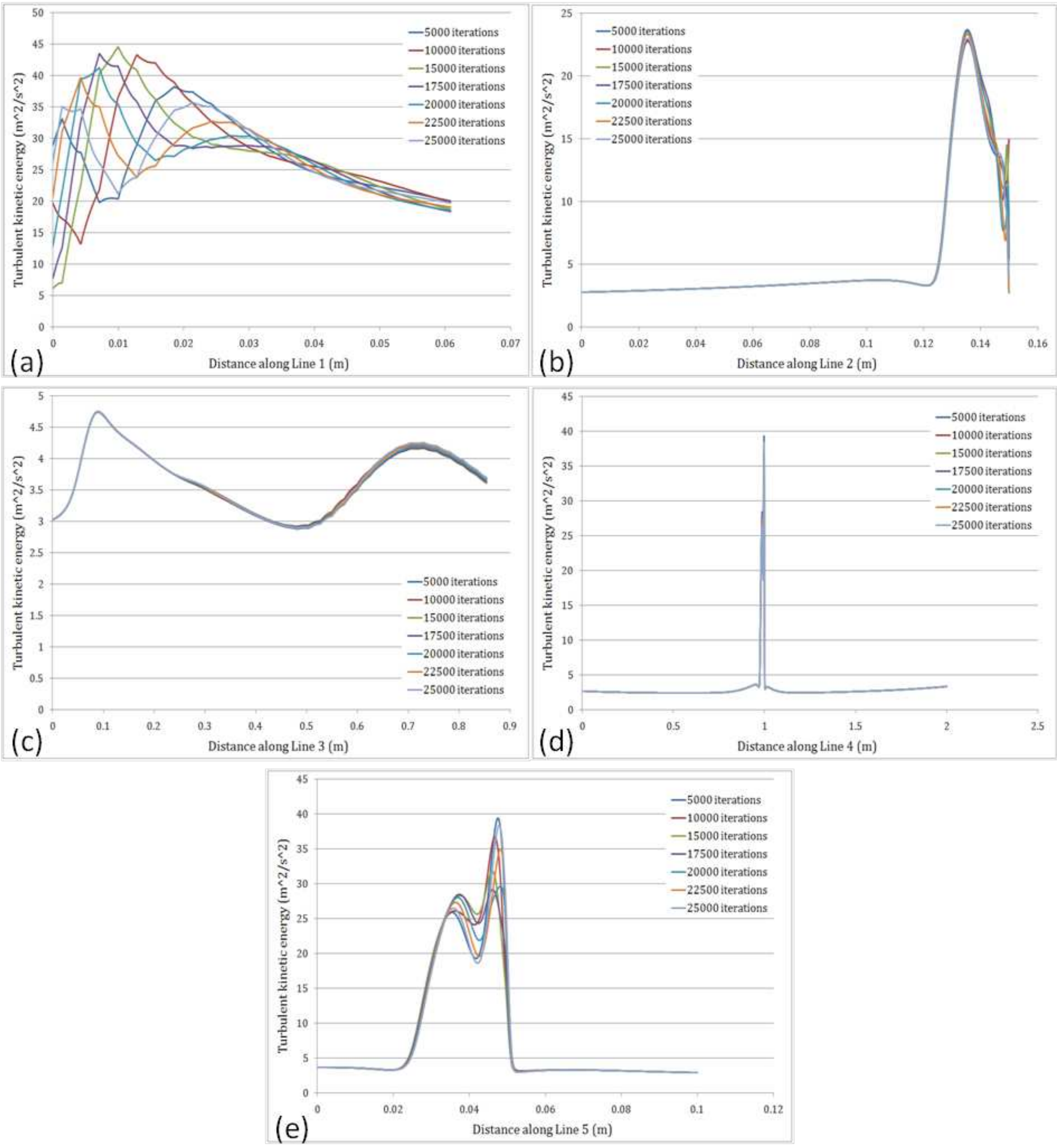

Figure 4.2.12: X-Y plots for each line in the domain for Mesh 7

The turbulence intensity contour plots in Figure 4.2.9 and x-y plots show that shedding does not occur for meshes 1, 2 and 3, the coarser meshes. It was therefore decided to rule out the use of the coarser meshes as it is clear that mesh independence had not been reached. The finer meshes 4, 5, 6 and 7 were then further examined to test for mesh independence.

On investigation of the turbulence kinetic energy x-y plots for the finer meshes, a maximum and minimum value for turbulence kinetic energy associated with shedding could be determined from the plots of line 1 (see Figure 4.2.13) and line 5 (see Figure 4.2.14), i.e. at what number of iterations did the maximum and minimum turbulent kinetic energy occur.

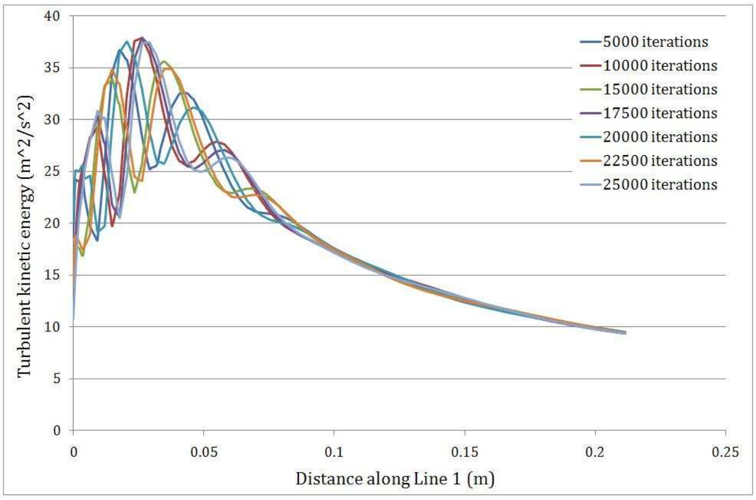

Figure 4.2.13: X-Y plot of turbulent kinetic energy for Mesh 4 along line 1

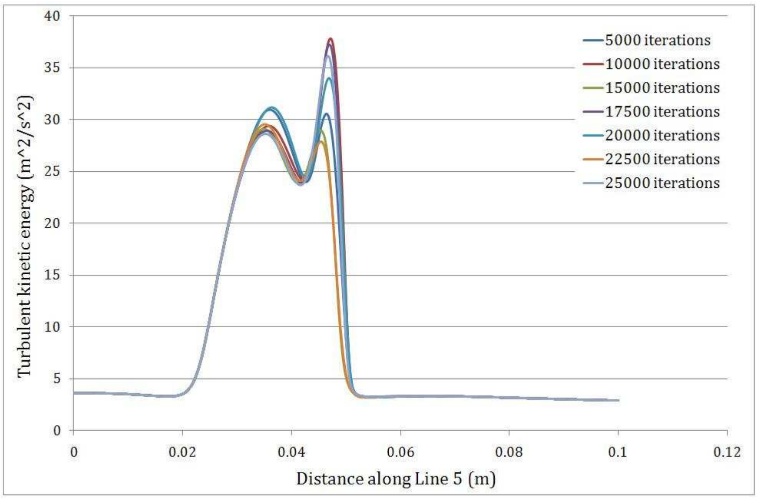

Figure 4.2.14: X-Y plot of turbulent kinetic energy for Mesh 4 along line 5

After determining the number of iterations for each mesh, the maximum and minimum values for dynamic pressure, velocity magnitude, surface wall shear stress and turbulence intensity were computed and are shown in Table 4.2.7. It is shown in the table that values for dynamic pressure, velocity magnitude and surface wall shear stress are not affected by the vortex shedding at the trailing edge and it is only the maximum value of turbulence intensity that changes. Values for all variables over all mesh densities are within an acceptable range of each other. Therefore, mesh 4 is the sufficient for the final analyses.

Mesh Number		Number of Iterations	Dynamic Pressure (Pa)		Velocity Magnitude (m/s)		Surface Wall Shear Stress (Pa)		Turbulence Intensity (%)	
			Min.	Max.	Min.	Max.	Min.	Max.	Min.	Max.
EM4	Max TKE	10000	0.015	1129.63	0	42.95	0	11.29	0.228	19.19
	Min TKE	22500	0.015	1129.66	0	42.95	0	11.29	0.228	18.71
EM5	Max TKE	25000	0.005	1176.88	0	43.83	0	18.85	0.050	20.87
	Min TKE	15000	0.005	1177.32	0	43.84	0	18.85	0.050	19.32
EM6	Max TKE	20000	0.006	1167.50	0	43.66	0	18.70	0.052	19.24
	Min TKE	25000	0.005	1167.39	0	43.66	0	18.70	0.050	18.80
EM7	Max TKE	15000	0.005	1173.24	0	43.77	0	21.59	0.032	21.09
	Min TKE	25000	0.004	1173.73	0	43.78	0	21.60	0.032	19.49

Table 4.2.7: Comparison of value ranges for each of the finer mesh at max. and min. TKE values for shedding

As shedding does occur at the trailing edge, it is evident that the solution should be treated as a transient solution. A mesh independence check was carried out by running transient cases for mesh numbers 4, 5 and 7. The method used for the transient mesh independence check was the same as the method for the steady-state mesh independence check. The calculation activities for transient cases have been outlined in Section 4.2.2.4. It was found that mesh 4 was also adequate for transient cases.

Therefore it was chosen that mesh 4 should be used for all cases and all models as it is the coarsest out of all the finer meshes within the acceptable range, hence would require the least computing cost. Steady-state and transient cases will be run at each percentage span to identify whether shedding does occur.

Details of all the CFD cases and the results of the analysis will be given in the following Section.

4.3 CFD Results

In this Section, results of the CFD analysis will be given. First a comparison between the steady-state and transient approaches will be given, followed by results of the rated and cut-in cases, focusing on the turbulence within the domain. This is because aerodynamic noise is directly related to turbulence about the walls of the aerofoil sections and noise is the focus of the current research.

4.3.1 Steady-State vs. Transient Cases

As outlined in Section 4.2.3, rated and cut-in cases were run with the steady-state approach for span distances from the hub of interest. Each case was run until the residual and monitor plots had reached convergence and all the plotted residuals and monitor lines had plateaued. Maximum and minimum values within the domain of velocity magnitude, turbulent kinetic energy, static pressure, dynamic pressure and wall shear stress were calculated at 25000, 40000 and the maximum number of iterations as a final check that convergence had been achieved. These values are given in Table I.0.1 in Appendix I. The evidence showed that all steady-state cases had converged to a satisfactory level.

During the mesh independence check, evidence of vortex structures were observed at the trailing edge in the wake region for the 15% span rated case. This indicates that a transient solution may be more appropriate. For this reason all cases were also run using the transient approach as described in Section 4.2.3 and compared to the steady-state results. The transient cases were run for sufficient time steps to allow the flow to have convected through the domain three times. Details for how many time-steps were needed for each case is given in Section 4.2.2.4.

As for the steady-state cases, the maximum and minimum values within the domain of velocity magnitude, turbulent kinetic energy, static pressure, dynamic pressure and wall shear stress were calculated for each of the three air passes through the domain. These values are given in Table I.0.2 in Appendix I. The evidence for the transient cases showed that each model was fully converged. Comparisons of the turbulent kinetic energy about the trailing edge between the steady-state and transient approaches for the 15% span and 20% span rated cases were carried out to identify whether there are any significant differences between the steady-state and transient approaches. The best approach for analysis of the remaining cases is determined from these comparisons.

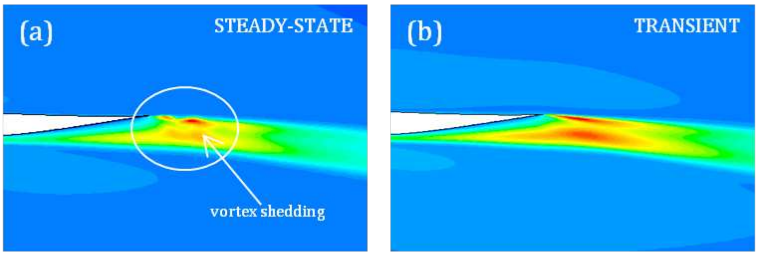

Figure 4.3.1: Comparison of steady-state (a) vs transient (b) turbulent kinetic energy contour plots for the 15% span rated case

Figure 4.3.1 shows that the 15% transient case did not show evidence of oscillating vortex structures at the trailing edge. The magnitude of the turbulent kinetic energy in the wake region behind the aerofoil trailing edge serves to give an indication of the differences between the steady-state and transient cases. The maximum turbulent kinetic energy occurs in the region behind the trailing edge for each case so an investigation of the maximum turbulent kinetic energy for all the cases gives an indication of how different the steady-state and transient cases are for the cut planes at each percentage span.

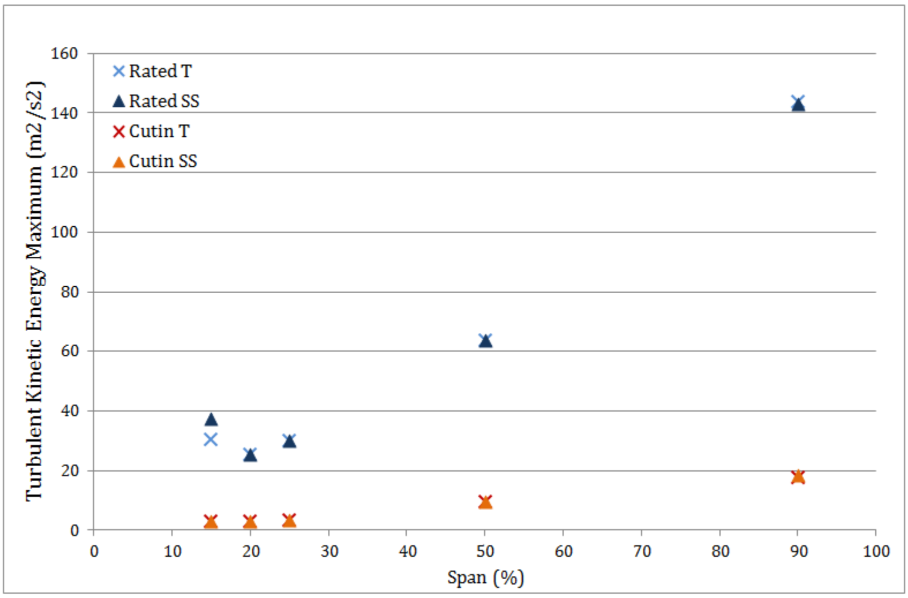

Figure 4.3.2: Graph showing the comparison between steady-state and transient results of max TKE for all cases

Figure 4.3.2 shows the magnitude of the maximum turbulent kinetic energy within the domain for each of the percentage span cut planes. Results are presented for the rated and cut-in cases using both the steady-state and transient approaches. It is noted from Figure 4.3.2 that the 15% rated case is the only case where the maximum turbulent kinetic energy is different for the steady-state and transient cases. This is a sign that evidence of vortex shedding is only observed for the 15% span rated case. The resultant angle of attack reduces very quickly at increasing distances from the hub (see Table 4.2.3) and it is expected that further from the turbine hub, vortex shedding will not occur, Figure 4.3.2 serves to prove this expectation. However, further verification has been sought by inspecting the 20% span rated case to check that there is no evidence of vortex structures.

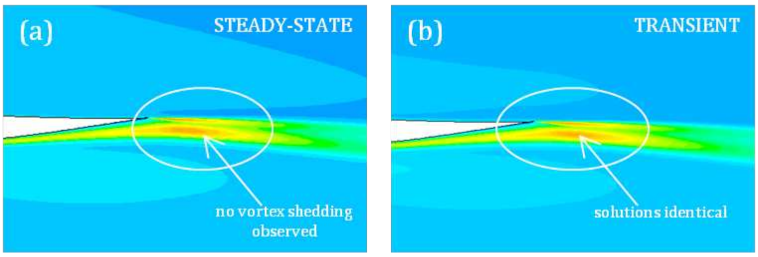

Figure 4.3.3: Comparison of steady-state (a) vs transient (b) for the 20% span rated case

The turbulent kinetic energy contours in the region behind the aerofoil trailing edge were examined for the steady-state and transient 20% span rated cases (see Figure 4.3.3(a) and (b) respectively). It was observed that vortex shedding does not occur at the trailing edge of the aerofoil for either approaches. This is due to the reduction in chord length from 198mm to 180mm as well as a reduction in resultant angle of attack from 10º to 8º and an increase in resultant aerofoil velocity further from the hub. For the 20% span rated case, the solution for the steady-state and transient cases are identical. This is proven from the contours of turbulent kinetic energy (see Figure 4.3.3) and the plot in Figure 4.3.2. The transient approach of modelling the flow comes at a high computational cost compared to the steady-state approach and except for the 15% span rated case, the transient and steady-state cases are identical. It was therefore decided that the steady-state results were satisfactory to describe the flow and further results are given only for the steady-state cases.

In the following Section comparisons are made between the rated and cut-in cases with a focus on the turbulence near the aerofoil wall. This is because turbulence is directly related to aerodynamic noise, the focus of this research.

4.3.2 Rated vs. Cut-In Cases

The maximum turbulent kinetic energy within the domain for all the cases gives an indication of how much self noise the aerofoil will produce. This is because in all the models, the highest regions of turbulence occur close to the aerofoil wall. Figure 4.3.4 shows that for distances further from the hub, the maximum magnitude of the turbulent kinetic energy is higher, hence the likely amount of aerodynamic noise the aerofoil blade sections will produce is also highest furthest from the hub. This relationship for the cut-in cases appears to be linear, however this is not the case for the rated cases. The relationship for the 20% span, 25% span and the 50% span cases indicates a linear relationship, however the maximum value of turbulent kinetic energy increases faster the further from the hub the aerofoil blade section is.

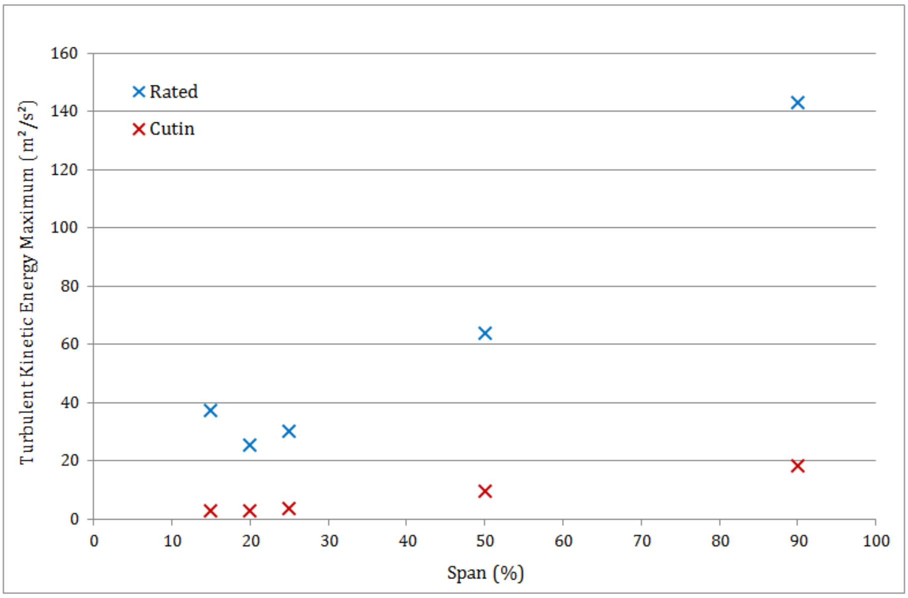

Figure 4.3.4: Graph showing the comparison between rated and cutin results of max TKE for all span distances

Contours of the static pressure give a good indication of the validity of the results by verifying that the pressure and suction sides of the aerofoil exist as expected. Static pressure contours for the whole domain and close to the aerofoil walls are given for the 20% span cut-in (a) and rated (b) cases in

Figure 4.3.5 (Similar contour plots for the 50% span and 90% span cases are given in Appendix J in Figures J.1.1 and J.1.2 respectively). The region of increased pressure on the upper wall (pressure side) of the aerofoil is larger for the rated case than the corresponding cut-in case. This means increased lift on the aerofoil and hence a faster rotational speed of the rotor at higher wind speeds. The region of increased pressure on the upper side of the aerofoil increases for blade sections further from the hub, except for aerofoil sections close to the tip. For aerofoil blade sections close to the tip such as the 90% span case, the region of increased pressure on the upper wall of the aerofoil is lower for the rated case than the cut-in case. This indicates that due to the small chord length at 90% span of 65mm compared to 180mm at 20% span, the lower angle of attack and the increase in resultant velocity of the flow of air over the aerofoil section, the blade sections at the outer parts of the wind turbine rotor play less of a role in providing the lift which causes the rotor to turn. This effect is magnified when the wind speeds are faster. The lower contribution to the lift which occurs at the outer regions of the aerofoil means that the tips of the turbine blades may flutter[5], this is a potential noise source.

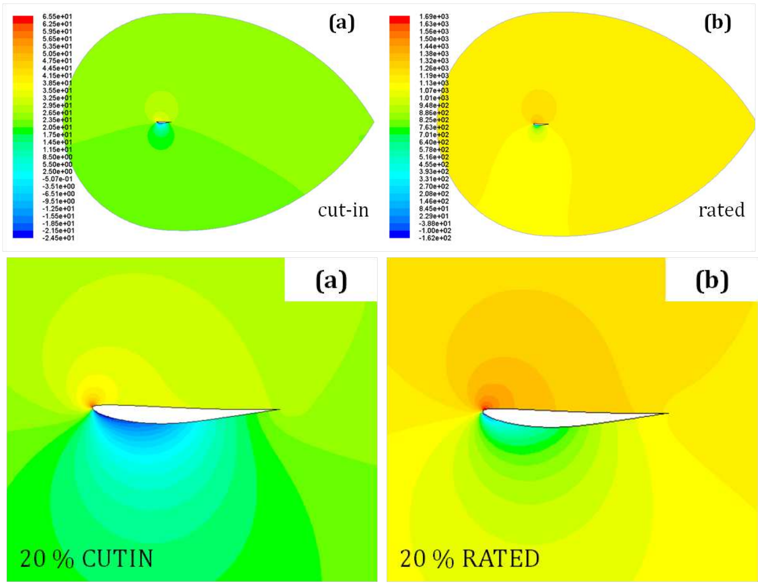

Figure 4.3.5: Static pressure contours for the whole domain and close to the aerofoil for the 20% cutin (a) and rated (b) cases

[5] Blade flutter is the self-excited vibration of a blade, due to the interaction of structural-dynamic and aerodynamic forces. At the tip, the chord length is small at 64.6mm and the air velocities are very high at up to 85m/s. This means the blade tips are more likely to suffer from flutter aerodynamic forces will be high compared to the structural forces. A more detailed analysis of flutter at the blade tip is outside the scope of this research but is recommended for further work.

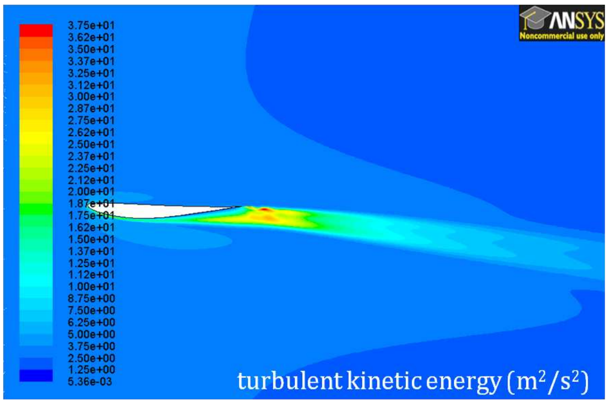

Figure 4.3.6: Contours of turbulent kinetic energy around the aerofoil and downstream at 15% rated steady-state case

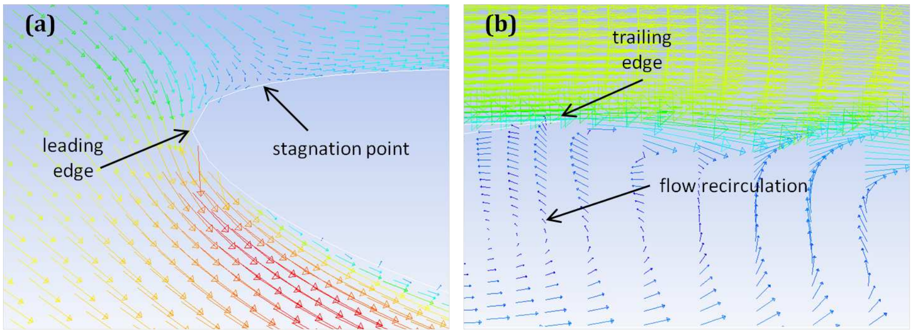

Figure 4.3.7: Close up velocity vectors for the 15% span rated steady-state case at the leading and trailing edges

From the plot of maximum turbulent kinetic energy against span percentage in Figure 4.3.4, it would appear that the 15% span rated case is an anomaly, however this is not the case. As suggested previously, evidence of vortex structures were seen downwind of the trailing edge for the 15% span steady-state rated case (as seen in Figure 4.3.6). These structures occur due to the high angle of attack of the blade section, the velocity of the air flowing over the aerofoil and the chord length of the aerofoil section. Plots of velocity vectors (Figure 4.3.7) at the leading (a) and trailing (b) edge for the 15% span rated case demonstrate that there is a large amount of flow separation and recirculation of the flow at the trailing edge, this phenomenon contributes to the vortex shedding mechanism and therefore also means that high levels of noise at the trailing edge are likely for the 15% span rated case. Further from the hub, the angle of attack reduces dramatically, and hence the flow does not separate downwind of the trailing edge (see Figure 4.3.9 for velocity vectors at the trailing edge for the rated cases at increasing distances from the hub) and hence vortex shedding does not occur. Plots of the velocity vectors at the leading edge for the rated cases at increasing distances from the hub (Figure 4.3.8) also shows that the stagnation point moves closer to the leading edge the further from the hub the aerofoil section is, another reason why less flow separation occurs around the aerofoil wall further from the hub. Further velocity vector plots around the whole aerofoil for the rated and cut-in cases and at the leading and trailing edge for the cut-in cases can be found in Appendix J. Even less flow separation occurs at the trailing edge for the cut-in cases because the magnitude of the air flow over the aerofoil blade sections is significantly lower, hence much less noise is expected from the trailing edge for the cut-in cases.

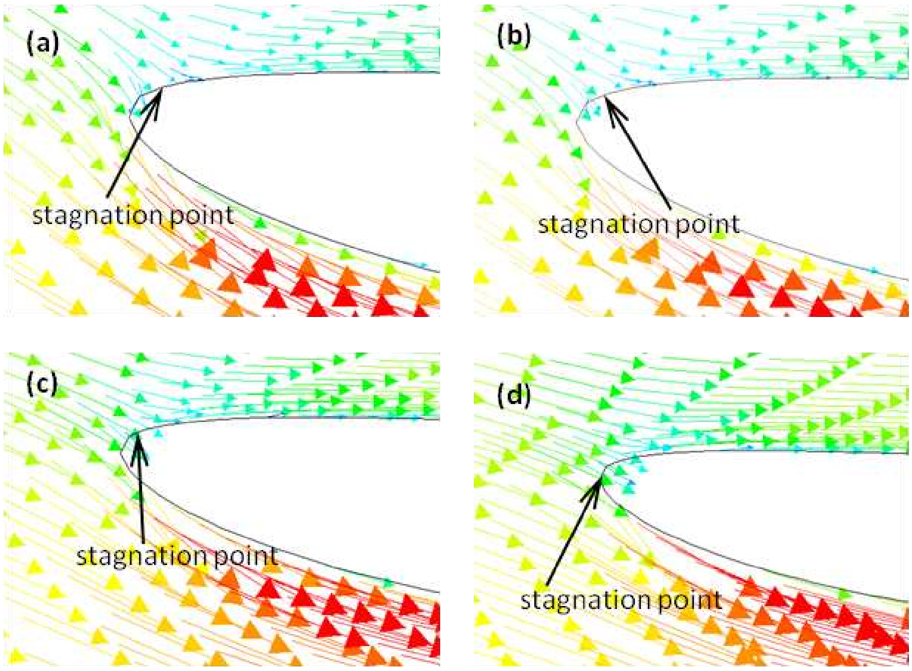

Figure 4.3.8: Comparison of the leading edge velocity vectors for 20% (a), 25% (b), 50% (c), and 90% (d) span rated cases

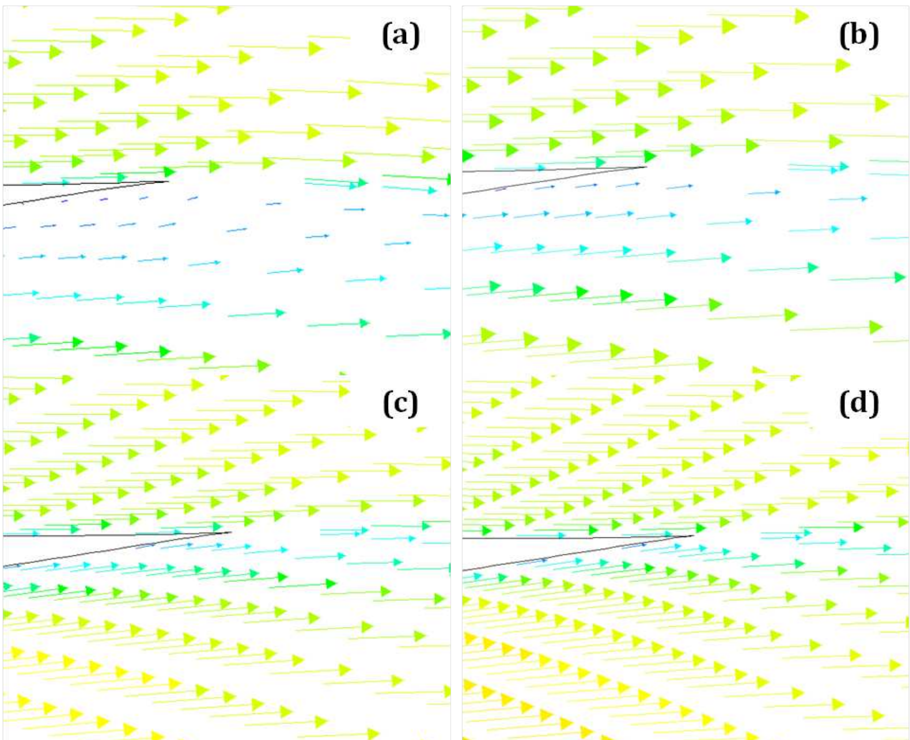

Figure 4.3.9: Comparison of the trailing edge velocity vectors for 20% (a), 25% (b), 50% (c), and 90% (d) span rated cases

The plots of the velocity vectors have shown that further from the hub, less flow separation should occur around the aerofoil wall because the angle of attack and the chord length of the blade sections decrease further from the hub. If the noise created from the turbine is purely due to flow separation less turbulence and hence noise would be expected for blade sections further from the hub. This is not the case. The chart of maximum turbulent kinetic energy against percentage span in Figure 4.3.4 is an indication that for both the rated and cut-in cases, aerofoil sections further from the hub will produce increased self noise because the maximum value of the turbulent kinetic energy increases, except for the 15% rated case where the angle of attack is high enough so vortex shedding will occur due to high flow separation. This shows that the magnitude of the velocity of the flow of air over the aerofoil blade section is an important indicator of the likely turbulence that will be produced. It is therefore important to consider how the turbulence varies over the areas around the aerofoil wall.

Although vortex shedding does not occur at distances from the hub greater than 15% span or for any of the cut-in cases, there is a region of high turbulence at the suction side of the trailing edge extending into the aerofoil wake for the 20% rated case. This shows that for the high air flow velocities over the aerofoil of the rated cases, there is a higher maximum turbulent kinetic energy particularly at the trailing edge and hence it would be expected that increased trailing edge noise will occur. This is shown in Figure 4.3.10, in the contours of the 20% span rated case over the whole aerofoil (b) and at the trailing edge (f).

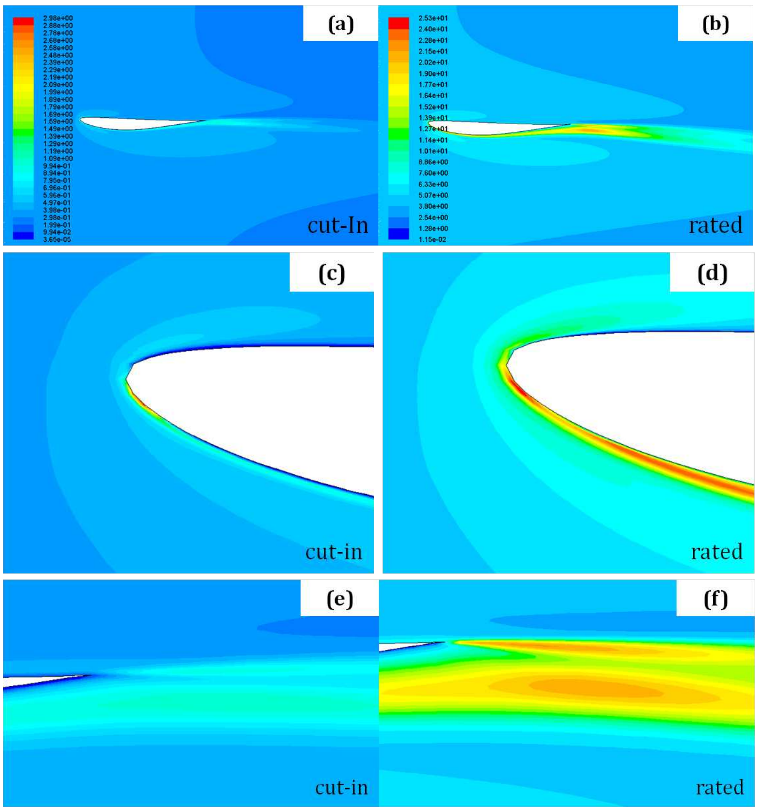

Figure 4.3.10: TKE contours for the 20% span cut-in (a) and rated (b) cases

For the rated cases shown, where the angle of attack reduces for distances further from the hub, the region of high turbulence at the suction side trailing edge decreases. This means the point where the maximum turbulent kinetic energy occurs, is not at the trailing edge but moves to the leading edge. At higher rotational speeds and wind velocities, the inflow turbulence noise is a much more important indicator of aerofoil self noise, although trailing edge noise does still occur, the high turbulence at the leading edge is more significant. This can clearly be seen when comparing Figures 4.3.11(b), 4.3.11(d) and 4.3.11(f) (the rated 50% case contours for the whole aerofoil, the leading edge and the trailing edge respectively) with Figures 4.3.12(b), 4.3.12(d) and 4.3.12(f) (the rated 90% case contours for the whole aerofoil, the leading edge and the trailing edge respectively). The maximum turbulent kinetic energy occurs close to the leading edge for both cases. As the distance from the hub increases, and hence the resultant air flow velocities over the aerofoil section increases, the size of the region of high turbulence close to the leading edge increases significantly, a phenomenon clearly visible in Figure 4.3.12(b).

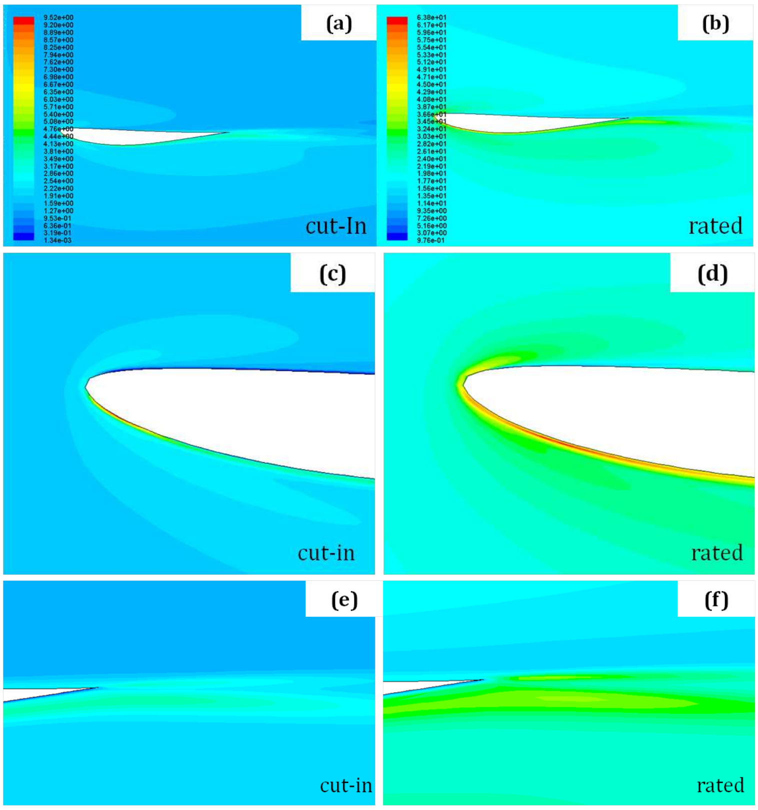

Figure 4.3.11: TKE magnitude contours for the 50% span cut-in (a) and rated (b) cases

The maximum turbulent kinetic energy is lower for all the cut-in cases compared to the rated cases, indicating that when resultant air speeds are lower, less aerofoil self noise is produced and for the cut-in cases the maximum kinetic energy always occurs at the leading edge. For low wind speeds where the turbine rotor is rotating slowly, inflow turbulence noise is always more significant than trailing edge noise.

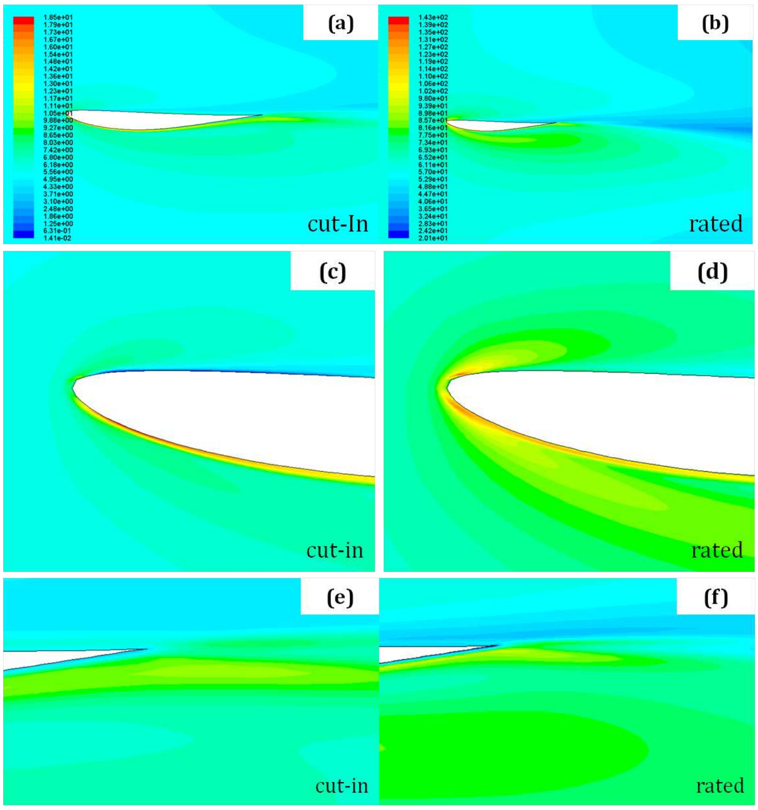

Figure 4.3.12: TKE magnitude contours for the 90% span cut-in (a) and rated (b) cases

These results are shown as 2D cases where interaction of the flow from the other blades on the turbine is not represented. This is not applicable to a real turbine case as the results do not take into account how the flow around the aerofoil blade sections may interact with the rest of the aerofoil blade. The micro wind turbine type M1 used to carry out the CFD work is a three bladed turbine, therefore the following blade will cut through the wake of the preceding blade. This is because the rotational speeds of micro turbines is very high at up to 1200rpm. For a three bladed micro turbine, this equates to a blade pass frequency of 60Hz. As the air is turbulent in the wake region, the following aerofoil will experience turbulence at the leading edge and hence inflow turbulence noise. The wake length and spread for aerofoil sections furthest from the hub are smaller than for sections close to the hub. However, the length and spread of the wake for the rated and cut-in cases for a given percentage span do not vary much between the two. This is shown in Figures 4.3.13, 4.3.14 and 4.3.15, velocity contours over the whole domain for the 15% span, 50% span and 90% span cut-in (a) and rated (b) cases respectively. The magnitude of the velocity of the flow over the aerofoil wall plays less of a role in determining the size of the wake than the chord length and angle of attack because although the magnitude of the velocity is much higher for the rated cases than the cut-in cases, the spread and length of the wakes are roughly equal. In the wake region and on the pressure side of the aerofoil the magnitude of the velocity is lower compared to the free stream velocity. At the leading edge the flow is accelerated to the suction side of the aerofoil. Turbulence is created in these regions due to the shear between different layers of the flow, therefore the size and shape of the accelerated and decelerated regions of the flow close to the aerofoil wall at the leading and trailing edge and on the pressure and suction sides of the aerofoil will determine how much turbulence is produced. Turbulence in these regions will interact with the rest of the blade and the following blade will encounter the wake from the preceding turbine blade, hence potentially producing increased inflow turbulence noise. These phenomena will be magnified for resultant air flows with a higher magnitude.

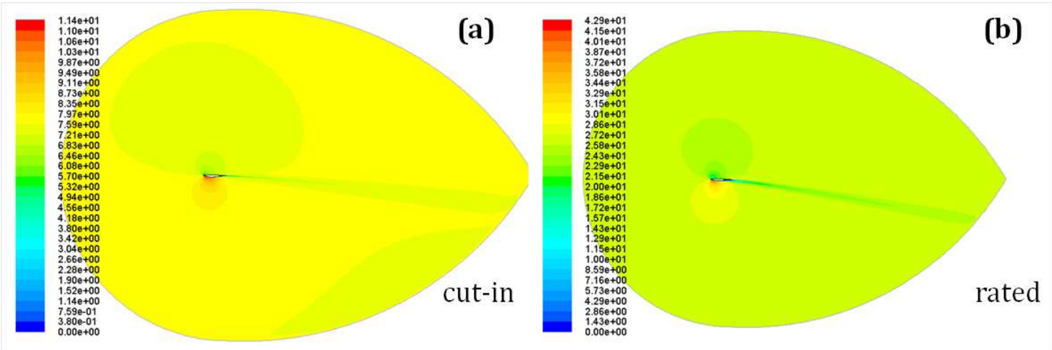

Figure 4.3.13: Velocity magnitude contours for the 15% span cut-in (a) and rated (b) cases

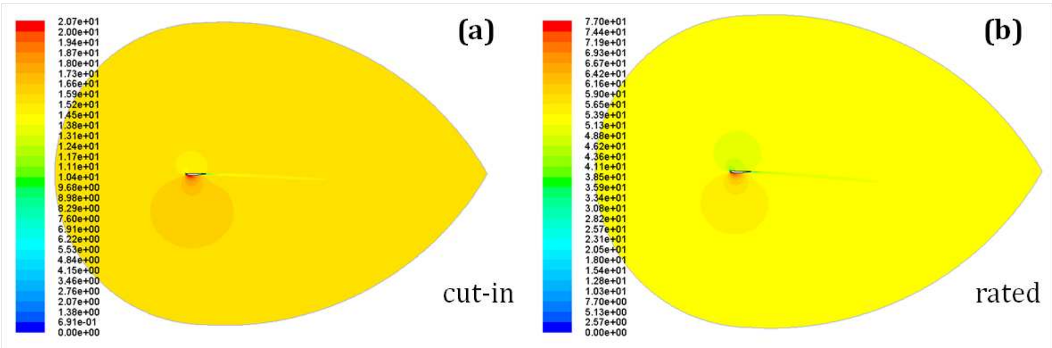

Figure 4.3.14: Velocity magnitude contours for the 50% span cut-in (a) and rated (b) cases

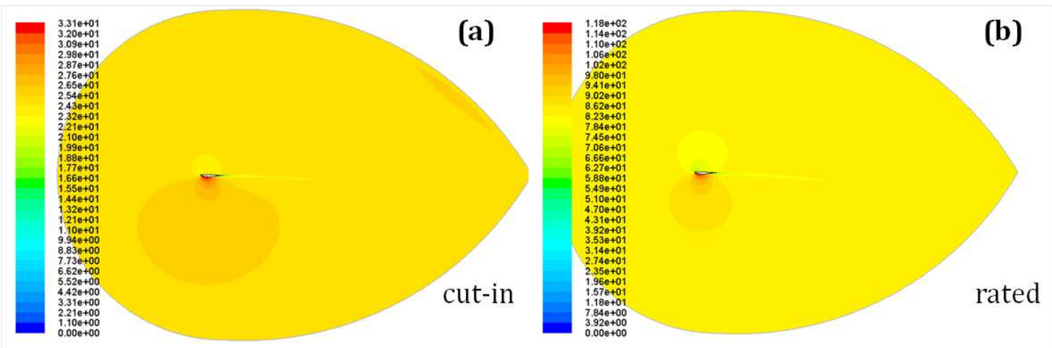

Figure 4.3.15: Velocity magnitude contours for the 90% span cut-in (a) and rated (b) cases

In summary, the combination of the air velocity over the blade sections, the angle of attack and the chord lengths all play a key role in determining how much turbulence and hence noise is generated by an aerofoil. These factors also determine where around the aerofoil wall the noise is likely to be produced. At higher wind speeds when the turbine is rotating faster, inflow turbulence noise is significant at the blade tips, closer to the hub trailing edge noise is important, as is noise due to flow separation at the leading and trailing edge. How this trailing edge turbulence will interact with the rest of the rotor and the turbine hub should be considered. As expected for the cut-in cases, at low wind speeds and rotor rotational speeds, inflow turbulence noise is always more significant than trailing edge noise, but the maximum turbulent kinetic energy is lower than the rated cases, so less aerofoil self noise on the whole is is expected. The length of the wake as indicated by the velocity vectors and contours will also affect the amount of aerodynamic noise generated by the aerofoil. These findings need to be taken into consideration accounting for the limitations of the 2D modelling method. In the following Section a conclusion of the CFD results will be given, including the implications for the overall work. Suggestion will be made for further work.

4.4 Conclusions of the CFD Work

The aims and objectives of the noise modelling work have been achieved. The likely noise mechanisms associated with small wind systems have been identified by using computational fluid dynamics to model the flow fields around 2D blade sections at increasing span distances from the hub of the micro turbine type M1. By analysing the flow field around the 2D blade sections for rated and cut-in cases, the turbulence and hence regions of high noise have been identified. The method and results from this part of the research have together verified that the CFD method adopted could be appropriate for small wind system manufacturers to assess the noise mechanisms associated with a particular small or micro wind turbine design. Although the results do not give the absolute levels of noise from the blade sections tested, comparisons between different turbine designs would identify which is best in terms of low aerodynamic noise production. The drivers for the CFD part of the research have hence been met.

It has been found that the key noise mechanisms associated with the micro wind turbine type M1 are inflow turbulence noise, trailing edge noise and separation stall noise (see Section 1.2 for a full description of these noise mechanisms). Each of these noise mechanisms generate a broadband sound which are likely to manifest themselves as a swooshing sound, however the nature of the noise mechanisms may change when encountering other parts of the turbine structure. For example, the blade pass frequency and the size of the turbine mast may have an effect on the sounds generated. Depending on the magnitude of the angle of attack separation stall noise can be generated at the trailing edge or from the whole chord length. Separation stall noise and tip noise were not included in Lowson's [16] semi-empirical model for prediction as this noise mechanism requires a detailed prediction of local aerodynamic parameters. The CFD method is a good way to resolve these aerodynamic parameters and hence fill the gap in the semi-empirical noise prediction method. This also indicates that CFD was the most appropriate method to adopt for the current research.

For the rated cases, at 12m/s wind speeds and 1200rpm rotor rotational speeds, close to the hub where the resultant angle of attack is high compared to at span distances further from the hub, separation of the flow occurs upwind of the trailing edge on the suction side of the aerofoil. This causes flow recirculation and vortex shedding and the maximum magnitude of the turbulent kinetic energy occurs in this region of the domain. At distances further from the hub, local flow velocities are increased and as a result of this, the maximum magnitude of the turbulent kinetic energy also increases; an indication that higher noise levels due to the turbulence occur at distances further from the hub. However, from analysis of the results, it is clear that the separation stall noise mechanism does not occur further from the hub because the angle of attack is close to zero. The contours of turbulent kinetic energy show that further from the hub, inflow turbulence noise becomes significant and the maximum magnitude of the turbulence occurs close to the leading edge. Due to the extremely high velocities of the flow up to 117m/s at 90% span, the flow field is extremely disturbed at the leading edge and the flow can separate close to the leading edge causing high turbulence in this region. For the cut-in cases, (3m/s wind speeds and 300rpm rotor rotational speeds) the maximum magnitude of the turbulent kinetic energy is lower than for the equivalent rated cases and inflow turbulence noise is always the most significant noise mechanism. Even closer to the hub, separation stall noise and vortex shedding does not occur for the cut-in cases. This is due to the low local flow velocities.

A comparison of the wake sizes for blade sections at increasing distances from the hub at rated and cut-in wind speeds show that the length and spread of the wakes of the equivalent rated and cut-in cases are approximately the same, even though the local flow velocities for the rated cases are significantly higher. Furthest from the hub the wake has the smallest length and spread. This signifies that it is the chord length and resultant angle of attack of the blade section that is the main contributing factor to the size of the wake. It is important to consider the size of the wake because the flow will be turbulent in this region. The way the wake from a 2D blade section interacts with the rest of the rotor and the turbine hub should also be considered and these phenomena are not represented in the results; a limitation of the work carried out. This is especially important for the blade sections where inflow turbulence noise is the largest contribution factor to the overall turbulence in the domain. For all the blade sections modelled, the leading edge is encountering a uniform flow and the turbulence at the leading edge is generated by the aerofoil itself. If the leading edge is encountering randomly fluctuating turbulent flow from the wake of the preceding blade it is likely that inflow turbulence noise will become even more significant. Amiet [88], described the acoustic radiation of an aerofoil in a turbulent stream. It was stated in Amiet's research that the unsteady loading the inflow turbulence causes on an aerofoil causes the noise, further supporting inflow turbulence noise as an important noise mechanism for small wind systems.

The conclusions given here are a snapshot of the key findings of the noise modelling research carried out. The results show the way in which a small or micro wind turbine manufacturer could use the CFD methods to assess noise from different turbine designs. In Chapter 5, comparisons will be made between the results of the noise modelling analysis and analysis of the data collected for the studies of the psychological and health impacts of small wind systems as well as the noise measurement results.

There are limitations to the noise modelling work. Due to limited availability of computational resource (as is expected to be the case for small wind system manufacturers) for the current research, the RANS k-ω SST has been used. If computing resource continues to become more readily available, it is conceivable that more expensive methods such as large eddy simulation (LES) as used by researchers such as Moroianu [114] could become accessible for the prediction of noise from small wind systems. It is however, more likely that hybrid RANS and LES methods such as a zonal RANS-LES approach such as that used by Mathey [107] will be used in the near future.

A significant limitation of the work is that only 2D blade sections from one micro turbine type have been investigated. The turbulent flows seen from the analysis of the 2D sections will interact with the rest of the turbine blade and the turbine structures. Due to the fast rotation of small wind system rotors, the turbulent flow and the wakes generated by a blade will also cause disturbance of the flow encountered by the following blade, hence increased turbulence and noise levels. The way small wind systems behave is dynamic, for example they tend to change orientation very quickly into and out of the wind direction. For this reason, the flow encountered by a small wind system aerofoil will not be uniform like the flow field used for the CFD analysis in the current research. The work carried out for this research can be considered as a starting point for future work. First a 3D analysis of the turbulent flow fields and hence likely noise from the full blade should be considered followed by a 3D analysis of the whole micro or small turbine structure.

It has not been the intention of this research to develop new methods within CFD but to verify that CFD could be used by small wind system manufacturers to analyse likely noise production from different designs of turbines. The work has also allowed an analysis of the likely noise mechanisms associated with small wind systems. If the methods within CFD for predicting noise such as the broadband noise sources method are further developed, they should be considered for future work.

In the following and final Chapter of the Thesis, a full comparison between the three key methods adopted for the whole research will be given, including a full assessment of the whether the objectives of the research have been achieved and the drivers for the work satisfied.

Chapter 5

Conclusions of the Thesis

In this Chapter of the Thesis, final conclusions of the work will be given drawing together the three methods adopted to achieve the objectives of the overall research and to satisfy the drivers of the work. The general aim of the research was to better understand the noise levels generated by small and micro wind turbines, the characteristics of the noise and people's reactions to this noise. The research fills a gap in the literature, which is currently principally based on large scale turbines in rural environments rather than small wind systems in built up areas. The current research is an interdisciplinary study incorporating the subject areas of Engineering; to measure and characterise the noise from small wind systems and to investigate the flow around aerofoil blade sections which is directly related to noise, and Psychology; to identify the type of people who are most likely to perceive small wind system noise and the effect the noise has on them.

The three main objectives of the research were:

1. **Noise Measurement -** to measure and characterise the noise levels and noise mechanisms at real small and micro wind turbine installations to estimate the turbine noise levels over and above the background noise at each installation, including a spectral analysis and assessment of the noise attenuation.

2. **Public Perceptions of Noise -** to survey individuals living close to small and micro wind turbine installations to investigate the level and type of noise perceived and to link this to individuals' attitudes towards wind turbines and personality and temperamental characteristics. To confirm the results with an experimental recordings study and compare the results of the two studies with the results of the noise measurements and noise modelling.

3. **Noise Modelling -** to identify the noise mechanisms associated with small wind systems by modelling the turbulent flow and hence noise around a turbine blade to compare to the noise measurement results.

In the following Sections conclusions of the three methods adopted to satisfy the above objectives will be given including a drawing together of the results from the three methods adopted. This will be followed by an outline of the contributions of the Thesis to the literature and finally, recommendations for future work.

5.1 A Comparison of the Three Methods

The noise measurement part of the research has shown that the sound pressure levels measured at real turbine installations are not of a high level as the maximum sound pressure levels measured at locations closest to the turbines are equivalent to the sound levels of general speech. The further from the turbines the measurements were taken, the lower the magnitude of the wind turbine sounds. These findings were found to be the same for both the small turbine type S1 and the micro turbine type M1. From analysis of the domestic study data it has been shown the the overall perceived turbine loudness and occurrence scores as reported by respondents were of a low level. The data have also shown that respondents living in zones furthest from the turbines perceived the least turbine noise. These findings therefore support the noise measurement results in indicating that small wind system noise levels are low and attenuate to locations further from the turbines. The attenuation of the turbine sounds observed from the noise measurement data are also in agreement with the sound maps generated using the software package CadnaA and the attenuation levels quoted by the manufacturers of turbine types M1 and S1.

Although the measured and reported noise levels due to the turbines at real small wind system installations are low, the spectral analysis and analysis of the sounds reported from the results of the domestic study at real small wind system installations have shown that the characteristics of the noise vary between the two turbine types (M1 and S1), as well as in different wind speeds and conditions. For example, they types of sounds the turbines make varies depending on the wind conditions. The portion of the frequency spectrum the sounds occupy also varies as the wind speed and turbine rotational speed varies. It is these characteristics of the sounds that are likely to cause annoyance and increase the perception levels of the turbine sounds. For example, the humming sound the small wind turbine makes is tonal in nature and may cause annoyance where audible. This finding is further supported by the recordings survey results. Although the turbine sounds perceived in each recording by respondents to the recordings study matched well to the sounds expected to be perceived, it was also expected that the recordings taken in the highest wind speeds would be reported as containing the loudest turbine sounds compared to recordings at lower wind speed. This, however was not always the case and it appeared that is was the sound characteristics in the recordings which influenced the level of sound perceived. As expected, the recording that did not contain any wind turbine noise was reported as having the least turbine noise by the participants.

During the measurement data collection, the sounds typically heard from the micro turbine type M1 were swooshing in all reference wind speeds, squeaking at low to mid reference wind speeds and at high reference wind speeds the swooshing sound turned to a fan sound due to the very high rotational speeds of the rotor. For measurement taken inside, humming was audible as a sound transmitted through the building structure the micro turbine was mounted on.

The results of the domestic study of the psychological and health impacts of small wind systems have shown that the sounds perceived the most readily from the micro turbine type M1 at real installations by respondents to the questionnaire were humming, swooshing, whistling and buzzing. These reported sounds are in agreement with the sounds heard during measurement data collection and from observation of the associated frequency spectra. However, it was not possible from the domestic study results to identify in what type of weather conditions these turbine sounds were experienced by the respondents. The recordings study allowed the researcher to control the sounds the participants were exposed to by selecting recordings which capture the typical sounds experienced from the micro turbine type M1 in different wind conditions. From the sound recording of turbine M1 in moderate wind speeds (recording 1) the sounds reported by respondents were whistling, swooshing, high frequency and screeching. For the sound recording of M1 taken at very high wind speeds (recording 6) the sounds reported were low frequency, humming, swooshing and buzzing or throbbing.

Hence, for the micro turbine type M1, the key comparisons between the measurement data collected and the domestic and recordings studies were as follows:

- Sounds reported as perceived from the micro turbine installations and the recordings of micro turbine noise were in good agreement with the sounds observed from the spectral analysis.
- A broadband swooshing sound occurs for all wind speeds above 1000Hz. From a knowledge of the noise mechanisms associated with wind turbines it is known that it is likely that this sound occurs due to the inflow turbulence, separation stall and turbulent boundary layer trailing edge noise mechanisms. The swooshing sound has been perceived both from micro turbines at real turbine installations and from both sound recordings of micro turbine noise used for the recordings study.
- At high wind speeds the swooshing sound can change to a fan type sound and is still broadband in nature but occurs over a larger portion of the frequency spectrum. The fan sound could still be due to the same noise mechanisms as swooshing but the nature of the sound changes due to the very fast rotational speeds of the micro turbine rotor up to 1200rpm.
- Recording 6 represented the micro turbines at installation (d) in very high wind speeds. The low frequency, humming and throbbing sounds perceived by respondents from this recording could all be associated with the fan type sound heard during measurement data collection.
- At low to mid wind speeds, a tonal squeaking sound was observed in the frequency spectra at high frequencies around 1600Hz to 4000Hz during measurement data collection. As the squeaking sound is associated with the rotor rotational speed and is tonal in nature it is not clear which noise mechanism it is associated with. It could be tip noise interacting with other parts of the turbine structure or one of either laminar boundary layer trailing edge noise or blunt trailing edge noise. Further work is required to verify the source of the squeaking sound.

- Recording 1 represented the micro turbines at installation (d) in mid wind speeds. The perceived sounds by the respondents from this sound recording were whistling, high frequency and screeching. These sounds perceived agree very will with the measurement data.

During the measurement data collection, the sounds typically heard from the small turbine type S1 were swooshing and humming in all reference wind speeds, and at high reference wind speeds the swooshing sound turned to a chopping sound due to the increased rotational speeds of the rotor. On some occasions in low wind speeds, if the rotor turned to face out of the wind direction a whistling type sound was heard as the rotor slowed down before returning to face the wind direction.

The humming sound is an electro-mechanical sound emitted from the base of the mast. Due to the source of the humming sound being near ground level, it attenuates quickly because obstacles such as fences or low buildings have a large affect on the attenuation of the sound. As the aerodynamic sounds such as swooshing are emitted from the rotor hub, they travel further without encountering any obstructions to attenuate the sound.

The results of the domestic study have shown that the sounds perceived the most readily from the small turbine type S1 at real installations from respondents to the questionnaire were scratching, swooshing, humming, thumping and low frequency. These reported sounds are in agreement with the sounds heard during measurement data collection and from observation of the associated frequency spectra. As with the micro turbine type, it was not possible from the domestic study results to identify in what type of weather conditions these turbine sounds were experienced by respondents. The recordings study allowed the researcher to control the sounds the participants were exposed to by selecting recordings which capture the typical sounds experienced from the small turbine type S1 in different wind conditions. From the video recording of turbine S1 taken in very low wind speeds (recording 7), the sounds reported by participants were swooshing, scratching, low frequency and whistling. For the video recording at moderate wind speeds (recording 3) the sounds reported were low frequency, humming, swooshing and throbbing. For the sound recording of turbine S1 at moderate wind speeds (recording 2), participants perceived low frequency, humming, swooshing and throbbing sounds the most. For the sound recording at very high wind speeds (recording 5), participants reported swooshing, scratching, low frequency and throbbing.

The key comparisons between the measurement data collected and the domestic and recordings studies for the small turbine type S1 were as follows:

- Sounds reported as perceived from the small turbine installations and the four recordings of small turbine noise were in good agreement with the sounds observed from the spectral analysis.
- As with the micro turbine type M1, broadband swooshing sound occurs for all wind speeds above 1000Hz. From a knowledge of the noise mechanisms associated with wind turbines it is known that it is likely that this sound occurs due to the inflow turbulence, separation stall and turbulent boundary layer trailing edge noise mechanisms. The swooshing sound has been perceived both

from small turbines at real turbine installations and from all four sound recordings used for the recordings study.

- At high wind speeds the swooshing sound changes to a chopping sound and is still broadband in nature but occurs over a larger portion of the frequency spectrum. The chopping sound is still be due to same noise mechanisms as swooshing but the nature of the sound changes due to the fast rotational speeds of the turbine rotor up to 230rpm.

- Recording 5 represented the small turbine at installation (c) in very high wind speeds. The scratching, low frequency and throbbing sounds perceived by respondents from this recording could all be associated with the chopping sound heard during measurement data collection.

- Recording 7 represented the small turbine at installation (a) at low wind speeds when the rotor turns to face away from the wind direction. A whistling sound was heard during data collection as the rotor slowed. Whistling was indeed also perceived by respondents to the recordings study in recording 7.

- The humming noise mechanism heard from the small turbine type during noise measurements in all wind speeds have been observed from the analysed frequency spectra to be tonal in nature and occur in the frequency spectrum at 100Hz to 125Hz and 200Hz to 400Hz. This noise mechanism is not an aerodynamic sound source but due to the electro-mechanical workings of the small turbine at the base of the turbine mast.

- At measurement locations further from the turbine the humming is not audible as the sound has attenuated due to low obstructions. Only recordings 2 and 3 taken at installations (a) and (b) respectively were taken close enough to the turbine for the humming noise to be audible. Indeed, humming was perceived by participants from recordings 2 and 3 but not recordings 6 and 7.

- Recordings 6 and 7 were taken at installations (c) and (a) respectively at locations Ma4 and Mc9. The measurement data has shown that humming is not observed in the frequency spectra for these measurement locations.

Overall, the findings show that the range of sounds perceived from the micro turbine type M1 are similar to the sounds perceived from the small turbine type S1. However, sounds associated with higher frequencies such as screeching are perceived more readily from the micro turbine type and lower frequency sounds are heard more readily from the small turbine type. This is due to the different characteristics of the two turbine types such as the rotor diameter and rated rotational speeds. Although swooshing is reported from both the small and micro turbine types, lower frequency sounds are associated with the small turbine type as the rotor is larger than the micro turbine type rotor, rotating at a lower rotational speed. Hence, the exact frequencies of the sounds perceived depends on the wind speeds and conditions and the sizes and rotational speeds of the rotor.

A summary of the analysis of how individual differences and attitudes to wind turbines affects small wind system noise perception and symptom reporting from both the domestic and recordings survey has shown that whilst some work has associated turbine noise with increased symptoms of ill health for those living close to wind turbines [54], the current study suggests that this approach may be too simplistic. Any model aiming to examine the effects of small wind system installations more fully should assess the role of individual differences and differential effects of perceived and typical noise on symptoms including the level of exposure. The role of negative oriented personality has been shown to be key in understanding how perception of environmental negative characteristics (such as noise from small wind systems) may be translated into symptoms of ill health. Specifically, those with a more negative attitude to wind turbines, the more noise they perceive and the more noise that is perceived, the more symptoms of ill-health they report. These relationships are moderated by personality and are only significant for individuals with higher NOP; specifically high neuroticism, high levels of negative affect and high levels of frustration intolerance and emotional intolerance.

To complete the overall picture of small wind system noise an analysis of the flow fields around 2D blade sections of turbine type M1 has been carried out. The aim was to verify that the noise mechanisms observed from the spectral analysis of the measurement data and the sounds perceived by participants from both the domestic and recordings studies are comparable to the regions of high turbulence around a turbine blade section.

The CFD analysis has shown that the regions of high turbulence around a 2D micro turbine blade section occur at the leading edge and trailing edge and the flow separates from the aerofoil wall upwind of the trailing edge on the suction side, generating turbulence. It can be deduced from this that the noise mechanisms associated with the micro wind turbine type M1 are inflow turbulence noise, trailing edge noise and separation stall noise (see Section 1.2 for a full description of these noise mechanisms). Each of these noise mechanisms generate broadband sounds which are likely to manifest themselves as a swooshing sound. The swooshing sound has been observed from the noise measurement spectral analysis and perceived by respondents to both the domestic and recordings studies. The nature of the sounds the noise mechanisms generate may change when encountering other parts of the turbine structure and could account for the changes in turbine noise at different wind speeds such as the squeaking noise heard for the micro turbine type at lower wind speeds and the fan noise heard at very fast wind speeds. This is because in these varying wind conditions the interaction of the turbulence with the rest of the blade and the turbine structure will change the exact noise mechanism occurring, i.e. the blade pass frequency and the size of the turbine mast may have an effect on the sounds generated. The sounds which occur due to interaction of the local flow fields with other parts of the turbine structure such as the squeaking sound from the micro turbine type M1 could be represented using CFD if full 3D analyses were carried out. A full 3D analysis would require a large domain with fine grid spacing close the wind turbine aerofoil walls and periodic boundaries utilised to represent a full three bladed micro turbine. The computational cost for a full 3D analysis was prohibitively high for the current research and outside the scope of the work. A detailed 3D analysis is recommended for future work and could be a full research project in it's own right if the resource were available. It is not possible to represent the electro-mechanical humming sound from the small turbine type using CFD as this is not an aerodynamic noise source.

The CFD results show that separation stall noise occurs for blade sections close to the hub at higher reference wind speeds where the pitch angle is high. Turbulent boundary layer trailing edge noise is also significant for blade sections close to the hub. For blade sections closer to the tip where the local flow velocities are high, inflow turbulence noise and separation of the flow at the leading edge becomes more significant. For lower wind speeds inflow turbulence noise is always more significant for blade sections at all distances from the hub. The length of the wake should also be observed to give an indication of how the turbulence in the wake will interact with the rest of the turbine structure and with the following blade during rotation. The chord length and the angle of attack are the key factors in determining the length of the wake rather than the local flow velocities.

In summary, the overall level of small wind system noise likely to be experienced is of a low level but the nature of the sounds emitted increase the likely perception of the sounds. Swooshing, humming, chopping and squeaking sounds are the sounds most likely to be perceived. This is seen from both the spectral analysis and the studies of the psychological and health impacts of the noise. The swooshing, chopping and fan type sounds are broadband sounds and are hence associated with the inflow turbulence, turbulent boundary layer and separation stall noise observed from analysis of the local flow fields and the turbulence around 2D blade sections of the micro turbine type M1 using CFD. The squeaking and humming sounds perceived are tonal in nature. These sounds are attributed to the electro-mechanical workings of the turbines. They could also be due to the interaction of the turbulent wake observed from the local flow fields with the rest of the turbine structure. However, it is not possible to capture these interactions with the 2D analysis using CFD. The characteristics of the noise potentially increase the perception of small wind system noise levels and the the sound levels alone are not enough to predict the amount of noise which could be perceived. An individual's attitude to wind turbines and personality traits further explain how small wind system noise is perceived. Individuals experiencing the noise in the most negative manner with high NOP are also likely to experience increased symptoms of ill health.

5.2 Thesis Contribution to the Literature

The Thesis has satisfied the drivers of the research which were to provide the following benefits:

- A better understanding of the real levels of small wind system noise experienced by individuals living near where they are sited;
- Hence information to planners and policy makers for better guidance regarding siting of turbines;
- An accessible method to estimate the noise issues associated with small wind aerofoil for small wind system manufacturers;

- Information about the type of individuals likely to perceive small wind system noise and the effect this will have on their general health;
- Hence guidance on how information about small wind systems can be better relayed to the general public based on those who are likely to oppose installations.

The Thesis is the first of its kind to draw together three methods from two disciplines to get an overall picture of small wind system noise levels and characteristics and how the noise is perceived. Research available in the current literature is principally based on large scale turbines generally focusing on one aspect of the issues surrounding their implementation, for example only the measurement of the noise levels. There is a large gap in the research in all subject areas for small wind systems noise. This is the first study which seeks to link noise perception with individual differences and attitudes to wind turbines and not just noise annoyance. A full understanding incorporating the two disciplines has been essential to satisfy the overall aim of the work.

The specific contributions to the literature are as follows:

- It is now understood from noise measurements that the level of noise generated by small wind systems is of a low level and it has been confirmed that it is the characteristics of the noise which cause annoyance to individuals living near small wind system installations. It is also the characteristics of the sounds which makes them more perceivable, i.e. as small wind systems are very dynamic in their behaviour, the sounds generated can change rapidly making them more noticeable. Different turbine types and sizes generate different sounds depending on their characteristics.
- A full analysis of the type of sounds observed from the noise measurement data and those perceived by respondents to both questionnaires has been carried out. The sounds measured and those perceived have found to be in agreement. This gives information to planners and policy makers regarding the likely noise levels that will be perceived at proposed turbine installations of a particular turbine design.
- Environmental noise measurements have proven to be an acceptable way to measure the noise levels and to characterise the noise from small wind systems at real installations. The method would be appropriate for planners and policy makers to assess the noise levels at existing or proposed small wind system installations.
- The studies of the psychological and health impacts have given a model for the type of individual most likely to perceive small wind system noise, proving that personality does play an important role, and that those perceiving the most noise experience more symptoms of ill-health.
- The CFD method for assessing likely noise sources for a particular small wind system design has been shown to be accessible to small wind system manufacturers. The flow field around 2D blade sections has also given an indication of the regions of high turbulence and hence likely

noise mechanisms. This means that different turbine designs can be compared to assess which may generate the lowest or most acceptable noise levels.

- The overall conclusions of the research are useful for turbine designers, planners, policy makers and potential turbine installers by allowing a better understand of small wind system noise. The conclusions could also help in achieving a consistent planning process for new small wind system installations and give guidance to local councils on how to engage the general public at the early stages of a new small wind system proposal. By having a knowledge of those likely to perceive and oppose new small wind system installations it is possible to engage these individuals in the most appropriate manner to aid understanding of the actual noise levels likely to be experienced. Fear of the unknown is often the biggest obstacle to overcome.

Finally and most importantly, it has been shown that measuring the absolute noise levels of the turbines is not enough to assess how small wind system noise is experienced and all aspects of the study should be taken into consideration. Simply measuring the absolute noise alone would have returned a result that small wind systems generate a low level of noise and should not cause a nuisance. By considering all aspects of the study, measurements have shown that although small wind systems are quiet, the studies of the psychological and health impacts have shown that the sounds are still perceivable and do affect individuals living nearby. These studies have also shown that it is not the actual noise levels from the turbines experienced but the perceived noise levels which predict symptoms of ill-health. Therefore a method such as CFD flow field analysis of new small wind system designs should always be adopted so the best possible designs of small wind systems in terms of their noise production are used.

5.3 Recommendations for Future Work

Specific recommendations for further work are as follows:

- Noise measurements should be taken continuously over a number of weeks and weather conditions at real small wind system installations. Wind speeds at hub height should also be measured simultaneously with the noise measurements. This would allow quantification of the sound power levels from different turbine types in a range of wind speeds and a full assessment of the directionality of the sound and the attenuation of small wind system noise. Analysis of the agreement between noise measurement attenuation and the inverse power law would then be possible.
- Continuous environmental noise measurements should also be carried out at a selection of questionnaire respondents dwellings to obtain more information about the noise perceived by individuals living close to a real small wind system installation.
- The focus of the current research has been on aerodynamic noise, however the results suggest that mechanical noise is present at the base of a small turbine tower. The results also suggest

that if a micro turbine is building mounted, noise is transmitted through the structure of the building and is audible inside. For this reason, a full continuous assessment of vibration and mechanical noise should also be carried out.

- More sophisticated methods for measuring aerodynamic noise from small and micro wind turbine aerofoils could be considered if the resource is available. These include, the use of a wind tunnel or PIV, new methods are also becoming available such as the use of an acoustic camera. These methods would allow confirmation of the noise mechanisms associated with the sounds heard from the small and micro wind turbines and quantification of the absolute noise levels.

- It would be advantageous to compare the measurement data collected to manufacturers' data and include more turbine types in the analysis to get a more complete picture of the nature of small wind system noise. The current study is a starting point focusing on the small wind turbine type S1 and the micro wind turbine type M1.

- The domestic study carried out is a cross-sectional study. Future research should implement a longitudinal before and after design to capture any changes in symptom reporting and attitudes throughout the whole process of implementation of a new small wind system installation.

- Extending the recordings study to increase the number of participants would increase the validity of the results to compare to any further domestic studies.

- The CFD work carried out for this research can be considered as a starting point for future work. A 3D analysis of the turbulent flow fields around a full turbine blade should be carried out followed by a 3D analysis of the whole micro or small turbine structure. This would allow an assessment of how the turbulence around the 2D blade sections interacts the the rest of the turbine blade as well as the other blades on the turbine and the structure of the turbine itself.

- If the methods within CFD for predicting noise such as the broadband noise sources method are further developed, they should be considered for future work. In addition to this, if the cost of computational resource continues to be reduced methods such as large eddy simulation could also be considered to get a better picture of the turbulence.

The research carried out in the Thesis is the first of its kind, incorporating the subject areas of Engineering and Psychology to get an overall picture of small wind system noise. Any further work carried out would only add to the findings and conclusions made in this Thesis and should not ignore the implications of the psychological or engineering aspects of the work. This means always using an interdisciplinary approach to assess small wind system noise and never focusing on one aspect in isolation.

Bibliography

[1] B. Lapillone. World energy use in 2010: over 5 percent growth. Technical report, Enerdata, 2011.

[2] Climate Change 2007: The Physical Science Basis. Contribution of Working Group I to the Fourth Assessment Report of the Intergovernmental Panel on Climate Change. Technical report, IPCC, 2007.

[3] DTI. Meeting the Energy Challenge: A White Paper on Energy, 2007.

[4] Power stations expected to close before 2025, 2011. URL `http://www.aepuk.com/uploads/downloads/Power5.pdf`.

[5] *The UK Renewable Energy Strategy*, 2009. HM Government, The Stationary Office.

[6] Wind Power and the UK Wind Resource. Technical report, University of Oxford, 2005.

[7] *The UK Low Carbon Transition Plan. National strategy for climate and energy.*, 2009. HM Government, The Stationary Office.

[8] UKWED Statistics, 2011. URL `http://www.bwea.com/ukwed/index.asp`.

[9] P. Devine-Wright. Beyond NIMBYism: towards an integrated framework for understanding public perceptions of wind energy. *Wind Energy*, 8(2), pp125–139, 2005.

[10] M. Wolsink. Wind power implementation: The nature of public attitudes: Equity and fairness instead of 'backyard motives'. *Renewable and Sustainable Energy Reviews*, 11(6), pp1188–1207, 2007.

[11] BWEA. BWEA Small Wind Systems UK Market Report - 2008. Technical report, BWEA, 2008.

[12] RenewableUK. RenewableUK Small Wind Systems UK Market Report - April 2011. Technical report, RenewableUK, 2011.

[13] M. Wolsink, M. Sprengers, A. Keuper, T. H. Pedersen, and C. A. Westra. Annoyance from wind turbine noise on sixteen sites in three contries. In *Proceedings of the European Community Wind Energy Conference*, Pages: 273–276, Lubeck, Travemunde, 1993.

[14] E. Pedersen, F. van den Berg, and R. Bakker. Response to noise from modern wind farms in The Netherlands. *Journal of the Acoustical Society of America*, 126(2), pp634–643, 2009.

[15] Planning Policy Statement 22: Renewable Energy, 2004. URL `http://www.communities.gov.uk/publications/planningandbuilding/pps22`.

[16] M. V. Lowson. Assessment and Prediction of Wind Turbine Noise. Technical report, 1993.

[17] S. Wagner, R. Bareiss, and G. Guidati. *Wind Turbine Noise*. Springer, Berlin, 1996.

[18] F. W. Grosveld. Prediction of Broadband Noise from Horizontal Axis Wind Turbines. *Journal of Propulsion and Power*, 1(4), pp292–299, 1985.

[19] T. F. Brooks, D. S. Pope, and M. A. Marcolini. Airfoil self-noise and prediction. Technical report, 1989.

[20] M. V. Lowson. New prediction model for wind turbine noise. IEE Conference Publication, Pages: 177–182, London, UK, 1993. Publ by IEE, Stevenage, England.

[21] P. J. Moriarty, G.o Guidati, and P. Migliore. Prediction of turbulent inflow and trailing-edge noise for wind turbines. Volume: 2 of *Collection of Technical Papers - 11th AIAA/CEAS Aeroacoustics Conference*, Pages: 1040–1055, 2005.

[22] S. A. L. Glegg, S. M. Baxter, and A. G. Glendinning. Prediction of Broadband Noise from Wind Turbines. *Journal of Sound and Vibration*, 118(2), pp217–239, 1987.

[23] A. R. George. Comparison of Broadband Noise Mechanisms, Analyses, and Experiments on Rotors. *Journal of Aircraft*, 21(8), pp583–592, 1984.

[24] Product Certification Scheme Requirements: Micro and Small Wind Turbines, Microgeneration Certification Scheme: MCS 006, BWEA, July 2009.

[25] Small Wind Turbine Performance and Saftey Standard, BWEA, February 2008.

[26] Wind Turbine Generator Systems Acoustic Noise Measurement Techniques, British Standards, BS61400-11(2003), 2003.

[27] B. D. Vick and R. N. Clark. Using Rotor Tip Speed in the Acoustical Analysis of Small Wind Turbines. Volume: 1334 of *46th AIAA Aerospace Sciences Meeting and Exhibit*, Pages: 16275–16285, Reno, Nevada, January 2008.

[28] A. de Bruijn, W. J. Stam, and W. B. de Wolf. Determination of the Acoustic Source Power Levels of Wind Turbines. Commission of the European Communities, (Report) EUR, Pages: 889–894, Hamburg, West Germany, 1985.

[29] R. Meir, M. L. Legerton, M. B. Anderson, B. Berry, A. Bullmore, M. Hayes, M. Jiggins, E. Leeming, P. Musgrove, D. J. Spode, H. A. Thomas, E. Tomalin, M. Trinicik, and J. Warren. The Assessment and Rating of Noise from Wind Farms. Technical report, Noise Working Group, 2006.

[30] Method for Rating industrial noise affecting mixed residential and industrial areas, British Standards, BS4142:1997, 1997.

[31] Acoustics - Attenuation of sound during propagation outdoors, Part 1: Calculation of the absorption of sound by the atmosphere, International Organisation for Standards, ISO 9613-1:1993, 1993.

[32] Acoustics - Attenuation of sound during propagation outdoors, Part 2: General method of calculation, International Organisation for Standards, ISO 9613-2:1996, 1996.

[33] Occupational and Community Noise, 2001. URL `http://www.who.int/mediacentre/factsheets/fs258/en`

[34] S. Oerlemans, P. Sijtsma, and B. Mendez Lopez. Location and quantification of noise sources on a wind turbine. *Journal of Sound and Vibration*, 299(4-5), pp869–883, 2007.

[35] P. Migliore, J. Van Dam, and A. Huskey. Acoustic tests of small wind turbines. Collection of ASME Wind Energy Symposium Technical Papers AIAA Aerospace Sciences Meeting and Exhibit, Pages: 529–542, Reno, NV, United States, 2004.

[36] Y. Nii, H. Matsumiya, and T. Kogaki. Acoustic performances of a vertical board for wind turbine noise immission measurements. *Acoustical Science and Technology*, 24(2), pp83–89, 2003.

[37] Y. Nii. Sound level distributions on a circular ground board for wind turbine noise measurements. *Noise Control Engineering Journal*, 50(3), pp81–89, 2002.

[38] M. Bjorkman. Long time measurements of noise from wind turbines. *Journal of Sound and Vibration*, 277(3), pp567–572, 2004.

[39] S. S. Jung, W. S. Cheung, C. Cheong, and S. H. Shin. Experimental Identification of Acoustic Emission Characteristics of Large Wind Turbines with Emphasis on Infrasound and Low-Frequency Noise. *Journal of the Korean Physical Society*, 53(4), pp1897–1905, 2008.

[40] P. Migliore and S. Oerlemans. Wind tunnel aeroacoustic tests of six airfoils for use on small wind turbines. Collection of ASME Wind Energy Symposium Technical Papers AIAA Aerospace Sciences Meeting and Exhibit, Pages: 543–557, Reno, NV, United States, 2004.

[41] T. Cho, C. Kim, and D. Lee. Acoustic measurement for 12 percent scaled model of NREL Phase VI wind turbine by using beamforming. *Current Applied Physics*, 10, ppS320–S325, 2010.

[42] W. Merzkirch. *Flow visualization.* Academic Press, Orlando, 2nd edition, 1987.

[43] A.J. Smits T.T. Lim, editor. *Flow visualization techniques and examples.* Imperial College Press, London, 2000.

[44] T. Nakano, N. Fujisawa, Y. Oguma, Y. Takagi, and S. Lee. Experimental study on flow and noise characteristics of NACA0018 airfoil. *Journal of Wind Engineering and Industrial Aerodynamics*, 95(7), pp511–531, 2007.

[45] A. Nashimoto, N. Fujisawa, T. Nakano, and T. Yoda. Visualization of aerodynamic noise source around a rotating fan blade. *Journal of Visualization*, 11(4), pp365–373, 2008.

[46] D. E. Neff and R. N. Meroney. Mean wind and turbulence characteristics due to induction effects near wind turbine rotors. *Journal of Wind Engineering and Industrial Aerodynamics*, 71, pp413–422, 1997.

[47] S. Tomimatsu and N. Fujisawa. Measurement of aerodynamic noise and unsteady flow field around a symmetrical airfoil. *Journal of Visualization*, 5(4), pp381–388, 2002.

[48] M. Raffel, C. Willert, and J. Kompenhans. *Particle image velocimetry, a practical guide*. Experimental fluid mechanics. Springer, Berlin, 1998.

[49] Summary Test Report For Ampair 600/230 Mk 2.5 Version 2, 2009. URL `http://www.ampair.com/downloads`.

[50] Evance Iskra R9000 Acoustic Noise Assessment according to BWEA Performance and Safety Standard - Summary Issue 2, 2009. URL `www.windturbine.ltd.uk/downloads/evance/21-evancenoisereport/download`.

[51] K. P. Waye and E. Ohrstrom. Psycho-acoustic characters of relevance for annoyance of wind turbine noise. *Journal of Sound and Vibration*, 250(1), pp65–73, 2002.

[52] L. A. Page, K. J. Petrie, and S. C. Wessely. Psychosocial responses to environmental incidents: A review and a proposed typology. *Journal of Psychosomatic Research*, 60(4), pp413–422, 2006.

[53] K. J. Petrie, B. Sivertsen, M. Hysing, E. Broadbent, R. Moss-Morris, H. R. Eriksen, and H. Ursin. Thoroughly modern worries - The relationship of worries about modernity to reported symptoms, health and medical care utilization. *Journal of Psychosomatic Research*, 51(1), pp395–401, 2001.

[54] Nina Pierpont. *Wind Turbine Syndrome: A Report on a Natural Experiment*. K-Selected Books, 2009.

[55] K. Kroenke and R. L. Spitzer. Gender differences in the reporting of physical and somatoform symptoms. *Psychosomatic Medicine*, 60(2), pp150–155, 1998.

[56] J. W. Pennebaker. THE Symptom-Guessing Game. *Psychology Today*, 16(1), pp51, 1982.

[57] S. McMahan and J. Meyer. Symptom prevalence and worry about high voltage transmission lines. *Environmental Research*, 70(2), pp114–118, 1995.

[58] E. Ferguson, K. Daniels, and D. Jones. Negatively oriented personality and perceived negative job characteristics as predictors of future psychological and physical symptoms: A meta-analytic structural modelling approach. *Journal of Psychosomatic Research*, 60(1), pp45–52, 2006.

[59] A. M. Simon. A Summary of Research Conducted into Attitudes to Wind Power from 1990-1996, 1996. URL `http://www.bwea.com/ref/surveys-90-96.html`.

[60] G. Belojevic, B. Jakovljevic, and O. Aleksic. Subjective reactions to traffic noise with regard to some personality traits. *Environment International*, 23(2), pp221–226, 1997.

[61] S. A. Stansfeld and M. P. Matheson. Noise pollution: non-auditory effects on health. *British Medical Bulletin*, 68, pp243–257, 2003.

[62] K. Kroenke. Studying symptoms: Sampling and measurement issues. *Annals of Internal Medicine*, 134(9), pp844–853, 2001.

[63] N. D. Weinstein. Individual-differences in reactions to noise - longitudinal-study in a college dormitory. *Journal of Applied Psychology*, 63(4), pp458–466, 1978.

[64] E. Pedersen and H. i Halmstad. Noise Annoyance from Wind Turbines: a review, Report 5308. Technical report, Swedish Environmental Protection Agency, 2003.

[65] E. Pedersen and K. P. Waye. Wind turbines - low level noise sources interfering with restoration? *Environmental Research Letters*, 3(1), pp1–5, 2008.

[66] E. Pedersen and K. P. Waye. Wind turbine noise, annoyance and self-reported health and well-being in different living environments. *Occupational and Environmental Medicine*, 64(7), pp480–486, 2007.

[67] N. M. Moreira and M. E. Bryan. Noise annoyance susceptibility. *Journal of Sound and Vibration*, 21(4), pp449–end, 1972.

[68] P. Lercher. Environmental noise and health: an integrated research perspective. *Environment International*, 22, pp117–128, 1996.

[69] S. A. Stansfeld, D. S. Sharp, J. Gallacher, and W. Babisch. Road traffic noise, noise sensitivity and psychological disorder. *Psychological Medicine*, 23(4), pp977–985, 1993.

[70] I. M. Engelhard, M. A. van den Hout, and M. Kindt. The relationship between neuroticism, pre-traumatic stress, and post-traumatic stress: a prospective study. *Personality and Individual Differences*, 35(2), pp381–388, 2003.

[71] D. K. Kennedy and B. M. Hughes. The optimism-neuroticism question: An evaluation based on cardiovascular reactivity in female college students. *Psychological Record*, 54(3), pp373–386, 2004.

[72] T. R. Schneider. The role of neuroticism on psychological and physiological stress responses. *Journal of Experimental Social Psychology*, 40(6), pp795–804, 2004.

[73] D. C. Glass and J. E. Singer. *Urban Stress. Experiments on Noise and Social Stressors.* Academic Press, New York, 1972.

[74] N. D. Weinsten. Individual differences in critical tendencies and noise annoyance. *Journal of Sound and Vibration*, 68, pp241–248, 1980.

[75] C. Lawrence. Measuring individual responses to aggression-triggering events: Development of the Situational Triggers of Aggressive Responses (STAR) scale. *Aggressive Behavior*, 32(3), pp241–252, 2006.

[76] G. W. Evans and R. Stecker. Motivational consequences of environmental stress. *Journal of Environmental Psychology*, 24(2), pp143–165, 2004.

[77] J. Hatfield, R. F. S. Job, A. J. Hede, N. L. Carter, P. Peploe, R. Taylor, and S. Morrell. Human response to environmental noise: The role of perceived control. *International Journal of Behavioral Medicine*, 9(4), pp341–359, 2002.

[78] D. Watson and J. W. Pennebaker. Health complaints, stress, and distress - Exploring the central role of negative affectivity. *Psychological Review*, 96(2), pp234–254, 1989.

[79] J. P. David, P. J. Green, R. Martin, and J. Suls. Differential roles of neuroticism, extraversion, and event desirability for mood in daily life: An integrative model of top-down and bottom-up, influences. *Journal of Personality and Social Psychology*, 73(1), pp149–159, 1997.

[80] N. Harrington. The frustration discomfort scale: Development and psychometric properties. *Clinical Psychology & Psychotherapy*, 12(5), pp374–387, 2005.

[81] D. Watson, L. A. Clark, and A. Tellegen. Development and validation of brief measures of positive and negative affect - The PANAS Scales. *Journal of Personality and Social Psychology*, 54(6), pp1063–1070, 1988.

[82] L. R. Goldberg, J. A. Johnson, H. W. Eber, R. Hogan, M. C. Ashton, C. R. Cloninger, and H. C. Gough. The International Personality Item Pool and the future of public-domain personality measures. *Journal of Research in Personality*, 40, pp84–96, 2006.

[83] M. Isaac, A. Janca, K. C. Burke, J. A. C. E. Silva, S. W. Acuda, A. C. Altamura, J. D. Burke, C. R. Chandrashekar, C. T. Miranda, and G. Tacchini. Medically unexplained somatic symptoms in different cultures a preliminary report from phase 1 of the world health organization international study of somatoform disorders. *Psychotherapy Psychosomatics*, 64, pp88–93, 1995.

[84] B. J. Zhang, L. L. Shi, and G. Q. Di. The influence of the visibility of the source on the subjective annoyance due to its noise. *Applied Acoustics*, 64(12), pp1205–1215, 2003.

[85] M. J. Lighthill. On Sound Generated Aerodynamically .1. General Theory. *Proceedings of the Royal Society of London Series a-Mathematical and Physical Sciences*, 211(1107), pp564–587, 1952.

[86] M. J. Lighthill. On Sound Generated Aerodynamically .2. Turbulence as a source of sound. *Proceedings of the Royal Society of London Series a-Mathematical and Physical Sciences*, 222 (1148), pp1–32, 1954.

[87] J. E. Ffowcs-Williams and D. L. Hawkings. Sound Generation by Turbulence and Surfaces in Arbitrary Motion. *Philosophical Transactions of the Royal Society of London*, 264(No. a 1151), pp321–342, 1969.

[88] R. K. Amiet. Acoustic Radiation from an Airfoil in a Turbulent Stream. *Journal of Sound and Vibration*, 41(4), pp407–420, 1975.

[89] H. Lamb. *Hydrodynamics*. Dover Publications, New York, 6th edition, 1932.

[90] N. Curle. The influence of solid boundaries upon aerodynamic sound. *Proceedings of the Royal Society*, A231, pp505–514, 1955.

[91] O. Fleig, M. Iida, and C. Arakawa. Blade tip flow and noise prediction by Large-Eddy Simulation in horizontal axis wind turbines. Pages: 689–698, 2005.

[92] P. J. Moriarty, G. Guidati, and P. G. Migliore. Recent improvement of a semi-empirical aeroacoustic prediction code for wind turbines. Volume: 3 of *Collection of Technical Papers - 10th AIAA/CEAS Aeroacoustics Conference*, Pages: 2742–2757, Manchester, United Kingdom, 2004.

[93] R. H. Schlinker and R. K. Amiet. Helicopter rotor trailing edge noise. Page: 149, 1981.

[94] M. R. Fink. Noise Component Method for Airframe Noise. *Journal of Aircraft*, 16(10), pp659–665, 1979.

[95] M. S. Howe. Review of the Theory of Trailing Edge Noise. *Journal of Sound and Vibration*, 61 (3), pp437–465, 1978.

[96] P. A. Nelson and C. L. Morfey. Aerodynamic sound production in low speed flow ducts. *Journal of Sound and Vibration*, 79(2), pp263–289, 1981.

[97] R. H. Schlinker. Airfoil Trailing Edge Noise Measurements with a Directional Microphone. Pages: 77–1269. AIAA Paper, 1977.

[98] M. R. Fink, R. H. Schlinker, and R. K. Amiet. Prediction of Rotating-Blade Vortex Noise of Non-rotating Blades. *NASA*, CR-2611. NASA, 1976.

[99] P. Fuglsang and H. A. Madsen. Wind turbine design with numerical optimization and a semi-empirical noise prediction model. *Wind Engineering*, 22(1), pp31–41, 1998.

[100] P. Moriarty. NWTC Design Codes (NAFNoise by Pat Moriarty), 2005. URL `http://wind.nrel.gov/DesignCodes/simulators/NAFNoise/`.

[101] P. J. Moriarty. Development and validation of a semi-empirical wind turbine aeroacoustic code. Collection of ASME Wind Energy Symposium Technical Papers AIAA Aerospace Sciences Meeting and Exhibit, Pages: 577–586, Reno, NV, United States, 2004.

[102] C. L. Burley and T. F. Brooks. Rotor Broadband Noise Prediction with Comparison to Model Data. *Journal of the American Helicopter Society*, 49(1), pp28–42, 2004.

[103] M. Drela and H. Youngren. XFOIL Subsonic Airfoil Development System, 2000. URL `http://web.mit.edu/drela/Public/web/xfoil/`.

[104] W. J. Zhu, N. Heilskov, W. Z. Shen, and J. N. Sorensen. Modeling of aerodynamically generated noise from wind turbines. *Journal of Solar Energy Engineering, Transactions of the ASME*, 127 (4), pp517–528, 2005.

[105] C. J. Doolan. A review of airfoil trailing edge noise and its prediction. *Acoustics Australia*, 36 (1), pp7–13, 2008.

[106] R. D. Sandberg and N. D. Sandham. Direct numerical simulation of turbulent flow past a trailing edge and the associated noise generation. *Journal of Fluid Mechanics*, 596, pp353–385, 2008.

[107] F. Mathey. Aerodynamic noise simulation of the flow past an airfoil trailing-edge using a hybrid zonal RANS-LES. *Computers & Fluids*, 37(7), pp836–843, 2008.

[108] E. Manoha, B. Troff, and P. Sagaut. Trailing-edge noise prediction using large-eddy simulation and acoustic analogy. *AIAA Journal*, 38(4), pp575–583, 2000.

[109] M. Iida, O. Fleig, C. Arakawa, and M. Shimooka. Wind turbine flow and noise prediction by large eddy simulation. 43rd AIAA Aerospace Sciences Meeting and Exhibit - Meeting Papers, Pages: 15017–15028, Reno, NV, United States, 2005.

[110] O. Fleig and C. Arakawa. Aeroacoustics simulation around a wind turbine blade using compressible LES and linearized Euler equations. Volume: 2 D of *Proceedings of the ASME/JSME Joint Fluids Engineering Conference*, Pages: 2607–2614, Honolulu, HI, United States, 2003.

[111] O. Fleig, M. Iida, and C. Arakawa. Wind turbine blade tip flow and noise prediction by large-eddy simulation. *Journal of Solar Energy Engineering, Transactions of the ASME*, 126(4), pp1017–1024, 2004.

[112] M. Wang and P. Moin. Computation of trailing-edge flow and noise using large-eddy simulation. *AIAA Journal*, 38(12), pp2201–2209, 2000.

[113] W. Z. Shen and J. N. Sorensen. Aero-acoustic modelling using Large Eddy simulation - art. no. 012085. *Science of Making Torque from Wind*, 75, pp12085–12085, 2007.

[114] D. Moroianu and L. Fuchs. Prediction of wind turbine noise generation and propagation based on an acoustic analogy. Pages: 271–274, 2007.

[115] A. Humpf, E. Ferrer, and X. Munduate. Investigation of computational aeroacoustic tools for noise predictions of wind turbine aerofoils - art. no. 012086. *Science of Making Torque from Wind*, 75, pp12086–12086, 2007.

[116] A. Tadamasa and M. Zangeneh. Numerical prediction of wind turbine noise. *Renewable Energy*, 36(7), pp1902–1912, 2011.

[117] S. Y. Lin and T. H. Shieh. Study of aerodynamical interference for a wind turbine. *International Communications in Heat and Mass Transfer*, 37(8), pp1044–1047, 2010.

[118] M. S. Campobasso, A. Zanon, E. Minisci, and A. Bonfiglioli. Wake-tracking and turbulence modelling in computational aerodynamics of wind turbine aerofoils. *Proceedings of the Institution of Mechanical Engineers Part a-Journal of Power and Energy*, 223(A8), pp939–951, 2009.

[119] J. M. M. Monteiro, J. C. Pascoa, and F. MR. P. Brojo. Simulation of the Aerodynamic Behaviour of a Micro Wind Turbine. International Conference on Renewables Energies and Power Quality (ICREPQ'09), Valencia, Spain, April 2009.

[120] F. Wang, L. Bai, J. Fletcher, J. Whiteford, and D. Cullen. The methodology for aerodynamic study on a small domestic wind turbine with scoop. *Journal of Wind Engineering and Industrial Aerodynamics*, 96(1), pp1–24, 2008.

[121] H. K. Versteeg. *An introduction to computational fluid dynamicsthe finite volume method*. Pearson Prentice Hall, Harlow, 2nd edition, 2007.

[122] J. Wendt and J. Anderson. *Computational fluid dynamics, an introduction*. Springer, Berlin, 3rd edition, 2009.

[123] *Ansys Fluent 12.0 User's Guide*. 2009.

[124] *Ansys Fluent 12.0 Theory Guide*. 2009.

[125] D. Howitt and D. Cramer. *An introduction to statistics in psychology*. FT Prentice Hall, Harlow, 4th edition, 2008.

[126] A. Aron, E.e Aron, and E. J. Coups. *Statistics for psychology*. Pearson Prentice Hall, Upper Saddle River, N.J., 5th edition, 2009.

[127] J. Pallant. *SPSS survival manual a step by step guide to data analysis using SPSS for Windows*. Open University Press, Maidenhead, 3rd edition, 2007.

[128] Barbara G. Tabachnick and Linda S. Fidell. *Using multivariate statistics*. Pearson/Allyn & Bacon, Boston, 5th edition, 2007.

[129] S. H. Miller. *Experimental design and statistics*. New essential psychology. Routledge, London, 1989.

[130] K. J. Preacher, P. J. Curran, and D. J. Bauer. Computational tools for probing interactions in multiple linear regression, multilevel modeling, and latent curve analysis. *Journal of Educational and Behavioral Statistics*, 31(4), pp437–448, 2006.

Appendix A

Sound Fields from Simple Sources

A.1 Monopole

A monopole sound source radiates sound equally in all directions and the wave front is a perfect sphere hence is radially symmetric. Figure A.1.1 shows the directivity pattern of a monopole which is omnidirectional. The simplest example of a monopole is a pulsating sphere which removes and introduces fluid into the medium alternately (a fluctuating injection of matter) such as is the case with a siren. Monopole sound is also radiated by moving volumes such as a wind turbine rotor blade. The strength of a monopole sound source depends on the rate of change of the mass inflow and outflow as a scalar quantity.

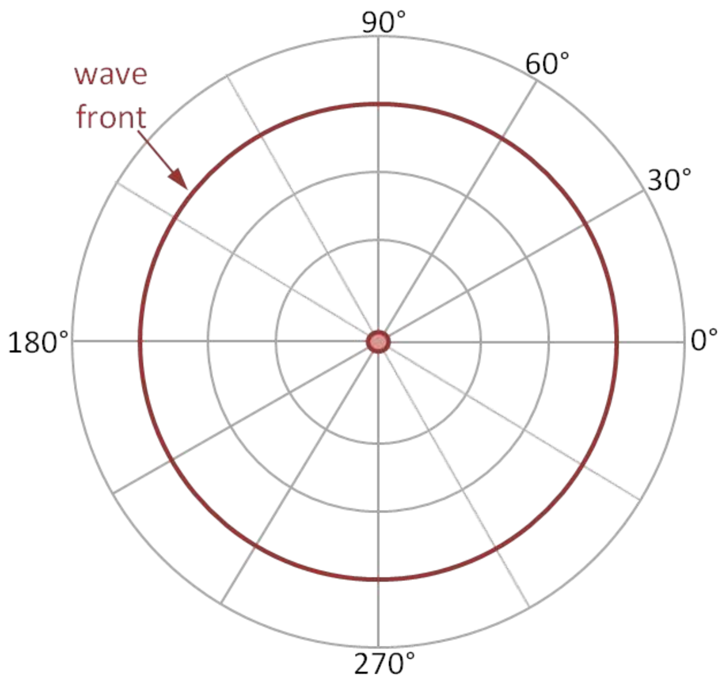

Figure A.1.1: Figure showing the directivity pattern of a monopole

A.2 Dipole

A dipole sound source is simply two monopole sources which alternately introduce and remove fluid into the medium with equal strength but opposite phase, i.e. as one monopole source introduces fluid, the other monopole source removes fluid from the medium (i.e. a fluctuating injection of momentum or an unsteady force acting on a fluid). The two monopoles are separated by a small distance compared with the wavelength of the sound. See Figure A.2.1 for the directivity pattern of a monopole sound source. It can be seen in Figure A.2.1 that the sound is not radiated equally in all directions but is similar to a figure of eight (two lobes). The sound is cancelled at 90º and 270º but radiates well at 0º and 180º. A sphere which oscillates back and forth acts as a dipole sound source. A dipole sound can also be generated by moving surfaces such as a propeller or fan by rotation and fluctuating forces on the blades. The strength of a dipole sound source depends on the force acting on the fluid as a vector quantity.

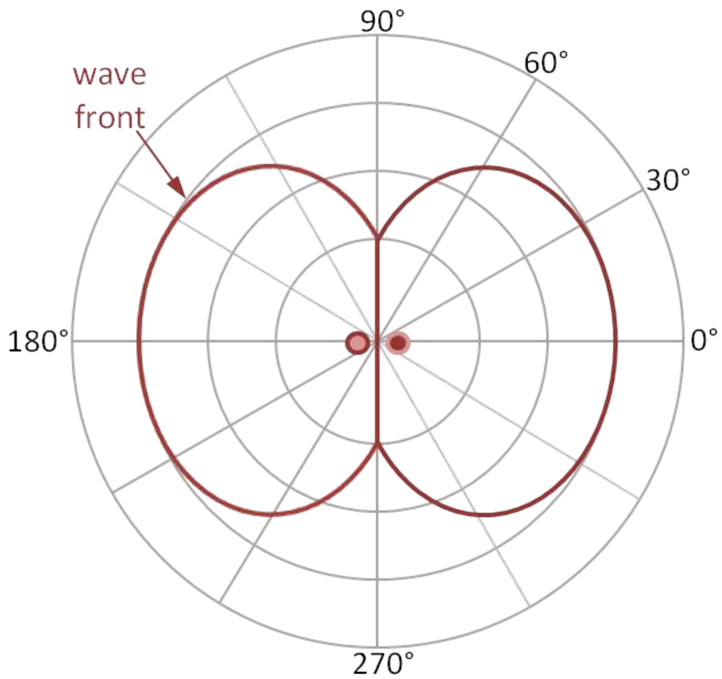

Figure A.2.1: Figure showing the directivity pattern of a dipole

A.3 Quadrupole

Two opposite phase dipoles make up a quadrupole which do not lie along the same line and are actually four monopoles with alternating phase at the corners of a square. The physical mechanism is a system of normal and shear stresses and fluctuating Reynolds stresses. Figure A.3.1 shows the directivity pattern of a quadrupole which is similar to a four leaf clover (four lobes). Sound is radiated well in the 0º, 90º, 180º and 270º directions (i.e. in front of each monopole source) but is cancelled at 45º, 135º, 215º and 315º directions (i.e. at points equidistant from adjacent opposite monopoles).

Sound with quadrupole character occurs in all turbulent flows. The simplest form of a quadrupole is a deforming sphere. The strength of a quadrupole sound source depends on the Lighthill tensor (see Section 4.1.1.1)

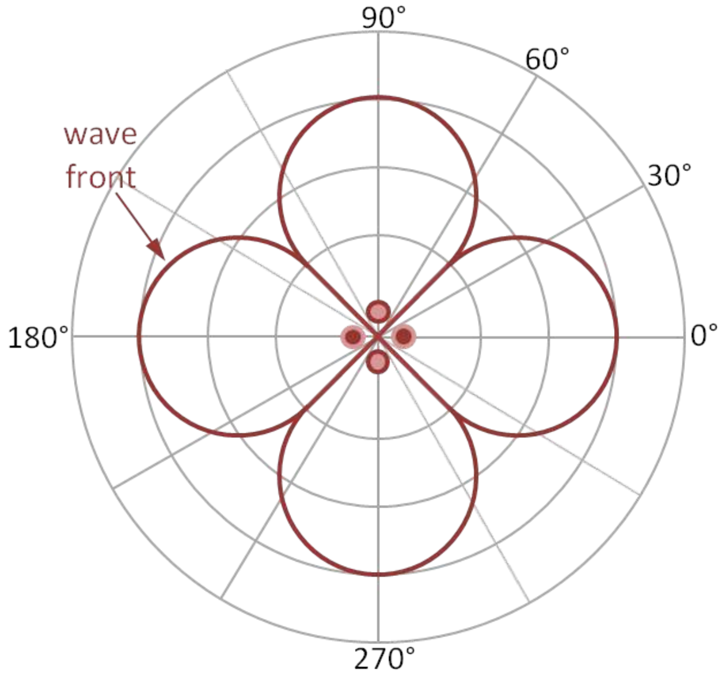

Figure A.3.1: Figure showing the directivity pattern of a lateral quadrupole

Appendix B

A-weighting values

Frequency (Hz)	Weighting (dB)	Frequency (Hz)	Weighting (dB)
16	-56.4	500	-3.2
20	-50.4	630	-1.9
25	-44.7	800	-0.8
31.5	-39.4	1000	0.0
40	-34.6	1250	0.6
50	-30.2	1600	1.1
63	-26.2	2000	1.2
80	-22.5	2500	1.3
100	-19.1	3150	1.2
125	-16.1	4000	1.1
160	-13.4	5000	-0.5
200	-10.9	6300	-0.1
250	-8.6	8000	-1.1
315	-6.6	10000	-2.5
400	-4.8	12500	-4.3

Appendix C

Noise Measurement Plots

C.1 Installation (a)

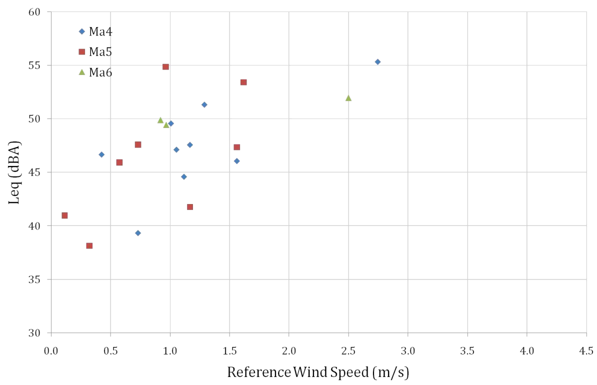

Figure C.1.1: Scatter chart showing how noise levels vary with wind speed for measurement locations at installation (a)

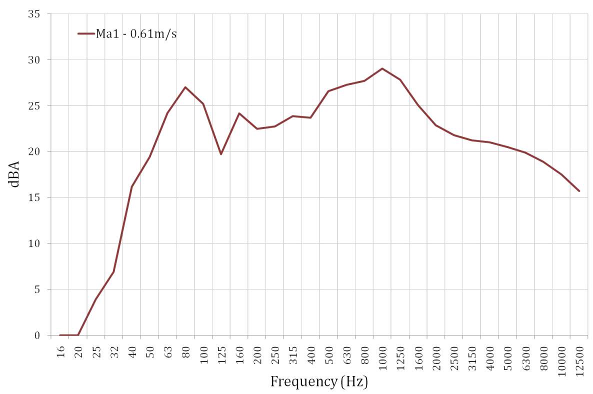

Figure C.1.2: Frequency spectrum when turbine not turning with a low reference wind speed approximately 0.61m/s

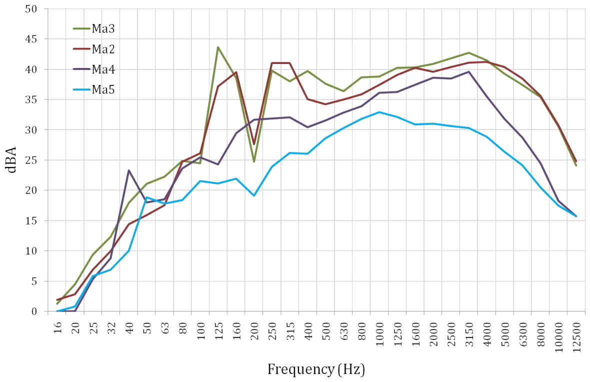

Figure C.1.3: Measurements at increasing distances from the turbine with low reference wind speeds approximately 1.17m/s

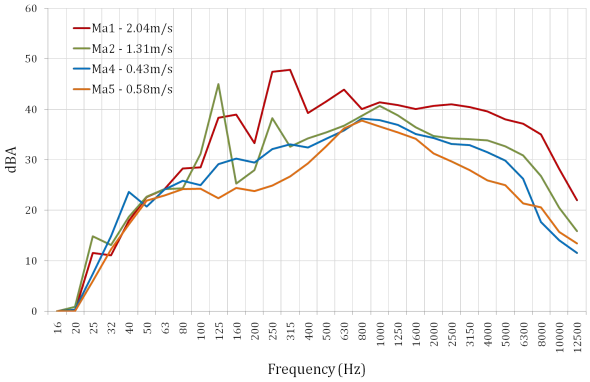

Figure C.1.4: Measurements at increasing distances from the turbine with reference wind speeds up to 2.04m/s

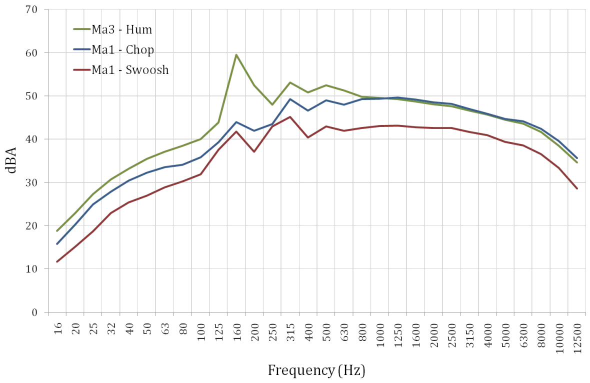

Figure C.1.5: Comparison of different turbine sounds with high reference wind speeds of approximately 3.67m/s

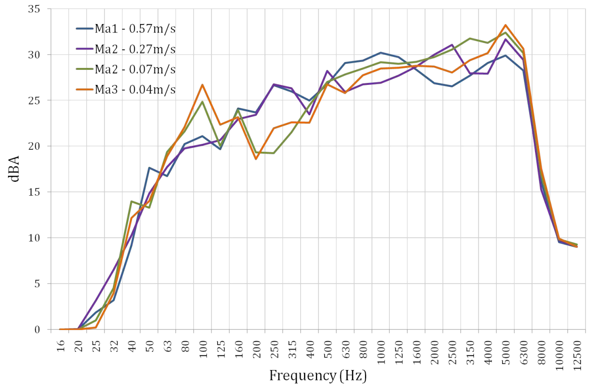

Figure C.1.6: Measurements showing directionality of the noise close to the turbine with low reference wind speeds up to 0.57m/s

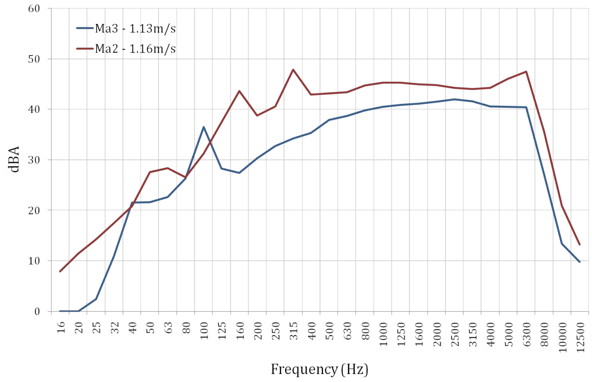

Figure C.1.7: Measurements showing directionality of the noise close to the turbine with low reference wind speeds up to 1.16m/s

C.2 Installation (b)

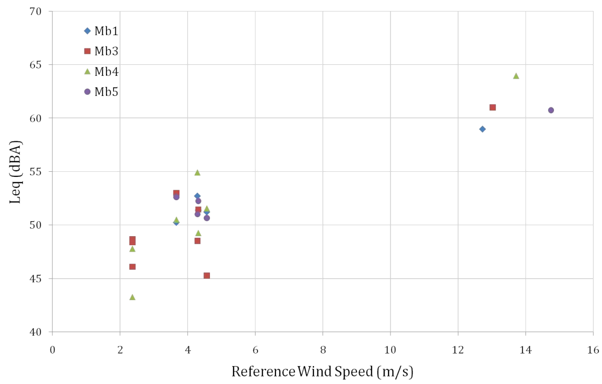

Figure C.2.1: Scatter chart showing how noise levels vary with wind speed for measurement locations at installation (b)

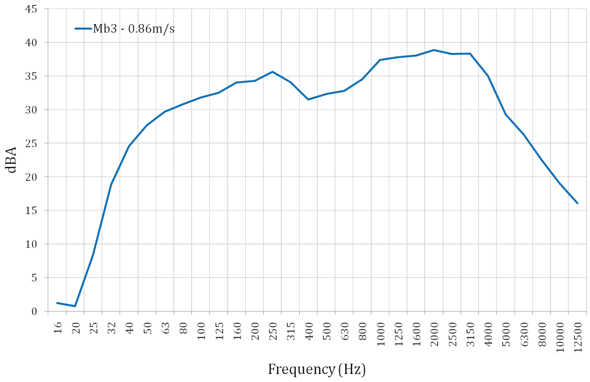

Figure C.2.2: Frequency spectrum when turbines not turning with a low reference wind speed approximately 0.86m/s

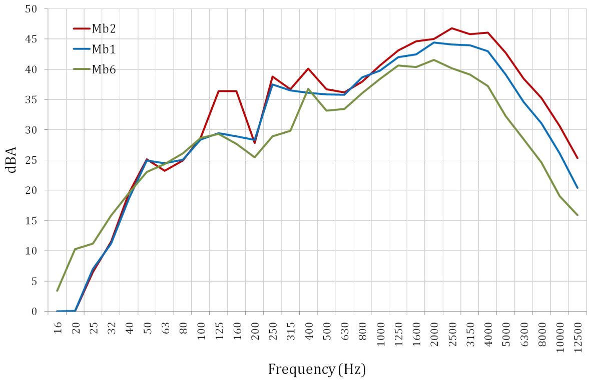

Figure C.2.3: Measurements at increasing distances from the turbines with low reference wind speeds approximately 1.56m/s

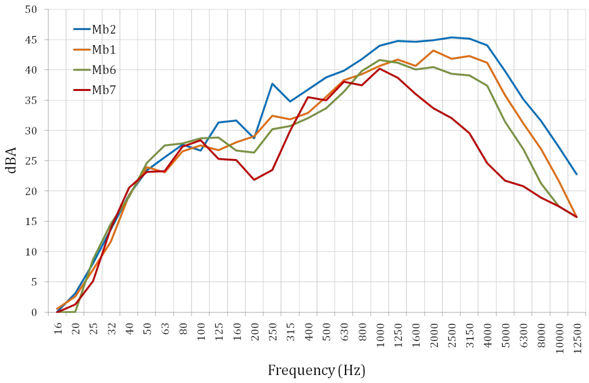

Figure C.2.4: Measurements at increasing distances from the turbines with low reference wind speeds approximately 1.57m/s

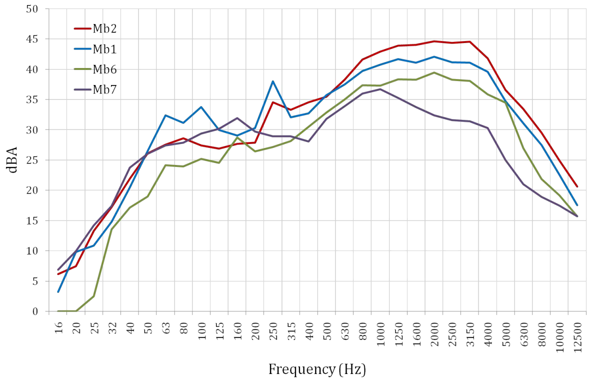

Figure C.2.5: Measurements at increasing distances from the turbines with low reference wind speeds approximately 1.66m/s

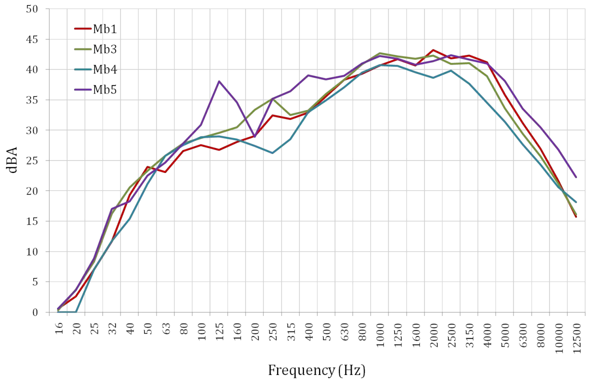

Figure C.2.6: Measurements showing directionality of the noise close to the turbines with low reference wind speeds up to 1.57m/s

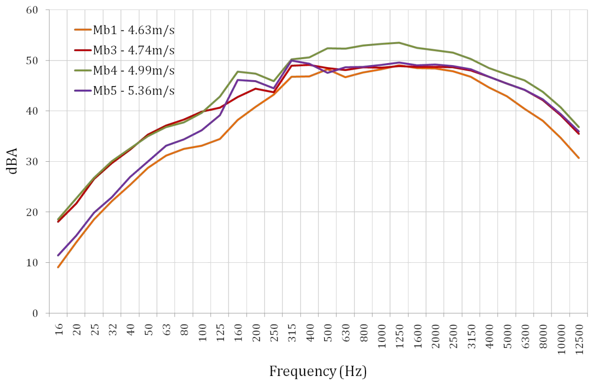

Figure C.2.7: Measurements showing directionality of the noise close to the turbines with high reference wind speeds up to 5.36m/s

C.3 Installation (c)

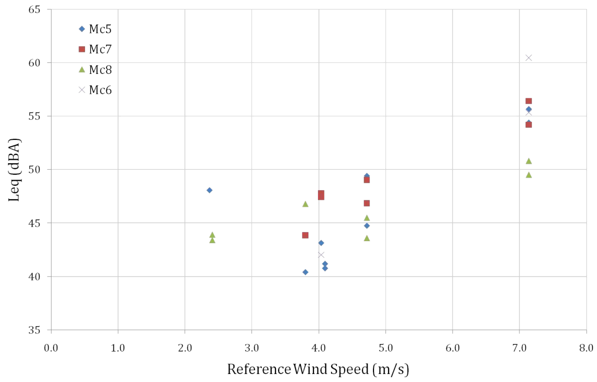

Figure C.3.1: Scatter chart showing how noise levels vary with wind speed for measurement locations at installation (c)

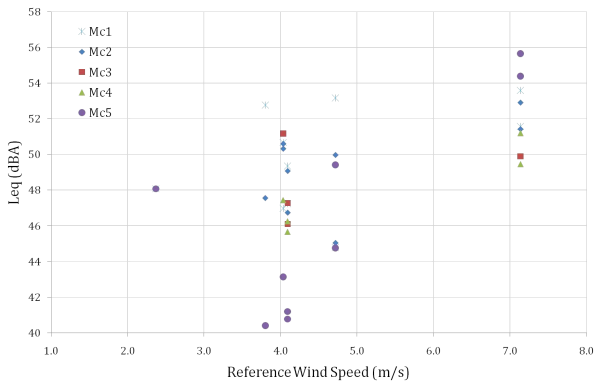

Figure C.3.2: Scatter chart showing how noise levels vary with wind speed for measurement locations at installation (c)

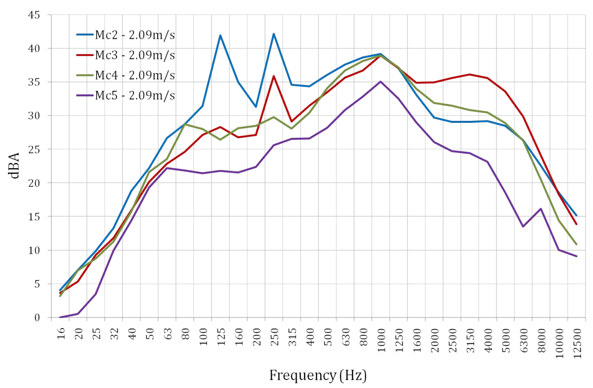

Figure C.3.3: Measurements at increasing distances from the turbine with mid reference wind speeds approximately 2.09m/s

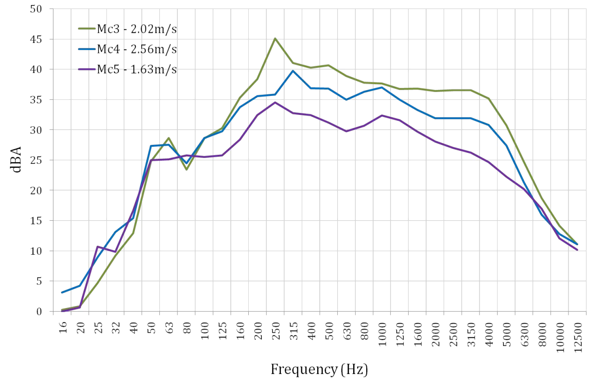

Figure C.3.4: Measurements at increasing distances from the turbine with mid reference wind speeds up to 2.56m/s

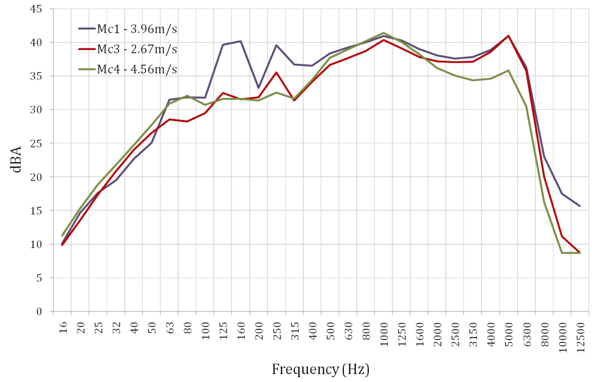

Figure C.3.5: Measurements at increasing distances from the turbine with high reference wind speeds up to 4.56m/s

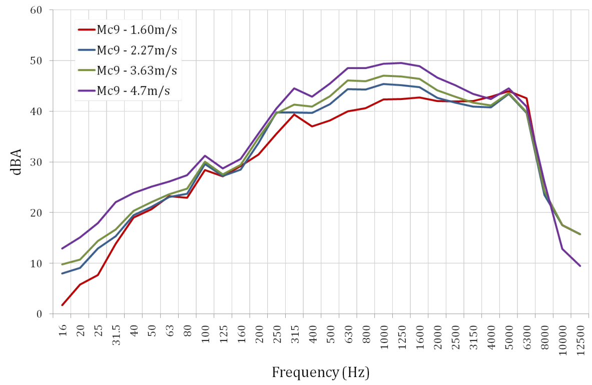

Figure C.3.6: Comparison of different turbine sounds measured at the same location with varying reference wind speeds up to 4.70m/s

C.4 Installation (d)

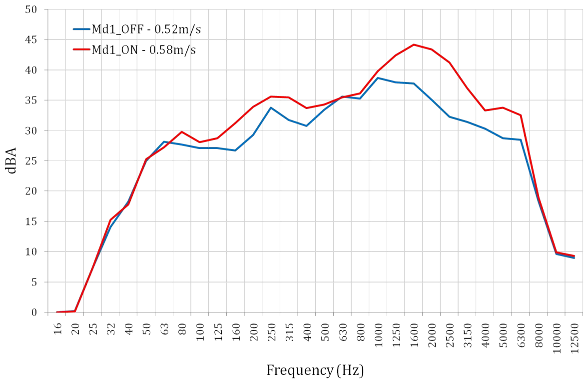

Figure C.4.1: Measurements with the turbines on and off with low reference wind speeds approximately 0.58m/s

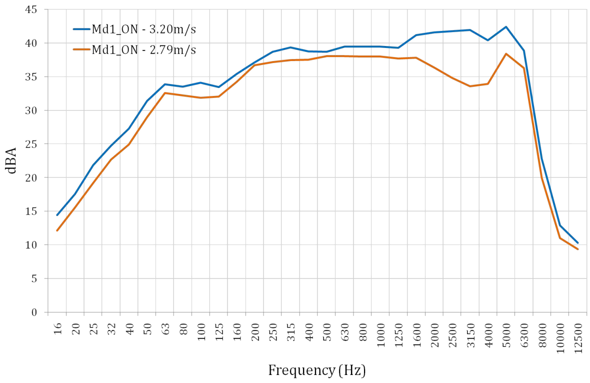

Figure C.4.2: Measurements with the turbines on and off mid reference wind speeds up to 3.20m/s

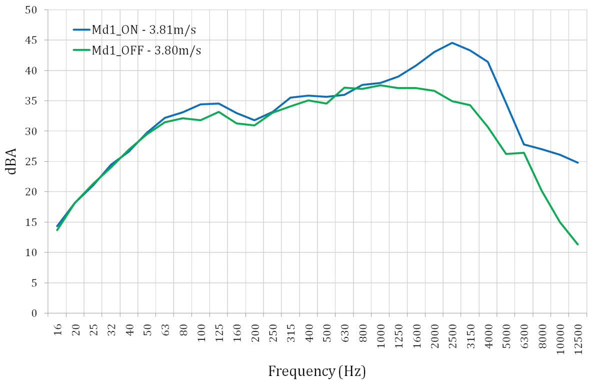

Figure C.4.3: Measurements with the turbines on and off with high reference wind speeds approximately 3.81m/s

C.5 Installation (e)

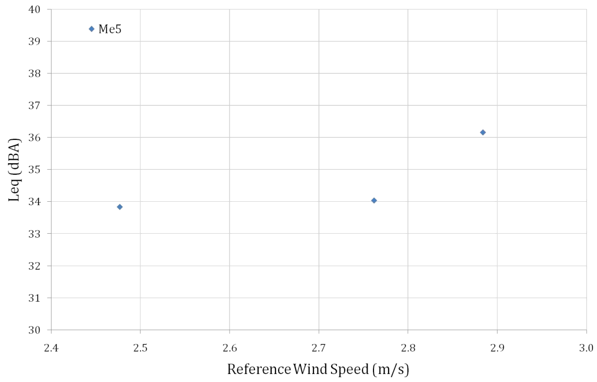

Figure C.5.1: Scatter chart showing how noise levels vary with wind speed for measurement locations at installation (e)

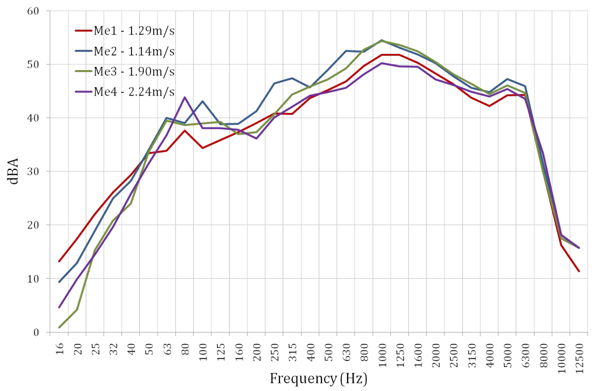

Figure C.5.2: Measurements at increasing distances from the turbine with reference wind speeds up to 2.24m/s

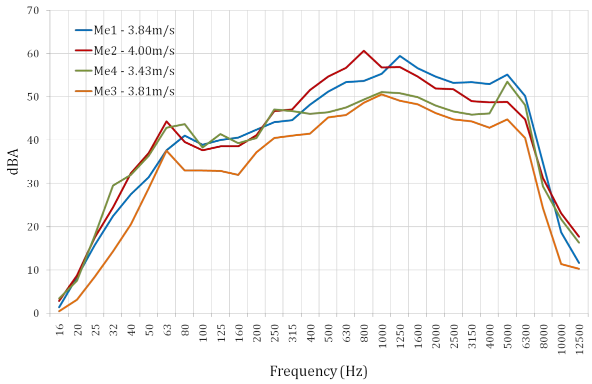

Figure C.5.3: Measurements at increasing distances from the turbine with high reference wind speeds up to 4.00m/s

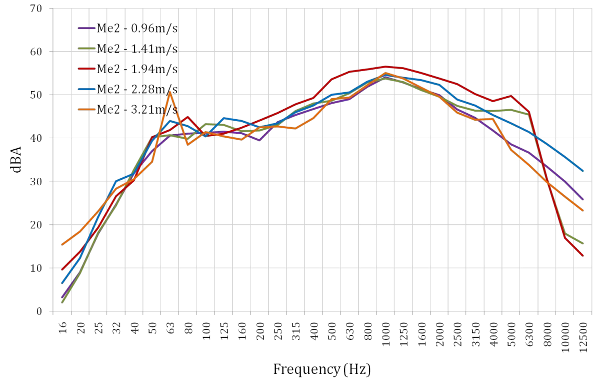

Figure C.5.4: Measurements taken in the same location with increasing reference wind speeds up to 3.21m/s

C.6 Installation (f)

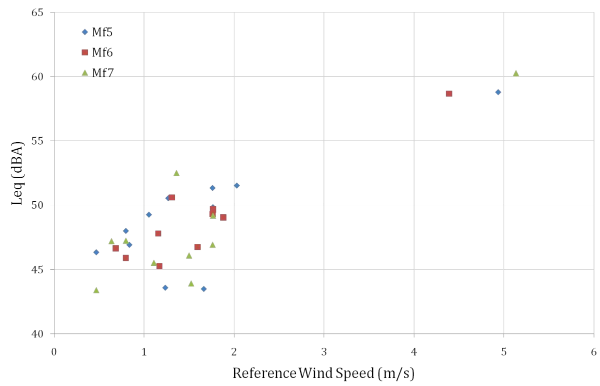

Figure C.6.1: Scatter chart showing how noise levels vary with wind speed for measurement locations at installation (f)

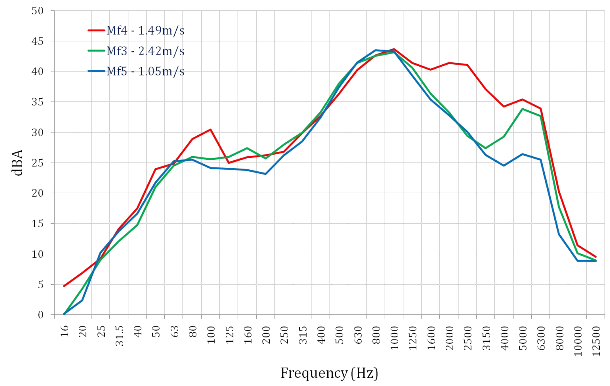

Figure C.6.2: Measurements at increasing distances from the turbine with reference wind speeds up to 2.42m/s

C.7 Installation (g)

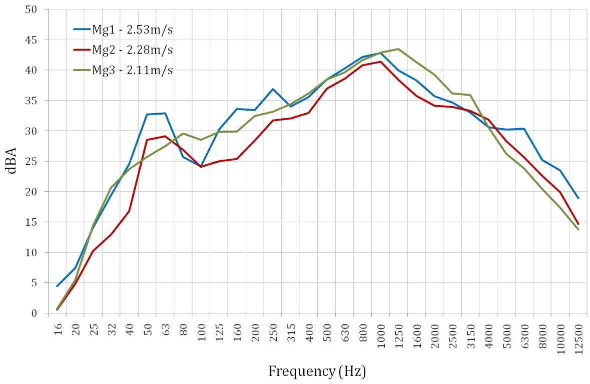

Figure C.7.1: Measurements at from all measurement locations with reference wind speeds up to 2.53m/s

Appendix D

CadnaA Sound Maps

D.1 Colour Palettes

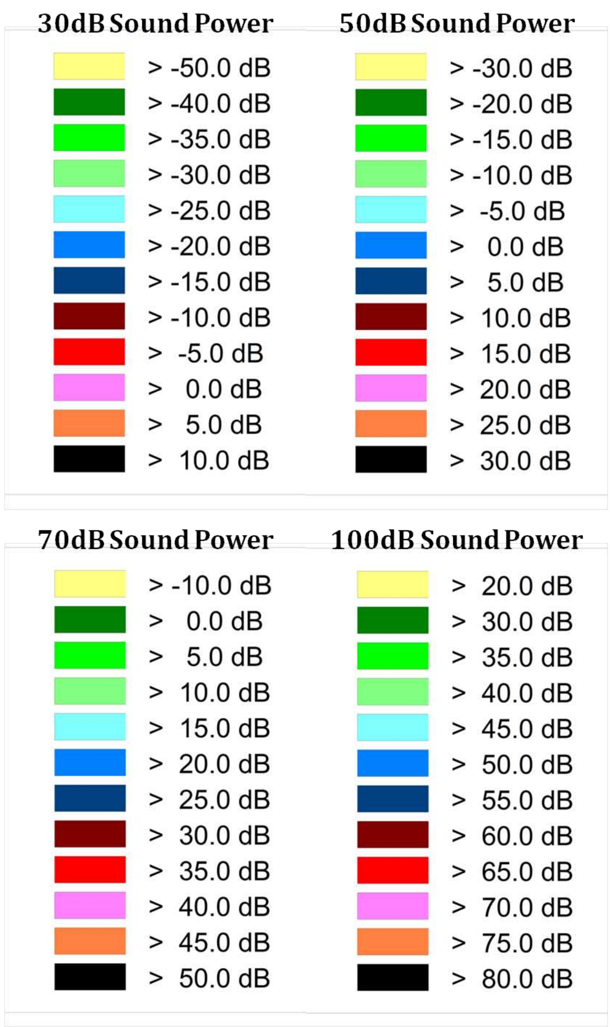

Figure D.1.1: Colour palettes for sound maps produced using CadnaA software package for a 30dB, 50dB, 70dB and 100dB sound power point source

D.2 Sound Maps

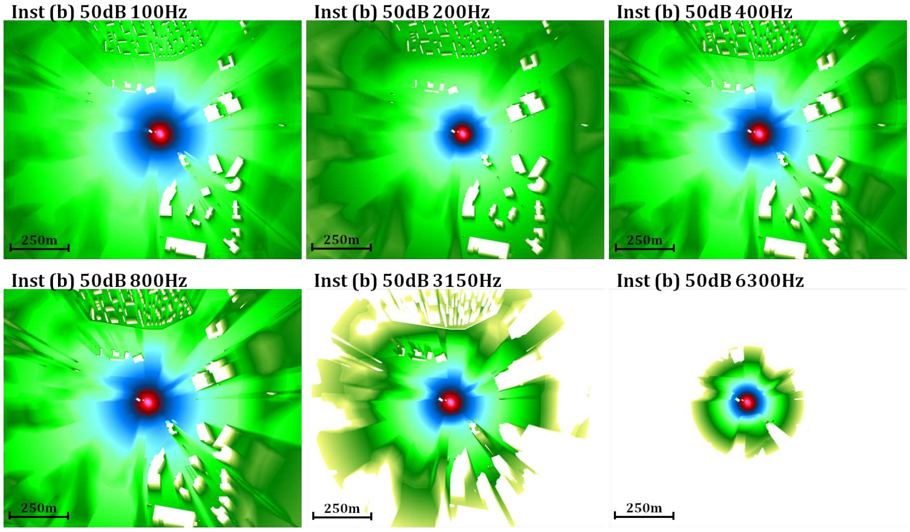

Figure D.2.1: Sound maps for installation (b) with a point sound source at each of the turbine hubs with a sound power of 50dB at 100Hz, 200Hz, 400Hz, 800Hz, 3150Hz and 6300Hz

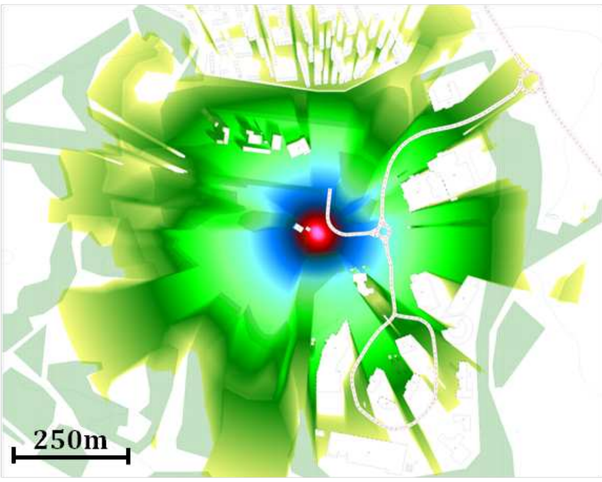

Figure D.2.2: Map of installation (b) showing area topography, sound pressure levels at building facades and the sound pressure contours.

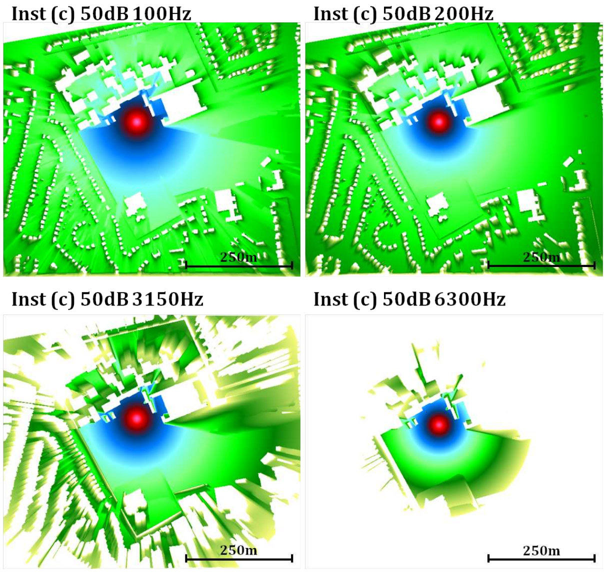

Figure D.2.3: Sound maps for installation (c) with a point sound source at the turbine hub with a sound power of 50dB at 100Hz, 200Hz, 3150Hz and 6300Hz

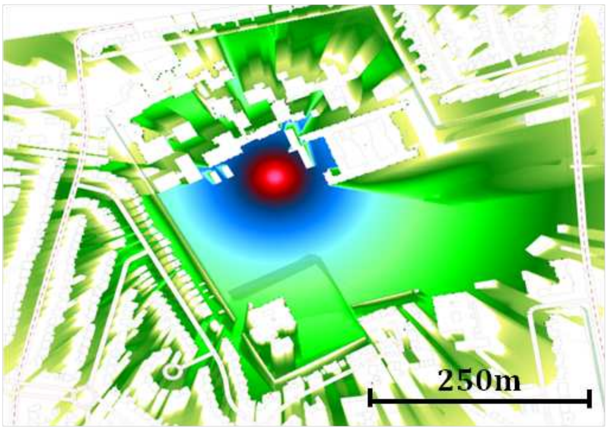

Figure D.2.4: Map of installation (c) showing area topography, sound pressure levels at building facades and the sound pressure contours.

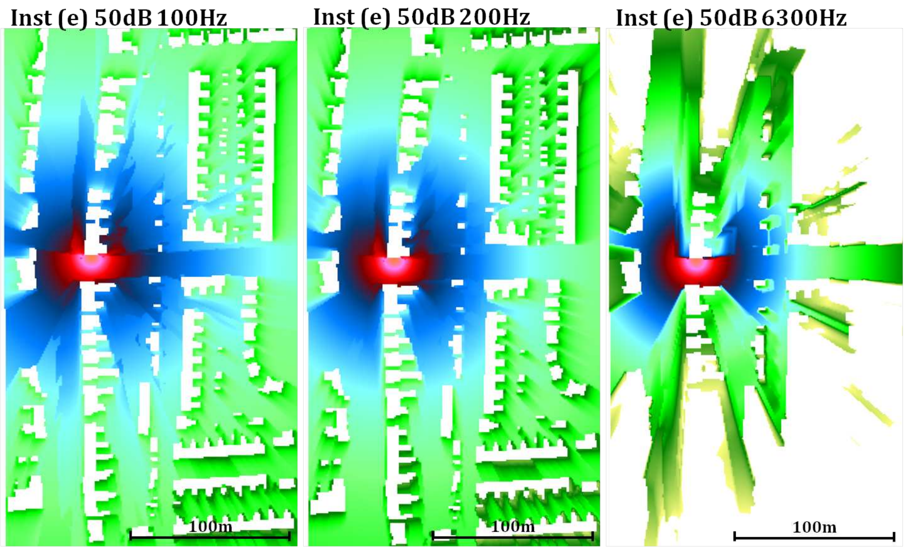

Figure D.2.5: Sound maps for installation (e) with a point sound source at the turbine hub with a sound power of 50dB at 100Hz, 200Hz and 6300kHz

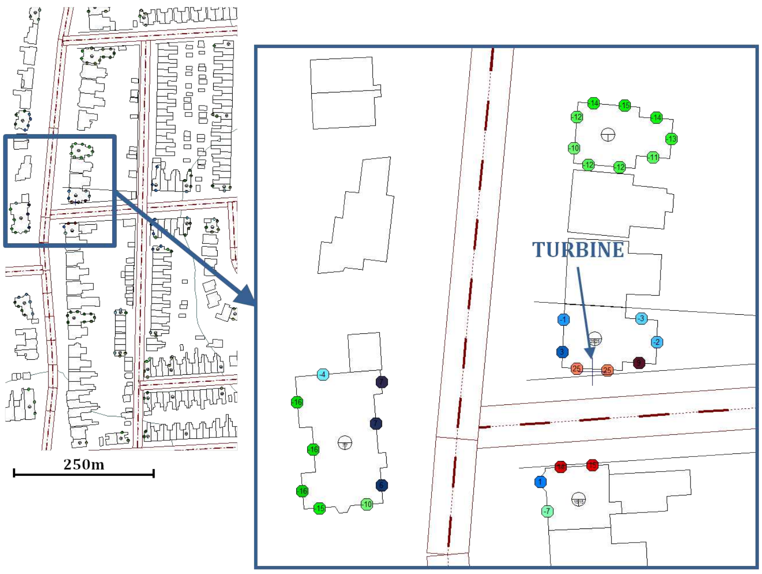

Figure D.2.6: Map of installation (e) showing area topography and sound pressure levels at building facades close to the turbines

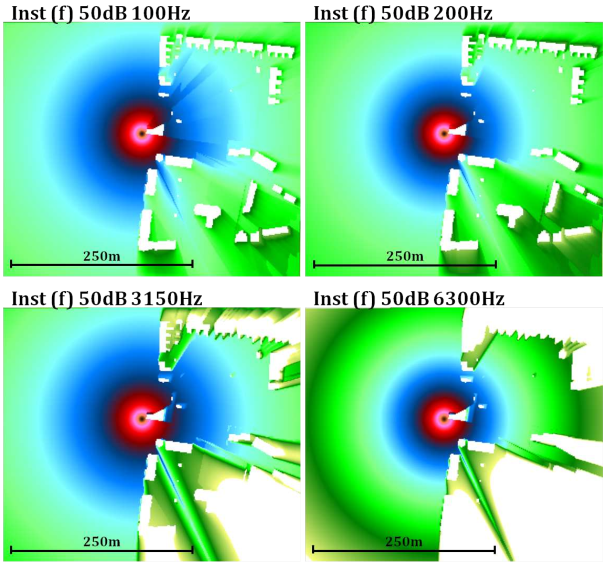

Figure D.2.7: Sound maps for installation (f) with a point sound source at the turbine hub with a sound power of 50dB at 100Hz, 200Hz, 3150Hz and 6300Hz

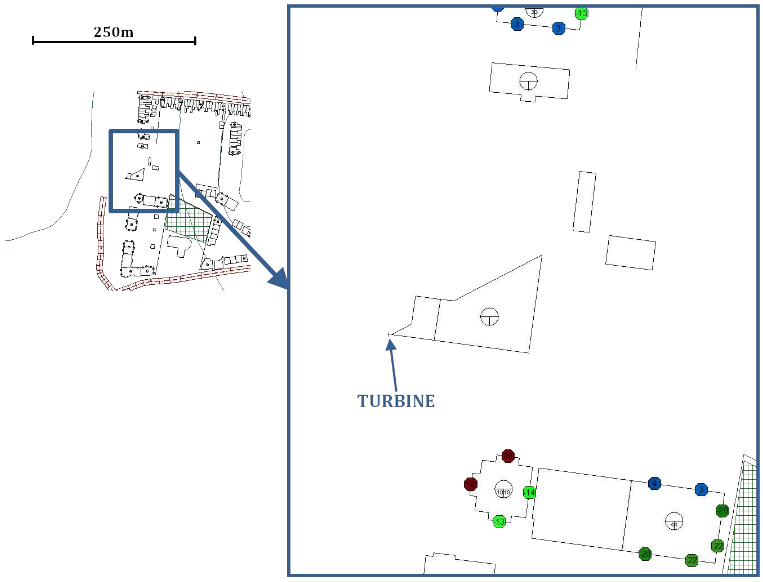

Figure D.2.8: Map of installation (f) showing area topography and sound pressure levels at building facades close to the turbines

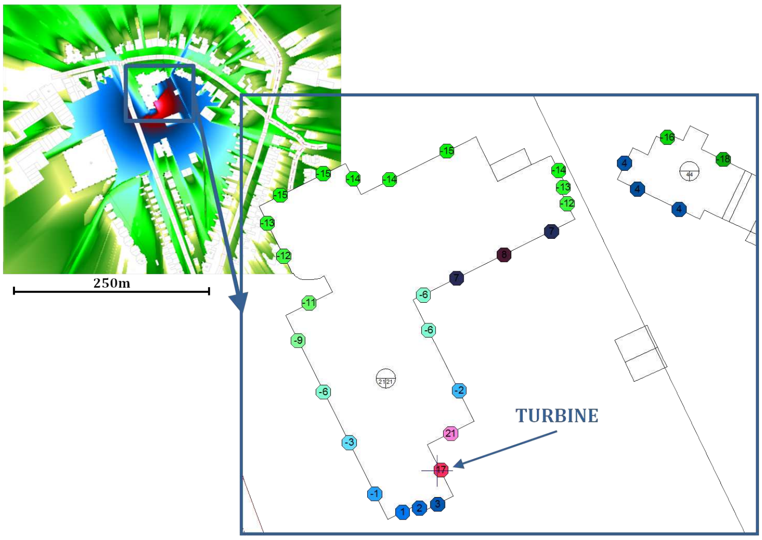

Figure D.2.9: Map of installation (g) showing area topography and sound pressure levels at building facades close to the turbines

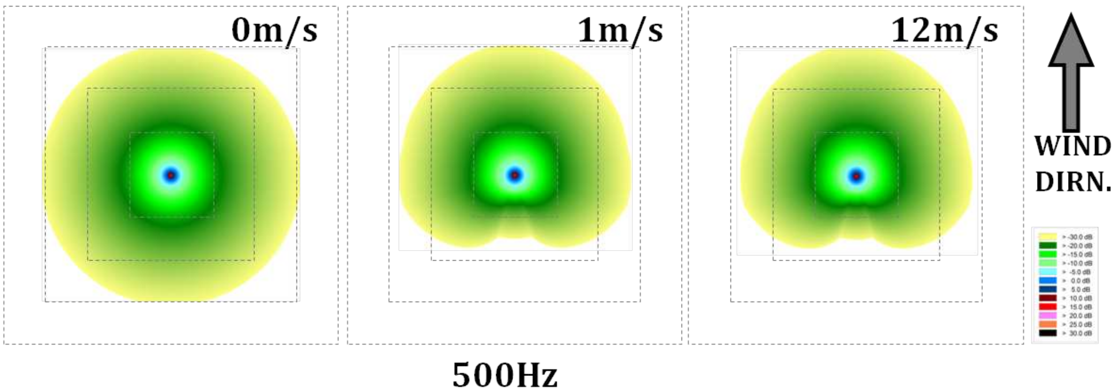

Figure D.2.10: Sound map showing the effect of wind speed on a 50dB point source of sound at 12.5Hz

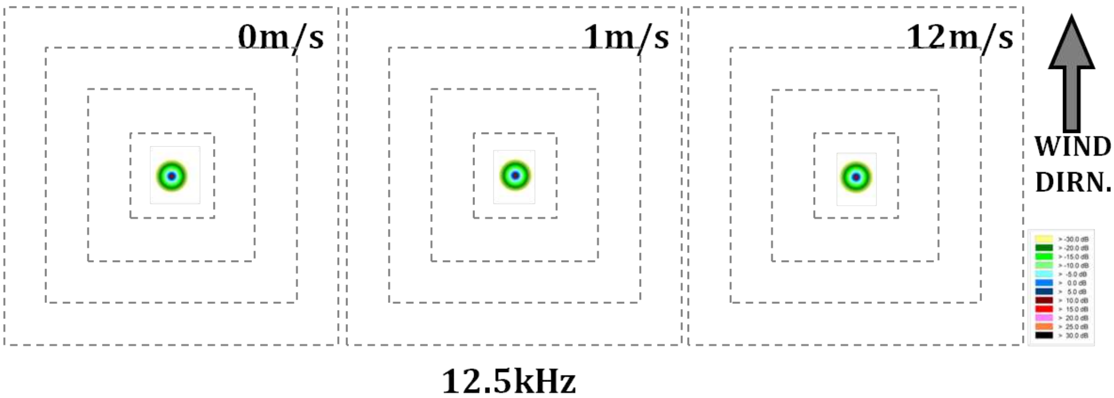

Figure D.2.11: Sound map showing the effect of wind speed on a 50dB point source of sound at 12.5kHz

Appendix E

Statistics Theory

This Section introduces the theory behind the statistical tests that are required for the psychological and health impacts studies. The theory presented in the following Sections is taken from the following text books [125, 126, 127, 128].

E.1 SPSS

The statistical package SPSS can be used as a tool to input data from a study, it is also possible to explore the data, check for errors and carry out all the statistical analyses required for this study. SPSS has the capability to carry out all the types of analyses required for the study using the techniques described as below, all the tests can be carried out quickly with clear output of data for further analysis. SPSS can handle all types of data and can be exploited in a custom way if necessary.

E.2 Definitions

This Section contains some essential definitions which will be required for the reader to follow through the outlines of the methods used within this research.

Independent and Dependent Variables A prediction is a statement that a change in one thing is due to a change in another. The variable causing the change is known as the independent variable (IV for short) and the variable changing as a result of a changing IV is known as the dependent variable (abbreviated as DV). Independent variables are sometimes known as predictor variables and dependent variables are also sometimes known as criterion variables [129].

Continuous Data Continuous variables change values smoothly and can take any value in the range of the scale, the size of the number represents the amount of the variable, for example, 32 years of age, £12,550 income or a 72/100 score on a test. Continuous data may also be called interval or quantitative data.

Discrete Data Discrete variables take on a finite and usually small number of values and there is no smooth transition from one value or category to the next, for example, type of dwelling, or colour of hair. Discrete variables can be used as if continuous to categorise a variable, for example categories of age instead of a continuous age, i.e. a continuous 32 years could by categorised in a discrete 30-39 years group. Discrete data may also be described as nominal, categorical or qualitative data.

Ordinal Data Ordinal variables can indicate which value is best or higher but does not indicate by how much. Often, ordinal variables are treated as continuous, an example of such a scale is a Likert scale where subjects are asked to respond to which answer best describes their attitude e.g. 1="strongly agree", 2="agree", 3="neither agree nor disagree", 4="disagree" and 5="strongly disagree". Ordinal data is sometimes called a ranking scale data.

Dichotomous Data Dichotomous variables only have two possible levels; an example of a dichotomous variable is sex, i.e. male or female. Some discrete or continuous variables could be changed to a number of dichotomous variables if necessary i.e. a discrete variable categorising religion, Christian, Jewish, Muslim etc could by dichotomised to Jewish and Non-Jewish. Dichotomous data may also be described as nominal, categorical or qualitative data.

Non-Parametric Test A non-parametric test does not rely on assumptions made about the data, for a non-parametric test the data should be measured as discrete or dichotomous.

Parametric Test A parametric test demands that the underlying populations of scores should be normally distributed and with equal variances. The scores should also have been obtained from a continuous scale of measurements. Parametric tests are more reliable than non-parametric tests provided the assumptions have been met.

E.3 Exploring the Data

Before carrying out any detailed analysis it is essential to explore the data, there are a few reasons for this. First, to check for errors which may have occurred during input of the data, second, to check that the demographic of the sample population is well spread and represents the whole population relevant to the study and finally to get a feel for the data before carrying out any detailed analysis. Initial exploration of the data can be done in a number of ways as described in the following Sections.

E.3.1 Describing data graphically

Tables, graphs and diagrams are very powerful for showing key trends in data and for this reason they should always be clear and concise. The appropriate type of diagram or table depends largely on the type of data to be plotted, i.e. whether the data is continuous or discrete? For discrete data, pie charts or bar charts showing frequencies are appropriate. Continuous data can be categorised so that histograms or frequency tables can be plotted. Likert scale type data can also be easily plotted as a histogram to show frequencies at each level.

E.3.2 Describing data numerically

In many cases it is more efficient to use numerical values to describe the data, with values such as the mean (Equation E.3.1), variance (Equation E.3.2) or standard deviation (Equation E.3.3). These numerical measures can only be used for continuous data and ordinal data when it is treated as continuous and can be calculated as below.

$$\overline{X} = \frac{\sum X}{N} \tag{E.3.1}$$

$$Variance = \frac{\sum \left(X - \overline{X}\right)^2}{N} \tag{E.3.2}$$

$$SD = \sqrt{Variance} \tag{E.3.3}$$

The mean and standard deviation values are useful for finding major differences between two sets of data. The mean, mode and median are measures of the central tendency of the data, whereas the variance and standard deviation are measures of the spread and variability of the data, where the standard deviation is simply the square root of the variance and is the standard unit of measurement in statistics. The standard deviation is otherwise known as the average amount that the scores on a variable differ from the mean centre score and gives the researcher the ability to standardise scores which do not normally have a standard value (i.e. the standard unit of length is m and the standard for mass is kg but there is no standard value such as this for statistics in Psychology).

E.3.3 Distribution of data

The distribution of the data is very important in statistics and refers to the shape and characteristics of the frequency distribution or histogram. Many statistical tests rely on the data being normally distributed about the mean and this is one of many factors which must be considered when examining the data distribution. Distributions are often distorted about the mean; this distortion is referred to as the skewness and kurtosis. Negative skew indicates that more of the scores are to the left of the mode than to the right and that the mean and median are smaller than the mode and the opposite is true for positive skew. Some distributions may look much like they follow the normal distribution but are steeper or shallower than would be expected; a positive kurtosis means the curve is steep, where a negative value indicates a flat curve.

E.3.4 The z-score

The z-score (Equation E.3.4) is an important statistic which measures the number of standard deviations a value is from the mean and is useful because with the z-score it is possible to express standard statistical units in terms of standard deviations. This means that many measures can be expressed consistently with the minimum number of concepts used. For example if the size of the standard deviation is 5 and a particular value is 20 above the mean, it is 20/5 or 4 standard deviations from the mean, all scores can be stated as the number of standard deviations from the mean they are, and this is applicable no matter what is being measured. The z-score may also be known as the *standard score*, they are used for many advanced statistical techniques which will be discussed in the following Sections.

$$z - score = \frac{\left(X - \overline{X}\right)}{SD} \tag{E.3.4}$$

E.4 Scale Reliability

For psychological studies scales are often used to measure where an individual rates on a particular aspect. For example, the neuroticism scale measures an individual's level of trait neuroticism, the scale consists of a number of personality items measuring an individual's level of neuroticism with the mean or the sum of their scores from all the items as the final measure. It is important to check that the scale is in fact measuring neuroticism and not something else.

In order to test the reliability, it would be expected that the items would correlate with each other to some extent and also with the total score; this is called item-total or item-whole correlation. Another test could involve checking that a score on half the items correlates with scores based on the remainder of the items, this is called the split-half reliability or Cronbach's alpha. These tests measure the *internal consistency* of psychological measures, also known as the *reliability*.

E.4.1 Item-total correlation

This method involves calculating the Pearson correlation coefficient measuring the correlation between each scale item and the total (or mean) score from each individual for all the items. The correlation with the total score excluding the item in question can also be calculated helping to identify the weakest items on the scale. If any items are particularly weakly correlated, it is possible to consider removing these items and re examining the reliability. Checks should also be made that all correlation coefficients are positive.

E.4.2 Split-half reliability

Split-half reliability involves splitting the items in the scale into two halves and computing scores based on each half of the items; the split-half reliability is then the correlation between these scores. There are no rules as to which item should be on which half, however the spilt is often made between odd and even items or with the split between the first and second half of the items. The major problem with split half reliability is that the results will vary depending on which item is allocated to which half. A solution to this problem would be to calculate every possible combination of the split half reliabilities and then take the average of these.

E.4.3 Alpha reliability

Calculating every possible combination of the split half reliabilities with items in each half and taking the average of these is known as the coefficient alpha, or Cronbach's alpha. Cronbach's alpha values above 0.7 are acceptable but values above 0.8 are preferable. SPSS can calculate the Cronbach's alpha easily; it will also give an indication of the Cronbach's alpha if each item were deleted from the scale, this gives a further indication of whether the reliability of the scale would be improved if items were deleted.

E.5 Significance Testing

Significance testing is important to establish whether any effect that an independent variable has on the dependent variable does not occur simply by chance, i.e. whether the null hypothesis is true (the null hypothesis is a statement that there is no relationship between two variables). It is also important because all statistical tests are carried out on samples which generalise about a population; significance testing is called *inferential statistics* and refers to how well the sample applies to the population. To check significance, a statistical test is used to determine the probability that the observed results could have occurred under the null hypothesis, i.e. if the probability that differences are due to the null hypothesis is less than or equal to 0.05 ($p \leq 0.05$), the null hypothesis is rejected in favour of the alternative hypothesis and the results are said to be significant. Hence the lower the p value, the more significant the effect between the independent and dependent variables. The selection of an appropriate significance test depends on the type of data and the analysis used.

E.6 Standard Error

The standard error is the term for the standard deviation of a number of sample means and is a very important term theoretically. The difficulty with the concept of standard error is it is a comparison of a number of samples in a given population; however most often data is only available for one sample in the population. It is however possible to estimate the standard error for the characteristics of a sample of scores. The estimated standard error can be calculated as in E.6.1.

$$standard\ error = \frac{\sqrt{\frac{\sum X^2 - \frac{(\sum X)^2}{N}}{N-1}}}{\sqrt{N}} \tag{E.6.1}$$

E.7 Independent samples t-tests

The independent samples t-test (Equation E.7.1) is used to compare the means of two different samples or conditions to find out whether they are significantly different, i.e. how likely is it that there are differences between the groups. A requirement of the t-test is that the two samples are similar in terms of their distributions. In a t-test the null hypothesis is tested, where any differences between the two samples or conditions occur only due to chance or that there is no difference between the two samples. In other words the t-test examines the probability that two sets of scores come from the same population. To carry out the t-test the t value must be calculated, the t-value is the number of standard errors by which the difference between the two samples means differ from the population mean of 0. It is necessary to use a significance table to identify the threshold t-values for the degrees of freedom of the test above which the groups are statistically significant.

$$t = \frac{\overline{X}_1 - \overline{X}_2}{\sqrt{\left(\frac{\left(\sum X_1^2 - \frac{(\sum X_1)^2}{N_1}\right) + \left(\sum X_2^2 - \frac{(\sum X_2)^2}{N_2}\right)}{N_1 + N_2 - 2}\right)\left(\frac{1}{N_1} + \frac{1}{N_2}\right)}} \tag{E.7.1}$$

E.8 Correlation

Correlation is used to measure the association between two continuous variables and is the measure of the size and direction of the relationship between the variables, the correlation squared gives an indication of the strength of the association between the two variables. The Pearson product-moment correlation coefficient (often known as the Pearson r or simply the Pearson coefficient) shows the strength and direction of the correlation and gives the average cross product of the two standardised variables. The Pearson coefficient must lie in the range -1.00 to +1.00. A value of 0 indicates that there is no correlation where a value of -1.00 or +1.00 shows a perfect correlation in the negative or positive direction respectively. If the Pearson r is squared, this gives the coefficient of determination which gives an indication of variation in the Y scores that can be accounted for by knowing X.

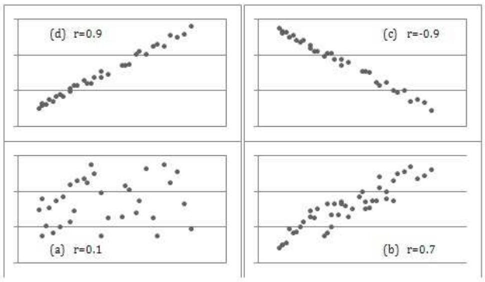

Figure E.8.1: Scatter chart illustrating correlation relationships

A scatter chart is a good way of visually showing how two variables are related giving an indication of the correlation, scatter charts showing the Pearson r for different types of relationships between variables are shown in Figure E.8.1.

The Spearman's rank order correlation r_s is the non parametric alternative to the Pearson product-moment correlation.

E.9 Regression

Where correlation is used to measure the size and direction of an association between two continuous variables, a regression analysis is used to predict the score of one (dependent) variable based on the score of one or more (independent) variables, where linear regression is the most commonly applied. In a simple bivariate linear regression Y (the dependent variable) is predicted from X by finding the best fit line.

$$Y' = A + BX \tag{E.9.1}$$

Y'(dependent variable) is the predicted score, A is the intercept value, B is the gradient (the regression coefficient) and X (independent variable) is the value which is used to predict Y.

Multiple regression is an extension of bivariate regression where more than one independent variable can be included in the analysis, the regression equation for multiple regression is based on that for bivariate regression but includes regression coefficients for each IV (independent variable).

$$Y' = A + B_1X_1 + B_2X_2 + ... + B_kX_k \tag{E.9.2}$$

Where k is the number of IVs included in the regression equation.

The best fitting regression coefficients produce a prediction equation where $(Y - Y')^2$ are at a minimum (Y is the actual value of the dependent variable), this is the least squared solution.

The sum of squares method is used to determine the squared multiple correlation R^2, which is the proportion of the sum of squares for regression in the total sum of squares for Y, in other words it is the proportion of variation in the DV (dependent variable) that is predictable for the best linear combination of the IVs or explained by the IVs. The multiple correlation R is the correlation between the values of Y and Y'.

$$R^2 = \frac{SS_{reg}}{SS_Y} \tag{E.9.3}$$

$$SS_Y = SS_{reg} + SS_{res} \tag{E.9.4}$$

SS_Y is the total sum of squares; SS_{reg} is the sum of squares due to the portion of the variation in Y that is explained by the use of the IVs as the predictors and SS_{res} represents errors in the prediction (or the residuals). Each sum of squares value can be calculated with the following equations.

$$SS_Y = \sum \left(Y - \overline{Y}\right)^2 \tag{E.9.5}$$

$$SS_{reg} = \sum \left(Y' - \overline{Y}\right)^2 \tag{E.9.6}$$

$$SS_Y = \sum \left(Y - Y'\right)^2 \tag{E.9.7}$$

SS_Y can be calculated directly from the available data but in order to evaluate SS_{reg} and SS_{res} the regression equation must be solved to find the correct set of B values. This is done using basic matrix algebra.

$$R^2 = \sum_{i=1}^{k} r_{yi}\beta_i \tag{E.9.8}$$

Where β_i is the standardised regression coefficient for the ith IV which would be applied to the standardised X_i value (the z-score of the X_i value) to predict the standardised Y'. r_{yi} is the correlation between the DV and the ith IV.

The matrix form of equations is as follows:

$$R^2 = \boldsymbol{R}_{yi}\boldsymbol{B}_i \tag{E.9.9}$$

$$\boldsymbol{B}_i = \boldsymbol{R}_{ii}^{-1}\boldsymbol{B}_{iy} \tag{E.9.10}$$

Where:

$\boldsymbol{B}_i$	Column matrix of standardised regression coefficients for the IVs
$\boldsymbol{R}_{iy}$	Column matrix of correlations between the DV and IVs
$\boldsymbol{R}_{yi}$	Row matrix of correlations between the DV and IVs
$\boldsymbol{R}_{ii}^{-1}$	Inverse of the matrix of correlations among the IVs

To determine the unstandardised regression coefficients, the beta weights are multiplied by the ratio of standard deviations of the DV and the IV.

$$B_i = \beta_i \left(\frac{S_Y}{S_i} \right) \tag{E.9.11}$$

The intercept of the regression equation is then determined with the following equation.

$$A = \overline{Y} - \sum_{i=1}^{k} (B_i \overline{X}_i) \tag{E.9.12}$$

There are several types of multiple regression which are used to answer different questions such as "How good is the regression equation?", "Does the regression equation provide a better than chance prediction?" and "Which independent variables are important in the equation?" However, the fundamental equations for each type of multiple regression are the same, the differences occur due to the order in which the IVs are entered into the equation. The different types of multiple regression relevant for this study are outlined in the following Sections.

E.9.1 Standard Multiple Regression

Differences in the types of multiple regression regimes primarily involves what happens to the overlapping variability due to correlated IVs, and the order the IVs enter the equation. Take for example the Venn diagram in Figure E.9.1a which shows three IVs and one DV. Each IV explains some of the variance in the DV, area a comes uniquely from IV_1, area c comes uniquely from IV_2 and area e comes uniquely from IV_3. However area b can either be attributed to IV_1 or IV_2 and area d could either be attributed to IV_2 or IV_3. In this case $R^2 = a + b + c + d + e$. The decision as to which IV the shared areas should be attributed to depends on the choice of method of regression.

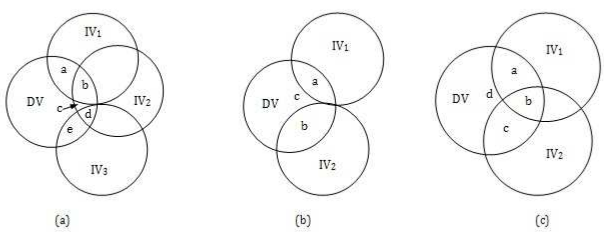

Figure E.9.1: Venn diagram illustrating overlapping variance sections

In standard multiple regression, all the relevant IVs are entered into the equation at once and each one is assessed as if it had entered the regression after all the other IVs have been assessed, i.e. it is assessed in terms of what it adds to the prediction of the DV. Referring to Figure E.9.1a again, each IV only gets credit for the unique contribution it gives to the DV, i.e. in this situation area a is assigned to IV_1, area c is assigned to IV_2 and area e is assigned to IV_3. Consider Figure E.9.1b, if the IVs are uncorrelated, the issue of shared variance is not a problem as no area is shared by both IVs. Where shared variance does occur the importance of each IV depends solely on the type of regression used. The Venn diagram in Figure E.9.1c as well as Equations E.9.13 to E.9.18 show how unique and shared variance is handled for standard multiple regression.

$$r_i^2 \qquad IV_1 \qquad {}^{(a+b)}\!/_{(a+b+c+d)} \tag{E.9.13}$$

$$r_i^2 \qquad IV_2 \qquad {}^{(c+b)}\!/_{(a+b+c+d)} \tag{E.9.14}$$

$$sr_i^2 \qquad IV_1 \qquad {}^{(a)}\!/_{(a+b+c+d)} \tag{E.9.15}$$

$$sr_i^2 \qquad IV_2 \qquad {}^{(c)}\!/_{(a+b+c+d)} \tag{E.9.16}$$

$$pr_i^2 \qquad IV_1 \qquad {}^{(a)}\!/_{(a+d)} \tag{E.9.17}$$

$$pr_i^2 \qquad IV_2 \qquad {}^{(c)}\!/_{(c+d)} \tag{E.9.18}$$

The semi-partial correlation sr_i^2 represents the unique contribution of the ith IV on the DV, therefore when IVs are correlated and there is some shared variance, the sum of the semi partial correlations in standard multiple regression does not equal R^2, the difference between these two values represents the magnitude of the shared variance. In partial correlation (pr_i^2) the influence of the other IVs is taken out of both the IV and the DV.

To test significance of B_i, βi, pr_i^2 and sr_i^2 in standard multiple regression, Equation E.9.19 should be applied. These significance tests assess the unique variance the IV adds to R^2.

$$F_i = \frac{sr_i^2}{\left(1 - R^2\right)/df_{res}} \tag{E.9.19}$$

Where $df_{res} = (N - k - 1)$

E.9.2 Hierarchical Regression

In hierarchical regression, the IVs are entered into the equation in an order specified by the researcher in steps; selection of the order is usually based on theory or logical reasoning. Consider again Figure E.9.1a, if the IVs are entered in order 1 to 3. Areas a and b are assigned to IV_1, area c and area d are assigned to IV_2 and area e is attributed to IV_3. If however, the IVs were entered in a different order the areas would be assigned differently. It is often the case that the most causally important variables are entered first, however sometimes the reverse is true, where nuisance variables are entered first in order to control for these variables, i.e. to find the contribution of the more causally important variables over and above the contribution of the nuisance variables. IVs can be entered one at a time or in blocks.

When considering unique or shared variance for hierarchical regression, refer to Figures E.9.1c and Equations E.9.21 to E.9.25.

$$r_i^2 \qquad IV_1 \qquad {}^{(a+b)}/_{(a+b+c+d)} \tag{E.9.20}$$

$$r_i^2 \qquad IV_2 \qquad {}^{(c+b)}/_{(a+b+c+d)} \tag{E.9.21}$$

$$sr_i^2 \qquad IV_1 \qquad {}^{(a+b)}/_{(a+b+c+d)} \tag{E.9.22}$$

$$sr_i^2 \qquad IV_2 \qquad {}^{(c)}/_{(a+b+c+d)} \tag{E.9.23}$$

$$pr_i^2 \qquad IV_1 \qquad {}^{(a+b)}/_{(a+b+d)} \tag{E.9.24}$$

$$pr_i^2 \qquad IV_2 \qquad {}^{(c)}/_{(c+d)} \tag{E.9.25}$$

In hierarchical regression, the semi-partial correlation sr_i^2 is interpreted as the amount of variance added to R^2 by each IV at the point it enters the equation. For hierarchical regression, R^2 does equal the sum of sr_i^2 for all the IVs. So the apparent importance of an IV depends on its point of entry into the equation. As seen in Figure E.9.1c IV_1 enters the equation before IV_2, therefore IV_1 gets credit for area a and area b, and IV_2 only gets credit for area c. However if the variables were entered into the equation the other way round, IV_2 would get credit for areas b and c and IV_1 would only get credit for area a. The partial correlation is handled in much the same way as standard multiple regression, but includes the shared variance area depending on which order the IVs are entered into the equation.

R^2 is important in hierarchical regression, as the change in R^2 at each step of the regression shows whether adding a set of IVs to the equation shows a significant contribution to the variance of the DV. The method for testing whether adding a subset of IVs shows a significant increase in R^2 is as Equation E.9.26.

$$F_i = \frac{\left(R_{wi}^2 - R_{wo}^2\right)/m}{\left(1 - R^2\right)/df_{res}} \tag{E.9.26}$$

Where R_{wo}^2 is R^2 before the subset of IVs has been added and R_{wi}^2 is R^2 after the subset of IVs has been added.

E.9.3 Statistical Regression

Statistical regression is a procedure where the entry of variables into the equation is based solely on statistical criteria, so that at each stage the most statistically important variables are entered first with no consideration of theory. Statistical regression can be used where the researcher enters particular variables in blocks into each step of the regression and then statistical regression can be used within these blocks to determine the most important variables. Statistical regression should be used with caution.

E.9.4 Checking the Assumptions of Multiple Regression

Sample Size Your sample size should be large enough that it can generalise to other samples. If your results do not generalise to other samples they do not have any real value. Tabachnick and Fidell [128] suggest that Equation E.9.27 should be used to check the size of the sample population.

$$N > 50 + 8m \tag{E.9.27}$$

Outliers Outliers are extreme cases with very low or very high scores compared to the average value, multiple regression is very sensitive to outliers as they have a large impact on the regression solution. Unless the extreme cases are representative of trends they should be deleted, re-scored or the variable transformed. Screening for outliers may be done before the regression is carried out or during the regression process via analysis of the residuals, i.e. outliers are defined as those with residual values above 3.3 or below -3.3. Identification of outliers should be carried out for both the independent and dependent variables and SPSS provides specialist tests for identifying multivariate outliers.

Multicollinearity and Singularity Multicollinearity occurs when independent variables in a multiple regression are highly correlated with one another, i.e. the have an r value of 0.9 or above. If there are high levels of multicollinearity among the independent variables, inversion of the correlations matrix $\boldsymbol{R}_{ii}$ is not possible. Singularity is also a problem for the inversion of $\boldsymbol{R}_{ii}$. Singularity occurs when one IV is actually a combination of other IVs, for example if there is an interaction between two IVs, the problems of singularity can be reduced by centering the variables about the mean, i.e. taking the actual score away from the mean score for the independent variables.

Normality, Linearity, Homoscedasticity and Independence of Residuals Normality, linearity, homoscedasticity and independence of residuals all refer to the distribution of scores and the nature of the underlying relationships between variables. Checking of these assumptions is done using the residuals plot that is generated during the multiple regression procedure (residuals are $(Y - Y')^2$ i.e. the differences between the actual and predicted values). Normality is where the residuals should be normally distributed around the mean of the predicted dependent variable, the residuals should also have a straight-line relationship with the predicted dependent variable scores, and this is known as linearity. The variance of the residuals about the predicted DV scores should be the same for all predicted scores, known as homoscedasticity. The independence of the residuals also represents the independence of errors; an assumption that must be met is that the errors in prediction are independent of one another.

E.10 Moderating Variables

A moderator is a variable that affects the strength and direction of the relationship between the independent and the dependent variable. For example, the relationship between symptom reporting and visits to a doctor may be larger for females than for males. A moderator may also change the direction of a relationship from positive to negative or vice versa. The essential properties of a moderator variable can be seen in Figure E.10.1, where a predictor (path a), moderator (path b) and interaction (path c) paths are visible. The criterion for a moderator variable is that path c should be significant. In contrast to mediating variables, moderator variables always act as an independent variable and do no shift from an effect to a cause.

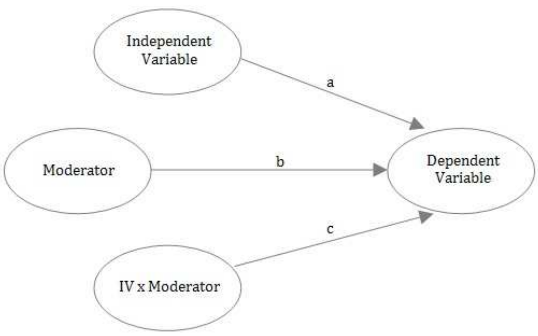

Figure E.10.1: The interaction between an IV, moderator and DV

The interaction path may violate the singularity assumption for a multiple regression analysis, for this reason the IVs should be transformed to mean centre scores i.e. taking the actual score away from the mean score for a variable. It is not necessary to transform the DV.

Moderation implies that the causal relationship between two variables changes as a function of the moderator, examining for moderation involves a statistical test which must measure and test this change. The method for these tests depends on the type of data used for the IVs and the moderator, for example continuous, categorical etc.

The method for testing for moderation involves the following steps in each with the DV as the criterion variables:

1. Linear regression test with IV set as the independent (path a)
2. Linear regression test with moderator set as the independent (path b)
3. Linear regression test with IV x moderator variable set as the independent (path c)

For a moderation to be present the interaction path should have a higher significance than the prediction and moderator paths.

The above test for moderation will clearly show whether or not a moderator is present in the equation, but the steps will not identify whether the stated IV or moderator is the true moderator. Consider Figure E.10.1, if the independent variable and the moderator were switched the calculated product is still the same and the steps for the analysis would also be the same. There are two possible methods to identify which variable is the moderator and at which levels of the moderator there is a significant relationship between the IV and the DV. For example, if the DV is set as score on a test, the IV is set as concentration levels and the moderator is set as sex, the above analysis shows that there is a significant relationship between the product of sex and concentration scores and the DV, test score. We know therefore that either sex or concentration level is acting as a moderator but we want to confirm that sex is the true moderator and whether the contribution of sex as the moderator to the DV occurs for both males and females or only males or females. The two methods for carrying out this analysis is using median splits or Preacher's [130] simple slopes. These two methods are outlined in the following Sections.

E.10.1 Median Splits

Median splits are a simple way to test whether the independent variable correlates significantly with the dependent values at different levels of the moderator. The method for carrying out median splits proceeds as follows:

1. Find the median value of the moderator
2. Convert the continuous moderator to a dichotomous variable
   (a) Values of the moderator $<$ median should be set to 0

   (b) Values of the moderator > median should be set to 1

3. Correlate the independent variable with the dependent variable for subjects with a moderator value of 0

4. Correlate the independent variable with the dependent variable for subjects with a moderator value of 1

5. Check for significance in the correlation results to identify whether there are interaction effects over varying levels of the moderator.

The median split method is a simple way to check interaction terms, however it is a fairly crude method that should be used with caution in some instances or where the interactions are complicated and where theory does not strongly back up the hypothesis being tested. One key drawback to using the median split method is that all subjects whose moderator takes the value of the median will be excluded from the analysis, this could result in a significantly reduced number of subjects and a less robust analysis. An alternative method to median splits is simple slopes. The method for simple slopes is outlined in the following Section.

E.10.2 Simple Slopes

As stated previously, an interaction shows that the magnitude of the relationship between one independent variable and the dependent variable is different across different levels of another predictor. It is easy to hypothesise based on theory that one IV is the predictor and the other IV the moderator, however this notation is arbitrary as the interaction and associated analysis is symmetrical about the dependent variable. It is therefore useful to analyse how the predictions will change over different levels of the hypothesised moderator and at which levels of the moderator the interaction is significant. Equation E.10.1 shows the general regression equation for the model implied value of Y, $\hat{y}$, with one predictor (x), one moderator (z) and one interaction effect (xz), the associated regression coefficients, $\hat{b}_1, \hat{b}_2, \hat{b}_3$ respectively with the intercept $\hat{b}_0$.

$$\hat{y} = \hat{b}_0 + \hat{b}_1 x + \hat{b}_2 z + \hat{b}_3 xz \tag{E.10.1}$$

Equation E.10.1 can be rearranged in terms of the simple intercept and the simple slope, with the simple intercept as E.10.4 and the simple slope as E.10.5.

$$\hat{y} = \left(\hat{b}_0 + \hat{b}_2 z\right) + \left(\hat{b}_1 + \hat{b}_3 z\right) x \tag{E.10.2}$$

$$\hat{y} = \hat{\omega}_0 + \hat{\omega}_1 x \tag{E.10.3}$$

$$\hat{\omega}_0 = \left(\hat{b}_0 + \hat{b}_2 z\right) \tag{E.10.4}$$

$$\hat{\omega}_1 = \left(\hat{b}_1 + \hat{b}_3 z\right) \tag{E.10.5}$$

Using expressionsE.10.4 and E.10.5 it is easy to evaluate how the estimates change over different levels of the moderator (z). For example, it is possible to evaluate whether the slopes over different levels of the moderator are significantly different to zero.

The traditional approach to evaluating simple slopes, (simple intercepts are rarely of any interest so will not be discussed in detail here) is to choose several conditional values of the moderator (z) and to evaluate the significance of the slope at each chosen level of z. The variance of the simple slope $\hat{\omega}_1$ should first be calculated using Equation E.10.6, values for the variances and covariances as required in E.10.6 can be found in the ACOV matrix in the output when carrying out a multiple regression text is SPSS.

$$var\left(\hat{\omega}_1 \mid z\right) = var\left(\hat{b}_1\right) + 2zcov\left(\hat{b}_1, \hat{b}_3\right) + z^2 var\left(\hat{b}_3\right) \tag{E.10.6}$$

The standard error of $\hat{\omega}_1 (SE_{\hat{\omega}_1})$ is then simply the square root of $var\left(\hat{\omega}_1 \mid z\right)$. Finally the critical ratio to perform the significance test can be determined as in Equation E.10.7 where the significance of which is determined by comparing the obtained t value to a t distribution for the required degrees of freedom $df = N - k - 1$.

predictor

$$t = \frac{\hat{\omega}_1}{SE_{\hat{\omega}_1}} \tag{E.10.7}$$

As stated previously, in order to carry out this method, conditional values of the moderator should be employed to evaluate Equations E.10.1 to E.10.1. These can be any values of scientific interest but are often taken at the mean of z and $1SD$ above and below the mean of z.

The simple slopes method relies on simply null hypothesis testing, however confidence intervals (CIs) can give more information than simple hypothesis testing and it is often recommended to test confidence intervals in addition to hypothesis testing. EquationE.10.8 shows the formula required for a $100 \times (1 - \alpha)\,\%$ CI for a simple slope.

$$CI_{\hat{\omega}_1} = \hat{\omega}_1 \pm t_{crit} SE_{\hat{\omega}_1} \tag{E.10.8}$$

As CI will vary as a function of moderator, if CI is plotted across all values of interest of z, the result if a pair of *confidence bands*.

These methods for evaluating interactions are not yet fully incorporated into modern statistical packages such as SPSS, however there are resources available online [130] which implement these techniques. Carrying out relevant multiple regression tests with the necessary predictors and criterion variables in SPSS will output the required statistics to be entered into an online simple slopes calculator. These online calculators carry out significance tests of the simple slopes across the required range of values of the moderator. It is also possible to obtain graphical outputs of the simple slopes E.10.2.

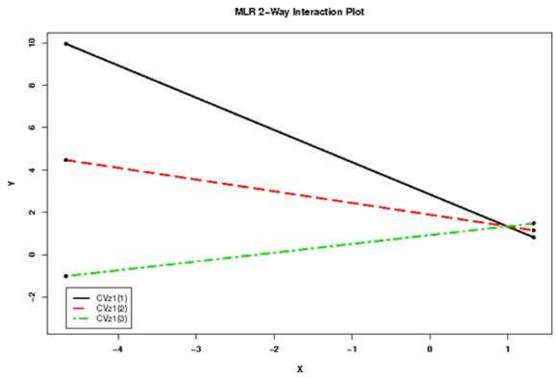

Figure E.10.2: Example output of simple slopes across conditional values of z

Appendix F

Domestic Questionnaire and Documents

University of Nottingham Wind Turbine Survey

Dear Participant,

Researchers at the University of Nottingham are exploring the way in which people perceive micro and small wind turbine noise and how this affects them. The project is funded by the UK Energy Research Centre (UKERC) but is being carried out by independent researchers within the School of Psychology, the Department of Mechanical, Materials and Manufacturing Engineering and the School of the Built Environment at the University of Nottingham and is in no way linked to any outside Council or Commercial Organisations.

We want to find out more about how people perceive small wind turbine noise and how this affects different individuals. Information collected from the survey will provide a better understanding of the nature of noise from small wind systems and how this can affect people's everyday lives which will have benefits for planners, policy makers and local communities.

You have been selected to receive a copy of this survey because you live near to a site where a micro or small wind turbine is either attached to a building or on a separate mast. You will not receive any more correspondence from us unless you consent to do so. Take time to look over the survey and this letter. If you are happy to participate then please complete the survey and return it to us in the prepaid envelope provided. If you would prefer to complete the survey online then please visit **http://tinyurl.com/wind-turbine-survey** and follow the instructions. Your responses will be used only for the purpose of this research. Please try to complete all the questions in the survey; however your survey is still useful to us even if you have missed out some questions, so please complete what you can and return it to us. Please complete this survey if you are over 18 years old. In addition, if there are any other adults living in your household, then extra copies can be sent to you on request (contact details are overleaf), or each person can complete the survey online.

This survey is voluntary and you do not have to complete it. Only the researchers will see the completed survey and all data will be kept securely, we will not pass on your information to anyone. You do not have to return the survey once you have started or return the survey once completed.

If you would like any further information about the study, please do contact a member of the research team. Our details are listed on the information sheet overleaf. Please contact us if you would like a large print version of this survey or instructions on how to complete the survey online. If you have any general concerns about stress or your health in general or would like more information on wind turbines, we have included a list of telephone numbers and websites of organisations that you may find useful.

When you have completed the survey, please send if back to us in the pre-paid envelope provided within two weeks, or as soon as possible after that. Alternatively you can complete the survey online.

Thank you in advance for you participation,
Yours sincerely,

Jennifer Taylor
PhD Research Student

Dr. Claire Lawrence
Supervisor

University of Nottingham Wind Turbine Survey
Information Sheet

Thank you for taking the time to read about our study. If you have any queries about the study please contact one of the project team. Our details are below:

Jennifer Taylor
Department of Mechanical, Materials and Manufacturing Engineering
☎ 0115 951 3832
💻 eaxjt@nottingham.ac.uk

Dr Claire Lawrence
School of Psychology
☎ 0115 951 5326
💻 claire.lawrence@nottingham.ac.uk

Dr Carol Eastwick
Department of Mechanical, Materials and Manufacturing Engineering
☎ 0115 951 3788
💻 carol.eastwick@nottingham.ac.uk

You may have some questions or concerns about stress, frustrations or your general health. Unfortunately we are unable to provide any personal support about this. If you do have any concerns about your health we would advise you in the first instance to contact your GP.

In addition, please find below the contact details for organisations that can provide specific advice about a number of health related topics:

- For general health advice:
  NHS Direct
  ☎ 0845 46 47
  💻 www.nhsdirect.nhs.uk

- For anyone seeking help or guidance, or wishing to discuss their problems in confidence:
  The Samaritans
  ☎ 08457 90 90 90
  💻 www.samaritans.org.uk

If you would like more information about wind turbines in general please contact the following organisations:

- British Wind Energy Association (BWEA)
  BWEA
  ☎ 020 7689 1960
  💻 www.bwea.com

University of Nottingham Wind Turbine Survey

If you would prefer to complete this survey online then please visit http://tinyurl.com/wind-turbine-survey and follow the instructions.

Can you see a small/micro wind turbine from where you live? (please circle) Yes / No
Is there a wind turbine attached to the building you live in? (please circle) Yes / No
Please rate how you feel about wind power in general (please circle a number below)
I feel very positive **1 2 3 4 5 6 7** I feel very negative

Listed below are a number of sounds you might hear coming from the wind turbine near your residence. Please rate the loudness of these sounds and the frequency you hear them by circling the answer that best relates to you.

	LOUDNESS					FREQUENCY				
	Never heard	Heard but not loud	Quite loud	Very loud	Extremely loud	Never noticed	Only noticed once or twice	Notice from time to time	Notice several times a week	Notice continuously
Swooshing	1	2	3	4	5	1	2	3	4	5
Screeching	1	2	3	4	5	1	2	3	4	5
Buzzing	1	2	3	4	5	1	2	3	4	5
Whistling	1	2	3	4	5	1	2	3	4	5
Humming	1	2	3	4	5	1	2	3	4	5
Throbbing	1	2	3	4	5	1	2	3	4	5
Thumping	1	2	3	4	5	1	2	3	4	5
Scratching	1	2	3	4	5	1	2	3	4	5
High Pitched	1	2	3	4	5	1	2	3	4	5
Low Pitched	1	2	3	4	5	1	2	3	4	5

When and in which weather conditions do you typically notice these sounds? CIRCLE AS MANY THAT APPLY.

	6am-9am	9am-5pm	5pm-10pm	10pm-6am	Wind	Rain	Sun	Fog	Cold	Hot
Swooshing	1	2	3	4	1	2	3	4	5	6
Screeching	1	2	3	4	1	2	3	4	5	6
Buzzing	1	2	3	4	1	2	3	4	5	6
Whistling	1	2	3	4	1	2	3	4	5	6
Humming	1	2	3	4	1	2	3	4	5	6
Throbbing	1	2	3	4	1	2	3	4	5	6
Thumping	1	2	3	4	1	2	3	4	5	6
Scratching	1	2	3	4	1	2	3	4	5	6
High Pitched	1	2	3	4	1	2	3	4	5	6
Low Pitched	1	2	3	4	1	2	3	4	5	6

This scale consists of a number of words that describe different feelings and emotions. Read each item and indicate to what extent you have felt this way DURING THE PAST MONTH by circling the appropriate answer next to that word.

	Very slightly or not at all	A little	Moderately	Quite a bit	Extremely
Interested	1	2	3	4	5
Distressed	1	2	3	4	5
Excited	1	2	3	4	5
Upset	1	2	3	4	5
Scared	1	2	3	4	5

Continued on next page

University of Nottingham Wind Turbine Survey

	Very slightly or not at all	A little	Moderately	Quite a bit	Extremely
Hostile	1	2	3	4	5
Enthusiastic	1	2	3	4	5
Proud	1	2	3	4	5
Irritable	1	2	3	4	5
Inspired	1	2	3	4	5
Nervous	1	2	3	4	5
Attentive	1	2	3	4	5

For each of the following statements, rate how accurately you feel they apply to you by circling the appropriate answer.

	Very inaccurate	Quite inaccurate	Neutral	Quite accurate	Very accurate
I often feel blue	1	2	3	4	5
I am very pleased with myself	1	2	3	4	5
I dislike myself	1	2	3	4	5
I am not easily bothered by things	1	2	3	4	5
I am often down in the dumps	1	2	3	4	5
I feel comfortable with myself	1	2	3	4	5
I have frequent mood swings	1	2	3	4	5
I seldom feel blue	1	2	3	4	5
I panic easily	1	2	3	4	5
I rarely get irritated	1	2	3	4	5

Listed below are a number of common thoughts and beliefs that people may have when they are distressed or frustrated. Please read each statement and decide how well this usually describes your own beliefs. Circle the answer that best indicates the strength of belief.

	Absent	Mild	Moderate	Strong	Very strong
I need the easiest way around problems	1	2	3	4	5
I must be free of disturbing feelings as quickly as possible; I can't bear it if they continue	1	2	3	4	5
I can't stand doing tasks that seem too difficult	1	2	3	4	5
I can't bear to feel that I am losing my mind	1	2	3	4	5
I can't stand doing tasks when I'm not in the mood	1	2	3	4	5
I can't bear to have certain thoughts	1	2	3	4	5
I can't stand having to push myself at tasks	1	2	3	4	5
I can't stand situations where I might feel upset	1	2	3	4	5
I can't stand the hassle of having to do things right now	1	2	3	4	5
I can't bear disturbing feelings	1	2	3	4	5
I can't stand doing things that involve a lot of hassle	1	2	3	4	5
I can't get on with my life or be happy if things don't change	1	2	3	4	5
I can't stand having to persist at unpleasant tasks	1	2	3	4	5
I can't stand to lose control of my feelings	1	2	3	4	5

Continued on next page

University of Nottingham Wind Turbine Survey

The following is a list of situations in which you may have felt aggressive. Please circle the answer, as honestly as possible, that relates to how accurate it is for you that each of the situations on the left make you feel aggressive.

I feel aggressive when....	Very inaccurate	Moderately inaccurate	Neither inaccurate nor accurate	Moderately accurate	Very accurate
A friend betrays me	1	2	3	4	5
I am the subject of a practical joke	1	2	3	4	5
People I live with show a lack of consideration	1	2	3	4	5
Someone steals something from me	1	2	3	4	5
I feel frustrated	1	2	3	4	5
Someone insults me	1	2	3	4	5
I have academic or work problems	1	2	3	4	5
I experience family dispute	1	2	3	4	5
I feel hot and crowded	1	2	3	4	5
Someone ignores me	1	2	3	4	5
Someone behaves in an inconsiderate manner towards me	1	2	3	4	5
I am in pain	1	2	3	4	5
I am goaded or provoked by someone	1	2	3	4	5
I've been let down by someone	1	2	3	4	5
I feel stressed	1	2	3	4	5
Someone is drunk and behaves inconsiderately towards me	1	2	3	4	5
I hear a noise that I cannot control	1	2	3	4	5
I am frustrated with services	1	2	3	4	5
Others around me are becoming aggressive	1	2	3	4	5
Someone makes offensive remarks to me	1	2	3	4	5
Another driver commits a traffic violation	1	2	3	4	5
I argue with a friend	1	2	3	4	5

How often have you experienced the following symptoms DURING THE LAST MONTH? (please circle)

	Never	Once or twice	Once or twice per week	Frequently	Daily
Headache	1	2	3	4	5
Dizziness	1	2	3	4	5
Palpitations	1	2	3	4	5
Weak / fatigued	1	2	3	4	5
Upset stomach	1	2	3	4	5
Pain in limbs	1	2	3	4	5
Pain in joints	1	2	3	4	5
Breathlessness	1	2	3	4	5
Sweatiness	1	2	3	4	5
Tingling hands/feet	1	2	3	4	5

Continued on next page

University of Nottingham Wind Turbine Survey

1. Age:___________
2. Sex: (please circle) MALE / FEMALE
3. Occupation:_________________________________
4. What type of dwelling do you live in? (please circle)
DETACHED SEMI-DETACHED TERRACED FLAT OTHER
5. How long have you lived at your current dwelling?_______________yrs
6. Do you have a garden or outside space at your residence? (please circle) Yes / No
7. If yes, approximately how much time per week do you spend there?______hrs

If you have any further comments you would like to add about the turbine/s in your area or this survey, please add them here:

If you are happy to be contacted in the future about other projects researching the effects of wind turbines please leave your details below (this is not compulsory):

Name:

Address:

Contact telephone:

Contact email:

Please note that this is a survey carried out by independent researchers at the University of Nottingham and is in no way linked to any outside Council or Commercial Organisations.

Thank you for your participation!

Office Use Only: Code

Appendix G

Recordings Questionnaire and Documents

University of Nottingham Wind Turbine Survey

Dear Participant,

Researchers at the University of Nottingham are exploring the way in which people perceive micro and small wind turbine noise and how this affects them. The project is funded by the UK Energy Research Centre (UKERC) but is being carried out by independent researchers within the School of Psychology and the Faculty of Engineering at the University of Nottingham.

We want to find out more about how people perceive small wind turbine noise and how this affects different individuals. Information collected from the survey will provide a better understanding of the nature of noise from small wind systems and how this can affect people's everyday lives which will have benefits for planners, policy makers and local communities.

You have been selected to complete this survey and will not receive any further correspondence from us unless you consent to do so. Take time to look over the survey and this letter. If you are happy to participate then please complete the survey as instructed by the leader of the session and return the completed survey at the end of the session. Your responses will be used only for the purpose of this research. Please try to complete all the questions in the survey; however your survey is still useful to us even if you have missed out some questions, so please complete what you can and return it to us. Please complete this survey if you are over 18 years old.

This survey is voluntary and you do not have to complete it. Only the researchers will see the completed survey and all data will be kept securely, we will not pass on your information to anyone. You do not have to return the survey once you have started or return the survey once completed.

If you would like any further information about the study, please do contact a member of the research team. Our details are listed on the information sheet overleaf. If you have any general concerns about stress or your health in general or would like more information on wind turbines, we have included a list of telephone numbers and websites of organisations that you may find useful.

When you have completed the survey, please return it to the session leader at the end of the session.

Thank you in advance for you participation,
Yours sincerely,

Jennifer Taylor
PhD Research Student

Dr. Claire Lawrence
Supervisor

Dr Carol Eastwick
Supervisor

University of Nottingham Wind Turbine Survey
Information Sheet

Thank you for taking the time to read about our study. If you have any queries about the study please contact one of the project team. Our details are below:

Jennifer Taylor
Energy and Sustainability Research Group, Faculty of Engineering
☎ 0115 951 3832
💻 eaxjt@nottingham.ac.uk

Dr Claire Lawrence
School of Psychology
☎ 0115 951 5326
💻 claire.lawrence@nottingham.ac.uk

Dr Carol Eastwick
Energy and Sustainability Research Group, Faculty of Engineering
☎ 0115 951 3788
💻 carol.eastwick@nottingham.ac.uk

You may have some questions or concerns about stress, frustrations or your general health. Unfortunately we are unable to provide any personal support about this. If you do have any concerns about your health we would advise you in the first instance to contact your GP.

In addition, please find below the contact details for organisations that can provide specific advice about a number of health related topics:

- For general health advice:
  NHS Direct
  ☎ 0845 46 47
  💻 www.nhsdirect.nhs.uk

- For anyone seeking help or guidance, or wishing to discuss their problems in confidence:
  The Samaritans
  ☎ 08457 90 90 90
  💻 www.samaritans.org.uk

If you would like more information about wind turbines in general please contact the following organisations:

- Renewable UK
  Renewable UK
  ☎ 020 7689 1960
  💻 www.bwea.com

CONSENT FORM

University of Nottingham Wind Turbine Noise Survey

Investigators: Jennifer Taylor, Dr Claire Lawrence (Supervisor), Dr Carol Eastwick (Supervisor)
Energy and Sustainability Research Group, Faculty of Engineering
And
School of Psychology,
University of Nottingham

The participant should complete the whole of this sheet himself/herself. Please cross out as necessary.

- Have you read and understood the participant information sheet YES/NO
- Have you had the opportunity to ask questions and discuss the study YES/NO
- Have all your questions (if any) been answered satisfactorily YES/NO
- Have you received enough information about the study YES/NO
- Do you understand that you are free to withdraw from the study:
  - at any time YES/NO
  - without having to give a reason YES/NO
- Do you agree to take part in the study YES/NO

"This study has been explained to me to my satisfaction, and I agree to take part. I understand that I am free to withdraw at any time."

Signature of the Participant: Date:

Name: (in block capitals)

"I have explained the study to the above participant and he/she has agreed to take part."

Signature of Researcher: Date:

University of Nottingham Wind Turbine Survey

Thank you for agreeing to participate in this survey about wind turbine noise.

PART 1

Please read the following questions and answer them to the best of your ability.

1. Age:________

2. Sex: **(please circle)** MALE / FEMALE

Please rate how you feel about wind power in general **(please circle a number below)**

I feel very positive	**1**	**2**	**3**	**4**	**5**	**6**	**7**	I feel very negative

This scale consists of a number of words that describe different feelings and emotions. Read each item and indicate to what extent you feel this way NOW by circling the appropriate answer next to that word.

	Very slightly or not at all	A little	Moderately	Quite a bit	Extremely
Interested	1	2	3	4	5
Distressed	1	2	3	4	5
Excited	1	2	3	4	5
Upset	1	2	3	4	5
Scared	1	2	3	4	5
Hostile	1	2	3	4	5
Enthusiastic	1	2	3	4	5
Proud	1	2	3	4	5
Irritable	1	2	3	4	5
Inspired	1	2	3	4	5
Nervous	1	2	3	4	5
Attentive	1	2	3	4	5

For each of the following statements, rate how accurately you feel they apply to you by circling the appropriate answer.

	Very inaccurate	Quite inaccurate	Neutral	Quite accurate	Very accurate
I often feel blue	1	2	3	4	5
I am very pleased with myself	1	2	3	4	5
I dislike myself	1	2	3	4	5
I am not easily bothered by things	1	2	3	4	5
I am often down in the dumps	1	2	3	4	5
I feel comfortable with myself	1	2	3	4	5
I have frequent mood swings	1	2	3	4	5
I seldom feel blue	1	2	3	4	5
I panic easily	1	2	3	4	5
I rarely get irritated	1	2	3	4	5

University of Nottingham Wind Turbine Survey

Listed below are a number of common thoughts and beliefs that people may have when they are distressed or frustrated. Please read each statement and decide how well this usually describes your own beliefs. Circle the answer that best indicates the strength of belief.

	Absent	Mild	Moderate	Strong	Very strong
I need the easiest way around problems	1	2	3	4	5
I must be free of disturbing feelings as quickly as possible; I can't bear it if they continue	1	2	3	4	5
I can't stand doing tasks that seem too difficult	1	2	3	4	5
I can't bear to feel that I am losing my mind	1	2	3	4	5
I can't stand doing tasks when I'm not in the mood	1	2	3	4	5
I can't bear to have certain thoughts	1	2	3	4	5
I can't stand having to push myself at tasks	1	2	3	4	5
I can't stand situations where I might feel upset	1	2	3	4	5
I can't stand the hassle of having to do things right now	1	2	3	4	5
I can't bear disturbing feelings	1	2	3	4	5
I can't stand doing things that involve a lot of hassle	1	2	3	4	5
I can't get on with my life or be happy if things don't change	1	2	3	4	5
I can't stand having to persist at unpleasant tasks	1	2	3	4	5
I can't stand to lose control of my feelings	1	2	3	4	5

Continued on next page

University of Nottingham Wind Turbine Survey

PART 2

You will now be played six different recordings (either a sound clip or a video) of sounds from a small or micro wind turbine, please listen to/watch the recordings carefully and answer the following questions for each recording.

RECORDING 1 (SOUND CLIP)

Listed below are a number of sounds you might hear in the recording due to the wind turbine. Please rate how loud you perceive each sound to be by circling the appropriate answer.

	LOUDNESS				
	Cannot hear	Hear but not loud	Quite loud	Very loud	Extremely loud
Swooshing	1	2	3	4	5
Screeching	1	2	3	4	5
Buzzing	1	2	3	4	5
Whistling	1	2	3	4	5
Humming	1	2	3	4	5
Throbbing	1	2	3	4	5
Thumping	1	2	3	4	5
Scratching	1	2	3	4	5
High Pitched	1	2	3	4	5
Low Pitched	1	2	3	4	5

If you heard any other sound NOT listed above, please state it/them here.

____

Please rate how annoying you find the sounds in this recording (please circle a number below)

Not at all annoying **1** **2** **3** **4** **5** Extremely annoying

How long do you feel you could put up with the sounds in this recording before you would have to switch it off? (please circle the appropriate answer)

Seconds Minutes Hours Days Wouldn't have to switch off

Continued on next page

This page is repeated for each of the seven recordings in the same format, without the introductory text.

University of Nottingham Wind Turbine Survey

PART 3

Finally please answer the following questions to the best of your ability, feel free to add any additional comments you may have about wind turbines or this survey.

How often have you experienced the following symptoms DURING THE LAST MONTH? (please circle)

	Never	Once or twice	Once or twice per week	Frequently	Daily
Headache	1	2	3	4	5
Dizziness	1	2	3	4	5
Palpitations	1	2	3	4	5
Weak / fatigued	1	2	3	4	5
Upset stomach	1	2	3	4	5
Pain in limbs	1	2	3	4	5
Pain in joints	1	2	3	4	5
Breathlessness	1	2	3	4	5
Sweatiness	1	2	3	4	5
Tingling hands/feet	1	2	3	4	5

If you have any further comments you would like to add this survey, please add them here:

If you are happy to be contacted in the future about other projects researching the effects of wind turbines please leave your details below (this is not compulsory):

Name:

Address:

Contact telephone:

Contact email:

Thank you for your participation!

Appendix H

The k-ω Turbulence Model

In the k-ω models, ω is the specific dissipation rate and is the ratio of ε to k. They are advantageous over the k-ε models as they are better equipped to deal with flow separation and hence external aerodynamic flows. However the solution of the standard k-ω model has a strong sensitivity to the free-stream values of k and ω. Therefore the use of the SST k-ω is recommended to overcome these sensitivities, it was developed to blend the accurate formulation of the standard k-ωmodel in the near-wall region with the free-stream independence of the k-ε model in the far field. The SST k-ωmodel is the most widely used of the models and is accurate in predicting the details of the wall boundary layer as it uses the enhanced wall treatment as default (for more information on wall treatments for the SST k-ω model see Section 4.2.1.3).

The k-ω model is another example of a two equation approach. The transport equations for k and ω respectively are as follows:

$$\frac{\partial(\rho k)}{\partial t} + div(\rho k \mathbf{u}) = div\left[\left(\mu + \frac{\mu_t}{\sigma_k}\right)\ grad\,(k)\right] + min\left(10\beta * \rho k\omega, 2\mu_t S_{ij}\,.\,S_{ij} - \frac{2}{3}\rho k \frac{\partial U_i}{\partial x_j}\delta_{ij}\right) - \beta * \rho k\omega \tag{H.0.1}$$

and

$$\frac{\partial(\rho\omega)}{\partial t} + div(\rho\omega\mathbf{u}) = div\left[\left(\mu + \frac{\mu_t}{\sigma_{\omega,1}}\right)\ grad\,(\omega)\right] + \gamma_2\left(2\rho S_{ij}\,.\,S_{ij} - \frac{2}{3}\rho\omega\frac{\partial U_i}{\partial x_j}\delta_{ij}\right) - \beta_2\rho\omega^2 + 2\frac{\rho}{\sigma_{\omega,2}\omega}\frac{\partial k}{\partial x_k}\frac{\partial \omega}{\partial x_k} \tag{H.0.2}$$

where, $\mu_t = a_1\rho k/max(a_1\omega, SF_2)$ is the eddy viscosity, $\delta_{ij}$is the Kronecker delta ($\delta_{ij} = 1$ if $i = j$, else $\delta_{ij} = 0$), the model constants are $\sigma_k = 1.0$, $\sigma_{\omega,1} = 2.0$, $\sigma_{\omega,2} = 1.17$ $\gamma_2 = 0.44$, $\beta_2 = 0.083$ and $\beta* = 0.09$.

Equation H.0.1 for k is the same as for the standard model, but the ε equation from the standard k-εmodel has been transformed into an ωequations by substituting in $\varepsilon = k\omega$ creating an extra source term on the right hand side representing a cross diffusion term.

Appendix I

CFD Convergence

Span (%)	Velocity (m/s)	Speed	Iteration Number	Velocity Magnitude (m/s)		Turbulent KE (m^2/s^2)		Turbulence Intensity (%)		Static Pressure (Pa)		Dynamic Pressure (Pa)		Wall Shear Stress (Pa)	
				min	max	min	max	min	max	min	max	min	max	min	max
15	26.22	Rated	40000	0.000	42.946	0.005	36.718	0.228	18.869	-176.740	1487.500	0.015	1129.658	0.000	11.290
15	26.22	Rated	25000	0.000	42.945	0.005	37.473	0.228	19.062	-176.733	1487.502	0.015	1129.642	0.000	11.290
15	7.61	Cutin	60000	0.000	11.392	0.000	2.888	0.050	18.326	-8.764	77.415	0.000	79.483	0.000	1.797
15	7.61	Cutin	40000	0.000	11.392	0.000	2.888	0.050	18.326	-8.764	77.415	0.000	79.483	0.000	1.797
15	7.61	Cutin	25000	0.000	11.392	0.000	2.888	0.050	18.326	-8.764	77.415	0.000	79.483	0.000	1.797
20	29.85	Rated	50000	0.000	47.329	0.011	25.294	0.293	13.726	-162.173	1688.133	0.062	1372.027	0.000	13.475
20	29.85	Rated	40000	0.000	47.329	0.011	25.298	0.293	13.726	-162.173	1688.132	0.062	1372.027	0.000	13.475
20	29.85	Rated	25000	0.000	47.329	0.011	25.298	0.293	13.726	-162.173	1688.133	0.062	1372.026	0.000	13.475
20	8.73	Cutin	50000	0.000	12.017	0.000	2.981	0.017	4.702	-24.521	65.533	0.011	88.450	0.000	1.929
20	8.73	Cutin	40000	0.000	12.017	0.000	2.981	0.017	4.702	-24.521	65.533	0.011	88.450	0.000	1.929
20	8.73	Cutin	25000	0.000	12.017	0.000	2.981	0.017	4.702	-24.521	65.533	0.011	88.450	0.000	1.929
25	33.57	Rated	50000	0.000	51.350	0.019	30.170	0.336	13.329	-252.214	1780.228	4.496	1615.072	0.000	15.053
25	33.57	Rated	40000	0.000	51.350	0.019	30.170	0.336	13.329	-252.214	1780.229	4.496	1615.072	0.000	15.053
25	33.57	Rated	25000	0.000	51.350	0.019	30.170	0.336	13.329	-252.214	1780.231	4.496	1615.072	0.000	15.053
25	9.87	Cutin	52000	0.000	13.169	0.000	3.624	0.065	15.764	-42.158	62.056	0.047	106.223	0.000	2.214
25	9.87	Cutin	40000	0.000	13.169	0.000	3.624	0.065	15.765	-42.158	62.056	0.047	106.223	0.000	2.214
25	9.87	Cutin	25000	0.000	13.169	0.000	3.624	0.065	15.765	-42.158	62.056	0.047	106.223	0.000	2.214
50	52.83	Rated	50000	0.000	77.000	0.976	63.811	1.526	12.327	-505.296	3323.969	42.735	3631.167	0.000	27.048
50	52.83	Rated	40000	0.000	76.996	0.976	63.811	1.526	12.327	-505.296	3323.968	42.736	3631.168	0.000	27.048
50	52.83	Rated	25000	0.000	77.000	0.976	63.811	1.526	12.327	-505.296	3323.969	42.735	3631.168	0.000	27.048
50	15.72	Cutin	50000	0.000	20.734	0.001	9.522	0.057	4.771	-110.196	114.842	0.483	263.312	0.000	5.074
50	15.72	Cutin	40000	0.000	20.734	0.001	9.522	0.057	4.771	-110.196	144.842	0.483	263.312	0.000	5.074
50	15.72	Cutin	25000	0.000	20.734	0.001	9.522	0.057	4.771	-110.196	144.842	0.483	263.312	0.000	5.074
90	84.45	Rated	50000	0.000	117.610	20.094	143.148	4.334	11.538	-929.592	7490.964	227.749	8472.199	0.000	58.634
90	84.45	Rated	40000	0.000	117.610	20.094	143.147	4.334	11.538	-929.591	7490.967	227.750	8472.197	0.000	58.635
90	84.45	Rated	25000	0.000	117.610	20.096	143.148	4.334	11.539	-929.592	7490.964	227.748	8472.194	0.000	58.635
90	25.26	Cutin	50000	0.000	33.124	0.014	18.517	0.384	13.911	-243.521	406.153	2.911	672.032	0.000	10.633
90	25.26	Cutin	40000	0.000	33.124	0.014	18.517	0.384	13.911	-243.521	406.153	2.911	672.032	0.000	10.633
90	25.26	Cutin	25000	0.000	33.124	0.014	18.517	0.384	13.911	-243.521	406.153	2.911	672.032	0.000	10.633

Table I.0.1: Table showing convergence for all steady-state cases

Span (%)	Velocity (m/s)	Speed	Time Step No.	Time (s)	Velocity Magnitude (m/s)		Turbulent KE (m^2/s^2)		Turbulence Intensity (%)		Static Pressure (Pa)		Dynamic Pressure (Pa)		Wall Shear Stress (Pa)	
					min	max	min	max	min	max	min	max	min	max	min	max
15	26.22	Rated	4250	0.1645	0.000	42.872	0.005	30.546	0.228	17.210	-173.853	1479.145	0.014	1125.774	0.000	11.273
15	26.22	Rated	8500	0.3290	0.000	42.872	0.005	30.531	0.228	17.206	-173.823	1479.092	0.014	1125.766	0.000	11.273
15	26.22	Rated	12771	0.4944	0.000	42.872	0.005	30.531	0.228	17.206	-173.824	1479.096	0.015	1125.768	0.000	11.273
15	7.61	Cutin	4250	0.5610	0.000	11.186	0.000	2.887	0.048	18.381	-10.935	73.593	0.000	76.646	0.000	1.836
15	7.61	Cutin	8500	1.1220	0.000	11.186	0.000	2.887	0.048	18.381	-10.935	75.593	0.000	76.646	0.000	1.836
15	7.61	Cutin	11500	1.5180	0.000	11.186	0.000	2.887	0.048	18.381	-10.935	73.593	0.000	76.646	0.000	1.856
20	29.85	Rated	4215	0.1311	0.000	47.329	0.011	25.298	0.293	13.726	-162.172	1688.131	0.062	1372.026	0.000	13.475
20	29.85	Rated	8430	0.2622	0.000	47.329	0.011	25.298	0.293	13.726	-162.172	1688.129	0.062	1372.025	0.000	13.475
20	29.85	Rated	12647	0.3933	0.000	47.329	0.011	25.298	0.293	13.726	-162.172	1688.129	0.062	1372.025	0.000	13.475
20	8.73	Cutin	4215	0.4468	0.000	12.017	0.000	2.981	0.056	16.077	-24.521	65.533	0.011	88.450	0.000	1.929
20	8.73	Cutin	8430	0.8936	0.000	12.017	0.000	2.981	0.056	16.077	-24.521	65.533	0.011	88.450	0.000	1.929
20	8.73	Cutin	12647	1.3406	0.000	12.017	0.000	2.981	0.056	16.077	-24.521	65.533	0.011	88.450	0.000	1.929
25	33.57	Rated	4105	0.1059	0.000	51.346	0.019	30.165	0.336	13.328	-252.305	1779.407	4.498	1614.786	0.000	15.049
25	33.57	Rated	8205	0.2117	0.000	51.350	0.019	30.170	0.336	13.329	-252.215	1780.217	4.496	1615.069	0.000	15.053
25	33.57	Rated	12315	0.3177	0.000	51.350	0.020	30.170	0.336	13.329	-252.214	1780.229	4.496	1615.071	0.000	15.053
25	9.87	Cutin	4105	0.3584	0.000	13.169	0.000	3.624	0.065	15.765	-42.158	62.056	0.047	106.223	0.000	2.214
25	9.87	Cutin	8215	0.7171	0.000	13.169	0.000	3.624	0.065	15.765	-42.158	62.056	0.047	106.223	0.000	2.214
25	9.87	Cutin	12260	1.0707	0.000	13.169	0.000	3.624	0.065	15.765	-42.158	62.056	0.047	106.223	0.000	2.214
50	52.83	Rated	3680	0.0427	0.000	76.992	0.976	63.800	1.526	12.326	-505.269	3323.039	42.747	3630.761	0.000	27.044
50	52.83	Rated	7360	0.0854	0.000	76.996	0.976	63.811	1.526	12.327	-505.297	3323.964	42.736	3631.173	0.000	27.048
50	52.83	Rated	11040	0.1281	0.000	76.996	0.976	63.811	1.526	12.327	-505.296	3323.960	42.735	3631.167	0.000	27.048
50	15.72	Cutin	3600	0.1400	0.000	20.734	0.001	9.522	0.190	16.029	-110.196	144.841	0.483	263.311	0.000	5.074
50	15.72	Cutin	7400	0.2879	0.000	20.734	0.001	9.522	0.190	16.029	-110.196	144.840	0.483	263.310	0.000	5.074
50	15.72	Cutin	11040	0.4295	0.000	20.734	0.001	9.522	0.190	16.029	-110.196	144.841	0.483	263.311	0.000	5.074
90	84.45	Rated	3030	0.0166	0.000	116.913	20.258	143.965	4.352	11.575	-1218.166	7193.773	219.788	8372.060	0.000	57.259
90	84.45	Rated	6050	0.0331	0.000	116.913	20.100	143.964	4.335	11.575	-1218.181	7193.734	219.789	8372.043	0.000	57.259
90	84.45	Rated	9070	0.0496	0.000	116.913	20.099	143.964	4.334	11.575	-1218.181	7193.735	219.789	8372.043	0.000	57.259
90	25.26	Cutin	3025	0.0551	0.000	33.056	0.004	17.605	0.200	13.564	-272.656	377.370	1.263	669.282	0.000	9.950
90	25.26	Cutin	6050	0.1101	0.000	33.056	0.004	17.605	0.200	13.564	-272.656	377.370	1.263	669.282	0.000	9.950
90	25.26	Cutin	9070	0.1651	0.000	33.056	0.004	17.605	0.200	13.564	-272.656	377.370	1.263	669.282	0.000	9.950

Table I.0.2: Table showing convergence for all transient cases

Appendix J

CFD Results

J.1 Static Pressure Contours

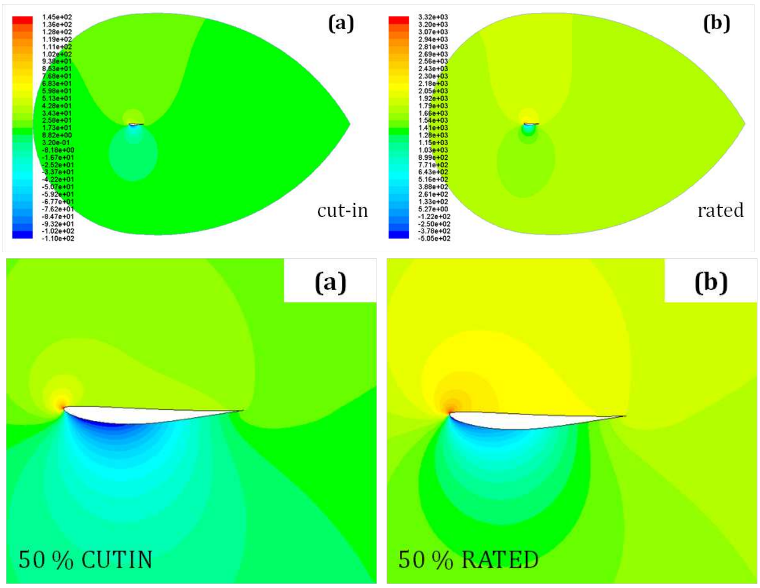

Figure J.1.1: Static pressure contours for the whole domain and close to the aerofoil for the 50% cutin (a) and rated (b) cases

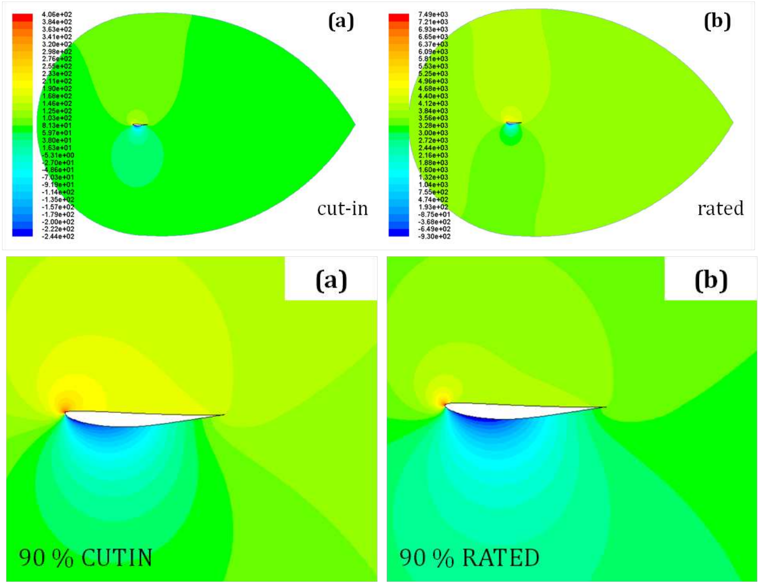

Figure J.1.2: Static pressure contours for the whole domain and close to the aerofoil for the 90% cutin (a) and rated (b) cases

J.2 Velocity Magnitude Vectors

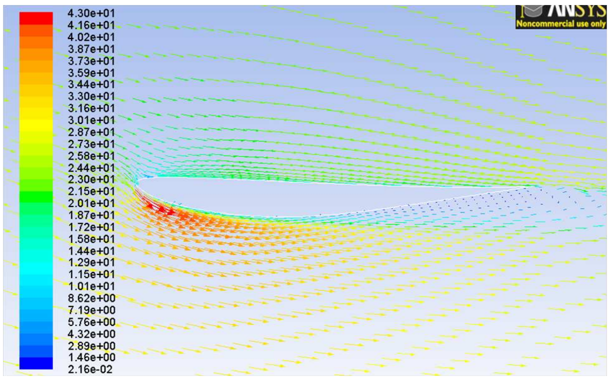

Figure J.2.1: Velocity vectors (m/s) for the whole 15% span aerofoil - steady-state rated case

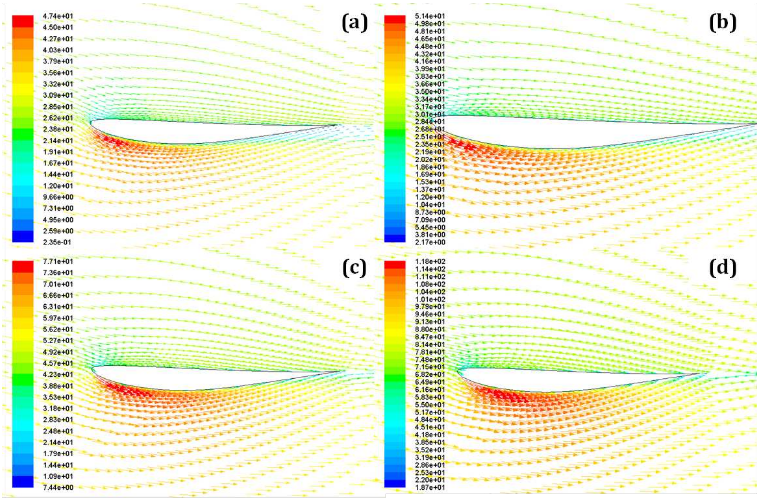

Figure J.2.2: Comparison of the velocity vectors around the aerofoil for 20% (a), 25% (b), 50% (c), and 90% (d) span rated cases

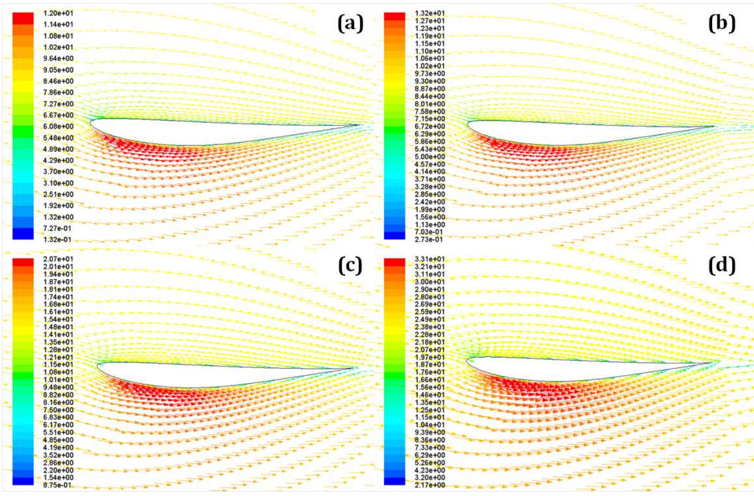

Figure J.2.3: Comparison of the velocity vectors around the aerofoil for 20% (a), 25% (b), 50% (c), and 90% (d) span cutin cases

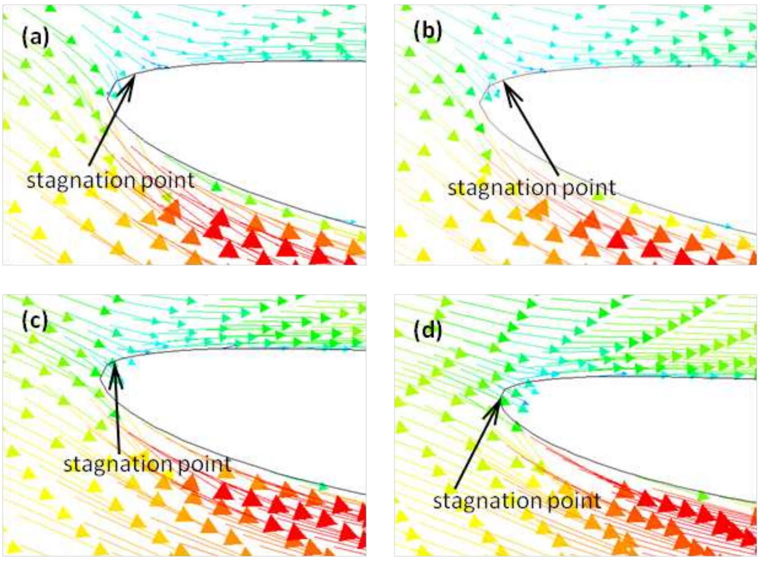

Figure J.2.4: Comparison of the leading edge velocity vectors for 20% (a), 25% (b), 50% (c), and 90% (d) span cutin cases

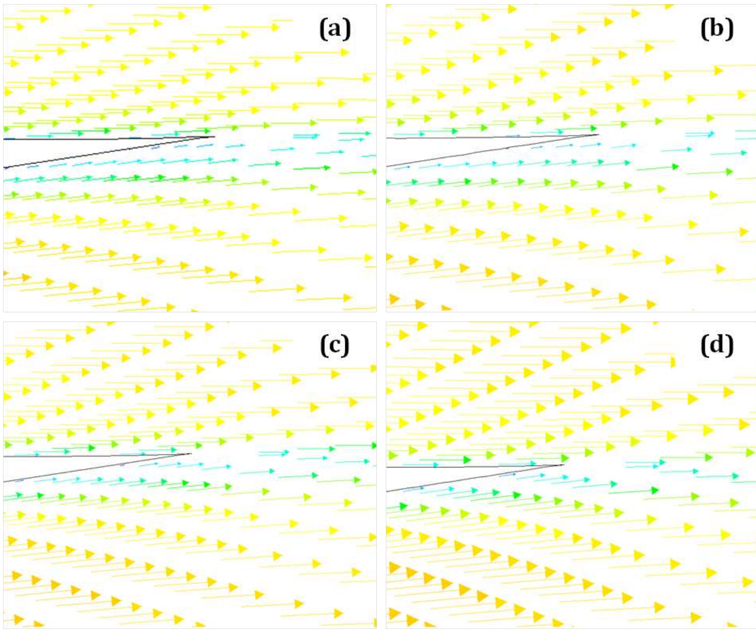

Figure J.2.5: Comparison of the trailing edge velocity vectors for 20% (a), 25% (b), 50% (c), and 90% (d) span cutin cases